Achieving High Reliability for Ambiguity Resolutions with Multiple GNSS Constellations

A THESIS

SUBMITTED TO THE FACULTY OF SCIENCE AND TECHNOLOGY

OF QUEENSLAND UNIVERSITY OF TECHNOLOGY

IN PARTIAL FULFILMENT OF THE REQUIREMENTS

FOR THE DEGREE OF

DOCTOR OF PHILOSOPHY

Jun Wang

October, 2012

Statement of Original Authorship

The work contained in this thesis has not been previously submitted to meet requirements for an award at this or any other higher education institution. To the best of my knowledge and belief, the thesis contains no material previously published or written by another person except where due reference is made.

Signature QUT Verified Signature

Date 30/10/2012

Abstract

Global Navigation Satellite Systems (GNSS)-based observation systems can provide high precision positioning and navigation solutions in real time, in the order of sub-centimetre if we make use of carrier phase measurements in the differential mode and deal with all the bias and noise terms well. However, these carrier phase measurements are ambiguous due to unknown, integer numbers of cycles. One key challenge in the differential carrier phase mode is to fix the integer ambiguities correctly. On the other hand, in the safety of life or liability-critical applications, such as for vehicle safety positioning and aviation, not only is high accuracy required, but also the reliability requirement is important. This PhD research studies to achieve high reliability for ambiguity resolution (AR) in a multi-GNSS environment.

GNSS ambiguity estimation and validation problems are the focus of the research effort. Particularly, we study the case of multiple constellations that include initial to full operations of foreseeable Galileo, GLONASS and Compass and QZSS navigation systems from next few years to the end of the decade. Since real observation data is only available from GPS and GLONASS systems, the simulation method named Virtual Galileo Constellation (VGC) is applied to generate observational data from another constellation in the data analysis. In addition, both full ambiguity resolution (FAR) and partial ambiguity resolution (PAR) algorithms are used in processing single and dual constellation data.

Firstly, a brief overview of related work on AR methods and reliability theory is given. Next, a modified inverse integer Cholesky decorrelation method and its performance on AR are presented. Subsequently, a new measure of decorrelation performance called orthogonality defect is introduced and compared with other measures. Furthermore, a new AR scheme considering the ambiguity validation requirement in the control of the search space size is proposed to improve the search efficiency. With respect to the reliability of AR, we also discuss the computation of the ambiguity success rate (ASR) and confirm that the success rate computed with the integer bootstrapping method is quite a sharp approximation to the actual integer least-squares (ILS) method success rate. The advantages of multi-GNSS constellations are examined in terms of the PAR technique involving the predefined

ASR. Finally, a novel satellite selection algorithm for reliable ambiguity resolution called SARA is developed.

In summary, the study demonstrats that when the ASR is close to one, the reliability of AR can be guaranteed and the ambiguity validation is effective. The work then focuses on new strategies to improve the ASR, including a partial ambiguity resolution procedure with a predefined success rate and a novel satellite selection strategy with a high success rate. The proposed strategies bring significant benefits of multi-GNSS signals to real-time high precision and high reliability positioning services.

Keywords: GNSS; Ambiguity Resolution; Multiple Constellations; Success Rate; Satellite Selection; Reliability

Acknowledgements

First of all, I would like to express my sincere appreciation to my supervisor, Prof. Yanming Feng, who creates an ideal environment for people like me to conduct the research that is of my genuine interests. His supervision, passion, inspiration, encouragement and openness gave me the confidence and made this work possible. I would also like to thank my associate supervisor, Dr Maolin Tang, for proofreading this thesis and other kind support.

I would like to acknowledge the generous financial support provided by the China Scholarship Council (CSC), and the top-up from the Cooperative Research Centre for Spatial Information (CRCSI).

I would like to thank Prof. Peter Teunissen from Curtin University and Dr Peiliang Xu from Kyoto University for their constructive suggestions and comments. The advice from and discussions with Dr Charles Wang and Dr Bofeng Li were also appreciated. Special thanks go also to my colleagues and friends at Queensland University of Technology, Feng Qiu, Jun Gao, Zhengrong Li, Hang Jin, Yan Shen, Ning Zhou, Nannan Zong, Hua Deng, Zhengyu Yang, Wen Wen, Yue Wu, Juan Li and Yue'e Liu, who made my life here wonderful, enjoyable and unforgettable. To my friends in China, I am grateful for their support and friendship.

Finally, I want to particularly thank my family for their constant encouragement and endless love. Above all, I would like to give my deepest thanks to my wife, Waiyee Ivy Lau, whose patient love encouraged me and accompanied me to complete this work.

Table of Contents

Abstract ..... **i**

Acknowledgements ..... **iii**

Table of Contents ..... **iv**

Abbreviations ..... **viii**

List of Figures ..... **x**

List of Tables ..... **xiv**

List of Publications ..... **xv**

Chapter 1: Introduction **1**

1.1 Background and Motivation 1
1.2 Description of Research Problems 3
1.3 Overall Aims of the Study 5
1.4 Specific Objectives of the Study 5
1.5 Account of Research Progress Linking the Research Papers 6

Chapter 2: Literature Review **10**

2.1 Overview of GNSS Systems 10
2.1.1 GPS and its modernisation 10
2.1.2 GLONASS and its modernisation 11
2.1.3 Compass and its development 13
2.1.4 Other GNSS systems 14
2.1.5 Compatibility and interoperability of GNSS 14
2.2 GNSS Observables 15
2.2.1 Pseudorange and carrier phase measurements 16
2.2.2 Measurement errors and mitigation 17
2.2.3 Phase differences 19
2.3 Integer Ambiguity Estimation Methods 22
2.3.1 Fundamental mathematic model 22
2.3.2 Integer rounding 24
2.3.3 Integer bootstrapping 25
2.3.4 Integer least-squares 26
2.3.5 Other ambiguity resolution methods 27
2.4 Decorrelation Methods 28
2.4.1 Integer Gaussian transformation 29

2.4.2 Lenstra–Lenstra–Lovász (LLL) algorithm 29
2.4.3 Inverse integer Cholesky decorrelation method 30
2.4.4 Measure of decorrelation performance 31
2.5 Reliability Theory 32
2.5.1 Internal reliability and external reliability 32
2.5.2 ADOP 34
2.5.3 Success rate 34
2.5.4 Computations of success rate 35
2.6 Satellite Selection Algorithms 36
2.6.1 Highest Elevation Satellite Selection Algorithm 37
2.6.2 Maximum Volume Algorithm 37
2.6.3 Quasi-Optimal Satellite Selection Algorithm 38
2.6.4 Multi-Constellations Satellite Selection Algorithm 38
2.7 Summary 39

Chapter 3: A Modified Inverse Integer Cholesky Decorrelation Method and Performance on Ambiguity Resolution 41

Statement of Contribution of Co-Authors 42
3.1 Introduction 44
3.2 Decorrelation Techniques 48
3.2.1 Integer Gaussian decorrelation 48
3.2.2 Lenstra–Lenstra–Lovász algorithm 49
3.2.3 Inverse integer Cholesky decorrelation (IICD) method 49
3.2.4 Modified inverse integer Cholesky decorrelation (MIICD) method 50
3.3 Random Simulation and Measuring Performance 51
3.3.1 Random simulation method 52
3.3.2 Virtual Galileo Constellation (VGC) model 53
3.3.3 Measuring performance 53
3.4 Experiments 54
3.5 Conclusions 62
3.6 Reference 63

Chapter 4: Orthogonality Defect and Search Space Size for Solving Integer Least-Squares Problems 65

Statement of Contribution of Co-Authors 66
4.1 Introduction 68
4.2 Integer Least-Squares 71
4.2.1 Ratio-Test 73

4.3 A Proposed AR Scheme 74
4.3.1 The ambiguity search space 74
4.3.2 A proposed AR scheme 76
4.4 Measure of Decorrelation Performance 79
4.4.1 Decorrelation number 80
4.4.2 Condition number 80
4.4.3 Orthogonality defect 80
4.5 Experiments and Analysis 83
4.6 Conclusions 92
4.7 References 94

Chapter 5: Computed Success Rates of Various Carrier Phase Integer Estimation Solutions and Their Comparison with Statistical Success Rates 96

Statement of Contribution of Co-Authors 97
5.1 Introduction 100
5.2 Integer Least Square (ILS) Solutions and Variations 103
5.3 Success Probability Computations 107
5.3.1 Integer least squares success probability 107
5.3.2 Construction and representation of ambiguity pull-in region 109
5.3.3 Integer rounding and integer bootstrapping success probability 113
5.3.4 Actual success rate statistic 114
5.4 Experimental analysis 115
5.5 Concluding remarks 121
5.6 References 122

Chapter 6: Reliability of Partial Ambiguity Fixing with Multiple GNSS Constellations 124

Statement of Contribution of Co-Authors 125
6.1 Introduction 127
6.2 Reliability Characteristics of Ambiguity Resolution 131
6.2.1 ADOP 131
6.2.2 Pull-in region and success rate of integer least-squares 132
6.2.3 Computation of success rates 133
6.3 Ambiguity Validation Decision Matrix 134
6.3.1 Ratio test 135
6.4 Partial Ambiguity Decorrelation 136
6.5 Partial Ambiguity Fixing With Indices of Success Rate and Ratio Test 140
6.6 Experimental Analysis 142

6.6.1 AR success rates, ratio-test values and AR validation outcomes 142
6.6.2 Reliability Performance of PAR in the case of a dual-constellation 146
6.7 Conclusions 151
6.8 References 152

Chapter 7: Satellite Selection Strategy for Achieving High Reliability Ambiguity Resolution with Multi-GNSS Constellations 156

Statement of Contribution of Co-Authors 157
7.1 Introduction 160
7.2 Existing Satellite Selection Algorithms 163
7.2.1 Highest Elevation Satellite Selection Algorithm 164
7.2.2 Maximum Volume Algorithm 164
7.2.3 Quasi-Optimal Satellite Selection Algorithm 165
7.2.4 Multi-Constellations Satellite Selection Algorithm 165
7.3 Reliability Criteria for Ambiguity Resolution 166
7.3.1 Internal reliability and external reliability 166
7.3.2 ADOP 168
7.3.3 Success Rate 169
7.3.4 Reliability criteria for satellite selection 170
7.4 Satellite-selection Algorithm for Reliable Ambiguity-resolution (SARA) 172
7.5 Experiments and Analysis 174
7.6 Conclusions and Future work 188
7.7 Reference 189

Chapter 8: Conclusions and Recommendations 192

8.1 Summary of Key Contributions 194
8.2 Recommendations for Future Work 195

BIBLIOGRAPHY 197

Abbreviations

ADOP	Ambiguity Dilution of Precision
AR	Ambiguity Resolution
ASR	Ambiguity Success Rate
CDMA	Code Division Multiple Access
CIR	Cascading Integer Resolution
CS	Commercial Service
DOF	Degree Of Freedom
EIA	Ellipsoidal Integer Aperture
FARA	Fast Ambiguity Resolution Approach
FASF	Fast Ambiguity Search Filter
FDMA	Frequency Division Multiple Access
GEO	Geostationary Orbit
GIOVE	Galileo In-Orbit Validation Elements
GNSS	Global Navigation Satellite Systems
GPS	Global Positioning System
HESSA	Highest Elevation Satellite Selection Algorithm
HMI	Hazardous Misleading Information
IA	Called Integer Aperture
ILS	Integer Least-Squares
IR	Integrity Risk
IRNSS	Indian Regional Navigation Satellite System
ITU	International Telecommunications Union
LAMBDA	Least-Squares Ambiguity Decorrelation Adjustment
LBS	Location Based Services
LEO	Low Earth Orbit
LLL	Lenstra–Lenstra–Lovász
LS	Least-Squares
LSAST	Least Squares Ambiguity Search Technique
MCSSA	Multi-Constellations Satellite Selection Algorithm
MDB	Minimum Detectable Bias
MEO	Medium Earth Orbit
MIICD	Modified Inverse Integer Cholesky Decorrelation
MVA	Maximum Volume Algorithm

MVNCDF	Multivariate Normal Cumulative Density Function
OMEGA	Optimal Method for Estimating GPS Ambiguities
OS	Open Service
PAR	Partial Ambiguity Resolution
PCF	Probability of Correct Fixing
PDOP	Position Dilution of Precision
PIF	Probability of Incorrect Fixing
PNT	Positioning, Navigation and Timing
PPS	Precise Positioning Service
PRS	Public Regulated Service
QOSSA	Quasi-Optimal Satellite Selection Algorithm
QZSS	Quasi-Zenith Satellite System
RAIM	Receiver Autonomous Integrity Monitoring
RF	Radio Frequency
RTK	Real-Time Kinematic
SAR	Search and Rescue
SARA	Satellite-selection Algorithm for Reliable Ambiguity-resolution
SoL	Safety-of-Life
SPS	Standard Positioning Service
TCAR	Three Carrier Ambiguity Resolution
TOA	Time of Arrival
UTC	Coordinated Universal Time
VGC	Virtual Galileo Constellation

List of Figures

Figure 1-1 Outline of the research parts conducted to complete the project..... 6

Figure 3-1 Condition numbers of $\mathbf{Q}_{\hat{N}}$ and $\mathbf{Q}_{\hat{N}dec}$ in L1L2 and L1L2L5 cases. Left plot: the float ambiguity variance-covariance matrix $\mathbf{Q}_{\hat{N}}$ Right plot: the decorrelated ambiguity vc- matrix $\mathbf{Q}_{\hat{N}dec}$ 46

Figure 3-2 Condition numbers of $\mathbf{Q}_{\hat{N}}$ and $\mathbf{Q}_{\hat{N}dec}$ in GPS and dual donstellations cases. Left plot: the float ambiguity variance-covariance matrix $\mathbf{Q}_{\hat{N}}$ Right plot: the decorrelated ambiguity vc- matrix $\mathbf{Q}_{\hat{N}dec}$ 47

Figure 3-3 Flowchart if the modified inverse integer Cholesky decorrelation method 51

Figure 3-4 The eigenvalues partition of the covariance matrix of the float ambiguities. Left plot: the three largest eigenvalues; Right plot: the remaining eigenvalues 53

Figure 3-5 Dimensions of the 300 random simulation examples..... 55

Figure 3-6 Condition numbers of simulated Q samples and results from LAMBDA, LLL, IICD and MIICD with Scenario 1..... 56

Figure 3-7 Condition Numbers of simulated Q samples, results from LAMBDA, LLL, IICD and MIICD in Scenario 2..... 56

Figure 3-8 Condition numbers of Q matrices, resulting from LAMBDA and MIICD with Scenario 3..... 58

Figure 3-9 Condition numbers of Q matrices, resulting from LAMBDA and MIICD with Scenario 4..... 59

Figure 3-10 Search candidate numbers, resulting from LAMBDA and MIICD with Scenario 3..... 59

Figure 3-11 Search candidate numbers, resulting from LAMBDA and MIICD with Scenario 4..... 59

Figure 3-12 Scatter plots of the search candidate number against the condition number..... 60

Figure 3-13 Computed success rates, resulting from LAMBDA and MIICD with Scenario 3..... 61

Figure 3-14 Computed success rates, resulting from LAMBDA and MIICD with Scenario 4..... 61

Figure 4-1 Illustrations of two-dimensional ILS pull-in regions and minimum volume boxes covering the ellipsoidal regions for the original ambiguity vc-matrix (left) and decorrelated vc-matrix, respectively. The blue dots stand for search grid points in minimum volume box; and the red dots for those falling in to the ellipsoidal region. 71

Figure 4-2 The search nodes and candidates in an integer-ambiguity search tree..... 73

Figure 4-3 Illustrations of two-dimensional ambiguity search space with different sizes, shapes and orientations. 77

Figure 4-4 Illustrations of increased search nodes for searching the second candidate with different search space sizes comparing the exact norm of the second candidate. 77

Figure 4-5 Flowchart of the proposed AR scheme 79

Figure 4-6 Correlation coefficients between the ambiguity search candidate number and its condition number, orthogonality defect and search-space size from the simulation data 85

Figure 4-7 Correlation coefficients between the ambiguity search node number and its condition number, orthogonality defect and search-space size from the simulation data 85

Figure 4-8 Correlation coefficients between the ambiguity search candidate number and its condition number, orthogonality defect and search-space size from a real-data set 86

Figure 4-9 Correlation coefficients between the ambiguity search node number and its condition number, orthogonality defect and search-space size from a real-data set 86

Figure 4-10 The ambiguity search-space sizes for LAMBDA and the new AR scheme of GPS and DCS 89

Figure 4-11 The search candidate numbers for LAMBDA and the new AR scheme of GPS and DCS 90

Figure 4-12 The search node numbers for LAMBDA and the new AR scheme of GPS and DCS 90

Figure 4-13 The ambiguity ratio-test values for LAMBDA and the new AR scheme of GPS and DCS 91

Figure 4-14 The ambiguity search CPU time difference between LAMBDA and the new AR scheme 91

Figure 5-1 Illustration of the Voronoi cell defined by the covariance matrix (22) for the L1 and L2 ambiguity variables where the correct integers are (0, 0). The Voronoi cell is represented using a two-dimensional matrix grid, which consists of 1,554 rows or grid points 111

Figure 5-2 Illustration of probability density over the Voronoi represented by the 2-dimensional grid as shown in Figure 5-1 112

Figure 5-3 Illustration of the cumulative probability integrated over the Voronoi cell as shown in Figure 5-1 112

Figure 5-4 Probability density contours for the covariance matrix (22) plotted over the pull-in region and bound box (-0.5, 0.5), showing very low probability density values outside the pull-in region. 113

Figure 5-5 Illustration of computed integer rounding success probabilities according to the integration of m-normal distribution function (23) with single-epoch unit-weight variance estimates, referring to computation scheme I 116

Figure 5-6 Illustration of computed integer rounding success probabilities according to the integration of m-normal distribution function (23) with the all-epoch variance estimate (see computation scheme II) 117

Figure 5-7 Illustration of computed integer bootstrapping success probabilities according to the integration of m-normal distribution function (24) (see computation scheme IV) 117

Figure 5-8 a Illustration of computed ILS lower-bound success probability according to the integration in the inequality (4) (see computation scheme V). b Illustration of computed ILS upper-bound success probability according to the integration in the inequality (4) (see computation scheme VI) 118

Figure 5-9 Illustration of computed ILS upper-bound success probability according to the right-hand integration in the inequality (3) (see computation scheme VII) ... 118

Figure 5-10 The positioning errors after integers are correctly fixed over all the epochs. The large errors show the impact of poor geometry instead of wrong integers. 119

Figure 6-1 Illustration of the pull-in region (*left*) and the probability density (*right*) of 2-dimensional matrix..... 133

Figure 6-2 The success rate P_{boot} in the case with no bias, with a bias of 0.01 cycles, and a bias of 0.1 cycles on a ten-dimensional matrix for different numbers of decorrelation steps..... 139

Figure 6-3 Illustration of effects of measurement biases on bootstrapping ambiguity solutions with consideration of the cases with no bias, a bias of 0.01 cycles, and a bias of 0.1 cycles. The dimension of the Q matrix is 10 and the decorrelation iteration run from 1 to 450 steps..... 139

Figure 6-4 The flowchart of partial ambiguity resolution with predefined success rate 141

Figure 6-5 Fixed ambiguity numbers of GPS, DCS, GPS (PAR) and DCS (PAR). 147

Figure 6-6 ADOPs of GPS, DCS, GPS (PAR) and DCS (PAR) 147

Figure 6-7 Bootstrapped success rates of GPS, DCS, GPS (PAR) and DCS (PAR)148

Figure 6-8 ADOP-approximated success rates of GPS, DCS, GPS (PAR) and DCS (PAR) 149

Figure 6-9 Ratio Test Values of GPS, DCS, GPS (PAR) and DCS (PAR) 149

Figure 6-10 XYZ Positioning errors of GPS, DCS, GPS (PAR) and DCS (PAR) .. 151

Figure 7-1 PDOP, ADOP and ASR of different ten satellites from fifteen satellites 163

Figure 7-2 The precision and change rate of the ADOP with increasing number of satellites..... 169

Figure 7-3 The redundancy number, minimum detectable bias and external global reliability of a dual-constellation design matrix for 1000 samples with the correspondent satellites of extreme values..... 171

Figure 7-4 The two options of SARA algorithm..... 173

Figure 7-5 The ASR difference between option 1 and option 2 in SARA algorithm 173

Figure 7-6 The sky plot of selected 14 visible satellites as an example from 18 visible satellites by SARA, □ denotes the selected satellite..... 174

Figure 7-7 ADOPs computed with four schemes: GPS, SARA, HESSA and MCSSA 176

Figure 7-8 ASRs computed with four schemes: GPS, SARA, HESSA and MCSSA 177

Figure 7-9 Redundancy number computed with four schemes: GPS, SARA, HESSA and MCSSA 177

Figure 7-10 MDB computed with four schemes: GPS, SARA, HESSA and MCSSA 178

Figure 7-11 External reliability computed with four schemes: GPS, SARA, HESSA and MCSSA 178

Figure 7-12 PDOP computed with four schemes: GPS, SARA, HESSA and MCSSA 179

Figure 7-13 XYZ position error computed with four schemes: GPS, SARA, HESSA and MCSSA. 179

Figure 7-14 Ratio Test values computed with four schemes: GPS, SARA, HESSA and MCSSA 180

Figure 7-15 ADOPs computed with four schemes: DCS, SARA, HESSA and MCSSA 182

Figure 7-16 ASRs computed with four schemes: DCS, SARA, HESSA and MCSSA 183

Figure 7-17 Redundancy number computed with four schemes: DCS, SARA, HESSA and MCSSA..... 183

Figure 7-18 PDOP computed with four schemes: DCS, SARA, HESSA and MCSSA 184

Figure 7-19 XYZ position error computed with four schemes: DCS, SARA, HESSA and MCSSA 184

Figure 7-20 Ratio Test values with four schemes: DCS, SARA, HESSA and MCSSA 185

Figure 7-21 Satellites number with four schemes: GPS, GPS (SARA), DCS and DCS (SARA) 186

Figure 7-22 ASR computed by HESSA with different satellites..... 186

Figure 7-23 Time cost of SARA method in single- and dual-constellation..... 187

List of Tables

Table 2-1 Comparison of systems 14

Table 2-2 A summary of GPS measurement errors and errors mitigation 19

Table 2-3 A summary of AR success rate computing algorithms as approximations to the actual AR success rates 36

Table 3-1 Lower condition number statistics derived from LLL, IICD and MIICD with respect to LAMBDA 57

Table 3-2 The correlation coefficients between search candidate numbers and condition numbers 60

Table 3-3 MIICD with respect to LAMBDA: data epochs with Lower condition numbers and search numbers and success rates derived from the 24-h data set 62

Table 4-1 Properties of decorrelation performance by the LAMBDA method 82

Table 4-2 Search candidate and search node with the same size of the search space 82

Table 4-3 Correlation Coefficients between different parameters 83

Table 4-4 The Means of Correlation Coefficients 87

Table 4-5 Statistical information of search CPU time for GPS and DCS case, respectively 92

Table 5-1 Description of data sets and settings in use of the geometry-based AR models (5) 116

Table 5-2 Summary of computational schemes and overall computed AR success probabilities and actual success rates 119

Table 6-1 A summary of AR success rates computing algorithms as approximations to the actual AR success rate 134

Table 6-2 AR probability outcomes from the ratio test decision under high and low AR success rates 136

Table 6-3 The impact of biases on decorrelated solutions of different decorrelation levels 138

Table 6-4 Statistical information of AR success rates, AR risk parameters, and ratio-test thresholds in the single-constellation case 143

Table 6-5 Statistical information of AR success rates, AR risk parameters, and ratio-test thresholds in the dual-constellations case 145

Table 6-6 The mean of the success rate, ADOP and the critical value of ratio-test 150

Table 6-7 The percentage of past ratio-test values with given thresholds 150

Table 7-1 The extreme values of redundancy number (RNUM), MDB and external global reliability (EXTR) 171

Table 7-2 The percentage of samples number for ratio test and ASR with given critical values 185

List of Publications

Journal Papers

Wang Jun, Feng Yanming, Wang Charles (2010) *A Modified Inverse Integer Cholesky Decorrelation Method and Performance on Ambiguity Resolution*. Journal of Global Positioning Systems, Vol. 9, No. 2, pp. 156-165 (***Chapter* 3**)

Feng Yanming, Wang Jun (2011) *Computed success rates of various carrier phase integer estimation solutions and their comparison with statistical success rates*. Journal of Geodesy, 85(2), pp. 93-103 (***Chapter* 5**)

Wang Jun, Feng Yanming (2012) *Orthogonality Defect and Search Space Size for Solving Integer Least-Squares Problems.* GPS Solutions, DOI 10.1007/s10291-012-0276-6, ISSN1080-5370 (***Chapter* 4**)

Wang Jun, Feng Yanming (2012) *Reliability of partial ambiguity fixing with multi-GNSS constellations.* Journal of Geodesy, DOI 10.1007/s00190-012-0573-4, ISSN 0949-7714 (***Chapter* 6**)

Wang Jun, Feng Yanming (2011) *Satellite Selection Strategy for Achieving High Reliability Ambiguity Resolution with Multi-GNSS Constellations*, submitted to Journal of Geodesy, November 2011 (***Chapter* 7**)

Conference Papers

Wang Jun, Feng Yanming (2009) *Integrity determination of RTK solutions in precision farming applications*. In Proceedings of the Surveying and Spatial Sciences Institute Biennial International Conference 2009, Adelaide Convention Centre, Adelaide, South Australia, pp. 1277-1291.

Wang Jun, Feng Yanming, Wang Charles (2009) *Rover autonomous integrity monitoring of GNSS RTK positioning solutions with multi-constellations*. In Proceedings of the 22nd International Technical Meeting of the Satellite Division of the Institute of Navigation, Institute of Navigation, Savannah International Convention Center, Savannah, Georgia, pp. 1361-1370

Chapter 1: Introduction

1.1 Background and Motivation

In the context of Global Navigation Satellite Systems (GNSSs), including GPS and GLONASS modernisation, Galileo and Compass in progress and worldwide construction of regional augmentation such as WAAS and EGNOS, there will be more than 100 satellites in orbit. The precise positioning technique, for instance, real-time kinematic (RTK) technique, can achieve three-dimensional positioning accuracy of a few centimetres in real-time or near real-time taking advantage of the dual frequency carrier phase signals from a single or multiple GNSS constellations. However, the prerequisite that RTK results in more precise positioning solutions than those by GNSS pseudorange measurements is the number of complete cycles between the receiver antenna and the satellites, that is, the integer ambiguity of the carrier phase can be resolved correctly (Kleusberg and Teunissen 1998; Kaplan and Hegarty 2006; Misra and Enge 2006; Hofmann-Wellenhof et al. 2008). Here the problem of mixed integer-real valued parameter adjustment or integer least-squares (ILS) arises to obtain the estimates of integer ambiguities (Grafarend 2000; Chang et al. 2005). Aside from accuracy, integrity is also a crucial performance factor when a positioning system is to be used for safety-critical and liability-critical operations such as aviation applications and some Location Based Services (LBS) (Feng and Ochieng 2006; Ober 1999).

Unlike the classical pseudorange integrity monitoring technique, for example receiver autonomous integrity monitoring, the main issues with the integrity of carrier phase positioning are reliability and robustness, which are dominated by the correctness of the ambiguity resolution (AR) and validation (Feng et al. 2009). Once integer ambiguities are fixed correctly, then the integrity monitoring algorithms are a direct extension of receiver autonomous integrity monitoring based on pseudorange measurements (Kuusniemi 2005). Henkel (2010) has shown that the risk of an integrity threat is two orders of magnitude lower than the probability of incorrect fixing (PIF) for some linear combinations of dual frequency. In general, the ambiguity success rate (ASR) is considered as an important measure which gives a

quantitative assessment of the probability of correct fixing (PCF) and thus providing the reliability information of the AR (Teunissen et al. 1999; Teunissen 2000; Verhagen 2005b). Since the theoretical ASR of the ILS problem is difficult to obtain, approximate computations of the ILS ASR are sought instead. The ASR is a significant factor, which can be predicated to evaluate the quality of the AR results, but it is not recommended to decide whether to accept the integer ambiguities based on the ASR value only, because the ASR computation does not involve any information of actual measurements. Hence, the concept of ambiguity validation is developed to determine the integer solution uniquely and reliably. Traditionally, the randomness of the integer estimators is often ignored when we use the methods of integer testing for the purpose of ambiguity validation. Nevertheless, the assumption is incorrect when the ASR is not large enough (Verhagen 2004). Moreover, the conclusion that the precision of the 'fixed' solution which is updated by the information of integer ambiguities from the real-valued least-squares (LS) 'float' solution, is better than the 'float' solution itself, which is only safely guaranteed when the ASR is sufficiently close to one (Teunissen 1999a).Unfortunately, the traditional ILS method does not necessarily satisfy this need for the high ASR requirement due to the number of visible satellites, when only a single GNSS constellation is applicable in a single epoch. In that case, there are two possible courses of action: to fix a subset of the ambiguities or to increase the strength of the model (Parkins 2009). The idea of a partial ambiguity resolution (PAR) technique derives from the former one, while the use of a longer observation time span is a typical example of the latter alternative. The PAR process can maintain a sufficiently high ASR, but sometimes the contribution of integer ambiguities on positioning precision will become insignificant if the number of fixed ambiguities is small. In contrast, the adoption of a long observation time span can maintain the benefits of ambiguity fixing, but it is certainly not preferable if the RTK process requires long initialization time. From both perspectives, the challenge is to achieve a good balance between the reliability of ambiguity solutions and and intialisation time. Although in the future the visiable satellites could be multipled, for various reasons, one may not necessarily expect that signals from all the visible satellites will be used by all types of receivers. This is because more GNSS systems operating in the same band may do more harm increasing the radio frequency. As a result, selective use of satellites or constellations could be applicable again to deal with the situation for the

optimal performance or cost saving purposes. However, the existing satellite selection algorithms based on the position dilution of precision (PDOP) have been developed for accuracy purpose (Kihara and Okada 1984; Mok and Cross 1994; Li et al. 1999; Park 2001; Roongpiboonsopit and Karimi 2009). With background knowledge for the above situation, this PhD work seeks to develop methods to improve efficiency and reliability for AR in the context of multiple GNSS constellations. The efforts includes development of new algorithm for efficient decorrelatoion in high-dimensional cases, ASR computation, improved PAR procedure for high ASR and an original easy-to-implement satellite selection algorithm based on the reliability criterion instead of PDOP in order to achieve high ASR.

1.2 Description of Research Problems

Correct integer ambiguity resolution is a prerequisite for centimetre real-time kinematic positioning with double-differenced phase measurements. During the past two decades, various ILS methods for AR have been proposed in the literature. These include the fast ambiguity resolution approach (FARA) (Frei and Beutler 1990), the least squares ambiguity search technique (LSAST) (Hatch 1990), the fast ambiguity search filter (FASF) (Chen and Lachapelle 1995) and the optimal method for estimating GPS ambiguities (OMEGA) (Kim and Langley 1999). Alongside these efforts, the least-squares ambiguity decorrelation adjustment (LAMBDA) method (Teunissen 1993) is both theoretically and practically at the top level among the ambiguity determination methods (Hofmann-Wellenhof et al. 2008). The LAMBDA method consists of two stages: decorrelation and search. The LAMBDA method uses the integer Gaussian transformation in the decorrelation progress to reduce the correlation coefficients and sizes of the ambiguity variance-covariance (vc-) matrix. However, the computational burden for ambiguity decorrelation could be a problem when there are dual or multiple GNSS constellations or signals from multiple carrier frequencies are processed together. In addition, it is noted that the standard LAMBDA method involve many redundant or repeated computations in the separated processes for ambiguity estimation and validation.

The pull-in-region is referred to the subset contains all real-valued ambiguity vectors that will be mapped to the same integer vector (Jonkman 1998). ASR is an important

measure which gives a quantitative assessment of the probability of correct fixing and thus provides the reliability information of AR (Teunissen 1998, 2000). ASR is predictable and dependant on the geometry embedded in the functional and stochastic model as well as the chosen method of integer ambiguity estimation (Teunissen 1999b). It has been proven that the ILS method has the largest ASR among integer rounding, integer bootstrapping and integer least-squares methods. The problem is that rigorous computation of the ASR for the more general ILS solutions has been considered difficult, because of complexity of the ILS ambiguity pull-in region and the computational load of the integration of the multivariate probability density function (Hassibi and Boyd 1998; Teunissen 1998; Xu 2006). Various lower and upper bounds of the ILS success rate haven been proposed and some of them have been proven to be good approximations of the actual success rate (Verhagen 2005b; Teunissen 2003c; Verhagen 2003). In existing works, an exact ASR formula for the integer bootstrapping estimator has been used as a sharp lower bound for the ILS ASR (Verhagen 2003). Nevertheless, the conclusion that the lower bound of the probability given as success probability predictions needs to be substantiated with numerical proof from real world examples.

Since ASR provides a measure for the reliability of integer solutions, it is natural to improve ASR performance in ambiguity resolution (Teunissen et al. 1999). The idea of the PAR technique, which means resolving a subset of the ambiguities, was suggested to maintain a sufficiently high success rate instead of the full set of the integer parameters (Teunissen et al. 1999b; Parkins 2009). In existing efforts to seek the ambiguity subset have been based on ambiguity variance, pre-defined subset sizes, elevation-ordering and linear combinations (Mowlam and Collier 2004). The PAR technique can indeed improve the ASR due to the reduced number of ambiguities fixing, but the contribution of ambiguity integer constraints on the precision of positioning solutions will lessen if the number of ambiguities fixed is too small. Though the concept of PAR may be applicable to multi-constellations, few studies have compared the PAR performance between the single-constellation case and the multi-constellations case (Cao et al. 2007; Cao et al. 2008a).

As mentioned in the previous section, due to the various reasons such as hardware limits and computation burdens, GNSS receivers may be designed to only track some

constellations or signals from certain satellites in instead of all visible satellites. The traditional satellite selection algorithms are based on the minimal PDOP within a given number of satellites. However, the difference between PDOP values would become insignificant for the different satellite subsets when the number of satellites is sufficiently large, such as over 10. In contrast, remarkable improvement of the ASR is still possible through selecting different satellites combinations.

In summary, to the following research questions have been identified to be relevant to data processing multiple GNSS signals::

(1) How to improve the performance of the ILS methods in general or the efficiency of the high-dimensional ambiguity decorrelation specifically?
(2) How to appropriately measure the ambiguity resolution reliability and how well the computed reliability agrees with the actual reliability statistics?
(3) How to achieve high reliability for ambiguity resolution solutions with multi-GNSS constellations?

1.3 Overall Aims of the Study

Given the background and the research problems identified above, the overall aim of this study is to evaluate and improve the ILS procedures to achieve better AR efficiency and high reliability in dealing with multiple GNSS constellations and multiple frequency signals. The thesis presents a novel satellite-selection algorithm to achieve the high reliability of integer ambiguity resolution in multiple GNSS constellations as a key contribution to the field of research.

1.4 Specific Objectives of the Study

In order to achieve the mentioned aim, the specific objectives of this study are as follows:

- Develop a new ambiguity decorrelation method to achieve a smaller condition number for the ambiguity vc-matrix;
- Compare different measures of the performance of ambiguity decorrelation methods and introduce a new measure to evaluate the relationship between

the ambiguity decorrelation performance and the ambiguity searching efficiency;

- Develop a new AR scheme with the combination of ambiguity estimation and validation requirement;
- Identify the best approximation index to assess the ASR of the ILS method in agreement with the actual ASR statistic
- Characterise the performance of the ambiguity validation method with different ASRs;
- Evaluate the performance of accuracy and reliability with multi-GNSS constellations;
- Develop a new multi-constellations satellite selection algorithm for high AR reliability.

1.5 Account of Research Progress Linking the Research Papers

Reliable ambiguity resolution is the key to real-time precise positioning with carrier phase measurements. To achieve high AR reliability with multi-GNSS constellations has been the overarching objective in our research program. In this thesis, the potential improvement of the integer ambiguity estimation method has been investigated based on both theoretical analysis and numerical study. Moreover, we have attempted to obtain a high ASR through the development of an original satellite selection algorithm. To this end, we have divided the following account of our research progress into four stages to highlight the contributions of our papers. Figure 1-1 outlines the stages undertaken in this study.

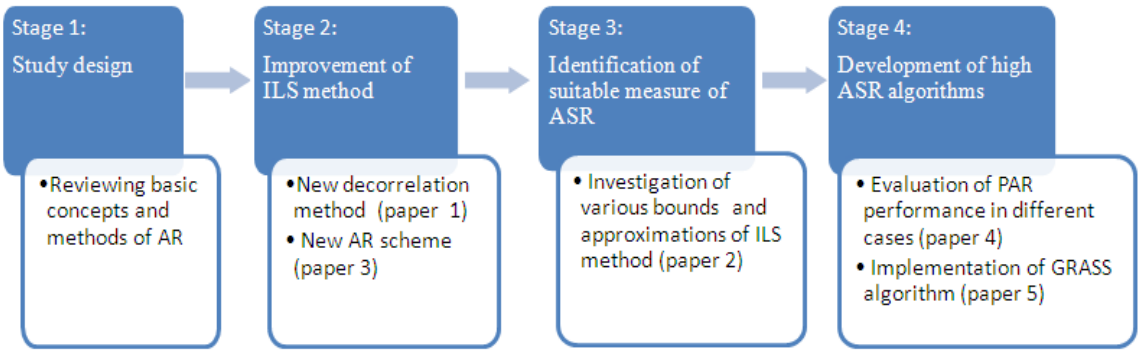

Figure 1-1 Outline of the research parts conducted to complete the project

In the beginning stage, an extensive literature review was carried out in the area of the integer ambiguity resolution method. As outlined in Chapter 2, an overview of GNSS evolution is given first. Next, the basic concepts and methods of ambiguity resolution are discussed. Specifically, the measure of AR reliability performance is reviewed. Various satellite selection algorithms are also inspected in this chapter. This exercise has been helpful in understanding the existing methods and algorithms and providing a basis for he design of the improved algorithms and identifying the focus areas of the whole PhD work.

Having identified potential improvement points for the existing ILS method, Chapter 3 and Chapter 4 investigates the current ILS method from the decorrelation perspective and the validation perspective. Effective decorrelation is a key to fast phase ambiguity resolution in GNSS real time data processing. In Chapter 3 (***paper* 1**), we have proposed a modified inverse integer Cholesky decorrelation (MIICD) technique. The simulation method employs the isotropic probabilistic model using a predefined eigenvalue which make the conclusion of this experiment more general and persuasive. Results from both random simulation data and real data suggest that the MIICD technique can outperform other decorrelation techniques in most situations. In Chapter 4 (***paper* 3**), the concept of the orthogonality defect is introduced as a new measure of the performance of ambiguity decorrelation techniques. The orthogonality defect is commonly used to evaluate the quality of reduced lattice vectors for a reduction process, but this is the first time has been used to evaluate decorrelation performance in the field of AR. Numerically, the orthogonality defect presents slightly better performance in measuring the correlation between decorrelation impact and computational efficiency than the condition number. In addition, a new AR scheme is proposed to improve the ambiguity search efficiency through the control of the ambiguity search space size. The new AR scheme combines the LAMBDA search and validation procedures, and results in a smaller search space size and higher computation efficiency, while retaining the same AR validation outcomes. In short, the results from Chapter 3 and 4 demonstrate the improvement of the ILS method through a joint effort.

After investigation of the measures of decorrelation techniques, in the next stage we conduct an inquiry into the measure for AR reliability performance. In existing works, an exact ASR formula for the integer bootstrapping estimator has been given

and used as a sharp lower bound for the ILS ASR, because its rigorous computation has been considered impractical. In Chapter 5 (***paper* 2**), we examine the variations of integer ambiguity estimators in accordance with the linear observational and stochastic models as well as data processing strategies. Furthermore, we present a study of the bivariate case where the pull-region is usually defined as a hexagon and the probability is obtained using a Matlab function called the multivariate normal cumulative density function (MVNCDF) at all the grid points within the convex polygon. Using a 24 hour GPS data set for a 21 km baseline, this chapter has compared the computed success probabilities of integer rounding, integer bootstrapping solutions and lower and upper bounds of ILS ASR with the actual success rate obtained from the ILS solutions. It is found that the unit–weight variance values taken in the probability formulas are as important as the construction of pull-in regions. Besides these findings, in Chapter 6 (***paper* 4**), an AR validation decision matrix is introduced to consider the impact of ASR. Numerical results from simulations clearly demonstrate that only when the ASR is very high, the AR validation with a lower and ratio-test threshold can provide the decisions about the correctness of AR which are close to real world, with both low AR risk and false alarm probabilities.

It is generally notated in the GNSS community that one of the key benefits that the multiple GNSS signals is that AR reliability can be improved significantly and thus the reliability of the real time kinematic solutions. However, simply adding all the measurements together does not automatically improve the reliability. In Chapter 6, with various probability parameters and an ambiguity validation decision matrix, we numerically examine how these parameters are related to each other. The experiment involves both the single constellation and dual constellations. It is shown that the computed ASR performance of the single constellation is better than that of the dual constellations when we use the traditional ambiguity estimation method. However, if we make use of the PAR method in those two situations, results show that the dual-constellation situation outperforms the single-constellation situation. Instead of choosing a subset of ambiguities to fix, Chapter 7 (***paper* 5**) proposes an original satellite selection algorithm to improve the ASR. Traditional satellite selection algorithms are focused on reducing the PDOP without consideration of the AR reliability requirement. In fact, if those algorithms are directly used in the RTK

technique, the positioning results may be worse than those of simply using all of the visible satellites. Therefore the so-called Satellite-selection Algorithm for Reliable Ambiguity-resolution (SARA) is proposed in this chapter. Validation results confirm that SARA can provide better ASR without loss of positioning accuracy. The SARA algorithm is not designed for specific constellations; however the evaluation results showed that SARA provides better performance in the dual-constellation system than in the single GPS constellation system. Both the PAR technique and the SARA algorithm result in an improvement of ASR performance in the context of multi-GNSS constellations.

Chapter 2: Literature Review

2.1 Overview of GNSS Systems

A satellite navigation system with global coverage can be termed as Global Navigation Satellite System (GNSS). Within the following decade, the evolution of GNSSs will see more than 100 GNSS satellites in orbits. At this stage, the constellation of Global Positioning System (GPS) consists of 32 satellites although the baseline constellation of onlt 24 satellites is ensured by the US Air Force (US Government's GPS page 2011). Besides GPS, the Russian GLONASS currently has 23 operational satellites, enabling nearly full global coverage in December 2011 (Russian Space Agency Information page 2011). As far as the European Galileo is concerned, the first two Galileo navigation satellites have been into orbit by the end of 2011 (European Space Agency Web 2011). The fully deployed Galileo constellation will consist of 30 satellites. The Chinese Compass/Beidou-2 is also a global satellite navigation system consisting of 35 satellites, which currently have 9 satellites in orbits and will complete the constellation for regional service by 2012 and full constellation for global services around 2020 (Compass navigation system web 2011). In addition to the four global systems, the Quasi-Zenith Satellite System (QZSS) developed by Japan and the Indian Regional Navigation Satellite System (IRNSS) developed by India are also providing navigation services for the regional areas. An overview of these systems configurations and signals are referred to the textbooks like (Misra and Enge 2006; Verhagen 2005a; Kleusberg and Teunissen 1998; Kaplan and Hegarty 2006; Hofmann-Wellenhof et al. 2008; Groves 2008) and relavent Wikipedia pages.

2.1.1 GPS and its modernisation

The world's most utilised satellite navigation system is the Navigation by Satellite Ranging and Timing (NAVSTAR) Global Positioning Systemand usually known simply as GPS. GPS consists of a three-segment architecture: the ground segment, the space segment and the user segment. GPS disseminates a form of Coordinated Universal Time (UTC). The nominal constellation is made up of 24 satellites arranged in 6 orbits with 4 satellites per plane. The system uses the concept of one-

way time of arrival (TOA) ranging or "pseudoranging". The satellites broadcast ranging codes and navigation data on two frequencies called L1 (1.57542 GHz) and L2 (1.22760 GHz) using the code division multiple access (CDMA) technique. Two types of pseudorange codes are modulated on these carriers: coarse/acquisition, C/A, and precision (encrypted), P(Y), codes. From these signals, two services are provided: the standard positioning service (SPS) and the precise positioning service (PPS) (Misra and Enge 2006; Kaplan and Hegarty 2006; Hofmann-Wellenhof et al. 2008; Groves 2008).

Due to the massive civil applications of GPS during the past decades and the new technologies used in the satellites and receivers, on January 25, 1999, the U.S government decided to extend the capabilities of GPS to satisfy the requirements of the civil community. The plans for GPS modernisation to benefit the civil users called for two new civil signals (Hofmann-Wellenhof et al. 2008; Kaplan and Hegarty 2006; Misra and Enge 2006):

- A signal on L2 (a C/A- code signal). The L2C signal is available for non safety-of-life (SoL) applications at the L2 frequency;
- Another signal (defined as L5=1.17645 GHz) to benefit civil aviation and other applications with SoL considerations.

By using the carrier phase of all three signals (L1 C/A, L2C and L5) and differential processing techniques, the ionospheric delay and ambiguity resolution will no longer be a nuisance (Feng 2008; Hatch et al. 2000; Li et al. 2009). For civil and military applications, all key performance elements like accuracy, availability, continuity, integrity and reliability will be improved significantly.

2.1.2 GLONASS and its modernisation

The GLONASS ("GLObalnaya NAvigatsionnaya Sputnikovaya Sistema") is nearly identical to GPS. Like GPS, it was also designed to support the positioning and navigation service for both civil and military applications. The first GLONASS satellite was launched in 1982. The operational space segment of GLONASS consists of 21 satellites in 3 orbital planes, with 3 on-orbit spares. Each satellite operates in circular 19,100 km orbits at an inclination angle of 64.8 degrees and each satellite completes an orbit in approximately 11 hours 15 minutes 44 seconds

(Groves 2008; Hofmann-Wellenhof et al. 2008). GLONASS employs frequency division multiple access (FDMA) technique for the transmission of its navigation signals. GLONASS offers a high-accuracy signal (P-code) for military users and a standard-accuracy signal (C/A-code) for civil users free of charge. For better differentiation from GPS, the GLONASS carrier frequencies are denoted using G instead of L. Hence the three carrier frequencies are allocated as G1 (1.602000 GHz), G2 (1.246000 GHz) and G3 (1.204704 GHz).

In August 2001, a modernisation program was instigated, rebuilding the constellation, introducing new signals, and updating the control segment (Groves 2008). The GLONASS modernisation program is an overall performance improvement initiative. Referring to the satellites, the main issues are the improvement of the satellite clock stability and a better dynamical model, for instance, the attitude determination of the satellite. Referring to the ground infrastructure, the number of monitor stations will be increased adequately. Moreover, the GLONASS reference system (PZ-90) will be refined. In addition, the code division multiple access (CDMA) signal will soon supplement GLONASS's FDMA signal. Lastly, the GLONASS time keeping system will be improved with the use of new system clocks with very high stability and the time synchronisation system will also be improved (Hofmann-Wellenhof et al. 2008).

2.1.1 Galileo and its development

The developing Galileo is made up of 30 satellites divided between three orbital planes inclined at 56 degrees at an altitude around 23, 000 km. The orbital period is 14 hours and 4 minutes, with ground track repeat every ten days (Misra and Enge 2006). The Galileo is designed for a service-oriented approach. These services mainly include: the open service (OS), the commercial service (CS), the safety-of-life (SoL) service, the public regulated service (PRS) and the search and rescue (SAR) service. The carrier frequencies of the Galileo navigation signals include: E1 (1.575420 GHz), E6 (1.278750 GHz), E5 (1.191795 GHz), E5a (1.176450 GHz) and E5b (1.207140 GHz). Different signals support different services, for instance, E1 supports PRS/OS/CS/SoL, E6 supports CS/PRS and E5 supports OS/CS/SoL. The Galileo satellite constellation nominally guarantees a minimum of six visible satellites to every user worldwide with 10° elevation mask angle. The maximum PDOP is less than 3.3 (Hofmann-Wellenhof et al. 2008).

The two experimental satellites officially named Galileo in-orbit validation elements (GIOVE) were launched on December 28 2005 and April 27 2008 respectively. These satellites aim to secure the frequencies allocated to Galileo by the International Telecommunications Union (ITU). After finalisation of the GIOVE satellites, on October 21 2011, the first pair of Galileo satellites were launched into orbit, bringing Europe's long-awaited GNSS program into a new phase (European Commission Enterprise and Industry 2011). Two more satellites will be launched in 2012. The provision of initial satellite navigation services will be provided in 2014 and the full service is expected by 2019.

2.1.3 Compass and its development

The People's Republic of China has started expanding their regional navigation system called Beidou-1 into an independent global satellite navigation system, that is, the Compass system (also known as Beidou-2). The Compass system will be a constellation of 30 medium earth orbit (MEO) satellites and 5 geostationary orbit (GEO) satellites(Compass navigation system 2011). In the early stage, the first two Beidou-1 satellites were placed at 80°E and 140°E longitude on geostationary orbits. The third satellite was placed at 110°E longitude. In the era of Compass, the MEO satellites will have an average satellite altitude of 21, 363 km in 3 orbital planes at 56° inclination. The Compass transponders operate S-band (2483-2500 MHz) and L-band (1610-1626.5 MHz) as communication links and four L-band as navigation links (Kaplan and Hegarty 2006). There are already fourteen Compass satellites in orbit at the time of this writing (Zhang X 2012). The global Compass coverage and operation is expected to be complete by 2020.

Table 2-1 shows a comparison of some of the key features of the four different GNSS systems (Satellite navigation 2011). The longer period of Galileo satellites is caused by the fact that the Galileo satellites fly in a higher orbit, while the higher number of Compass satellites is caused by the fact that there are additional five GEO satellites.

Table 2-1 Comparison of systems

System	GPS	GLONASS	Galileo	Compass
Political entity	United States	Russia	European Union	China
Coding	CDMA	FDMA/CDMA	CDMA	CDMA
Orbital height	20,180 km	19,100 km	23,616 km	21,150 km
Period	12.0 hours	11.3 hours	14.1 hours	12.6 hours
Number of satellites	24	24	30	35
Frequency	1.57542 GHz (L1) 1.22760 GHz (L2) 1.17645 GHz(L5)	1.602000 GHz (G1) 1.246000GHz (G2) 1.204704GHz (G3)	1.575420 GHz (E1) 1.278750 GHz (E6) 1.191795 GHz (E5) 1.176450 GHz (E5a) 1.207140 GHz (E5b)	1.561098 GHz (B1) 1.589742 GHz (B1-2) 1.20714 GHz (B2) 1.26852 GHz (B3)
Status	Operational	Operational	4 satellites operational	14 satellites operational

2.1.4 Other GNSS systems

In addition to the global navigation systems, Japan and India are developing their own regional navigation satellites systems. The Japanese Quasi-Zenith satellite system (QZSS) program was designed to support both mobile communications and GPS augmentation services. To meet the requirements for having satellites operating predominantly over Japan, three satellites are designed to be placed in a periodic highly elliptical orbit (Johannes 2005) with an elevation above 70°. Full operational status of QZSS is expected by 2013 (Japan Aerospace Exploration Agency 2011). The Indian Regional Navigation Satellite System (IRNSS) was approved to provide an autonomous navigation service for the Indian subcontinent in May 2006 (Hofmann-Wellenhof et al. 2008). The IRNSS constellation consists of seven satellites. The fully operation IRNSS is planned to be realised around 2014 (Sagar 2007).

2.1.5 Compatibility and interoperability of GNSS

In this context compatibility refers to the ability of more than one service to be used separately or together without interfering with each individual service or signal. Interoperability, in contrast, refers to the ability for the combined use of GNSSs to improve the performance, for example, accuracy, integrity, availability, continuity and reliability, at user level (Hofmann-Wellenhof et al. 2008). GNSS radio frequency

compatibility has become a focus of great attention for the system providers and user communities. RF compatibility between two signals or systems means that neither degrades the performance of the other in a significant way (Misra and Enge 2006). For instance, although Galileo signals overlay GPS signals in L1 and L5 bands, the impact has been shown to be negligible (Godet et al. 2002).

Meanwhile, the interoperability of systems and signals is guaranteed by an increasing number of agreements between the operators. The goal of GNSS interoperability is beyond the challenges of compatibility. The interoperability in the design of GNSS user hardware should be achieved at first. Receiver equipments need to consider the hardware issues involving the antenna, RF front-end and correlator channels (Hein 2006). Other interoperability issues are encountered in the coordinate reference and time reference systems. Fortunately, the reference system is only an issue for high-precision users, as the differences between these coordinate reference systems are just a few centimetres. Although the differences between GNSS time reference systems are significant, plans to broadcast time conversion data from different satellite constellations are under consideration to meet the requirement of interoperability (Groves 2008).

2.2 GNSS Observables

The most important observations of GNSS signals are pseudorange and carrier phase. The acquisition of pseudorange and carrier phase involves advanced techniques in electronics and digital signal processing. Instead of addressing the issue of code tracking and carrier tracking, this section focuses on dealing with the observation equations that directly apply to the pseudoranges and carrier phases to determine the position. Measurement errors are often categorised into three groups, namely, satellite-related errors, propagation-medium-related errors, and receiver-related errors. An overview of these errors and the corresponding mitigation methods are presented in this section. Last, we describe the differential GNSS (DGNSS) technique to reduce the measurement further for obtaining higher positioning accuracy, which usually includes single-difference (SD), double-difference (DD), and triple-difference (TD) (Hofmann-Wellenhof et al. 2008; Kaplan and Hegarty 2006; Kleusberg and Teunissen 1998; Misra and Enge 2006).

2.2.1 Pseudorange and carrier phase measurements

The pseudorange is the distance from the satellite antenna to the receiver antenna which involves the clock offsets of satellite and receiver as well as other biases. Therefore, the observation equations of the pseudorange and carrier phase measurements, P_i and ϕ_i, for the satellite S, the receiver R, and the carrier signal L can be expressed as

$$P_i = \rho + c(\delta t_S - \delta t_R) + I_i + T + \delta_{orb} + \delta_{mp} + \varepsilon_{Pi} \tag{2.1}$$

$$\phi_i = \rho + c(\delta t_S - \delta t_R) - I_i + T + \delta_{orb} + \delta_{m\phi} - \lambda_i(\varphi_S^0 - \varphi_R^0 + N)_i + \varepsilon_{\phi i} \tag{2.2}$$

with:

ρ	the geometric distance between satellite S and receiver R antennas
c	the speed of radio waves in vacuum, 299,792,458 m/s
δt_S	the satellite clock error of all components in unit of seconds
δt_R	the receiver clock error of all components in unit of seconds
I_i	the ionospheric delay on the frequency *i*
T	the tropospheric delay
δ_{orb}	the satellite orbital error in unit of metres
$\delta_{m\phi}$	the multipath error in carrier phase
δ_{mp}	the multipath error in pseudorange
λ_i	the wavelength of the carrier L_i in metres with frequency f_i in Hz
φ_S^0	the initial phase of the satellite oscillator (cycle), which is satellite-dependent
φ_R^0	the initial phase of the receiver oscillator (cycle), which is receiver-dependent
N_i	the integer ambiguity of the phase measurement in cycles
ε_{Pi}	the receiver code noise in metres
$\varepsilon_{\phi i}$	the receiver phase noise in metres

The geometric distance ρ between the receiver antenna and the satellite antenna is defined as

$$\rho = |X_S - X_R| = \sqrt{(x_S - x_R)^2 + (y_S - y_R)^2 + (z_S - z_R)^2} \tag{2.3}$$

with:

X_S	the position vector of satellite S in a geocentric coordinate system

X_R the position vector of receiver R in the same geocentric coordinate system as X_S

2.2.2 Measurement errors and mitigation

As the basic GNSS measurements described in (2.1) and (2.2) consist of different errors and noise, we will review the error sources and find out how to mitigate them in different approaches. Table 2-2 takes GPS as an example and gives a summary of these errors and their mitigation in differential mode (Misra and Enge 2006).

- Satellite clock errors. The GPS one-way ranging ultimately depends on the satellite clock. These satellite clock errors affect both the code and carrier phase users in the same way. These errors can be reduced with clock corrections message in broadcast ephemeris. The average clock modelling error is small as 2 metres rms.
- Ionosphere errors. The ionosphere starts 50km above the Earth and extends to higher than 1000km. GPS signals are delayed in proportion to the number of free electrons in the ionosphere and are also proportional to the inverse of the carrier frequency squared ($1/f^2$). Thus, the effect is dispersive. The density of free electrons varies significantly with the time of day and the latitude. The variations also depend on the solar cycles and seasons. The effects on the pseudorange and carrier phase are opposite in sign, that is, the delay of the carrier phase is advanced, see Eq. (2.2).

  So, we must correct the pseudorange or carrier to cater for the ionospheric delay. The first and simplest correction refers to the empirical model, for instance, the *Klobuchar* model broadcast by the GPS satellites navigation message (Klobuchar 1996). If we have the dual-frequency receivers, the ionospheric delay on frequency f_1 can be measured as

$$I_1 = \frac{f_2^2}{f_2^2 - f_1^2}(P_1 - P_2) \tag{2.4}$$

  or

$$I_1 = \frac{f_2^2}{f_2^2 - f_1^2}\left((\lambda_1 N_1 - \lambda_2 N_2) - (\phi_1 - \phi_2)\right) \tag{2.5}$$

- Troposphere errors. The troposphere is the lower part of the atmosphere. The tropospheric delay depends on the temperature, pressure and humidity. Both

the code and carrier will have the same delay. In the zenith direction, the total tropospheric delay is estimated to about 2.3 metres which consists of the hydrostatic component (responsible for 90%) and the wet component. For most users and circumstances, a simple model should be effective, one that is accurate to about 1 metre. Two famous tropospheric models include the Saastamoinen model and the Hopfield model (Hopfield 1969; Saastamoinen 1973).

- Orbit errors. These are also called ephemeris errors. Although the broadcast navigation messages transmit the satellites coordinates as their Keplerian elements, there are still with small errors. The rms ranging error attributable to ephemeris is about 2.1 metres (Parkinson 1996). Fortunately, the accuracy of the International GNSS Service (IGS) orbits can reach about 15 mm (1D global average) for each daily arc which brings great benefits to those high precision users (Griffiths and Ray 2009).
- Multipath errors. Multipath errors are caused by reflected signals entering the front end of the receiver and masking the real correlation peak. Due to the interference effect, the GPS signals can create a range error of several metres or more. Multipath error is a serious problem because of the difficulty of modelling. Hence, it is necessary to mitigate these errors by carefully sitting the site for receivers and choosing proper antennas. Generally, the impact to a moving user should be less than 1 metre under most circumstances with proper sitting and antenna selection.

Except for the above mitigation method, the most powerful method to eliminate or reduce these errors is the DGNSS technique. It is noted that the multipath errors cannot be mitigated by the DGNSS method. The mathematical model will be discussed in the next section. Table 2-2 gives a summary of these errors and their mitigation in DGPS mode for tens of kilometres baseline (Misra and Enge 2006).

Table 2-2 A summary of GPS measurement errors and errors mitigation

Source	Potential error size	Error mitigation
Satellite clock model	Clock modeling error: 2 m (rms)	DGPS: 0.0 m
Satellite ephemeris prediction	Component of the ephemeris prediction error along the line of sight: 2 m (rms)	DGPS: 0.1 m (rms)
Ionospheric delay	The code is delayed while the carrier is advanced by the same amount Delay in zenith direction: 2~10 m	Single-frequency receiver using broadcast model: 1-5 m Dual frequency receiver (compensates for the ionospheric delay but magnifies noise): 1 m (rms) DGPS: 0.2 m (rms)
Tropospheric delay	Code and carrier are both delayed by the same amount Delay in zenith direction at sea level ~ 2.3-2.5 m; lower at higher altitudes	Models based on average meteorological conditions: 0.1-1 m DGPS: 0.2 m (rms) plus altitude effect
Multipath error	In a normal circumstance: Code: 0.5-1 m Carrier: 0.5-1cm	Uncorrelated between reference and user receivers Mitigation through antenna design and siting a clean site

2.2.3 Phase differences

Differential positioning with GNSS, abbreviated by DGNSS, is a real-time positioning technique. DGNSS with phases is usually called real-time kinematic (RTK) technique. The basic concept of DGNSS is that most measurement errors, such as atmosphere errors, have strong spatial and time correlation, thus, we can mitigate these errors through differential operators. In general, there is a single-difference between receivers, double-difference between satellites, and triple-difference between epochs (Hofmann-Wellenhof et al. 2008). The principle of DGNSS with carrier phase is almost the same as DGNSS with pseudorange except including ambiguity items; therefore, we just show the basic mathematical modelling of phase differences.

Single-difference

Two receivers A, B and one satellite *j* are involved. Using Eq. (2.2), the carrier phase observation equations for receiver A and B are

$$\phi_A^j = \rho_A^j + c(\delta t_{S,j} - \delta t_{R,A}) - I_A^j + T_A^j + \delta_{A,orb}^j + \delta_{A,m\phi}^j - \lambda(\varphi_A^j + N_A^j) + \varepsilon_{A.\phi} \tag{2.6}$$

$$\phi_B^j = \rho_B^j + c(\delta t_{S,j} - \delta t_{R,B}) - I_B^j + T_B^j + \delta_{B,orb}^j + \delta_{B,m\phi}^j - \lambda(\varphi_B^j + N_B^j) + \varepsilon_{B,\phi} \tag{2.7}$$

and the difference of Eq. (2.6) and (2.7), we have

$$\phi_{AB}^j = \rho_{AB}^j - c(\delta t_{R,AB}) - I_{AB}^j + T_{AB}^j + \delta_{AB,orb}^j + \delta_{AB,m\phi}^j - \lambda(\varphi_{AB}^j + N_{AB}^j) + \varepsilon_{AB,\phi} \tag{2.8}$$

where

$$\begin{aligned}
\phi_{AB}^j &= \phi_B^j - \phi_A^j \\
\rho_{AB}^j &= \rho_B^j - \rho_A^j \\
\delta t_{R,AB} &= \delta t_{R,B} - \delta t_{R,A} \\
I_{AB}^j &= I_B^j - I_A^j \\
T_{AB}^j &= T_B^j - T_A^j \\
\delta_{AB,orb}^j &= \delta_{B,orb}^j - \delta_{A,orb}^j \\
\delta_{AB,m\phi}^j &= \delta_{B,m\phi}^j - \delta_{A,m\phi}^j \\
\varphi_{AB}^j &= \varphi_B^j - \varphi_A^j \\
N_{AB}^j &= N_B^j - N_A^j \\
\varepsilon_{AB,\phi} &= \varepsilon_{A,\phi} + \varepsilon_{B,\phi}
\end{aligned}$$

Note that the satellite clock bias $\delta t_{S,j}$ has cancelled, and the values of I_{AB}^j, T_{AB}^j, and $\delta_{AB,orb}^j$ would be very small, if the baseline is sufficiently short. In addition, we usually include residual $\delta_{AB,m\phi}^j$ in the error term $\varepsilon_{AB,\phi}$. Hence, Eq. (2.8) can be simplified as

$$\phi_{AB}^j = \rho_{AB}^j - c(\delta t_{R,AB}) - \lambda(\varphi_{AB}^j + N_{AB}^j) + \varepsilon_{AB,\phi}^j \tag{2.9}$$

Double-difference

A popular procedure for processing GNSS observations uses double-difference. Assuming two receivers A, B and two satellites *j*, *k* , we have two single-difference equations according to Eq. (2.9)

$$\phi_{AB}^{j} = \rho_{AB}^{j} - c(\delta t_{R,AB}) - \lambda(\varphi_{AB}^{j} + N_{AB}^{j}) + \varepsilon_{AB,\phi}^{j} \tag{2.10}$$

$$\phi_{AB}^{k} = \rho_{AB}^{k} - c(\delta t_{R,AB}) - \lambda(\varphi_{AB}^{k} + N_{AB}^{k}) + \varepsilon_{AB,\phi}^{k} \tag{2.11}$$

and the difference of Eq. (2.10) and (2.11), we have

$$\phi_{AB}^{jk} = \rho_{AB}^{jk} - \lambda(\varphi_{AB}^{jk} + N_{AB}^{jk}) + \varepsilon_{AB,\phi}^{jk} \tag{2.12}$$

where

$$\begin{aligned}
\phi_{AB}^{jk} &= \phi_{AB}^{k} - \phi_{AB}^{j} \\
\rho_{AB}^{jk} &= \rho_{AB}^{k} - \rho_{AB}^{j} \\
\varphi_{AB}^{jk} &= \varphi_{AB}^{k} - \varphi_{AB}^{j} \\
N_{AB}^{jk} &= N_{AB}^{k} - N_{AB}^{j} \\
\varepsilon_{AB,\phi}^{jk} &= \varepsilon_{AB,\phi}^{j} + \varepsilon_{AB,\phi}^{k}
\end{aligned}$$

Note that the receiver clock error $\delta t_{R,AB}$ has cancelled this time. The double-difference ambiguities thus can be parameterised as integers due to the absence of satellite and receiver clock errors. This advantage is important for those high-precision applications. It is necessary to emphasise that here we assume the wavelengths in Eq. (2.10) and (2.11) are the same; however, if the frequencies or wavelengths of Eq. (2.10) and (2.11) are different, for instance, for GLONASS carriers, the case is different. For more details on this subject, refer to the work of Wang (2000).

Triple-difference

When two epochs t_1 and t_2 are considered, according to Eq. (2.12) we have equations as

$$\phi_{AB}^{jk}(t_1) = \rho_{AB}^{jk}(t_1) - \lambda(\varphi_{AB}^{jk}(t_1) + N_{AB}^{jk}) + \varepsilon_{AB,\phi}^{jk}(t_1) \tag{2.13}$$

$$\phi_{AB}^{jk}(t_2) = \rho_{AB}^{jk}(t_2) - \lambda(\varphi_{AB}^{jk}(t_2) + N_{AB}^{jk}) + \varepsilon_{AB,\phi}^{jk}(t_2) \tag{2.14}$$

and the difference of Eq. (2.13) and (2.14), we have

$$\phi_{AB}^{jk}(t_{12}) = \rho_{AB}^{jk}(t_{12}) - \lambda\varphi_{AB}^{jk}(t_{12}) + \varepsilon_{AB,\phi}^{jk}(t_{12}) \tag{2.15}$$

where

$$\begin{aligned}
\phi_{AB}^{jk}(t_{12}) &= \phi_{AB}^{jk}(t_2) - \phi_{AB}^{jk}(t_1) \\
\rho_{AB}^{jk}(t_{12}) &= \rho_{AB}^{jk}(t_2) - \rho_{AB}^{jk}(t_1) \\
\varphi_{AB}^{jk}(t_{12}) &= \varphi_{AB}^{jk}(t_2) - \varphi_{AB}^{jk}(t_1) \\
\varepsilon_{AB,\phi}^{jk}(t_{12}) &= \varepsilon_{AB,\phi}^{jk}(t_1) + \varepsilon_{AB,\phi}^{jk}(t_2)
\end{aligned}$$

The advantage of triple-difference is the cancelling effect for the ambiguities, which eliminates the need to determine them. A triple-difference actually expresses a change in phase of the GNSS satellites, the main function of which is to detect and repair cycle slips.

2.3 Integer Ambiguity Estimation Methods

The prerequisite of the precise positioning and navigation with GNSS is to fix the ambiguities correctly. The purpose of AR is to determine the unknown integer cycles in carrier phase measurements, leading to recover the millimetre precision of ranging measurements between a satellite and a receiver (Li and Shen 2010). The pull-in regions define the integer estimator completely; therefore, one can define classes of integer estimators by imposing different conditions on the pull-in regions. The three best known integer estimators are integer rounding, integer bootstrapping and integer least-squares (Teunissen 1994).

2.3.1 Fundamental mathematic model

The GNSS double-difference (DD) linear observation equations are generally expressed as

$$\mathbf{L}=\mathbf{A}\mathbf{x}+\mathbf{B}\mathbf{N}+\mathbf{e} \tag{2.16}$$

and the criterion of least-squares solutions of Eq. (2.16) is given as

$$\min_{\mathbf{x},\mathbf{N}} \left\{ \left\| \mathbf{L} - \mathbf{A}\mathbf{x} - \mathbf{B}\mathbf{N} \right\|_{\mathbf{Q}_L}^2 , \mathbf{x} \in R^n, \mathbf{N} \in Z^k \right\} \tag{2.17}$$

where **L** is the *m*-vector of 'observed minus computed' DD observations; **A** is the $m \times n$ design matrix for the vector of real-valued unknowns $\mathbf{x}$; **B** is the $m \times k$ design matrix for the vector of integer DD ambiguities **N**; $\mathbf{Q}_{\mathbf{L}}$ is the vc-matrix of observables; **e** is the vector of unmodelled effects and measurement noise and $\|\cdot\|^2_{\mathbf{Q}_L} = (\cdot)^T \mathbf{Q}_L^{-1}(\cdot)$. The solution of the problem (2.17) is equivalent to the solution of the ILS problem

$$\breve{\mathbf{N}} = \min\left\{ \left\| \hat{\mathbf{N}} - \mathbf{N} \right\|^2_{\mathbf{Q}_{\hat{\mathbf{N}}}}, \mathbf{N} \in Z^k \right\} \tag{2.18}$$

where $\hat{\mathbf{N}}$ is a float ambiguity vector with the vc-matrix $\mathbf{Q}_{\hat{\mathbf{N}}}$ and $\breve{\mathbf{N}}$ is the estimated integer ambiguity vector. In general, $\mathbf{Q}_{\hat{\mathbf{N}}}$ has high correlation due to the DD geometry and correlation between measurements errors, which makes the search progress inefficient. Decorrelation or reduction techniques have been developed and applied in order to reduce the elongation and size of the search space, referring to Teunissen (1993 and 1994). The essence of decorrelation is to apply an admissible integer unimodular matrix **Z** to eliminate or reduce the size of the off-diagonal elements of $\mathbf{Q}_{\hat{\mathbf{N}}}$. This can be expressed as

$$\hat{\mathbf{N}}_{\mathbf{dec}} = \mathbf{Z}\hat{\mathbf{N}},\ \mathbf{N}_{\mathbf{dec}} = \mathbf{Z}\mathbf{N},\ \mathbf{Q}_{\hat{\mathbf{N}}_{\mathbf{dec}}} = \mathbf{Z}\mathbf{Q}_{\hat{\mathbf{N}}}\mathbf{Z}^{\mathbf{T}} \tag{2.19}$$

Therefore the ILS problem (2.18) is transformed as

$$\breve{\mathbf{N}}_{\mathrm{dec}} = \min\left\{ \left\| \hat{\mathbf{N}}_{\mathrm{dec}} - \mathbf{N}_{\mathrm{dec}} \right\|^2_{\mathbf{Q}_{\hat{\mathbf{N}}_{\mathrm{dec}}}}, \mathbf{N}_{\mathrm{dec}} \in Z^k \right\} \tag{2.20}$$

Due to the integer constraint $\mathbf{N}_{\mathrm{dec}} \in Z^k$, the solution $\breve{\mathbf{N}}_{\mathrm{dec}}$ of (2.20) must be obtained by virtue of a search process. Once we get $\breve{\mathbf{N}}_{\mathrm{dec}}$, $\breve{\mathbf{N}}$ can be easily obtained by $\mathbf{N} = \mathbf{Z}^{-1}\mathbf{N}_{\mathbf{dec}}$. In the last step, the remaining real-valued parameters $\hat{\mathbf{x}}$ can be updated due to the correlation with the ambiguities as

$$\breve{\mathbf{x}} = \hat{\mathbf{x}} - \mathbf{Q}_{\hat{\mathbf{x}}\hat{\mathbf{N}}}\mathbf{Q}_{\hat{\mathbf{N}}}^{-1}(\hat{\mathbf{N}} - \breve{\mathbf{N}}) \tag{2.21}$$

and

$$\mathbf{Q}_{\breve{\mathbf{x}}} = \underbrace{\mathbf{Q}_{\hat{\mathbf{x}}} - \mathbf{Q}_{\hat{\mathbf{x}}\hat{\mathbf{N}}}\mathbf{Q}_{\hat{\mathbf{N}}}^{-1}\mathbf{Q}_{\hat{\mathbf{N}}\hat{\mathbf{x}}}}_{1} + \underbrace{\mathbf{Q}_{\hat{\mathbf{x}}\hat{\mathbf{N}}}\mathbf{Q}_{\hat{\mathbf{N}}}^{-1}\mathbf{Q}_{\breve{\mathbf{N}}}\mathbf{Q}_{\hat{\mathbf{N}}}^{-1}\mathbf{Q}_{\hat{\mathbf{N}}\hat{\mathbf{x}}}}_{2} \tag{2.22}$$

Only when $\mathbf{Q}_{\breve{\mathbf{N}}}$ is very close to 0 can the integer ambiguities be considered deterministic which can guarantee the precision of the fixed solution better than the float solution because the second term of Eq. (2.22) can be omitted in this case. Hence it is critical to have measures to decide whether the integer ambiguities can be assumed deterministic (Verhagen 2005).

There are many methods to compute a float ambiguity vector $\hat{\mathbf{N}}$ to its integer ambiguity vector $\breve{\mathbf{N}}$. The integer estimator should be admissible, which is defined as (Teunissen 1999b)

1. $\bigcup_{N \in Z^k} S_N = R^k$

2. $S_{N_1} \bigcap S_{N_2} = \Theta, \ \forall N_1, N_2 \in Z^k, N_1 \neq N_2$

3. $S_N = N + S_0, \ \forall N \in Z^k$

where S_N is the pull-in region of the float ambiguity N with S_0 being the origin pull-in region . It is the region where all float solutions are mapped to the same fixed integer vector N (Jonkman 1998). The first property makes there is no gap covering the *k*-dimensional space. The second property is required to gurantte that the probability of $\hat{\mathbf{N}}$ lying on the boundary is zero. The last property states that when the float solution is moved by an integer, the corresponding integer solution is also moved by the same integer. Therefore, we can only work with the fractional parts of the float solution to avoid large numbers (Teunissen 1999b). All the following three estimators including integer rounding, interger bootstrapping and integer least-squares belong to this class estimator.

2.3.2 Integer rounding

The simplest way to obtain an integer ambiguities vector from the real-valued float solution is to apply a componentwise rounding scheme to the entries of $\hat{\mathbf{N}}$. This method may be used to set the size of the search space, but it can also be used as an integer estimator in its own right. It will not be an optimal estimator, but for

particular applications it may still perform well (Teunissen 1994), such as network based ambiguity resolution for RTK services and advanced GPS analysis software systems like GAMIT and Bernese. The corresponding integer estimator reads as

$$\breve{\mathbf{N}}_{\mathrm{R}} = \left(\left[\hat{\mathbf{N}}_1 \right], ..., \left[\hat{\mathbf{N}}_n \right] \right)^T \tag{2.23}$$

where '[ ]' denotes rounding to the nearest integer. The pull-in region of inter rounding is given as

$$S_{\text{rounding}} = \left\{ \mathrm{x} \in \mathrm{R}^{\mathrm{n}} \left| \left| \mathrm{c}_{\mathrm{i}}^{\mathrm{T}} (\mathrm{x}\text{-}\mathrm{z}) \right| \le 0.5, i = 1, ..., n \right. \right\}, \forall \mathrm{z} \in \mathrm{Z}^{\mathrm{n}} \tag{2.24}$$

where c_i denotes the *i*th canonical unit vector having a 1 as its *i*th entry and zeros otherwise.

2.3.3 Integer bootstrapping

Integer bootstrapping is another relatively simple integer ambiguity estimator(Blewitt 1989). This estimator can be regarded as an advanced integer rounding estimator, except that it takes some of the correlation between the ambiguities into account. In essence, integer bootstrapping follows from a sequential conditional LS adjustment (Teunissen 1994). The process of integer bootstrapping is given as follows. If *n* ambiguities are available, we start rounding the first ambiguity to the nearest integer. Then the remaining *n*-1 float ambiguities are corrected by virtue of their correlation with the first ambiguity. After fixing the first ambiguity, we start rounding the second float ambiguity with being already corrected to its nearest integer. Having obtained the second integer ambiguity, then the remaining *n*-2 ambiguities are corrected again by utilising the correlation with the second ambiguity. The process is continued until the *n*-1th ambiguity correlation is considered. The components of the integer ambiguity elements so obtained thus read

$$\begin{aligned}
&\left[\hat{N}_1 \right] = \left[\hat{N}_1 \right] \\
&\left[\hat{N}_{2|1} \right] = \left[\hat{N}_2 - \sigma_{\hat{N}_2 \hat{N}_1} \sigma_{\hat{N}_1}^{-2} \left(\hat{N}_1 - \left[\hat{N}_1 \right] \right) \right] \\
&\vdots \\
&\left[\hat{N}_{n|M} \right] = \left[\hat{N}_n - \Sigma_{i=1}^{n-1} \sigma_{\hat{N}_n \hat{N}_{i|I}} \sigma_{\hat{N}_{i|I}}^{-2} \left(\hat{N}_{i|I} - \left[\hat{N}_{i|I} \right] \right) \right]
\end{aligned} \tag{2.25}$$

where the symbol $\hat{N}_{i|I}$ stands for the *i*th LS ambiguity obtained through a conditioning on the previous $I=\{1,...,(i-1)\}$ sequentially rounded ambiguities and $\sigma_{\hat{N}_n\hat{N}_{i|I}}$ denotes the covariance between $\hat{N}_n$ and $\hat{N}_{i|I}$. Therefore, the integer bootstrapped solution is given as

$$\breve{\mathbf{N}}_{\mathrm{B}}=\left(\left[\hat{\mathbf{N}}_1\right],...,\left[\hat{\mathbf{N}}_{n|M}\right]\right)^T \tag{2.26}$$

The bootstrapped estimator is admissible. Note that integer rounding and integer bootstrapping are actually identical when the vc-matrix is diagonal. The float sequential conditional LS solution can be obtained by virtue of the triangular decomposition of the ambiguity vc-matrix, for instance, we have $\mathbf{Q}_{\hat{\mathbf{N}}}=LDL^T$, with a unit lower triangular matrix L and a diagonal matrix D. Hence, the pull-in region of integer bootstrapping is given as

$$S_{\text{bootstrapping}}=\left\{\mathrm{x}\in\mathrm{R}^{\mathrm{n}}\left|\left|\mathrm{c}_{\mathrm{i}}^{\mathrm{T}}\mathrm{L}^{-1}(\mathrm{x}\text{-}\mathrm{z})\right|\le 0.5, i=1,...,n\right.\right\}, \forall z\in \mathrm{Z}^{\mathrm{n}} \tag{2.27}$$

2.3.4 Integer least-squares

The optimal integer estimator in the Gaussian case is the integer least-squares (ILS) estimator. The optimality criterion used is that of maximising the probability of correct integer estimation, the so-called ambiguity success rate (ASR) (Teunissen 2003a). The ILS estimator minimises the weighted squared norm of the ambiguity residual over all integers which is defined as

$$\breve{\mathbf{N}}_{\mathrm{ILS}}=\arg\ \min_{z\in Z^n}\left\|\hat{\mathbf{N}}-\mathbf{z}\right\|^2_{\mathbf{Q}_{\hat{\mathbf{N}}}} \tag{2.28}$$

where $\|\cdot\|^2_{Q_{\hat{N}}}=(\cdot)^T\mathbf{Q}_{\hat{\mathbf{N}}}^{-1}(\cdot)$. This estimator was firstly introduced by Teunissen (1993). In contrast to the other two estimators mentioned previously, the ILS procedure requires a search process. The ambiguity search space is defined as

$$\Omega_{\mathrm{N}}=\left\{\mathbf{N}\in\mathbf{Z}^{\mathrm{n}}\left|(\hat{\mathbf{N}}-\mathbf{N})^{\mathrm{T}}\mathbf{Q}_{\hat{\mathbf{N}}}^{-1}(\hat{\mathbf{N}}-\mathbf{N})\le\chi^2\right.\right\} \tag{2.29}$$

with χ^2 the chosen positive constant. The search space (ellipsoidal region) is centred at the float ambiguity solution $\hat{\mathbf{N}}$, while the shape and orientation are governed by the corresponding vc-matrix $\mathbf{Q}_{\hat{\mathrm{N}}}$; its size can be controlled by the constant χ^2 (Teunissen et al. 1996). In order to search efficiently, one needs to make the vc-matrix as close as possible to a diagonal matrix and the search space size must not contain too many integer candidates. Therefore, the decorrelation technique (discussed in the next section) and close approximation of the search space size is necessary. The ILS pull-in region is constructed from intersecting half-spaces. It is a convex, symmetric set of volume 1, which also satisfies the conditions of admissible. The representation of the ILS pull-in region is given as

$$S_{\mathrm{ILS}}=\left\{\mathrm{x}\in\mathrm{R}^{\mathrm{n}}\left|\left|\mathrm{c}_{\mathrm{i}}^{\mathrm{T}}\mathrm{Q}_{\hat{\mathrm{N}}}^{-1}(\mathrm{x}\text{-}\mathrm{z})\right|\le 0.5\left\|\mathrm{c}_{\mathrm{i}}\right\|_{\mathrm{Q}_{\hat{\mathrm{N}}}}^{2},i=1,...,n\right.\right\},\forall z\in\mathrm{Z}^{\mathrm{n}} \tag{2.30}$$

2.3.5 Other ambiguity resolution methods

During the past two decades, various ILS methods for AR have been developed. These include the fast ambiguity resolution approach (FARA) (Frei and Beutler 1990), the least squares ambiguity search technique (LSAST) (Hatch 1990), the fast ambiguity search filter (FASF) (Chen and Lachapelle 1995) and the optimal method for estimating GPS ambiguities (OMEGA) (Kim and Langley 1999). Besides these efforts, the least-squares ambiguity decorrelation adjustment (LAMBDA) method (Teunissen 1993) is both theoretically and practically at the top level among the ambiguity determination methods (Hofmann-Wellenhof et al. 2008). The three carrier ambiguity resolution (TCAR) method was proposed for the purpose of resolving a three-frequency envisioned Galileo system (Vollath et al. 1999). Later, a similar approach to TCAR was also proposed and called cascading integer resolution (CIR) method in Jung *et al*. (2000) (Hatch et al. 2000; Jung et al. 2000). Another trend of AR method is to make use of some constraints for improving the computational efficiency. The ambiguity resolution using a constraint equation algorithm proposed by Park *et al.* (1996) uses the constraint equations in searching integer ambiguities (Park *et al.* 1996). Peter *et al.* (2009) developed a multiplatform instantaneous GNSS ambiguity resolution method for triple- and quadruple-antenna configurations with constraints. Li and Shen (2010) proposed a new method using the constraints conveniently derived from the normal equations which are primarily

obtained in accordance with the float solution. In their algorithm, only three independent ambiguities are needed to be searched (Li and Shen 2010).

The ambiguity validation procedure is used to determine the integer solution uniquely and reliably. For ambiguity validation purposes, a discrimination test is required to decide whether a set of integers is acceptable as the correct solution. The test methods may refer to the difference-test (Tiberius and Jonge 1995), the projector-test (Han 1997b), the W ratio-test (Wang et al. 1998) and the ratio-test (Euler and Schaffrin 1990; Teunissen and Verhagen 2009). Recent approaches called integer aperture (IA) estimators have been proposed with the combination of ambiguity estimation and validation. Two typical IA estimators are referred to as the penalised integer aperture estimator and the ellipsoidal integer aperture (EIA) estimator (Teunissen 2004, 2005). The most promising advantage of IA is that the fail-rate of ambiguity fixing is controllable.

2.4 Decorrelation Methods

Generally, the integer ambiguity search space is highly elongated. In order to make the search process more efficient, different decorrelation techniques have been developed. The essence of decorrelation is to apply an admissible integer unimodular matrix $\mathbf{Z}$ to eliminate the off-diagonal elements of $\mathbf{Q}_{\hat{N}}$ or reduce the size of the correlation coefficients. The LAMBDA method is based on the integer Gaussian decorrelation (Teunissen et al. 1995; Teunissen et al. 1997). A detailed description of this method is given by de Jonge and Tiberius (1996). Another algorithm named Lenstra–Lenstra–Lovász (LLL) was originally developed for lattice basis reduction, which can also be used to reduce the condition number of the matrix. This algorithm was suggested for the decorrelation of the integer ambiguities by Hassibi and Boyd (1998) and Grafarend (2000). Based on a modified LLL algorithm, Chang and Zhou (2007) developed a Matlab package for solving MILES problems and demonstrated higher computation efficiency than that achieved by the LAMBDA method (Chang and Zhou 2007). Xu (2001) also proposed an inverse integer Cholesky decorrelation method and demonstrated that this method outperformed LAMBDA and LLL methods.

2.4.1 Integer Gaussian transformation

Integer Gaussian decorrelation is actually performed as a sequence of integer Gaussian eliminations and permutations. Assuming there exist three elements q_{ii}, q_{jj} and q_{ij} of $\mathbf{Q}_{\hat{\mathbf{N}}}$ that satisfy $\left|q_{ij}\right| / \min(q_{ii}, q_{jj}) > 1/2$, then the unimodular matrix can be constructed as

$$\mathbf{Z_1} = \begin{bmatrix} 1 & & & & & & \\ & \ddots & & & & & \\ & & 1 & & & & \\ & & \vdots & \ddots & & & \\ & & -\left[q_{ij}/q_{ii}\right] & \cdots & 1 & & \\ & & & & & \ddots & \\ & & & & & & 1 \end{bmatrix} \tag{2.31}$$

if $q_{ii} \le q_{jj}$,or

$$\mathbf{Z_1} = \begin{bmatrix} 1 & & & & & & \\ & \ddots & & & & & \\ & & 1 & \cdots & -\left[q_{ij}/q_{jj}\right] & & \\ & & & \ddots & \vdots & & \\ & & & & 1 & & \\ & & & & & \ddots & \\ & & & & & & 1 \end{bmatrix} \tag{2.32}$$

if $q_{ii} > q_{jj}$. Here the operator [ ] denotes rounding to the nearest integer. Repeating the above steps, the final Z transformation matrix can be expressed as

$$\mathbf{Z=Z_n \cdots Z_2 Z_1} \tag{2.33}$$

2.4.2 Lenstra–Lenstra–Lovász (LLL) algorithm

The LLL algorithm was first introduced for decorrelation in GPS ambiguity resolution by Hassibi and Boyd (1998), followed with the contributions by Grafarend (2000), Xu (2001) and Chang (2007). The original LLL algorithm uses the integer Gram-Schmidt orthogonalisation process, however the Givens reflection based LLL algorithm can be numerically more robust performed in floating-point arithmetic

(Luk and Tracy 2008). Since the matrix $\mathbf{Q}_{\hat{\mathbf{N}}}$ is positive and definite, it can always be factorised as $\mathbf{Q}_{\hat{\mathbf{N}}} = \mathbf{V}^{\mathbf{T}}\mathbf{V}$. To compute the reduced or almost orthogonal basis $\mathbf{V_0}$, so that $\mathbf{V_0} = \mathbf{V}\mathbf{Z}^{-1}$, where $\mathbf{Z}$ is unimodular. After these steps, we have

$$\mathbf{Q}_{\hat{\mathbf{N}}} = \mathbf{V}^T\mathbf{V} = (\mathbf{V_0}\mathbf{Z})^T\mathbf{V}\mathbf{Z} = \mathbf{Z}^T\mathbf{V}_0^T\mathbf{V_0}\mathbf{Z} \tag{2.34}$$

Due to $\mathbf{V_0}$ being almost orthogonal, the target of decorrelation can be achieved with $\mathbf{Q}_{\hat{\mathbf{N}}\mathbf{dec}} = \mathbf{V}_0^T\mathbf{V_0}$.

2.4.3 Inverse integer Cholesky decorrelation method

The inverse integer Cholesky decorrelation (IICD) method applies the $\mathbf{LDL}^T$ factorisation as follows:

$$\mathbf{Q}_{\hat{\mathbf{N}}} = \mathbf{LDL}^T \tag{2.35}$$

where $\mathbf{L}$ is a unit lower triangular matrix, and $\mathbf{D}$ is a diagonal matrix with positive elements. Although $\mathbf{L}$ cannot be directly used for ambiguity decorrelation due to the real-valued elements, [$\mathbf{L}$] is obviously unimodular as well as [$\mathbf{L}^{-1}$]. Thus, we set $\mathbf{Z}_1 = \left[\mathbf{L}^{-1}\right]$ and can compute the decorrelated matrix as

$$\mathbf{H}_1 = \mathbf{Z}_1\mathbf{Q}_{\hat{\mathbf{N}}}\mathbf{Z}_1^T \tag{2.36}$$

Since in most cases $\mathbf{Z}_1$ is not equivalent to $\mathbf{L}$, $\mathbf{H}_1$ is no longer diagonal. Repeating the process

$$\mathbf{H}_n = \mathbf{Z}_n\mathbf{H}_{n-1}\mathbf{Z}_n^T \tag{2.37}$$

until the condition number of $\mathbf{H}_\mathrm{n}$ reaches the predetermined value, the final decorrelation can be expressed as

$$\mathbf{Q}_{\hat{\mathbf{N}}\mathbf{dec}} = (\mathbf{Z}_n \cdots \mathbf{Z}_2\mathbf{Z}_1)^T\mathbf{Q}_{\hat{\mathbf{N}}}(\mathbf{Z}_n \cdots \mathbf{Z}_2\mathbf{Z}_1) \tag{2.38}$$

To obtain larger off-diagonal elements of $\mathbf{L}$, we may rearrange the diagonal elements of $\mathbf{Q}_{\hat{\mathbf{N}}}$ and $\mathbf{H}_i$ in ascending order. Before finishing this section, we would like to make some arguments on this method. Firstly, what should be the predetermined

condition number for the decorrelated matrix? The answer is not easy to say, because it relates to the dimension and formation of the original matrix. Secondly, since this method involves an iterative process, sorting and stopping criteria would be very important for the IICD method. Simply comparing the condition numbers of $\mathbf{H}_n$ and $\mathbf{H}_{n-1}$ can lead to wrong decisions being made, because it is likely that the condition numbers of $\mathbf{H}_n$ and $\mathbf{H}_{n-1}$ are not in strictly descending order.

2.4.4 Measure of decorrelation performance

In order to evaluate the performance of the decorrelation process, the decorrelation number was introduced as a measure of the diagonality of the transformed matrix (Teunissen 1993, 1994). The decorrelation number equals one when the matrix is completely decorrelated, and it is close to zero when poorly decorrelated. Many other researchers use the condition number as the index to measure the correlation and to compare different decorrelation techniques (Liu et al. 1999; Xu 2001; Svendsen 2006; Wang et al. 2010a; Zhou 2010). A better decorrelation technique is expected to achieve a smaller condition number. The concept of the orthogonality defect is to evaluate the quality of reduced lattice vectors for a reduction process (Eisenbrand 2010; Xu 2011). Since the lattice theory can be applied to solve an ILS problem, it is natural to consider utilising this parameter to evaluate the performance of the decorrelation. As a result, the concept of the orthogonality defect is introduced as a possible index to analyse the decorrelation process.

Decorrelation Number

In two dimensions, the decorrelation number is defined as $\gamma = \sqrt{1-\rho^2}$, with ρ being the correlation coefficient between two ambiguities. Given the dimensions of a positive definite matrix **H** greater than two, the decorrelation number is defined as (Teunissen 1993, 1994),

$$\gamma(\mathbf{H}) = \sqrt{\det(R_H)} \qquad (0 \le \gamma(\mathbf{H}) \le 1) \tag{2.39}$$

where R_H is the correlation matrix of **H**. The decorrelation number equals one when the matrix is completely decorrelated, and it is close to zero when poorly decorrelated.

Condition Number

Given **H**, the condition number $\kappa(\mathbf{H})$ is the ratio between the maximum and minimum eigenvalues of **H** as,

$$\kappa(\mathbf{H}) = \left| \frac{\lambda_{\max}(\mathbf{H})}{\lambda_{\min}(\mathbf{H})} \right| \tag{2.40}$$

Orthogonality Defect

In order to quantitatively measure the orthogonality of a matrix, we can use the orthogonality defect $\delta(\mathbf{H})$ as a metric (Eisenbrand 2010) ,

$$\delta(\mathbf{H}) = \frac{\Pi_{k=1}^{N} \|\mathbf{h}_k\|}{|\det(\mathbf{H})|} \tag{2.41}$$

with $\delta(\mathbf{H}) \geq 1$ for all H and $\delta(\mathbf{H}) = 1$ if and only if the columns of **H** are orthogonal, where $\mathbf{h}_k$ is the basis vector.

2.5 Reliability Theory

The reliability criteria are referred to as the parameters to be used in the selection of satellites to achieve reliable ambiguity solutions in processing GNSS carrier phase measurements. The criteria include concepts of internal and external reliability from the traditional real-value least-squares estimation and the concepts of the ADOP and the ASR that is directly related to the ILS solutions' reliability. This section will introduce the internal and external reliability concept first, followed by the ADOP and success rate computations and numerical analysis regarding the reliability criteria.

2.5.1 Internal reliability and external reliability

A linearised Gauss-Markov model is defined by

$$\mathbf{y} = \mathbf{A}\mathbf{x} + \mathbf{e}, \quad \mathbf{e} \sim \left(0, \sigma_0^2 \mathbf{Q}\right) \tag{2.42}$$

where **y** is the observation vector, **x** is the unknown parameter vector, **e** is the random error vector, σ_0^2 is the variance of the unit-weight measurements and **Q** is the cofactor matrix. We have the weight matrix $\mathbf{P} = \mathbf{Q}^{-1}$. The redundancy number r_i is given as

$$r_i = (\mathbf{Q}_{vv}\mathbf{P})_{ii} \tag{2.43}$$

with a normal equation matrix

$$\mathbf{N} = \mathbf{A}^T\mathbf{P}\mathbf{A} \tag{2.44}$$

and a cofactor matrix for residuals

$$\mathbf{Q}_{vv} = \mathbf{Q} - \mathbf{A}\mathbf{N}^{-1}\mathbf{A}^T \tag{2.45}$$

The internal reliability measure is represented by the minimal detectable bias (MDB) as (Tang 1996; Teunissen 1998a) as

$$|\nabla_{0i}| = \frac{\delta}{\sqrt{r_i}}\sigma_i \tag{2.46}$$

where σ_i is the standard deviation of the *i*th observation and δ is the non-centrality parameter depending on the level of significance α and the power of the test β.

The external reliability is the influence of each of the MDBs on the estimated parameters. The effect of the blunder or the bias ∇_i in the *i*th observation is

$$\nabla_{\mathbf{x}} = \mathbf{N}^{-1}\mathbf{A}^T\mathbf{P}\mathbf{c}_i\nabla_i \tag{2.47}$$

where the **c**-vector takes the form $(0,...,1,...,0)^T$, with the 1 as the *i*th entry of **c**. Consequently, the impact of the MDB ∇_{0i} is given as

$$\nabla_{\mathbf{x}_{0i}} = \mathbf{N}^{-1}\mathbf{A}^T\mathbf{P}\mathbf{c}_i\nabla_{0i} \tag{2.48}$$

Baarda (1968) suggested the following alternative expression:

$$\lambda_{0i}^2 = \frac{\nabla_{\mathbf{x}_{0i}}^T \mathbf{N} \nabla_{\mathbf{x}_{0i}}}{\sigma_0^2} \tag{2.49}$$

The value λ_{0i}^2 is considered to be a measure of global external reliability. When the external reliability becomes large, the global falsification caused by a blunder or bias can be significant (Verhagen 2005a).

2.5.2 ADOP

Like the PDOP measure commonly used to describe the impact of receiver-satellite geometry on the positioning precision, the concept of the ADOP is introduced to measure the intrinsic precision characteristics of the ambiguities (Teunissen and Odijk 1997). It is defined as

$$\text{ADOP} = \sqrt{\left|\mathbf{Q}_{\hat{\text{N}}}\right|}^{\frac{1}{m}} \quad \text{(cycle)} \tag{2.50}$$

where $\mathbf{Q}_{\hat{\text{N}}}$ is the variance-covariance (vc-) matrix of the *m*-dimensional float ambiguities.

Smaller ADOP values imply more precise estimation of the float ambiguities and higher possibility of successful ambiguity validation. It is suggested that for successful AR the ADOP should be smaller than 0.15 cycles (Verhagen et al. 2010). For a short observation time span, the approximation of the ADOP can be expressed as (Takac 2006)

$$\text{ADOP} \approx m^{\frac{1}{2(m\text{-}1)}} \cdot \left(\frac{\sigma_\phi^2}{\sigma_p^2}\right)^{\frac{m\text{-}4}{4(m\text{-}1)}} \cdot \left(\frac{\sigma_\phi \sigma_p}{k\lambda_1\lambda_2}\right)^{\frac{1}{2}} \quad \text{(cycle)} \tag{2.51}$$

where σ_p^2 denotes the variance of code, σ_ϕ^2 denotes the variance of phase, λ_1 and λ_2 denote the wavelengths of L1 and L2, and *k* denotes the number of epochs.

2.5.3 Success rate

The success rate is defined as the integral of probabilistic density function of float ambiguity solutions over an ambiguity "Voronoi cell" (Hassibi and Boyd 1998) or

"Pull-in region" (Teunissen 1998c). The probability P_S of correct integer estimation in the case of ILS is defined as follows

$$P_S = P(\breve{\mathbf{N}} = \mathbf{N}) = \int_R f_{\hat{N}}(x)dX \tag{2.52}$$

where R and $f_{\hat{N}}(x)$ denote the ILS pull-in region and the probability density function of the float ambiguities $\hat{\mathbf{N}}$ respectively. In general, we assume the float ambiguity is normally distributed, e.g., $N(\mathbf{N}, \sigma_0^2\mathbf{Q}_{\hat{\mathbf{N}}})$. Therefore, the success rate can be expressed as

$$\begin{aligned} P_S &= \int_R N(\mathbf{N}, \sigma_0^2\mathbf{Q}_{\hat{\mathbf{N}}})dX \\ &= \int_R \frac{1}{(2\pi)^{\frac{1}{m}}\left|\sigma_0^2\mathbf{Q}_{\hat{\mathbf{N}}}\right|^{1/2}} \exp[-\frac{1}{2\sigma_0^2}(\mathbf{X}-\mathbf{N})^{\mathbf{T}}\mathbf{Q}_{\hat{\mathbf{Z}}}^{-\mathbf{1}}(\mathbf{X}-\mathbf{N})]dX \end{aligned} \tag{2.53}$$

2.5.4 Computations of success rate

The success rate of the integer bootstrapping formula is an exact formula and easy to evaluate (Teunissen 1998c). Teunissen (1999b) proved that of all integer estimators, the ILS estimator has the largest possible success rate. As a result, the bootstrapped success rate was widely used as a lower bound for the ILS success rate (O'Keefe et al. 2006; Pervan 1996; Feng and Wang 2011). Numerical experiment schemes and resuls have demonstrated that the success rate computed with the integer bootstrapping method is quite a sharp approximation to the actual ILS success rate (Feng and Wang 2011). The results also showed that variations or uncertainty of the unit–weight variance estimates from epoch to epoch will affect the computed success rates from different methods significantly, thus deserving more attention in order to obtain useful success probability predictions. Teunissen (2000) also gave the computations of lower and upper bounds of the ILS success rate based on the extreme eigenvalue of $\mathbf{Q}_{\hat{\mathbf{N}}_{\mathbf{dec}}}$. Biases that are unaccounted for will affect the success rate. Hence, a bias-affected bootstrapped success rate is studied to evaluate the bias robustness of AR (Teunissen 2001). In addition, another upper bound and approximation of the ILS success rate were given based on the ADOP using different

formulas (Teunissen 2003c; Verhagen 2003). An overview of the bounds and approximations is given in Table 2-3.

Table 2-3 A summary of AR success rate computing algorithms as approximations to the actual AR success rates

Methods	Approximations	References
P_{low}, P_{up1}, lower and upper bounds based on maximum and minimum eigenvalue	$P_{low} = [2\Phi(\frac{1}{2\sqrt{\lambda_{\max}}}) - 1]^k \le P(\breve{\mathbf{N}} = \mathbf{N})$ $\le P_{up1} = [2\Phi(\frac{1}{2\sqrt{\lambda_{\min}}}) - 1]^k$	(Teunissen 2000)
P_{boot}, lower bound based on bootstrapping	$P_{boot} = \prod_{i=1}^{k}\left[2\Phi\left(\frac{1}{2\sigma_{\hat{N}_i\|I}}\right)-1\right] \le P(\breve{\mathbf{N}} = \mathbf{N})$	(Teunissen 1998c)
P_{bias}, bias-affected on bootstrapped success rate	$P_{bias} = \prod_{i=1}^{m}\left[\Phi\left(\frac{1-2\beta_i}{2\sigma_{\hat{N}_i\|I}}\right)+\Phi\left(\frac{1-2\beta_i}{2\sigma_{\hat{N}_i\|I}}\right)-1\right] \le P_{boot}$	(Teunissen 2001)
P_{up2}, upper bound based on ADOP	$P_{up2} = P\left(\chi^2(k,0) \le \frac{c_k}{ADOP^2}\right) \ge P(\breve{\mathbf{N}} = \mathbf{N})$	(Teunissen 2003c; Verhagen 2003)
P_{adop}, approximation of P_{boot} based on ADOP	$P_{adop} = \left[2\Phi\left(\frac{1}{2\mathrm{ADOP}}\right)-1\right]^k \ge P_{boot}$	(Teunissen 2003c)

Note: $\Phi(t) = \int_{-\infty}^{t}\frac{1}{\sqrt{2\pi}}\exp(-\frac{1}{2}x^2)dx$, $c_k = \frac{\left(\frac{k}{2}\Gamma\left(\frac{k}{2}\right)\right)^{\frac{2}{k}}}{\pi}$, and β_i is the ith entry of the bias vector $L^{-1}b$.

2.6 Satellite Selection Algorithms

Several algorithms for selecting a subset of the satellites have been developed to find the minimal PDOP for a given number of satellites. The highest elevation satellite selection algorithm (HESSA) is the most popular used in the terrestrial applications since it provides reasonably good measurement geometries for terrestrial users, specifically, the vertical direction. Both the maximum volume algorithm (MVA) (Kihara and Okada 1984) and the four-step satellite selection algorithm (Li et al. 1999) were developed to select four satellites to form near optimal geometry. Park (2001) proposed the quasi-optimal satellite selection algorithm (QOSSA) for GPS

receivers used in low earth orbit (LEO) application, which can select any required number of satellites. A heuristic method combining the maximum volume algorithm and the redundancy technique, called the multi-constellations satellite selection algorithm (MCSSA), was developed to mitigate computational burdens while maintaining benefits of the combined navigation satellite systems (Roongpiboonsopit and Karimi 2009). Although low PDOP usually indicates good estimation accuracy, it does not yet hold true in terms of the system reliability. The reliability requirement is also of great importance within safety-critical and liability-critical applications. Until recently, however, no study has examined a method for selecting a subset of the satellites with the aim to achieve a high reliability system.

2.6.1 Highest Elevation Satellite Selection Algorithm

The highest elevation satellite selection algorithm (HESSA), which selects the highest elevation angles with reference to the user's position as its literal sense, is simple to utilise. The computation burden for this selection process is very low. However, the decision of the threshold of satellite elevation is often made experientially. Sometimes, if the threshold is too large, either the satellite number will be few or the geometry will be very poor.

2.6.2 Maximum Volume Algorithm

Kihara and Okada (1984) proposed the maximum volume algorithm (MVA) for selecting four satellites. The idea is based on the fact that PDOP tends to be inversely proportional to the volume of the tetrahedron form by unit vectors $\mathbf{a}_i$. The algorithm consists of the following three steps.

Step 1: Select the satellite (S1) with the highest elevation.

Step 2: Select the satellite (S2) which has the angle to S1 close to 109.5°.

Step 3: Select the other two satellites (S3 and S4).

It is shown that this algorithm provides a near-optimal geometry with a small computation time. However, for the purpose of reliability, specifically in the relative positioning application, it is required that more than four satellites be selected to increase estimation robustness.

2.6.3 Quasi-Optimal Satellite Selection Algorithm

Park (2001) introduced the quasi-optimal satellite selection algorithm (QOSSA) for selecting any number of satellites. The logic of this algorithm is to eliminate redundant satellites which are close or collinear to each other. The algorithm includes the following steps.

Step 1: Calculate the redundancy value of each visible satellite with respect to all the other visible satellites.
Step 2: Eliminate the satellite with maximum redundancy value.
Step 3: Return to step 1 until the predefined number of satellites is selected.

The implementation and computation of this algorithm is simple, nevertheless, the QOSSA was designed for GPS receivers used in LEO applications where the elevation angles are lower compared with those of terrestrial users. The predefined number of selected satellites is based on one's experience.

2.6.4 Multi-Constellations Satellite Selection Algorithm

Roongpiboonsopit and Karimi (2009) developed the multi-constellations satellite selection algorithm (MCSSA) to mitigate computational burdens and maintain benefits of the combined GNSS constellations. The MCSSA combines the strength of the MVA and the QOSSA. The MCSSA is not limited to any specific number of satellites and can provide sub-optimal satellite geometry. The procedure for the MCSSA can be summarised as follows.

Step 1: Define the number of selected satellites (n).
Step 2: Select the first four satellites based on the MVA from all of the candidate satellites.
Step 3: Remove the four satellites to selected satellites from the candidate satellites.
Step 4: Calculate the redundancy value of the remaining candidate satellites.
Step 5: Select the satellite with minimum redundancy value and remove the satellite to selected satellites from the candidate satellites
Step 6: Return to step 4 and continue until the predefined number of satellites is selected.

Though the MCSSA is fairly simple and provides the set of satellites with good geometry resulting in near-optimal PDOP, the criterion for the predefined number of selected satellites is not yet given.

2.7 Summary

The main findings from the literature review are:

(1) With the increasing number of satellites and signals, the traditional high precision positioning technique or concept is still affordable; however, some challenges and the potential for improving the reliability of positioning solutions have attracted our attention. Before we address this AR reliability issues, we need to have a good understanding of the ambiguity estimation method. The decorrelation process of the ILS method is important for improving the ambiguity search efficiency; nevertheless, the existing decorrelation methods do not perform well in high dimensional cases. Therefore, we developed a modified inverse integer Cholesky decorrelation method based on the work of Xu (2001). This approach is introduced in Chapter 3. In addition, finding a proper measure to evaluate the decorrelation methods performance is also a significant aspect. Traditionally, the decorrelation number and the condition number are considered. In Chapter 4, we will show another parameter, which has a similar function to that of the decorrelation number or condition number, to evaluate the decorrelation performance.

(2) For ambiguity validation purpose, the discrimination test is usually applied. The ratio-test is one of the powerful and common methods used to determine whether the integer ambiguities should be accepted or not. Although we consider the requirement of ambiguity validation in the ambiguity estimation process, for instance, we will estimate the best integer ambiguities and the second-best integer ambiguities for the ratio-test, other aspects of the combination of ambiguity estimation and validation have not been studied. Besides the decorrelation impact, the priori setting of the search space size χ^2 directly influences the search efficiency. Nevertheless, the existing approach of setting χ^2 ignores the information from the predefined critical

values of the ratio-test, sometimes, the χ^2 will be unnecessary large and thus reduce the search efficiency. A new χ^2 determination method will be discussed in Chapter 4.

(3) In terms of the evaluation of the AR reliability, according to the literature the ASR is generally used. However, the computation of the ILS ASR is very difficult, some approximations and bounds of the ILS ASR are reviewed. Though the ASR of bootstrapping is given as a good and sharp approximation of the ILS ASR, numerical examples are not seen in other work. Chapter 5 and Chapter 6 will address this issue.

(4) Due to the hardware limitation and computation burdens, it is no need to use all the available satellites into the computation, particularly in the context of multiple constellations. Quite a few algorithms for satellite selection have been studied in last two decades. However, these algorithms are almost all based on the minimisation of DOP. The author has not found an answer as to whether these algorithms are capable of improving the reliability of AR. Thus, an algorithm for satellite selection which improves the reliability of AR is even more badly needed. This issue is considered in Chapter 7.

Chapter 3: A Modified Inverse Integer Cholesky Decorrelation Method and Performance on Ambiguity Resolution

Statement of Contribution of Co-Authors

The authors listed below have certified that:

1. they meet the criteria for authorship in that they have participated in the conception, execution, or interpretation, of at least that part of the publication in their field of expertise;
2. they take public responsibility for their part of the publication, except for the responsible author who accepts overall responsibility for the publication;
3. there are no other authors of the publication according to these criteria;
4. potential conflicts of interest have been disclosed to (a) granting bodies, (b) the editor or publisher of journals or other publications, and (c) the head of the responsible academic unit, and
5. they agree to the use of the publication in the student's thesis and its publication on the Australasian Digital Thesis database consistent with any limitations set by publisher requirements.

In the case of this chapter:

Contributor	**Statement of contribution**
Jun Wang	Conducted all the experiments and data analysis, wrote the manuscript
Yanming Feng	Reviewed and revised the manuscript
Charles Wang	Reviewed and revised the manuscript

Principal Supervisor Confirmation

I have sighted email or other correspondence from all co-authors confirming their certifying authorship.

Yanming Feng		20-October-2012
Name	Signature	Date

A Modified Inverse Integer Cholesky Decorrelation Method and Performance on Ambiguity Resolution

Jun Wang, Yanming Feng, Charles Wang

Faculty of Science and Technology

Queensland University of Technology, Australia

Phone: +61 7 31389111, Fax: +61 7 31389390, Email: jun.wang@student.qut.edu.au

Abstract

One of the research focuses in dealing with integer least squares problem is the decorrelation technique to improve the efficiency of the integer parameter search progress. It remains a challenging issue and becomes even more critical in processing multi-GNSS signals. Currently, there are three main decorrelation techniques being employed: the integer Gaussian decorrelation, the Lenstra–Lenstra–Lovász (LLL) algorithm and the inverse integer Cholesky decorrelation (IICD) method. To measure the performance of decorrelation techniques, the condition number is usually used as the criterion. Additionally, the number of grid points in the search space can be directly utilised as a performance measure according to the decorrelation purpose. The success rate of integer bootstrapping is also calculated in terms of studying the ambiguity resolution reliability.

This paper presents a modified inverse integer Cholesky decorrelation (MIICD) method to improve the decorrelation performance out the other three techniques. Decorrelation performance is evaluated based on the condition number of the decorrelation matrix and the number of search candidates. Performance parameters are compared using both simulation and real data. The simulation experiment scenarios employ the isotropic probabilistic model using a predefined eigenvalue and without any geometry or weighting system constraints. Simulation analysis shows that MIICD method outperforms other three methods in terms of condition numbers achieved. The real data experiment scenarios involve both single and dual constellations cases. Experimental results demonstrate that in the single constellation case, the condition number of MIICD is smaller than that of LAMBDA over 78.65% times while the number of search candidate points is smaller over 98.92% of time. In the dual constellation case, these two numbers are 98.78% and 100% respectively.

Keywords: Modified Inverse Integer Cholesky Decorrelation, LLL, Condition Numbers, Ambiguity Resolution

3.1 Introduction

Integer ambiguity resolution is the key to high precision positioning using carrier phase measurements from Global Navigation Satellite System (GNSS). Given the GNSS linear observation equations

$$\mathbf{L} = \mathbf{A}\boldsymbol{\delta x} + \mathbf{B}\mathbf{N} + \mathbf{e} \tag{1}$$

and the criterion:

$$\min_{\boldsymbol{\delta x},\mathbf{N}} \left\{ \left\| \mathbf{L} - \mathbf{A}\boldsymbol{\delta x} - \mathbf{B}\mathbf{N} \right\|^2_{\mathbf{Q}_\mathbf{L}^{-1}}, \boldsymbol{\delta x} \in R^n, \mathbf{N} \in \mathbf{Z}^p \right\} \tag{2}$$

where **L** is a vector of 'observed minus computed' double-difference (DD) observations; **A** is the design matrix for the vector of real-valued unknowns $\boldsymbol{\delta x}$; **B** is the design matrix for the vector of integer DD ambiguities **N**; $\mathbf{Q}_\mathbf{L}$ is the corresponding variance matrix of observables and **e** is the vector of unmodelled error and measurement noise.

Solving the above mixed integer least-squares (MILS) problem has proved to be equivalent to the solution of the integer least-squares (ILS) problem:

$$\min_{\mathbf{N}} \left\{ \left\| \hat{\mathbf{N}} - \mathbf{N} \right\|^2_{\mathbf{Q}_{\hat{\mathbf{N}}}^{-1}}, \mathbf{N} \in \mathbf{Z}^p \right\} \tag{3}$$

where $\hat{\mathbf{N}}$ is a float ambiguity vector, with the corresponding variance-covariance matrix $\mathbf{Q}_{\hat{\mathbf{N}}}$. For more details on the procedure of solving MILS or ILS, see (Teunissen, 1995; Hassibi and Boyd, 1998; Grafarend, 2000; Chang and Zhou, 2007).

The integer ambiguity search space is defined as

$$(\hat{\mathbf{N}} - \mathbf{N})^T \mathbf{Q}_{\hat{\mathbf{N}}}^{-1} (\hat{\mathbf{N}} - \mathbf{N}) \le \chi^2 \tag{4}$$

It is actually a hyper-ellipsoid centred at $\hat{\mathbf{N}}$, its shape and orientation are governed by $\mathbf{Q}_{\hat{\mathbf{N}}}$ and its size can be controlled by χ^2. In general, $\mathbf{Q}_{\hat{\mathbf{N}}}$ has high correlation since the DD operation and correlation between measurements errors. Hence, the integer ambiguity search space is highly elongated. In order to make the search process more

efficient, different decorrelation techniques have been developed. The essence of decorrelation is to apply an admissible integer unimodular matrix $\mathbf{Z}$ to eliminate the off-diagonal elements of $\mathbf{Q}_{\hat{\mathbf{N}}}$ or reduce the size of the correlation coefficients. This can be expressed as

$$\hat{\mathbf{N}}_{\mathbf{dec}} = \mathbf{Z}\hat{\mathbf{N}},\ \mathbf{N}_{\mathbf{dec}} = \mathbf{Z}\mathbf{N},\ \mathbf{Q}_{\hat{\mathbf{N}}_{\mathbf{dec}}} = \mathbf{Z}\mathbf{Q}_{\hat{\mathbf{N}}}\mathbf{Z}^{\mathbf{T}} \tag{5}$$

Therefore the search space (4) can be transformed as

$$(\hat{\mathbf{N}}_{\mathbf{dec}} - \mathbf{N}_{\mathbf{dec}})^T \mathbf{Q}_{\hat{\mathbf{N}}_{\mathbf{dec}}}^{-1} (\hat{\mathbf{N}}_{\mathbf{dec}} - \mathbf{N}_{\mathbf{dec}}) \leq \chi^2 \tag{6}$$

The condition number is usually used to indicate the performance of decorrelation methods. For instance, the well-known least-squares ambiguity decorrelation adjustment (LAMBDA) method is based on integer Gaussian decorrelation (Teunissen et al., 1995, 1996 and 1998). A detailed description and implementation of this method is referred to (de Jonge and Tiberius 1996). Another algorithm named Lenstra–Lenstra–Lovász (LLL) was originally developed for lattice basis reduction, which can also be used to reduce the condition number of matrix(Lenstra et al. 1982). This algorithm was suggested for the decorrelation of the integer ambiguities by Hassibi and Boyd (1998) and Grafarend (2000). Based on a modified LLL algorithm, Chang and Zhou (2007) developed a Matlab package for solving MILES problems and demonstrated higher computation efficiency than LAMBDA. Xu (2001) developed a random simulation approach to compare the performance of different decorrelation method, but the simulation is more general, without referring to any particular satellite-receiver geometry, observation span and measurement weightings. This non-informativeness guarantees the statistical fairness of comparing different methods numerically because these three factors may favour a particular method. Xu also proposed an inverse integer Cholesky decorrelation method and demonstrated that this method outperformed LAMBDA and LLL method. However, the performance of these decorrelation methods in dealing with practical high dimension cases remains unknown (Xu, 2001; Svendsen, 2006). In the near future, more frequency signals, e.g. L1, L2 and L5 and more navigation satellites systems, e.g. GPS and Galileo could be used. Introducing more observations from three frequency signals and dual constellations changes the condition number of $\mathbf{Q}_{\hat{\mathbf{N}}}$.

Figure 3-1 plots the condition number of $\mathbf{Q}_{\hat{N}}$ and the corresponding decorrelated matrix $\mathbf{Q}_{\hat{N}dec}$ for both double and triple frequencies cases. It is clearly observed that the $\mathbf{Q}_{\hat{N}dec}$ condition numbers of triple frequencies are larger than that of double frequencies. Figure 3-2 compares the condition numbers of $\mathbf{Q}_{\hat{N}}$ and $\mathbf{Q}_{\hat{N}dec}$ between single GPS constellation and the simulated dual constellations, which refer to the combination of GPS measurements data sets recorded at two epochs separated by a few hours for data analysis (Feng, 2005) as outlined in Section 3.2 *Decorrelation Techniques*. It is seen that the condition numbers of $\mathbf{Q}_{\hat{N}dec}$ are larger than these for the single constellation. In this research effort, a modified inverse integer Cholesky decorrelation method is proposed to further decorrelate $\mathbf{Q}_{\hat{N}}$ and reduce the conditional numbers.

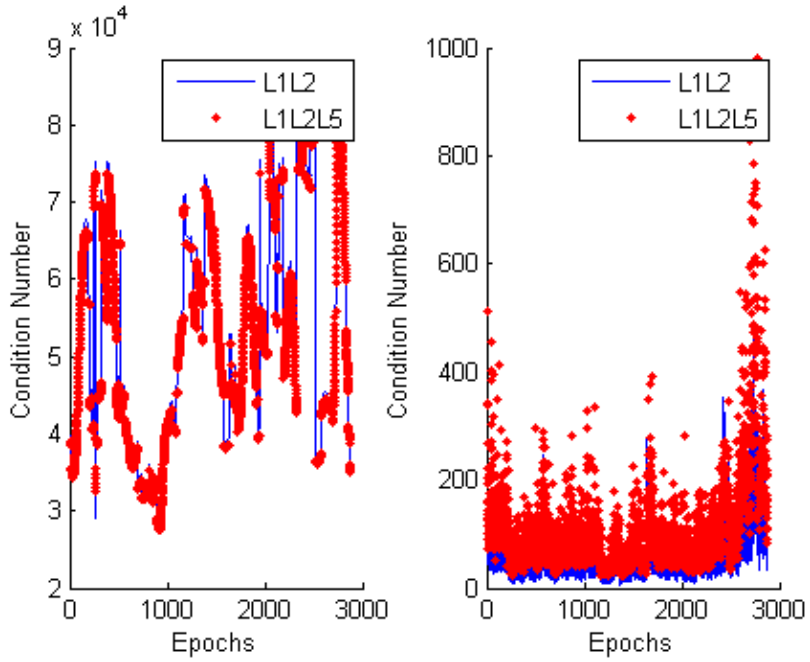

Figure 3-1 Condition numbers of $\mathbf{Q}_{\hat{N}}$ and $\mathbf{Q}_{\hat{N}dec}$ in L1L2 and L1L2L5 cases. Left plot: the float ambiguity variance-covariance matrix $\mathbf{Q}_{\hat{N}}$ Right plot: the decorrelated ambiguity vc- matrix $\mathbf{Q}_{\hat{N}dec}$

On the other hand, the condition properties of decorrelation methods may not necessarily link to the ambiguity searching efficiency. A simple way is to count the grid points within the search space. Although the volume of a search space has been demonstrated to be a fair approximation of the number of grid points on the average (Teunissen et al. 1996), the relation between the grid point number and condition

number have not been specifically examined. In the later context of this work, we will also compare the number of search grid points of different decorrelation methods to show their dependence.

Since the success rate of bootstrapping integer solutions could be a very good approximation of ILS success rate (Teunissen 1998c; Verhagen 2003) have numerically demonstrated close agreement with actual statistical results by Feng and Wang (2011), in this contribution, we will compute the success rate of ambiguity bootstrapping integer estimation with different decorrelation methods. It is also noticed that the work by Henkel (2007 and 2009) investigated the impact of biases inflation by integer decorrelation transformation.

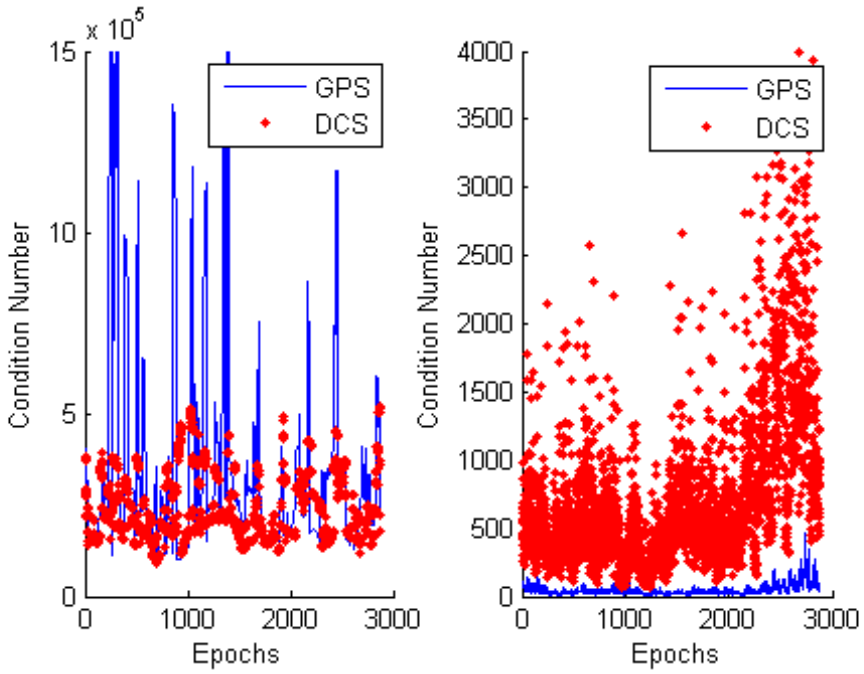

Figure 3-2 Condition numbers of $\mathbf{Q}_{\hat{N}}$ and $\mathbf{Q}_{\hat{N}dec}$ in GPS and dual donstellations cases. Left plot: the float ambiguity variance-covariance matrix $\mathbf{Q}_{\hat{N}}$ Right plot: the decorrelated ambiguity vc- matrix $\mathbf{Q}_{\hat{N}dec}$

The rest of paper is organised as follows. Section 3.2 *Decorrelation Techniques* briefly introduces different decorrelation techniques and introduces the modified inverse integer Cholesky decorrelation method. Section 3.3 presents the random simulation strategies, the concept of generating dual constellations and the criterion used to compare the performance of different decorrelation methods. Section 3.4

Experiments discusses the experimental results from four computation scenarios. The main findings of the paper are summarised in the final section.

3.2 Decorrelation Techniques

The variance-covariance matrix $\mathbf{Q}_{\hat{\mathbf{N}}}$ of DD float ambiguities possesses highly-correlated off-diagonal elements. The goal of a decorrelation process is to find a unimodular matrix Z to reduce the off-diagonal elements or reduce the size of the correlation coefficients. Since the matrix Z should be admissible and integer, the absolute decorrelation is impossible in most cases. The LAMBDA method based on integer Gaussian decorrelation has been proved to be highly efficient for ambiguity resolution in most situations (Teunissen et al. 1995; Teunissen et al. 1997). Although the LLL algorithm is developed for lattice basis reduction, the method can also be used to reduce the correlation of $\mathbf{Q}_{\hat{\mathbf{N}}}$ in ILS (Luk and Tracy 2008). The inverse integer Cholesky decorrelation (IICD) method uses the Cholesky decomposition instead of Gaussian decomposition for GPS decorrelation (Xu 2001). Based on IICD method, a modified inverse integer Cholesky decorrelation (MIICD) is proposed.

3.2.1 Integer Gaussian decorrelation

Integer Gaussian decorrelation is actually performed as a sequence of integer Gaussian eliminations and permutations. Assuming there exist three elements q_{ii}, q_{jj} and q_{ij} of $\mathbf{Q}_{\hat{\mathbf{N}}}$ that satisfy $\left|q_{ij}\right| / \min(q_{ii}, q_{jj}) > 1/2$, then the unimodular matrix can be constructed as

$$\mathbf{Z_1} = \begin{bmatrix} 1 & & & & & & \\ & \ddots & & & & & \\ & & 1 & & & & \\ & & \vdots & \ddots & & & \\ & & -\left[q_{ij}/q_{ii}\right] & \cdots & 1 & & \\ & & & & & \ddots & \\ & & & & & & 1 \end{bmatrix} \tag{7}$$

if $q_{ii} \le q_{jj}$,or

$$\mathbf{Z_1} = \begin{bmatrix} 1 & & & & & & \\ & \ddots & & & & & \\ & & 1 & \cdots & -\left[q_{ij}/q_{jj}\right] & & \\ & & & \ddots & \vdots & & \\ & & & & 1 & & \\ & & & & & \ddots & \\ & & & & & & 1 \end{bmatrix} \tag{8}$$

if $q_{ii} > q_{jj}$. Here the operator [ ] denotes rounding to the nearest integer. Repeating the above steps, the final **Z** transformation matrix can be expressed as

$$\mathbf{Z}=\mathbf{Z_n}\cdots\mathbf{Z_2Z_1} \tag{9}$$

Thus, the decorrelated matrix $\mathbf{Q}_{\hat{\mathrm{N}}\mathrm{dec}}$ can be obtained by equation (5).

3.2.2 Lenstra–Lenstra–Lovász algorithm

The LLL algorithm was first introduced for decorrelation in GPS ambiguity resolution by Hassibi and Boyd (1998), followed with the contributions by Grafarend (2000), Xu (2001) and Chang (2007). The original LLL algorithm uses the integer Gram-Schmidt orthogonalization process, however the Givens reflection based LLL algorithm can be numerically more robust performed in floating-point arithmetic (Luk and Qiao 2007; Luk and Tracy 2008). Since the matrix $\mathbf{Q}_{\hat{\mathrm{N}}}$ is positive and definite, it can always be factorised as $\mathbf{Q}_{\hat{\mathrm{N}}} = \mathbf{V^T V}$. Compute the reduced or almost orthogonal basis $\mathbf{V_0}$, so that $\mathbf{V_0} = \mathbf{VZ}^{-1}$, where **Z** is unimodular. After these steps, we have

$$\mathbf{Q}_{\hat{\mathrm{N}}} = \mathbf{V}^T\mathbf{V} = (\mathbf{V_0Z})^T\mathbf{VZ} = \mathbf{Z}^T\mathbf{V}_0^T\mathbf{V_0Z} \tag{10}$$

Due to V0 is almost orthogonal, the target of decorrelation can be achieved with $\mathbf{Q}_{\hat{\mathrm{N}}\mathbf{dec}} = \mathbf{V}_0^T\mathbf{V_0}$.

3.2.3 Inverse integer Cholesky decorrelation (IICD) method

The inverse integer Cholesky decorrelation (IICD) method applies the $\mathbf{LDL}^T$ factorization as follows:

$$\mathbf{Q}_{\hat{\mathrm{N}}} = \mathbf{LDL}^T \tag{11}$$

where **L** is unit lower triangular matrix, and **D** is a diagonal matrix with positive elements.

Although **L** cannot be directly used for ambiguity decorrelation due to the real-valued elements, [**L**] is obviously unimodular as well as [$\mathbf{L}^{-1}$]. Thus, we $\mathbf{Z}_1 = \left[\mathbf{L}^{-1}\right]$ and can compute the decorrelated matrix as

$$\mathbf{H}_1 = \mathbf{Z}_1 \mathbf{Q}_{\hat{\mathbf{N}}} \mathbf{Z}_1^T \tag{12}$$

Since in most cases $\mathbf{Z}_1$ is not equivalent to **L**, $\mathbf{H}_1$ is no longer diagonal. Repeating the process like

$$\mathbf{H}_n = \mathbf{Z}_n \mathbf{H}_{n-1} \mathbf{Z}_n^T \tag{13}$$

until the condition number of Hn reach the predetermine value, the final decorrelation can be express as (Xu 2001)

$$\mathbf{Q}_{\hat{\mathbf{N}}\mathbf{dec}} = (\mathbf{Z}_n \cdots \mathbf{Z}_2 \mathbf{Z}_1)^T \mathbf{Q}_{\hat{\mathbf{N}}} (\mathbf{Z}_n \cdots \mathbf{Z}_2 \mathbf{Z}_1) \tag{14}$$

To obtain larger off-diagonal elements of **L**, we may rearrange the diagonal elements of $\mathbf{Q}_{\hat{\mathbf{N}}}$ and $\mathbf{H}_i$ in ascending order. Before finishing this section, we would like to make some arguments on this method. Firstly, what should be the predetermined condition number of the decorrelated matrix? The answer is not easy to say, because it relates to the dimension and formation of the original matrix. Secondly, since this method involves iteration process, sorting and stopping criteria would be very important for the IICD method (private communication with Dr Xu on 25 June 2010). Simply comparing the condition number of $\mathbf{H_n}$ and $\mathbf{H_{n-1}}$ can lead to wrong decision, because it is likely to happen that the condition numbers of $\mathbf{H_n}$ and $\mathbf{H_{n-1}}$ are not in the strictly descending order. To overcome this shortcoming of IICD, we will propose a new method in the next section.

3.2.4 Modified inverse integer Cholesky decorrelation (MIICD) method

Instead of using the predetermined condition number as the iteration stopping criteria, we consider applying whether the abs($\mathbf{Z}_n$) is an identity matrix to stop the process of inverse integer Cholesky decorrelation, where abs( ) is the absolute value operator. In addition, we may also rearrange the diagonal elements of **H** in

descending order after stopping iteration and repeat the decorrelation process. It is observed that the condition numbers of $\mathbf{H_i}$ usually decrease with fluctuation, so we will record the condition number of $\mathbf{H_i}$ and transformation matrix $\mathbf{Z_i}$ each time while conducting the procedure of decorrelation. This function allows us to be able to find the smallest condition number by searching $\mathbf{H_i}$. Another iteration stopping criteria in this method is the predetermined iteration number. Figure 3-3 depicts this modified inverse integer Cholesky decorrelation method.

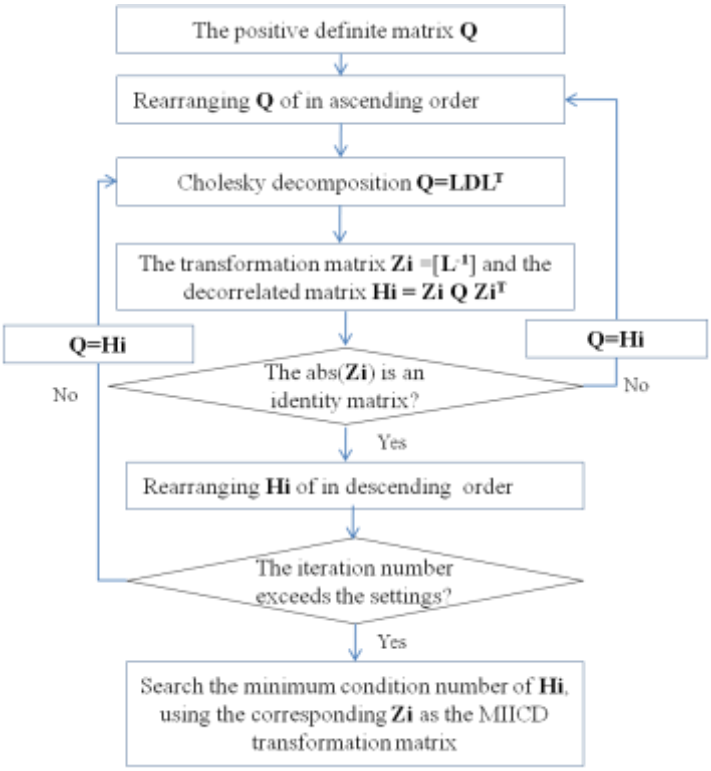

Figure 3-3 Flowchart if the modified inverse integer Cholesky decorrelation method

3.3 Random Simulation and Measuring Performance

In order to study the numerical performance of different decorrelation methods, an isotropic probabilistic model is used to simulate a positive definite matrix instead of a particular one (Xu 2002, 2001). In addition we apply the concept of Virtual Galileo Constellation (VGC) to generate useful data sets of dual-constellations (Feng 2005). The condition number is usually used to be an index of decorrelation methods performance (Svendsen 2006), but it might not directly reflect the integer candidates search efficiency. Therefore, the integer candidates search numbers can be compared with different decorrelation method.

3.3.1 Random simulation method

Any positive definite matrix **Q** can be decomposed by singular value decomposition as

$$\mathbf{Q} = \mathbf{U}\Lambda\mathbf{U}^T \tag{15}$$

where **U** is the normalised orthogonal eigenvector matrix and Λ is the diagonal matrix with positive eigenvalues $\lambda_1 \le \lambda_2 \le \cdots \le \lambda_n$. Then the simulation of **Q** is turned into design of **U** and Λ .

The isotropic probabilistic model is used to generation of an arbitrary **U**, which can be uniquely represented as

$$\mathbf{U}=\mathbf{U}_{n(n-1)}\cdots\mathbf{U}_{32}\mathbf{U}_{n1}\cdots\mathbf{U}_{31}\mathbf{U}_{21} \tag{16}$$

where

$$\mathbf{U_{ij}} = \begin{bmatrix} \mathbf{I_1} & \mathbf{0} & \mathbf{0} & \mathbf{0} & \mathbf{0} \\ \mathbf{0} & \cos\theta_{ij} & \mathbf{0} & \sin\theta_{ij} & \mathbf{0} \\ \mathbf{0} & \mathbf{0} & \mathbf{I}_2 & \mathbf{0} & \mathbf{0} \\ \mathbf{0} & -\sin\theta_{ij} & \mathbf{0} & \cos\theta_{ij} & \mathbf{0} \\ \mathbf{0} & \mathbf{0} & \mathbf{0} & \mathbf{0} & \mathbf{I}_3 \end{bmatrix}, \tag{17}$$

$\mathbf{I_1}$, $\mathbf{I_2}$ and $\mathbf{I_3}$ are the identity matrices of suitable orders, **0** is a zero matrix or vector and $-\pi/2 \le \theta_{ij} \le \pi/2$ (Xu, 2001and 2002).

The next step is to design Λ which is related to the eigenvalues of **Q**. Since the condition number of **Q** can be expressed as follows

$$cond(\mathbf{Q}) = \lambda_{\max} / \lambda_{\min} \tag{18}$$

Although we can generate all the eigenvalues equally separated with predetermined condition number or ratio, more complex assumption or constrains can be imposed. For single baseline geometry-based model, there are only three independent DD ambiguities and other DD ambiguities can be derived from those(Li and Shen 2010). Figure 3-4 shows the eigenvalue partition of the covariance matrix of the float

ambiguities in single baseline. Obviously there are three large ones and the remaining eigenvalues are significantly small.

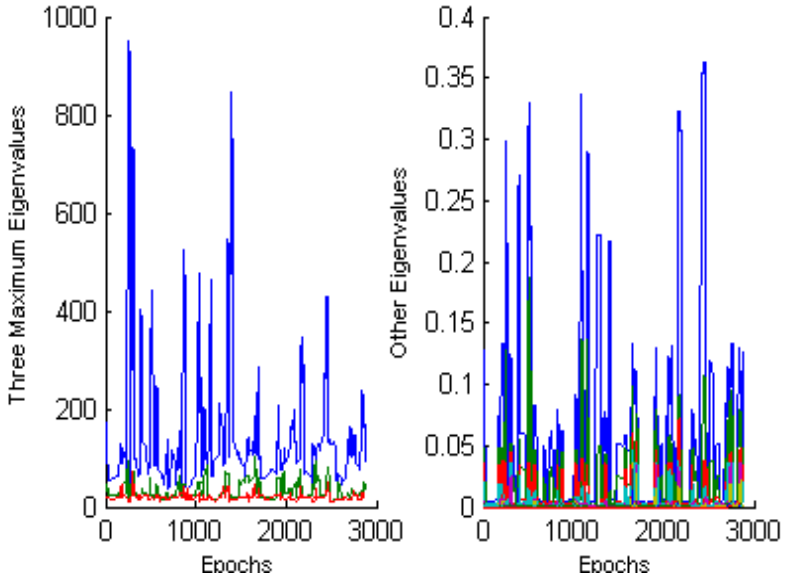

Figure 3-4 The eigenvalues partition of the covariance matrix of the float ambiguities. Left plot: the three largest eigenvalues; Right plot: the remaining eigenvalues

3.3.2 Virtual Galileo Constellation (VGC) model

The concept of VGC is to combine the GPS measurements data sets recorded at two epochs separated by a few hours to form dual constellations for data analysis. Feng (2005) showed that the separation can range from 1 to 2 hours. For GPS and VGC data sets, one can obtain the linear equations based on (1)

$$\begin{bmatrix} \mathbf{L}_{\text{gps}} \\ \mathbf{L}_{\text{gal}} \end{bmatrix} = \begin{bmatrix} \mathbf{A}_{\text{gps}} & \mathbf{B}_{\text{gps}} & \mathbf{0} \\ \mathbf{A}_{\text{gal}} & \mathbf{0} & \mathbf{B}_{\text{gal}} \end{bmatrix} \begin{bmatrix} \delta\mathbf{X} \\ \mathbf{N}_{gps} \\ \mathbf{N}_{gal} \end{bmatrix} + \begin{bmatrix} \mathbf{e}_{gps} \\ \mathbf{e}_{gal} \end{bmatrix} \tag{19}$$

where the subscript "gal" represents Galileo. It is noted that in (19), two data sets are assumed to have the same coordinates systems, but different sets of ambiguity parameters.

3.3.3 Measuring performance

Condition numbers are often used to compare the performance of different decorrelation techniques, which only reveal the ratio of the square of semi-major axis and semi-minor axis of search ellipsoid. It can only partially reflect the ILS search

progress efficiency; thus, the search numbers of grid points are also used to compare the impact of different decorrelation methods on search efficiency within the same search method. The details on how to compute the search numbers of candidates are referred to the instruction of LAMBDA and MILES (De Jonge and Tiberius, 1996; Chang and Zhou, 2007).

Furthermore, the success rate is computed considering ambiguity reliability requirements. The actual success rate of ILS is difficult to calculate; nevertheless the success rate of bootstrapping integer solution is a lower bound and a very good approximation of ILS (Teunissen, 1998; Feng and Wang, 2011), which can be computed as

$$\begin{aligned} &P(\hat{\mathbf{N}}|_{ILS}) \geq P(\hat{\mathbf{N}}|_{Boostrapping}) \\ &= \prod_{i=1}^{t} \int_{R_0} \frac{1}{(2\pi)^{1/2}\sigma_0\sqrt{\mathbf{Q_{i|I}}}} \exp[-\frac{(\mathbf{x}-\mathbf{z_i})^2}{2\sigma_0^2\mathbf{Q_{i|I}}}]dx \end{aligned} \tag{20}$$

where the diagonal elements of $\mathbf{Q_{i|I}}$ can be calculated by factorization based on (11).

3.4 Experiments

The purpose of the experimental analysis is to examine the decorrelation performance of LAMBDA, LLL, IICD and MIICD methods in different situations. Four computation scenarios are set up as follows:

Scenario 1: Performing LAMBDA, LLL, IICD and MIICD decorrelation with randomly simulated definite-positive covariance matrices;

Scenario 2: Performing LAMBDA, LLL, IICD and MIICD decorrelation with randomly simulated definite-positive covariance matrices where eigenvalues are constrained to certain values as discussed in Section 3.3;

Scenario 3: Performing LAMBDA and MIICD decorrelation in ILS processing of a real GPS data set for a 21 km baseline;

Scenario 4: Performing LAMBDA and MIICD decorrelation in ILS processing of the same data set as Scenario 3, but added with virtual GNSS data.

In Scenarios 1 and 2, 300 Q matrix samples are randomly generated for simulation experiments. We then set the condition number of original positive definite matrix Q based on the sample dimension size (as shown in Figure 3-5). The condition number

is set as 1×10^4, if $4 \le \dim(\mathbf{Q}) \le 20$; or 1×10^5, if $20 < \dim(\mathbf{Q}) \le 24$, where dim () is the matrix dimension operator.

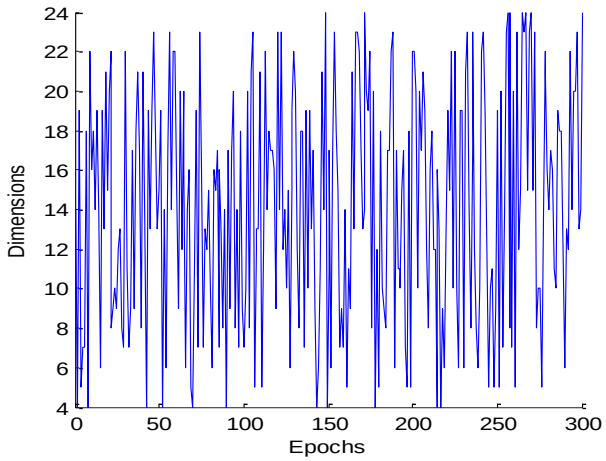

Figure 3-5 Dimensions of the 300 random simulation examples

Figure 3-6 shows the condition numbers of the original simulation matrix **Q** and the results for four decorrelation methods for Scenario 1. It is obvious that all decorrelation methods can significantly decrease the condition number of **Q**. Particularly, the condition numbers resulted from LLL and MIICD decorrelation are smaller than 200 and in most cases are smaller than 100. Meanwhile, the condition numbers resulted from other two methods; LAMBDA and IICD are slightly higher, mostly below 200 with occasional peaks to 400.

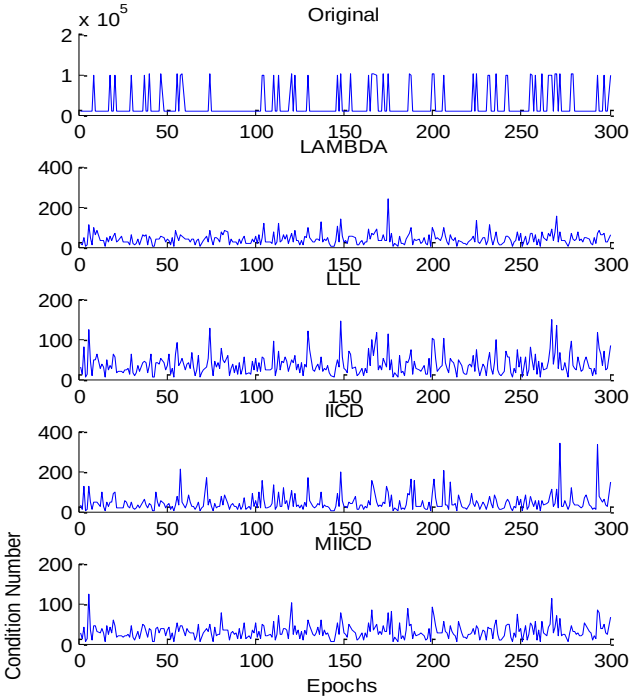

Figure 3-6 Condition numbers of simulated Q samples and results from LAMBDA, LLL, IICD and MIICD with Scenario 1

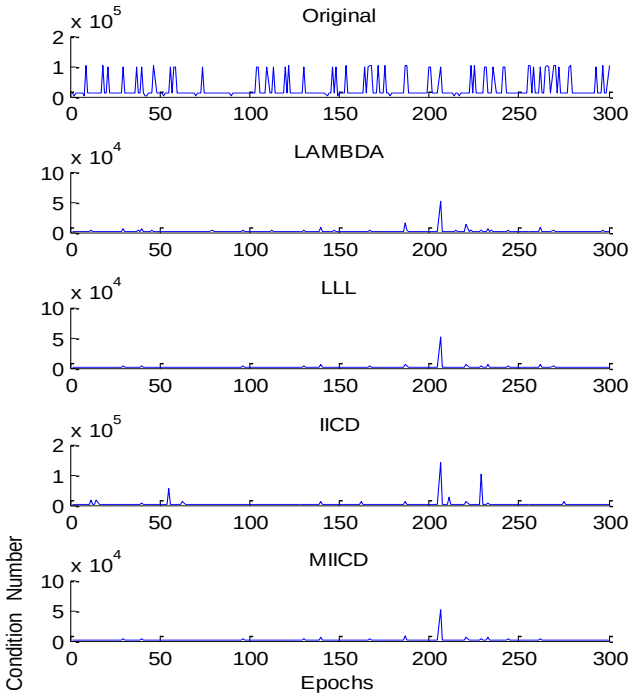

Figure 3-7 Condition Numbers of simulated Q samples, results from LAMBDA, LLL, IICD and MIICD in Scenario 2

For Scenario 2, constraint eigenvalues of **Q** were generated for performance evaluation as discussed in Section 3.1. The condition numbers of the original **Q** matrix and four decorrelation methods are shown in Figure 3-7. In this scenario, though most samples were successfully decorrelated by these methods, results indicate that the decorrelation may not occur at some epochs based on given stopping criteria on condition number comparison. For instance, at epoch 206, the decorrelation did not happen with IICD method.

Table 3-1 summarises the events and percentages when the condition numbers of decorrelated matrices from different methods are smaller than those from AMBDA method. It is clear that MIICD has the best performance in terms of condition numbers in both of two scenarios. It shows that MIICD method outperformed other three methods in terms of the events with smaller condition numbers than LAMBDA method. In particular, without eigenvalue constraints in the decorrelated matrices, in 235 out of 300 samples, or at 78.33% of time, MIICD conditional numbers are lower than LAMBDA condition numbers. With eigenvalue constraints, the samples and percentages grow to 245 and 81.67% of times, respectively. Therefore, for simplicity, only MIICD and LAMBDA method are compared for scenarios 3 and 4.

For Scenario 3 and Scenario 4, a real GPS data set of 24 hours collected at sampling rate of 30 seconds is used. The virtual Galileo constellation (VGC) used in Scenario 4 is generated from the collected dataset with time latency of 2 hours.

Table 3-1 Lower condition number statistics derived from LLL, IICD and MIICD with respect to LAMBDA

	Scenario 1	Scenario 2
LLL	161 (53.67%)	213 (71.00%)
IICD	178 (59.33%)	225 (75.00%)
MIICD	235 (78.33%)	245 (81.67%)

The condition numbers of LAMBDA and MIICD methods for Scenario 3 and Scenario 4 have been computed and shown in Figure 3-8 and Figure 3-9 respectively. It can be clearly seen that the condition number results of these methods have similar trends and fluctuations in most cases except the MIICD has smaller condition

numbers. In particular, the MIICD method has significant performance improvement in the dual constellation case where the peak condition number of LAMBDA is larger than 8000 while the peak MICCD condition number is about 1000.

The search candidate numbers of LAMBDA and MIICD methods for Scenarios 3 and 4 are shown in Figure 3-10 and Figure 3-11 respectively. It can be clearly observed that the search candidate numbers of LAMBDA are generally larger with respect to these of the MIICD method. Similarly to the condition number results, the improvement in the search candidate numbers of MIICD method is more significant in the dual constellation case. For instance in Scenario 4, the search numbers of LAMBDA are around 1×105 between epochs 2400 and 2800, whereas the MIICD search numbers are mostly less than 200 with the peak of 4000 during the time.

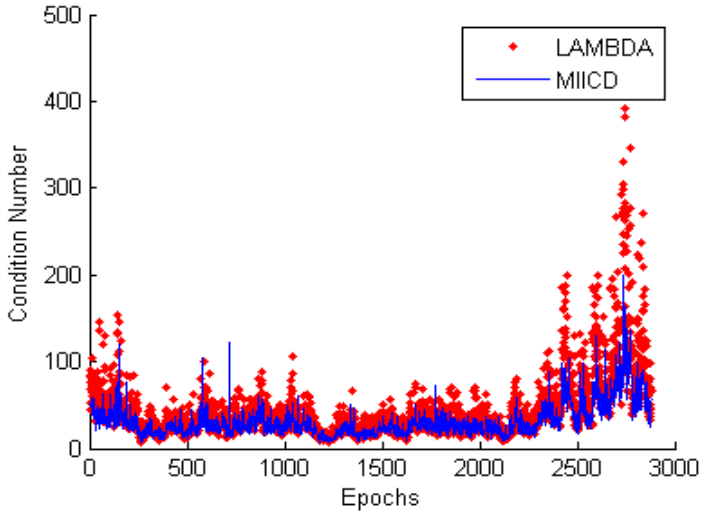

Figure 3-8 Condition numbers of Q matrices, resulting from LAMBDA and MIICD with Scenario 3

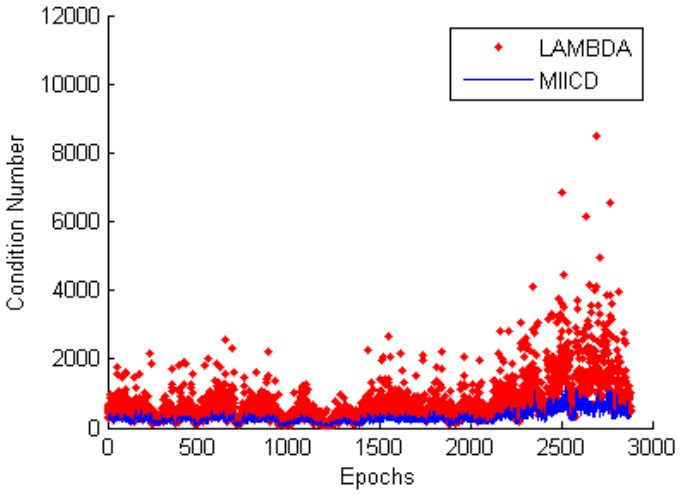

Figure 3-9 Condition numbers of Q matrices, resulting from LAMBDA and MIICD with Scenario 4

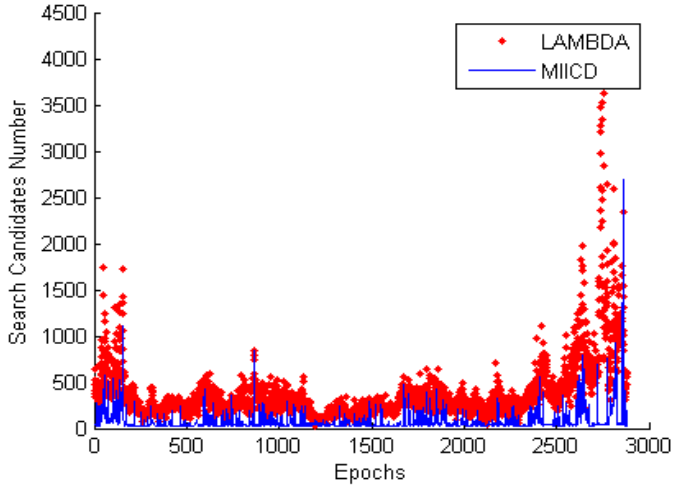

Figure 3-10 Search candidate numbers, resulting from LAMBDA and MIICD with Scenario 3

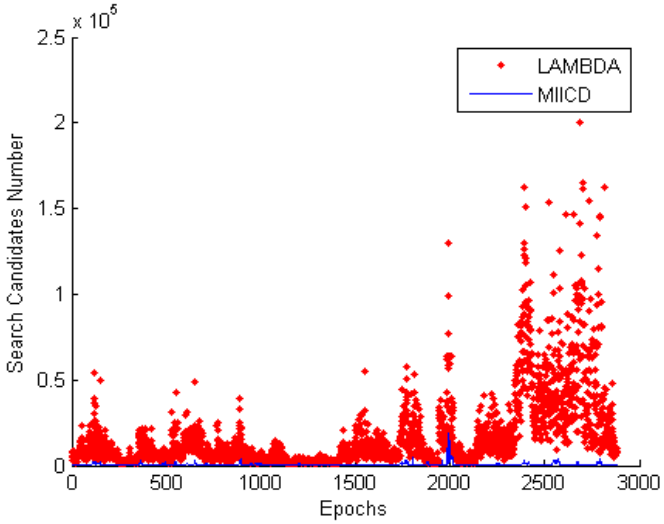

Figure 3-11 Search candidate numbers, resulting from LAMBDA and MIICD with Scenario 4

To investigate relations between condition numbers and search candidate numbers, we can either draw the scatter plots or calculate the correlation coefficients. Figure 3-12 shows the scatter plots of these two parameters. A linear dependence is clearly shown between the condition number and the search candidate number.

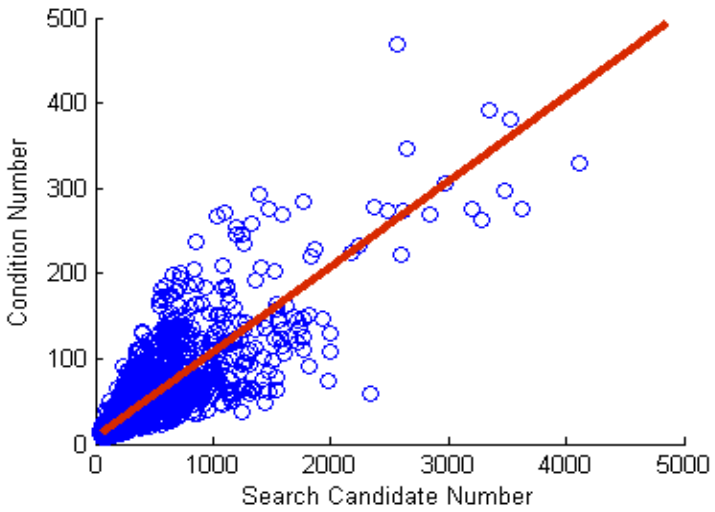

Figure 3-12 Scatter plots of the search candidate number against the condition number

Table 3-2 presents the correlation coefficients which also verify that the condition number is highly related to the candidate search number. On the other hand, the correlation coefficient 0.8050 also reveals that the condition numbers cannot totally be represented by the search candidate numbers.

Table 3-2 The correlation coefficients between search candidate numbers and condition numbers

Correlation coefficient	Search candidate number
Condition numbers	0.8050

The success rates of LAMBDA and MIICD method were computed with (20) for Scenario 3 Scenario 4 and shown in Figure 3-13 and Figure 3-14 respectively. It is seen that in most cases the computed success rates of LAMBDA are higher than MIICD, particularly for the dual constellation case as evidenced in Figure 3-15. However, the actual statistics for success rates are the same from both methods.

Table 3-3 summarises the statistics of LAMBDA and MIICD methods in the cases of Scenario 3 and Scenario 4.

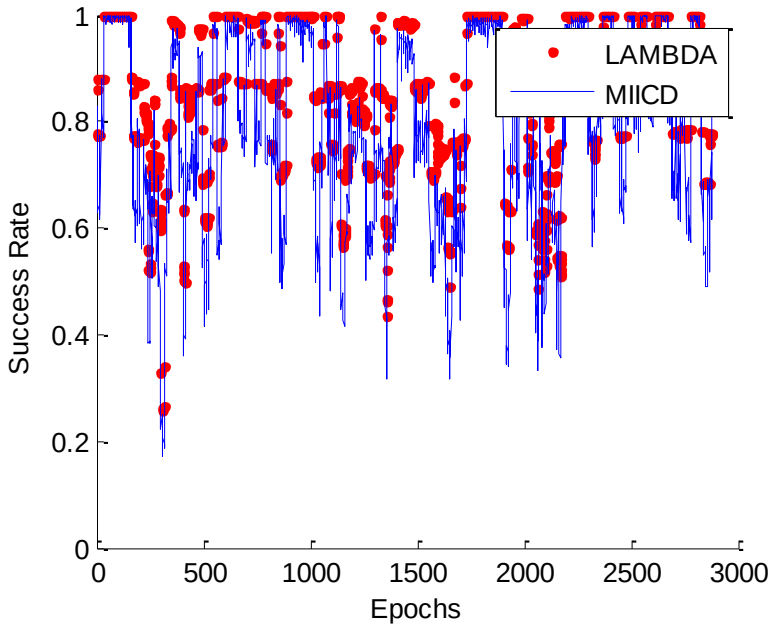

Figure 3-13 Computed success rates, resulting from LAMBDA and MIICD with Scenario 3

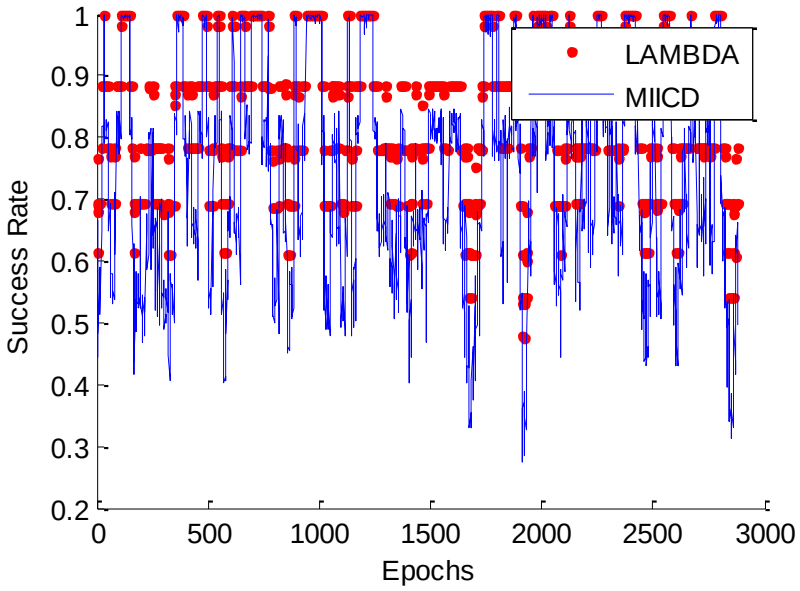

Figure 3-14 Computed success rates, resulting from LAMBDA and MIICD with Scenario 4

Table 3-3 MIICD with respect to LAMBDA: data epochs with Lower condition numbers and search numbers and success rates derived from the 24-h data set

	Scenario3	Scenario 4
Condition numbers	2265 (78.65%)	2816(97.78%)
Search numbers	2849(98.92%)	2880(100%)
Computed success rates	2878(99.93%)	2880(100%)
Actual success rates	0(0%)	0(0%)

From the above figures and tables, we can obtain the following useful observations:

- MIICD has better performance than LAMBDA in terms of condition numbers and search grid point numbers, especially in the high dimension case and the dual constellation case. For instance, 97.78% of the condition numbers and 100% of the search grid point numbers of MIICD method are smaller than those of LAMBDA method. In terms of the condition numbers, the improvement percentage (78.65%) of Scenario 3 is very close to the simulated case (78.33%) of Scenario 1;
- In terms of computed success rates of integer ambiguity bootstrapping solutions, the success rates of LAMBDA method is mostly higher than MIICD method. But both methods lead to the same actual success rates (100%). This may indicate that the bootstrapping success rate bound formula may not suit MIICD method well.

3.5 Conclusions

Effective decorrelation is the key to reliable and fast phase ambiguity resolution in GNSS real time data processing. Several decorrelation techniques have been developed and their performance have been discussed with a main focus on condition numbers. Although the inverse integer Cholesky decorrelation (IICD) method may outperform the LAMBDA method and LLL algorithm as shown through numerical analysis with random simulation (Xu, 2001), its performance with real world data has not been reported.

In this contribution, we have proposed a modified inverse integer Cholesky decorrelation (MIICD). Four different experiments from respective simulation data and real data have demonstrated that further improvement has been achieved by MIICD. In general, results from both random simulation and real data have suggested that MIICD can provide superior performance in most of the situations. In particular, the MIICD method can significantly reduce the condition numbers, at 78.65% and 97.78% of times, search numbers at 98.92% and 100% of times in single and dual constellation cases, respectively, comparing with the LAMBDA method. This performance improvement demonstrates its potential benefits for real world GNSS ambiguity resolution data processing.

3.6 Reference

Chang, X. W., and Zhou, T. (2007). MILES: MATLAB package for solving Mixed Integer LEast Squares problems. GPS Solutions, 11(4), 289-294.

De Jonge, P., and Tiberius, C. (1996). The LAMBDA method for integer ambiguity estimation: implementation aspects. Publications of the Delft Geodetic Computing Centre, 12.

Feng, Y. (2005). Future GNSS Performance Predictions Using GPS with a Virtual Galileo Constellation. GPS World, 16(3), 46-52.

Feng, Y. and Wang, J. (2010). Computed success rates of various carrier phase integer estimation solutions and their comparison with statistical success rates. Journal of Geodesy, 85: 93-103.

Grafarend, E. W. (2000). Mixed Integer-Real Valued Adjustment (IRA) Problems: GPS Initial Cycle Ambiguity Resolution by Means of the LLL Algorithm. GPS Solutions, 4(2), 31-44.

Hassibi, A., and Boyd, S. (1998). Integer parameter estimation in linear models with applications to GPS. IEEE Transactions on signal processing, 46(11), 2938-2952.

Henkel, P. A. G., Christoph (2007). Integrity Analysis of Cascade Integer Ambiguity Resolution with Decorrelation Transformations. Paper presented at the National Technical Meeting of the Institute of Navigation (NTM '07), San Diego, California, USA.

Henkel, P., and Günther, C. (2010). Partial integer decorrelation: optimum trade-off between variance reduction and bias amplification. Journal of Geodesy, 84: 51-63.

Lenstra, A. K., Lenstra, H. W., & Lovász, L. (1982). Factoring polynomials with rational coefficients. Mathematische Annalen, 261(4), 515-534.

Li, B., and Shen, Y. (2010). Global Navigation Satellite System Ambiguity Resolution with Constraints from Normal Equations. Journal of Surveying Engineering, 136(2), 63-71.

Luk, F. T., and Qiao, S. (2007). Numerical properties of the LLL algorithm. Paper presented at the Advanced Signal Processing Algorithms, Architectures, and Implementations XVII, Franklin T. Luk, Editors, 669703.

Luk, F. T., and Tracy, D. M. (2008). An improved LLL algorithm. Linear Algebra and its Applications, 428(2-3), 441-452.

Sanzheng, Q. (2008). Integer least squares: sphere decoding and the LLL algorithm. Paper presented at the Proceedings of the 2008 C3S2E conference.

Svendsen, J. (2006). Some properties of decorrelation techniques in the ambiguity space. GPS Solutions, 10(1), 40-44.

Teunissen, P. J. G. (1995). The least - squares ambiguity decorrelation adjustment: a method for fast GPS integer ambiguity estimation. Journal of Geodesy, 70(1), 65-82.

Teunissen, P. J. G., De Jonge, P. J., & Tiberius, C. (1995). The LAMBDA-Method for fast GPS Surveying. Proceedings of International Symposium GPS technology applications, Bucharest, Romania, September 26-29, pp. 203-210.

Teunissen, P., De Jonge, P., & Tiberius, C. (1996). The Volume of the GPS Ambiguity Search Space and its Relevance for Integer Ambiguty Resolution. Proceedings of ION GPS-96, 9th International Technical Meeting of the Satellite Division of the Institute of Navigation, Kansas City, Missouri, Sept. 17-20, pp. 889-898.

Teunissen, P. J. G., De Jonge, P. J., & Tiberius, C. C. J. M. (1997). The least-squares ambiguity decorrelation adjustment: its performance on short GPS baselines and short observation spans. Journal of Geodesy, 71(10), 589-602.

Teunissen, P. J. G. (1998). Success probability of integer GPS ambiguity rounding and bootstrapping. Journal of Geodesy, 72(10), 606-612.

Verhagen, S. (2003). On the approximation of the integer least-squares success rate: which lower or upper bound to use. Journal of Global Positioning Systems, 2(2), 117-124.

Xu, P. (2001). Random simulation and GPS decorrelation. Journal of Geodesy, 75(7-8), 408-423.

Xu, P. (2002). Isotropic probabilistic models for directions, planes and referential systems. Proceedings of the Royal Society London, Series A, 458, 2017–2038.

Chapter 4: Orthogonality Defect and Search Space Size for Solving Integer Least-Squares Problems

Statement of Contribution of Co-Authors

The authors listed below have certified that:

1. they meet the criteria for authorship in that they have participated in the conception, execution, or interpretation, of at least that part of the publication in their field of expertise;
2. they take public responsibility for their part of the publication, except for the responsible author who accepts overall responsibility for the publication;
3. there are no other authors of the publication according to these criteria;
4. potential conflicts of interest have been disclosed to (a) granting bodies, (b) the editor or publisher of journals or other publications, and (c) the head of the responsible academic unit, and
5. they agree to the use of the publication in the student's thesis and its publication on the Australasian Digital Thesis database consistent with any limitations set by publisher requirements.

In the case of this chapter:

Contributor	**Statement of contribution**
Jun Wang	Conducted all the experiments and data analysis, wrote the manuscript
Yanming Feng	Reviewed and revised the manuscript

Principal Supervisor Confirmation

I have sighted email or other correspondence from all co-authors confirming their certifying authorship.

Yanming Feng		20-October-2012
Name	Signature	Date

Orthogonality Defect and Search Space Size for Solving Integer Least-Squares Problems

Jun Wang, Yanming Feng

Faculty of Science and Technology

Queensland University of Technology, Australia

Phone: +61 7 31389111, Fax: +61 7 31389390, Email: jun.wang@student.qut.edu.au

Abstract

In the context of ambiguity resolution (AR) of Global Navigation Satellite Systems (GNSS), decorrelation among entries of an ambiguity vector, integer ambiguity search and ambiguity validations are three standard procedures for solving integer least-squares problems. This paper contributes to AR issues from three aspects. Firstly, the orthogonality defect is introduced as a new measure of the performance of ambiguity decorrelation methods, and compared with the decorrelation number and with the condition number which are currently used as the judging criterion to measure the correlation of ambiguity variance-covariance matrix. Numerically, the orthogonality defect demonstrates slightly better performance as a measure of the correlation between decorrelation impact and computational efficiency than the condition number measure. Secondly, the paper examines the relationship of the decorrelation number, the condition number, the orthogonality defect and the size of the ambiguity search space with the ambiguity search candidates and search nodes**.** The size of the ambiguity search space can be properly estimated if the ambiguity matrix is decorrelated well, which is shown to be a significant parameter in the ambiguity search progress. Thirdly, a new ambiguity resolution scheme is proposed to improve ambiguity search efficiency through the control of the size of the ambiguity search space. The new AR scheme combines the LAMBDA search and validation procedures together, which results in a much smaller size of the search space and higher computational efficiency while retaining the same AR validation outcomes. In fact, the new scheme can deal with the case there are only one candidate, while the existing search methods require at least two candidates. If there are more than one candidate, the new scheme turns to the usual ratio-test procedure. Experimental results indicate that this combined method can indeed improve ambiguity search efficiency for both the single constellation and dual constellations respectively, showing the potential for processing high dimension integer parameters in multi-GNSS environment.

Keywords: *Condition number · Orthogonality defect · Ambiguity search-space size · GNSS ambiguity decorrelation ·*

4.1 Introduction

Correct integer ambiguity resolution is a prerequisite for centimeter real-time kinematic (RTK) positioning with double-differenced phase measurements. To fix the phase ambiguities into integers, the first step is to obtain float ambiguity solutions and the corresponding variance-covariance (vc-) matrix using the standard least-squares estimation. In the second step, the real-valued float solution of the ambiguities is mapped into integer values. Integer rounding, integer bootstrapping and integer least-squares are three integer estimators. The ILS method has been proved to be the optimal one as it achieves the maximal success rate of ambiguity resolution (AR) (Teunissen 1999) among the three methods. Much research effort has been given to this topic over nearly two decades, including the least-squares ambiguity decorrelation adjustment (LAMBDA) method by Teunissen (1993). The third step of AR is the ambiguity validation procedure, which is essentially a discrimination test to decide whether a set of integers is acceptable as the correct solution. The test methods may refer to the difference-test (Tiberius and Jonge 1995), the projector-test (Han 1997), the W ratio-test (Wang et al. 1998) and the ratio-test (Euler and Schaffrin 1990; Teunissen and Verhagen 2009). Once the integer solutions are found, the remaining real-valued parameters, such as user-position states, can be updated due to the correlation with the ambiguities.

The entire ILS estimation for AR consists of three processes: decorrelation, integer search and ambiguity validation. The decorrelation process is also known as a reduction process in lattice theory to make the search process easier and more efficient (Chang and Zhou 2007). A few methods have been proposed for AR, including the integer Gaussian decorrelation (Teunissen 1993), the Lenstra–Lenstra–Lovász (LLL) algorithm (Hassibi and Boyd 1998), the united ambiguity decorrelation (Liu et al. 1999), the inverse integer Cholesky decorrelation (Xu 2001), the paired Cholesky integer transformation (Zhou 2010), and the modified inverse integer Cholesky decorrelation (Wang et al. 2010). In order to evaluate the performance of the decorrelation process, the decorrelation number was introduced as a measure of the diagonality of the transformed matrix (Teunissen 1993, 1994). The decorrelation number equals one when the matrix is completely decorrelated, and is close to zero when poorly decorrelated. Many other researchers use the

condition number as the index to measure the correlation and to compare different decorrelation techniques (Liu et al. 1999; Xu 2001; Svendsen 2006; Wang et al. 2010; Zhou 2010). A better decorrelation technique is expected to achieve a smaller condition number. The concept of the orthogonality defect is to evaluate the quality of reduced lattice vectors for a reduction process (Eisenbrand 2010). Since lattice theory can be applied to solve an ILS problem, it is natural to consider use of this parameter to evaluate decorrelation performance. As a result, the concept of the orthogonality defect is introduced as a possible index to analyze the decorrelation process.

The search process of integer ambiguities can be performed on the original ambiguities as well, however, the efficiency is much lower than that of the decorrelation transformed ambiguities (De Jonge and Tiberius 1996). Teunissen (1993, 1994) used the least-squares ambiguity search (LSAS) criterion in the LAMBDA method. The search is implemented through LDL^T decomposition and sequential conditional least-squares estimation. Cai (2009) developed a so-called total optimal search criterion for resolving integer ambiguities in both coordinate and ambiguity domains and proved that the total optimal search criterion and the LSAS criterion led to the same objective function and the same numerical results. Setting the size of the search space is an important aspect because it is relevant to the number of search grid points, which implies the efficiency of a search process. The search space (ellipsoidal region) is centered at the float ambiguity solution $\hat{\mathbf{N}}$, while the shape and orientation are governed by the corresponding vc-matrix $\mathbf{Q}_{\hat{\mathbf{N}}}$; its size can be controlled by the constant χ^2 (Teunissen et al. 1996). Some qualitative characteristics of the volume of GPS ambiguity search space and its relevance to AR have already been discussed in previous work (Teunissen et al. 1996). The quantitative evaluation of the size χ^2 may help understand its impact on the integer search efficiency. Figure 4-1 shows an example of two-dimensional ILS pull-in regions, constraint ellipsoidal regions and minimum volume boxes (Teunissen 1995; Hassibi and Boyd 1998) for an original ambiguity vc-matrix and the corresponding decorrelated matrix respectively. Figure 1 also shows that the area of the search ellipsoidal space is kept constant (the same number of dots in the ellipsoid), whereas the area of the minimum volume box is reduced in the decorrelation process (seeing

no blue dots in the right box). It is worth noting that not only has the shape of the minimum volume box been changed but also the area has reduced during the decorrelation process. An undersized χ^2 will fail to contain the correct solution, while an oversized χ^2 will contain too many redundant ones. If the size χ^2 of the search ellipsoid contains only the correct integer solution, (e.g., see the red ellipse in Figure1), the search efficiency is much higher than those with larger χ^2 values. Hence study of both the variation of the size χ^2 during the ambiguity decorrelation process and the choice of χ^2 in the ambiguity search process is of interest. In practice, the bootstrapped integer solution (after decorrelation) has been used to set the size of the search space in the released LAMBDA method (De Jonge and Tiberius 1996). Meanwhile, the success rate of integer bootstrapping has been proved to be very close to the success rate of ILS (Teunissen 1998; Feng and Wang 2011).

In addition, searching the second-best integer ambiguity candidates is needed for the validation purpose, based on the ratio-test, for instance. This implies that the ellipsoidal region should contain at least two sets of integer candidates. In fact, since the search ellipsoidal region of two integer candidates is larger than the region which contains a single integer candidate, the minimum volume box, along with the search steps, is consequently increased with the same search rules. Unlike the traditional AR procedure, which processes ambiguity validation after obtaining two integer candidates and decorrelated vc-matrices, the new scheme builds the validation requirement into the integer search process, in order to reduce the majority of redundant search nodes or grid points. Studying efficient AR schemes is motivated by the needs to deal with a much higher dimension of integer parameters in processing multi-GNSS and multi-frequency carrier phase measurements.

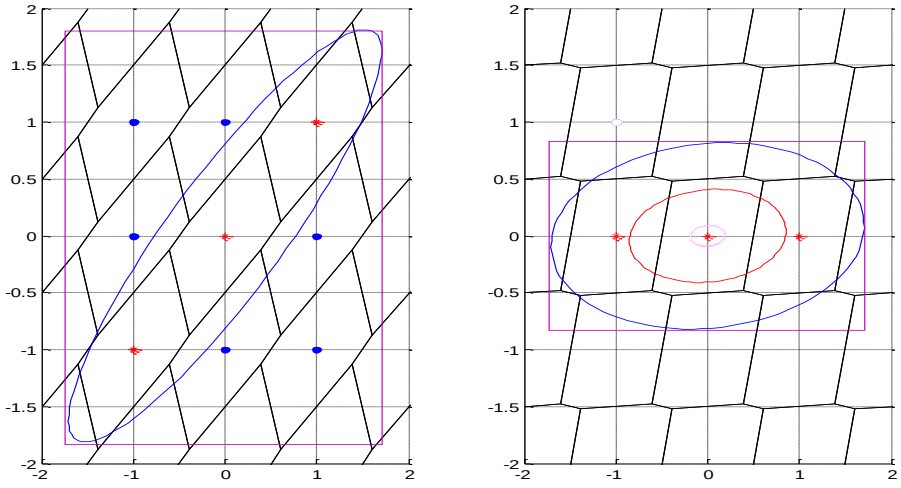

Figure 4-1 Illustrations of two-dimensional ILS pull-in regions and minimum volume boxes covering the ellipsoidal regions for the original ambiguity vc-matrix (left) and decorrelated vc-matrix, respectively. The blue dots stand for search grid points in minimum volume box; and the red dots for those falling in to the ellipsoidal region.

The remainder of this paper is organized as follows. Section 4.2 *Integer Least-Squares* describes the problem of integer least-squares and the general ILS procedure. Section 4.3 *A Proposed AR Scheme* briefly reviews the LAMBDA method, with special attention paid to the size of ambiguity search space. The section also presents a new AR scheme that combines the LAMBDA search and validation procedures together. In Section 4.4 *Measure of Decorrelation Performance*, three parameters − decorrelation number, condition number and orthogonality defect, are examined as indicators of the measure of decorrelation performance. In Section 4.5 *Experiments and Analysis*, numerical analysis is provided to examine the correlation of both the ambiguity search node number and the candidate number with the three measures of decorrelation performance and with the size of the search space respectively. The analysis also demonstrates the advantages of the proposed AR scheme. Finally, the main research findings achieved in this work are summarized.

4.2 Integer Least-Squares

The GNSS linear observation equations are generally expressed as

$$\mathbf{L}=\mathbf{A}\delta\mathbf{x}+\mathbf{B}\mathbf{N}+\mathbf{e} \quad (1)$$

and the criterion

$$\min_{\delta x,N}\left\{\left\|\mathbf{L}-\mathbf{A}\boldsymbol{\delta}\mathbf{x}-\mathbf{B}\mathbf{N}\right\|_{\mathbf{Q}_L}^2,\boldsymbol{\delta}\mathbf{x}\in R^n,\mathbf{N}\in Z^p\right\} \tag{2}$$

where **L** is the m-vector of 'observed minus computed' double-difference (DD) observations; **A** is the $m\times n$ design matrix for the vector of real-valued unknowns $\boldsymbol{\delta}\mathbf{x}$; **B** is the $m\times p$ design matrix for the vector of integer DD ambiguities N; $\mathbf{Q}_\mathbf{L}$ is the variance matrix of observables; **e** is the vector of unmodelled effects and measurement noise; and $\|\cdot\|_{\mathbf{Q}_L}^2=(\cdot)^T\mathbf{Q}_L^{-1}(\cdot)$. The solution of the problem (2) is equivalent to the solution of the integer least-squares problem

$$\breve{\mathbf{N}}=\arg\min_{\mathbf{N}\in Z^p}\left\{\left\|\hat{\mathbf{N}}-\mathbf{N}\right\|_{\mathbf{Q}_{\hat{\mathbf{N}}}}^2\right\} \tag{3}$$

where $\hat{\mathbf{N}}$ is a float ambiguity vector with the variance matrix $\mathbf{Q}_{\hat{\mathbf{N}}}$ and $\breve{\mathbf{N}}$ is the estimated integer ambiguity vector. In general, $\mathbf{Q}_{\hat{\mathbf{N}}}$ has high correlation due to the geometry and correlation between DD measurements. Hence, the search space is highly elongated. In order to make the search process easier and more efficient, different decorrelation techniques have been developed. The essence of decorrelation is to apply an admissible integer unimodular matrix **Z** to eliminate the off-diagonal elements of $\mathbf{Q}_{\hat{\mathbf{N}}}$ or to reduce the size of the correlation coefficients. This can be expressed as

$$\hat{\mathbf{N}}_{\mathbf{dec}}=\mathbf{Z}\hat{\mathbf{N}},\ \mathbf{N}_{\mathbf{dec}}=\mathbf{Z}\mathbf{N},\ \mathbf{Q}_{\hat{\mathbf{N}}_{\mathbf{dec}}}=\mathbf{Z}\mathbf{Q}_{\hat{\mathbf{N}}}\mathbf{Z}^{\mathbf{T}} \tag{4}$$

Therefore the ILS problem (3) is transformed to

$$\breve{\mathbf{N}}_{\text{dec}} = \underset{\mathbf{N}_{\text{dec}} \in Z^p}{\arg\min} \left\{ \left\| \hat{\mathbf{N}}_{\text{dec}} - \mathbf{N}_{\text{dec}} \right\|^2_{\mathbf{Q}_{\hat{\mathbf{N}}_{\text{dec}}}} \right\} \tag{5}$$

Due to the integer constraint $\mathbf{N}_{\text{dec}} \in Z^p$, the solution of (5) must be obtained by virtue of a search process. The ambiguity search space is defined as

$$\left\| \hat{\mathbf{N}}_{\text{dec}} - \mathbf{N}_{\text{dec}} \right\|^2_{\mathbf{Q}_{\hat{\mathbf{N}}_{\text{dec}}}} \leq \chi^2 \tag{6}$$

An integer-ambiguity search tree example for 3 ambiguity elements is depicted in Figure 4-2. A search node is a record consisting of one or more grid points in the search space that links to other nodes. A search candidate vector is defined as a rooted tree that contains a leaf node of the bottom level (De Jonge and Tiberius 1996; Knuth 1997). For instance, the level of z3 has nodes {4} and {5}, while a full candidate can be {4 4 2}. Both search candidate and search node can be used as indices to evaluate the search efficiency of the ILS method.

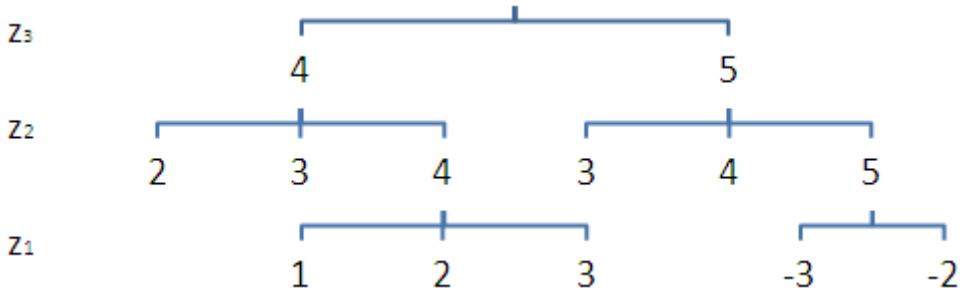

Figure 4-2 The search nodes and candidates in an integer-ambiguity search tree

4.2.1 Ratio-Test

For ambiguity validation purposes, most validation techniques need at least two sets of integer candidates with the minimum quadratic form of integer ambiguities

residuals, and the second-minimum one. The ratio-test, a popular discrimination test and, is given as

$$\text{Accept } \breve{\mathbf{N}} \text{ if: } \frac{\left\|\hat{\mathbf{N}}-\breve{\mathbf{N}}_2\right\|^2_{\mathbf{Q}_{\hat{\mathbf{N}}}}}{\left\|\hat{\mathbf{N}}-\breve{\mathbf{N}}\right\|^2_{\mathbf{Q}_{\hat{\mathbf{N}}}}} \geq k \tag{7}$$

where $\breve{\mathbf{N}}_2$ is the second-best integer ambiguity candidate and k is an empirically tolerance value. The ratio-test actually tests the closeness of the float ambiguity to its nearest integer candidate. The critical value of k actually determines how much closeness the user will choose. In general k can be chosen as 2 or 3 (Leick 2004). Teunissen and Verhagen (2009) propose an alternative approach to choose k based on setting a threshold for the failure rate, which makes the acceptance test model-driven. This approach does not affect the following proposed scheme.

4.3 A Proposed AR Scheme

The LAMBDA method (Least-squares AMBiguity Decorrelation Adjustment) was proposed to estimate the integer ambiguity of carrier phase measurement based on the float ambiguities and their vc-matrix (Teunissen 1993, 1994). It consists of two stages: decorrelation and search. A detailed description of this method is given by de Jonge and Tiberius (1996). In this work, special attention is paid to the ambiguity search space which is a multivariate ellipsoidal region. As Teunissen (1996) noted, "From the point of view of computational efficiency, it is important that the search for the integer least-squares solution, and in case of validation, also the search for the next-best integer solution, can be performed in a speedily manner". We will demonstrate the importance of the ambiguity search space in both their aspects.

4.3.1 The ambiguity search space

The ambiguity search space is already defined in (6) and discussed previously. The volume of the ellipsoidal region is given by

$$V_n = \chi^n U_n \sqrt{\left|\mathbf{Q}_{\hat{\mathbf{N}}}\right|} \tag{8}$$

where n is the dimension of the vc-matrix $\mathbf{Q}_{\hat{\mathbf{N}}}$. According to Teunissen (1996), the volume V_n gives a good indicator of the number of grid points inside the search space if the number of candidates is large enough. The volume of the unit sphere U_n is given as

$$U_n = \pi^{n/2} / \Gamma(n/2+1) \tag{9}$$

where $\Gamma(x)$ is the gamma function. Obviously, given the matrix $\mathbf{Q}_{\hat{\mathbf{N}}}$, the order n and the volume V_n, it is easy to compute the size χ^2 of the ambiguity search space based on (8). However, when the number of required candidates is small, for instance, less than n, the relation of (8) is not accurate and the size χ^2 is generally much larger than needed, which would be detrimental for the search efficiency. The algorithm of calculating χ^2 implemented in the LAMBDA method is based on the bootstrapping estimator to guarantee the required number of candidates to be not more than a few (De Jonge and Tiberius 1996; Joosten 2001). The bootstrapped estimator sequentially determines the integers as follows:

$$\begin{aligned}
&\breve{N}_{b,1} = \left[\hat{N}_1 \right] \\
&\breve{N}_{b,2} = \left[\hat{N}_{2|1} \right] = \left[\hat{N}_2 - \sigma_{\hat{N}_2\hat{N}_1} \sigma_{\hat{N}_1}^{-2} (\hat{N}_1 - \breve{N}_{b,1}) \right] \\
&\quad \vdots \\
&\breve{N}_{b,n} = \left[\hat{N}_{n|N} \right] = \left[\hat{N}_n - \sum_{i=1}^{n-1} \sigma_{\hat{N}_n\hat{N}_{i|I}} \sigma_{\hat{N}_{i|I}}^{-2} (\hat{N}_{i|I} - \breve{N}_{b,i}) \right]
\end{aligned} \tag{10}$$

where the shorthand notation $\hat{N}_{i|I}$ stands for the *i*th float ambiguity obtained through a condition on the previous $I = \{1,...,(i-1)\}$ sequentially rounded ambiguities. In other words, the integer vector $\breve{\mathbf{N}}_b$ is determined within the search space $\chi^2 = \left\| \breve{\mathbf{N}}_b - \hat{\mathbf{N}} \right\|^2_{\mathbf{Q}_{\hat{\mathbf{N}}_b}}$. We can obtain more other candidates $\breve{\mathbf{N}}^p$ with small norms

$\left\|\breve{\mathbf{N}}^{p}-\hat{\mathbf{N}}\right\|$ by rounding all ambiguities but one to their nearest integer, and one ambiguity to the next-nearest integer (De Jonge and Tiberius 1996). Both $\breve{\mathbf{N}}_{b}$ and $\breve{\mathbf{N}}^{p}$ can be used to form the search space. For instance, if the second set of candidates is requested, we can use the candidate $\breve{\mathbf{N}}^{p}$ with the second-smallest norm instead of $\breve{\mathbf{N}}_{b}$, to assure that the requested number of candidates will be obtained within the search space.

4.3.2 A proposed AR scheme

Current validation procedures require both the integer least-squares estimate $\breve{\mathbf{N}}$ and the second-best candidate set $\breve{\mathbf{N}}_{2}$. If the size χ^{2} is large, it would take a long time to search integer solutions $\breve{\mathbf{N}}$ and $\breve{\mathbf{N}}_{2}$, which is detrimental to the computational efficiency. Figure 4-3 shows the ambiguity search space with different ellipsoidal region sizes, shapes and orientations. The area of red ellipse is determined by the float solution and the closest integer solution, while the area of the black ellipse is two times of that of the red ellipse. Δ indicates the float ambiguity. The left picture has the same ambiguity variance matrix with the middle one but a different float ambiguity; while it has the same float ambiguity with the right picture but a different ambiguity variance matrix. The left one shows that the black ellipse contains two candidates while the middle one and the right one only contains one candidate due to the search space sizes, shapes and orientations. It implies that though the method of setting the size χ^{2} and the number of requested candidates are the same, the search efficiency can be different. This is to say that the area of black ellipse does not necessarily cover two candidates in the search space. In other words, other close candidates are located outside the black ellipse, or the area of the black ellipse is smaller than those determined by other candidates. It is easy to infer that the values of ratio-test in the middle and right of the figure will be larger than 2, even the value of the second candidate is not known. This fact implies that if the ratio-test can be guaranteed to pass for a given critical value, there is no need to find the second-best integer candidate set. Figure 4-4 shows increased search nodes with different search space sizes by comparing the exact norm of the second candidate set, the original search space size χ^{2} and the new search space size χ^{2}. Four simulation experiments are considered and the number of samples in each case is 1000. The exact norm of

second candidate is computed directly from $\left\|\hat{\mathbf{N}}-\breve{\mathbf{N}}_2\right\|^2_{\mathbf{Q}_{\hat{\mathbf{N}}}}$, the original χ^2 is obtained by the sub-function *chistart* of LAMBDA method (Joosten 2001), and the new χ^2 is equal to $2\cdot\left\|\hat{\mathbf{N}}-\breve{\mathbf{N}}\right\|^2_{\mathbf{Q}_{\hat{\mathbf{N}}}}$. It can be clearly seen that when the *k* value of ratio-test is larger or equal to 2, the increased search nodes are significantly reduced.

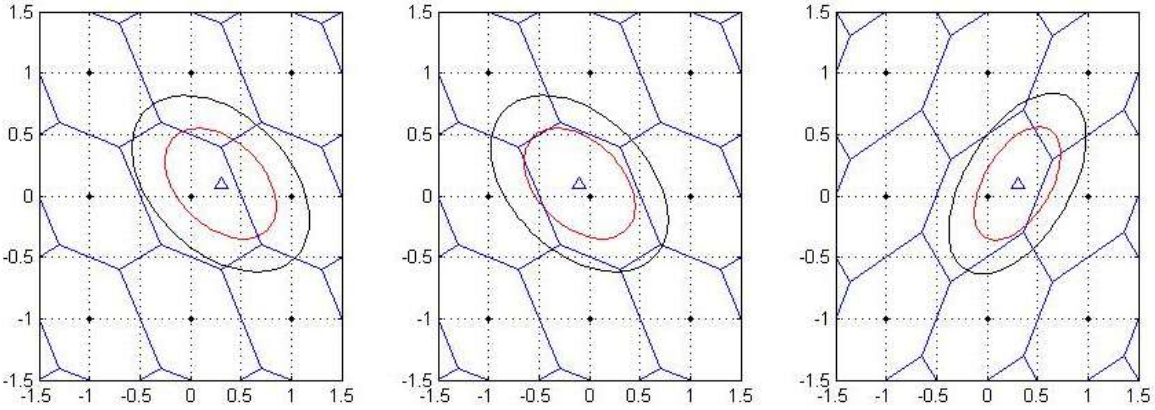

Figure 4-3 Illustrations of two-dimensional ambiguity search space with different sizes, shapes and orientations.

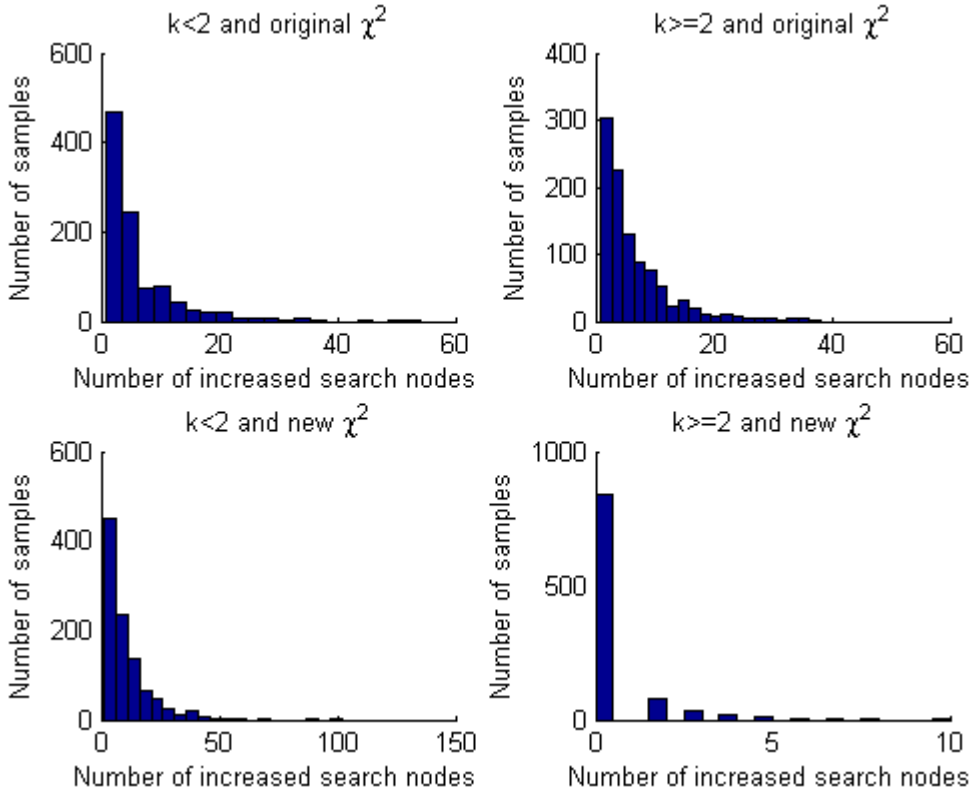

Figure 4-4 Illustrations of increased search nodes for searching the second candidate with different search space sizes comparing the exact norm of the second candidate.

Based on the above visual analysis, we propose a new AR scheme which does not necessarily require the solution $\breve{\mathbf{N}}_2$ but can still meet the validation purpose. The new scheme can deal with the case where there is only one candidate. When there are more than one candidate, the new scheme can automatically return to the usual ratio-test procedure. This idea is shown as a flowchart in Figure 5. Compared to the original LAMBDA method, the new procedure is unique in the step of setting the adjustable search space size χ^2, which is expressed as follows

$$\chi^2 = \min\left(k \cdot \left\|\hat{\mathbf{z}} - \breve{\mathbf{N}}_b\right\|^2_{\mathbf{Q}_{\hat{\mathbf{z}}}}, \left\|\hat{\mathbf{z}} - \breve{\mathbf{N}}^p\right\|^2_{\mathbf{Q}_{\hat{\mathbf{z}}}}\right), \tag{11}$$

The equation (11) by definition ensures that the size of χ^2 is smaller than, or at most equal to, that of the *chistart* function by LAMBDA method if the candidates number is less than *n* (Joosten 2001). There are two reasons for this choice. First, the success rate of the bootstrapped integer solutions $\breve{\mathbf{N}}_b$ of the decorrelated ambiguities is a sufficiently sharp approximation of the success rate of the ILS solutions **z** (Teunissen 1998). In other words, their integer solutions are coincident with each other in most cases (Feng and Wang 2011). Second, we assume that once the ambiguity validation tests are passed, the integer solutions should be treated as if they have the same level of acceptability, though the values of discernibility or discrimination test will be different. The second reason is practical because many software packages use a fixed value as the ratio-test of the best and the second-best solutions (Leick 2004).

As the smaller value between $k \cdot \left\|\hat{\mathbf{z}} - \breve{\mathbf{N}}_b\right\|^2_{\mathbf{Q}_{\hat{\mathbf{z}}}}$ and $\left\|\hat{\mathbf{z}} - \breve{\mathbf{N}}^p\right\|^2_{\mathbf{Q}_{\hat{\mathbf{z}}}}$ is chosen, the search is performed within the smaller space defined by χ^2. However, the search space meets the validation requirement without performing the ratio-test if there is just one candidate in the search space. Because this situation can only happen when $\chi^2 = k \cdot \left\|\hat{\mathbf{z}} - \breve{\mathbf{N}}_b\right\|^2_{\mathbf{Q}_{\hat{\mathbf{z}}}}$, and the property of χ^2 already guarantees the ratio of the second-nearest solution to the best solution to be larger than *k*. When k>1, there could be more candidates to be examined and the usual ratio-test is to be performed. However,

by definition, the search space setting (11) is always smaller or at most equal to the traditional search space $\left\|\hat{\mathbf{z}}-\breve{\mathbf{N}}^{p}\right\|_{Q_{\hat{z}}}^{2}$.

The proposed procedure has been implemented in Matlab (R2010a) following the flowchart in Figure 4-5. The performance of this new AR scheme and its efficiency is demonstrated in the experimental results in section *Experiments and Analysis*.

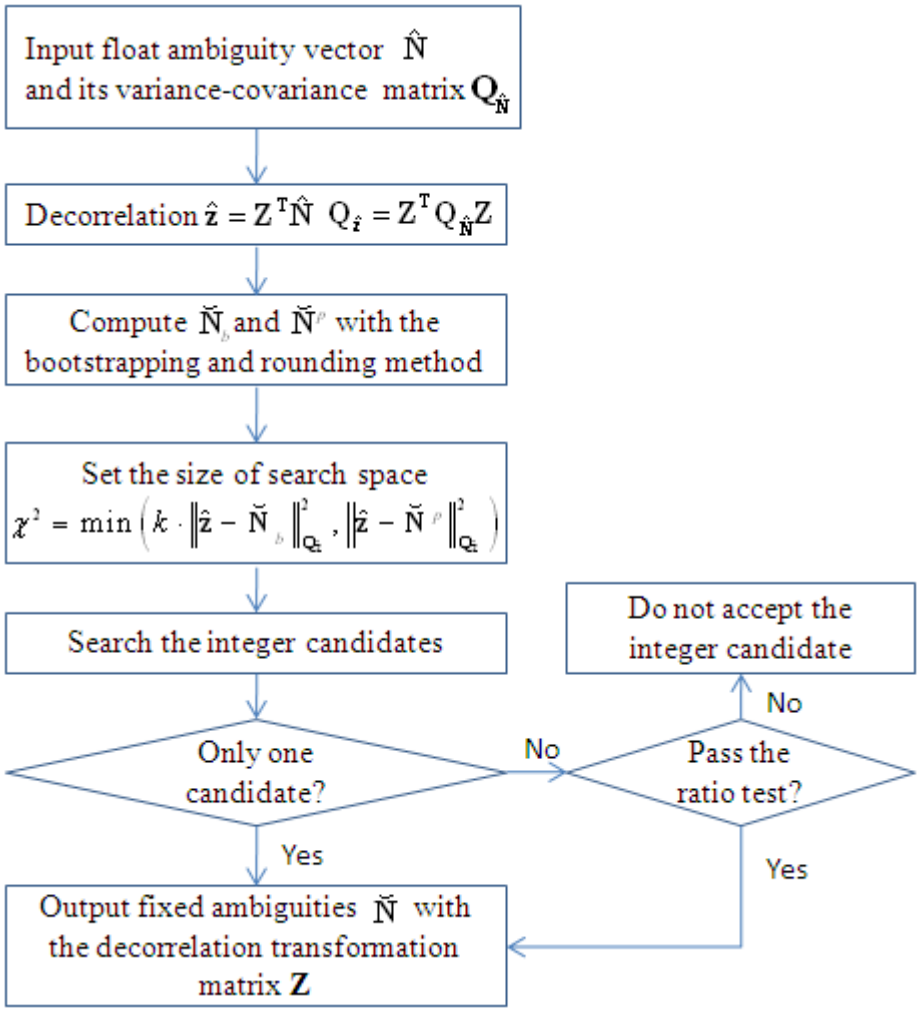

Figure 4-5 Flowchart of the proposed AR scheme

4.4 Measure of Decorrelation Performance

In addition to the decorrelation number, we also choose the condition number and the orthogonality defect to evaluate the performance of the decorrelation process. Since

an iterative procedure is used to create the integer unimodular matrix **Z** in the decorrelation stage of the LAMBDA method, we will compute the three indicators as well as the size of the search space, the number of the search candidates and the search nodes in each step to show their impact on search efficiency.

4.4.1 Decorrelation number

In two dimensions, the decorrelation number is defined as $\gamma = \sqrt{1-\rho^2}$, with ρ being the correlation coefficient between two ambiguities. Given the dimensions of a positive definite matrix **H** higher than two, the decorrelation number is defined (Teunissen 1993, 1994) as,

$$\gamma(\mathbf{H}) = \sqrt{\det(R_H)} \qquad (0 \le \gamma(\mathbf{H}) \le 1) \tag{12}$$

where R_H is the correlation matrix of **H**.

4.4.2 Condition number

Given **H**, the condition number $\kappa(\mathbf{H})$ is the ratio between the maximum and minimum eigenvalues of **H** (Xu 2001) as,

$$\kappa(\mathbf{H}) = \left| \frac{\lambda_{\max}(\mathbf{H})}{\lambda_{\min}(\mathbf{H})} \right| \tag{13}$$

4.4.3 Orthogonality defect

In order to quantitatively measure the orthogonality of a matrix, we can use the orthogonality defect $\delta(\mathbf{H})$ as a metric (Eisenbrand 2010),

$$\delta(\mathbf{H}) = \frac{\Pi_{k=1}^{N} \left\| \mathbf{h}_k \right\|}{\left| \det(\mathbf{H}) \right|} \tag{14}$$

with $\delta(\mathbf{H}) \geq 1$ for all H and $\delta(\mathbf{H}) = 1$ if and only if the columns of H are orthogonal.

We use an artificial four dimensional example to illustrate the concepts of three different decorrelation measures. Given the float ambiguity vector

$$\hat{\mathbf{N}} = \begin{bmatrix} -6.0187 & -2.0308 & -3.9991 & -0.2374 \end{bmatrix}^{'}$$

and its vc-matrix

$$\mathbf{Q}_{\hat{\mathbf{N}}} = \begin{bmatrix} 43.8803 & 1.8034 & 22.1973 & 6.3808 \\ 1.8034 & 7.7854 & 5.6033 & -2.9633 \\ 22.1973 & 5.6033 & 37.9287 & 0.4903 \\ 6.3808 & -2.9633 & 0.4903 & 2.3099 \end{bmatrix}$$

The results of different measures of decorrelation performance in each iteration step of the LAMBDA method are listed in Table 1. Note that iteration numbers {1, 2, 4, 5, 8, 9} run the operation of integer Gauss transformation, while iteration numbers {3, 6, 7} run the operation of the conditional variances permutation. These three measures of decorrelation performance change in those steps of integer Gauss transformation, while they remain invariant in other steps. From Table 4-1, we can see that decorrelation numbers are increasing while condition numbers and orthogonality defects are decreasing during the decorrelation process. However, both search candidates and search nodes have a good variation trend with the size of the search space. In the iterations {1} and {4}, though the search-space sizes and search candidates are the same, search nodes are different. This may be because although the search ellipsoidal regions have the same sizes, thus including the same number of candidates, these candidates can be found more efficiently due to the improvement of the search space geometry configuration.

Table 4-1 Properties of decorrelation performance by the LAMBDA method

Iteration number	Decorrelation number	Condition number	Orthogonality defect	Search space size	Search candidate	Search node
1	0.05	10000.00	21189.73	0.64	14	102
2	0.06	4735.76	21429.47	0.64	14	102
3	0.06	4735.76	21429.47	0.40	9	44
4	0.07	3953.81	10637.25	0.64	14	92
5	0.30	185.28	334.72	0.64	14	92
6	0.30	185.28	334.72	0.28	5	18
7	0.30	185.28	334.72	0.27	3	14
8	0.38	72.89	337.01	0.27	3	14
9	0.82	5.43	17.03	0.27	3	14

Table 4-2 shows that for a given fixed size of the search space, the number of search candidates remains unchanged, while the number of search nodes varies during the iteration process. A smaller size of the search space leads to a smaller number of search candidates. These results demonstrate that the decorrelation process influences AR from two aspects: to reduce the correlation coefficients and sizes of the ambiguity vc-matrix and to assist in reducing the size of the search space.

Table 4-2 Search candidate and search node with the same size of the search space

The size of the search space Case 1				The size of the search space Case 2			
Iteration number	Search space size	Search candidate	Search node	Iteration number	Search space size	Search candidate	Search node
1	0.27	3	30	**1**	0.64	14	102
2	0.27	3	30	**2**	0.64	14	102
3	0.27	3	26	**3**	0.64	14	92
4	0.27	3	26	**4**	0.64	14	92
5	0.27	3	26	**5**	0.64	14	92
6	0.27	3	14	**6**	0.64	14	34
7	0.27	3	14	**7**	0.64	14	29
8	0.27	3	14	**8**	0.64	14	29
9	0.27	3	14	**9**	0.64	14	29

The correlation coefficient r_{xy} is utilized as a measure of the strength of the linear relationship between two vectors (XY), given by

$$r_{xy} = \frac{\sum_{i=1}^{n}(x_i - \bar{x})(y_i - \bar{y})}{\sqrt{\sum_{i=1}^{n}(x_i - \bar{x})^2 \sum_{i=1}^{n}(y_i - \bar{y})^2}} \tag{15}$$

We calculate correlation coefficients between the three decorrelation performance measure parameters mentioned in this section, as well as search space size, with search candidate and search node respectively. Table 4-3 gives the correlation coefficients between the different factors listed in Table 4-1. It can be clearly observed that the search space size has correlation coefficients of 0.99 with the search candidate and 1 with the search node.

Table 4-3 Correlation Coefficients between different parameters

Correlation coefficients	Search candidates	Search nodes
Decorrelation number	-0.69	-0.65
Condition number	0.66	0.68
Orthogonality defect	0.65	0.64
Search-space size	0.99	1.00

4.5 Experiments and Analysis

Both simulation and real data experiments are conducted in order to verify whether the orthogonality defect can be treated as a new measure of decorrelation performance along with the decorrelation number and the condition number. We calculate the correlation coefficients between these measure parameters and the search efficiency indices: search candidates and search nodes. In terms of the simulation data, an isotropic probabilistic model is used to generate 200 samples of random positive-definite 14-dimensional matrix rather than a particular one (Xu 2002).

Figure 4-6 shows the correlation coefficients between the three decorrelation performance measures and the size χ^2 of the search space respectively, with the number of ambiguity search candidates. It is easy to find out that the correlation coefficients between the number of search candidate and the search space size are larger than the correlation coefficients between the number of search candidate and other parameters. Figure 4-7 shows the correlation coefficients between the number of ambiguity search nodes and the other four parameters from the simulation data. Figure 4-8 and Figure 4-9 show correlation coefficients of the number of the ambiguity search candidate/node and other parameters in the case of real data.

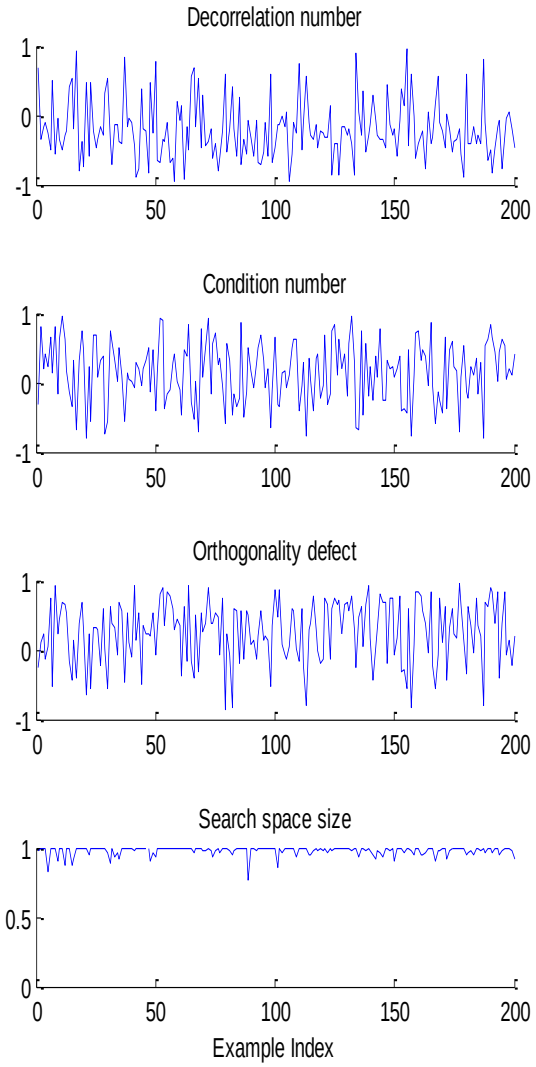

Figure 4-6 Correlation coefficients between the ambiguity search candidate number and its condition number, orthogonality defect and search-space size from the simulation data

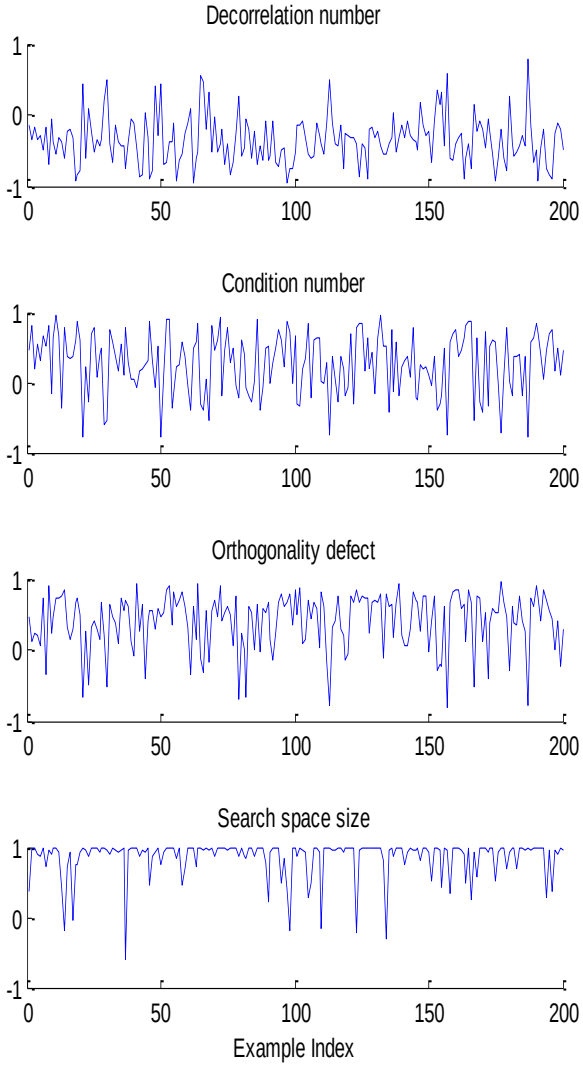

Figure 4-7 Correlation coefficients between the ambiguity search node number and its condition number, orthogonality defect and search-space size from the simulation data

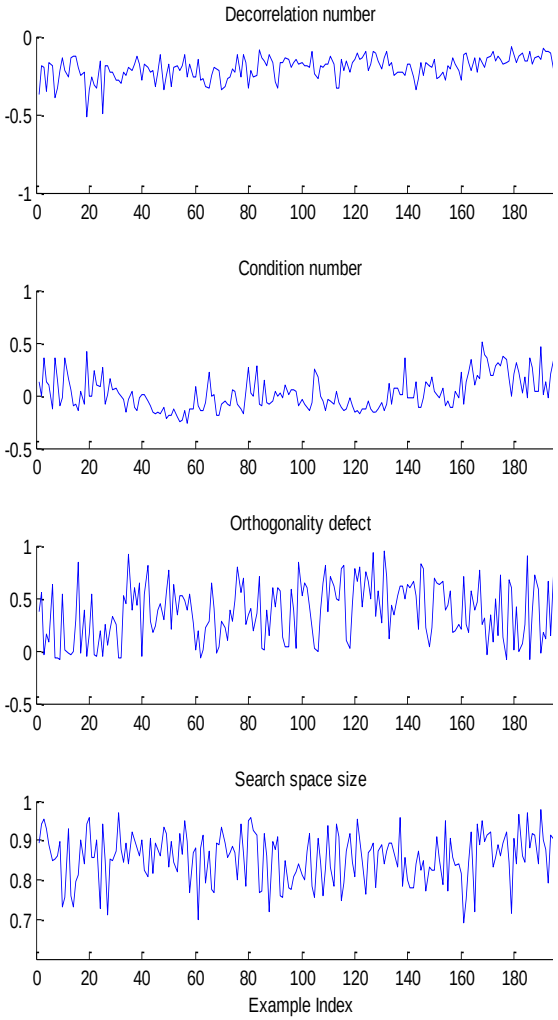

Figure 4-8 Correlation coefficients between the ambiguity search candidate number and its condition number, orthogonality defect and search-space size from a real-data set

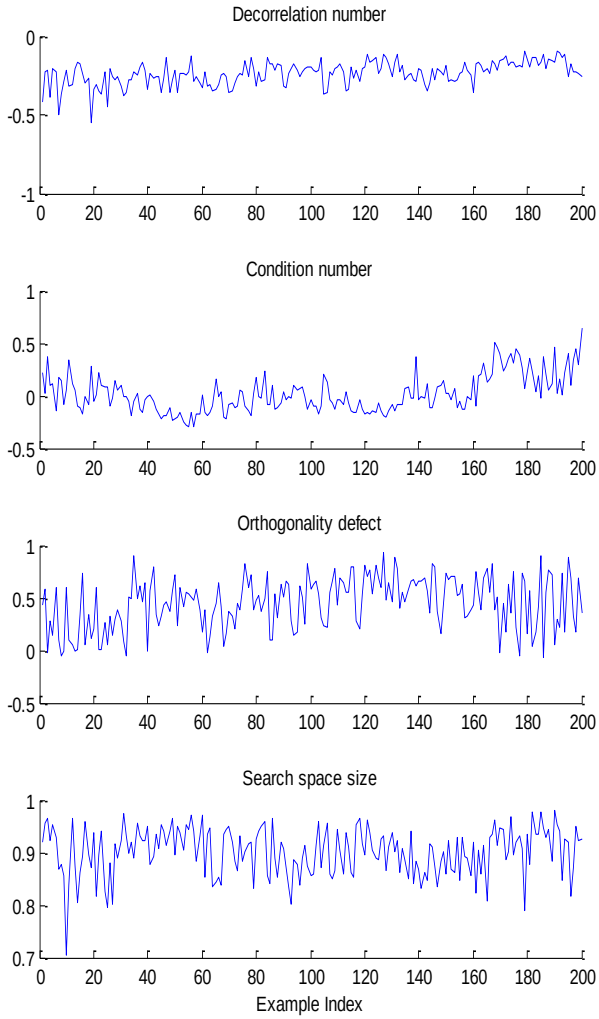

Figure 4-9 Correlation coefficients between the ambiguity search node number and its condition number, orthogonality defect and search-space size from a real-data set

The means of the correlation coefficients to quantitatively evaluate these measures of decorrelation performance are shown in Table 4-4. It is seen that the decorrelation number has negative correlation with the search candidate/node while the condition number and the orthogonality defect have positive correlation with the search candidate/node. Furthermore we observe that the overall value of the correlation coefficients between orthogonality defect and search candidate/node are higher than that of the condition number obtained from both simulation data and real data. In addition, it is clear that there is a much stronger correlation between the size of the search space and the number of search candidates/nodes. Therefore setting a suitable value of the search-space size is very important for the improvement of the computational efficiency.

Table 4-4 The Means of Correlation Coefficients

Correlation Coefficients	Simulation Data		Real Data	
	Search candidates	Search nodes	Search candidates	Search nodes
Decorrelation number	-0.20	-0.36	-0.20	-0.24
Condition number	0.15	0.27	0.03	0.02
Orthogonality defect	0.26	0.40	0.37	0.45
Search space size	0.98	0.85	0.85	0.90

We also used a dual frequency data set of a 21 km baseline to verify the better computational performance of the previously proposed ambiguity resolution scheme by comparison to the released LAMBDA. A total of 2880 epochs (24 hours) of data were available for analysis with the sample interval of 30s. The virtual Galileo constellation (VGC) method is applied to simulate the virtually real data to form the dual constellations (DCS) data set (Feng 2005). The concept is to combine the GPS measurements data sets recorded at two epochs separated by a few hours, and compute the user state parameters for the two different epochs. The critical value of k is chosen as 2 here for both cases. Figure 4-10 illustrates the computed search-space sizes based on the LAMBDA method and proposed AR scheme of GPS and DCS over the whole the observation period. The search-space sizes of the new scheme are smaller and more stable than the LAMBDA method. The χ^2 values of the LAMBDA method from most sample epochs are larger than 40, whereas the χ^2 values of the new scheme from most epochs are less than 20 in the case of GPS. In

the DCS case, it is observed that the search space size of the LAMBDA method can be as large as hundreds whereas the search space size of the new scheme remains the level of tens. Figure 4-11 shows the number of search candidates of these two AR methods. The number of search candidates of the new AR scheme is 1 in most of samples. These epochs with 1 search candidate are actually corresponding to those epochs with the predefined ratio-test value k shown in Figure 4-13. This is because the predefined confidence ellipsoidal region already implies that the ratio of these second-best solutions to best candidates is larger than the priori given tolerance value k. It is also seen that there are more epochs with more than 1 candidate of the new AR scheme in the case of DCS than those in the single constellation. Figure 4-12 compares that the numbers of search nodes computed by the new AR scheme are much less than those computed by the LAMBDA method. Especially the search node difference between these two methods becomes much larger in the case of DCS. In the worse case where the search node number are higher than the most, the new AR scheme can still guarantee that their search nodes are less or equal to that of the LAMBDA method. This characteristic of the new AR scheme is directly related to the ILS search efficiency. Figure 4-13 shows the ratio-test values of two methods. For the sake of clarity, only the ratio-test values less than 10 are shown to demonstrate the variations of the new AR scheme. The k values of the new scheme are mostly equal to 2 as the predetermined value while the ratio-test values of the LAMBDA method are mostly larger than 2. It is also shown that there are more epochs with small ratio-test value in the DCS case than in the GPS case. Referring to the fact all the AR solutions are correct in the experiment, it implies that the k value in the case of DCS should be set smaller to reduce the probability of wrong rejection (false alarm rate) by the ratio-test. The effectiveness of the new AR scheme is that the search efficiency can be improved at the acceptable cost of the smaller discrimination test value. In fact, the ratio-test values of the LAMBDA method and the new scheme are the same when k is less than the predetermined value.

Figure 4-14 shows the difference of CPU time between the LAMBDA method and the new AR scheme as well as the percentages of time saved in their search process. Since the search-space sizes of the new AR scheme are not larger than those of the LAMBDA method, ideally the search time of the new AR scheme should be always less. However, there are a few occasions where the new AR scheme costs more time

than the LAMBDA method. This is likely because of the randomness of PC computation itself. Table 4-5 summarizes the time performance of the LAMBDA method and the new AR scheme. It is confirmed that the proposed AR scheme can improve the search efficiency about 47.1% and 79.9% for GPS and DCS respectively.

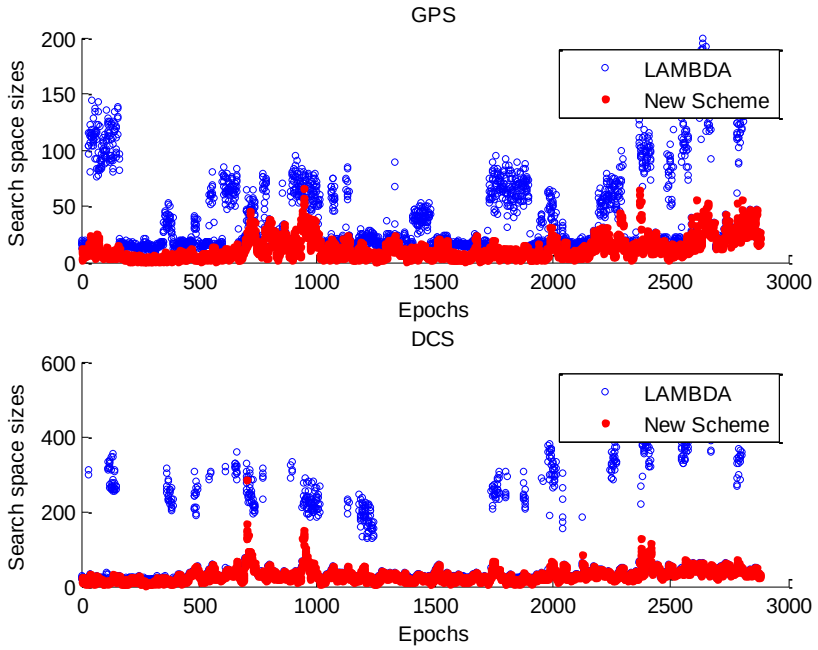

Figure 4-10 The ambiguity search-space sizes for LAMBDA and the new AR scheme of GPS and DCS

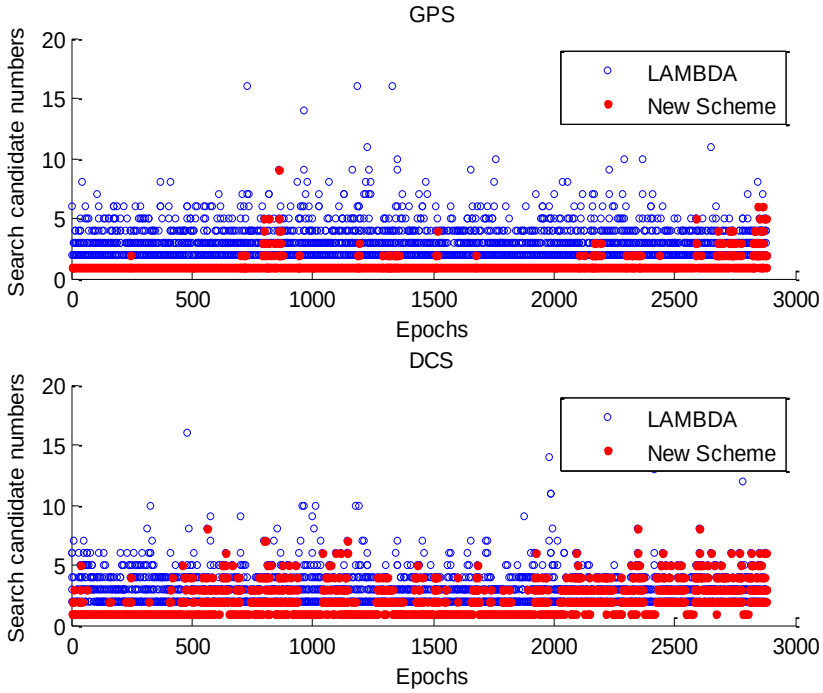

Figure 4-11 The search candidate numbers for LAMBDA and the new AR scheme of GPS and DCS

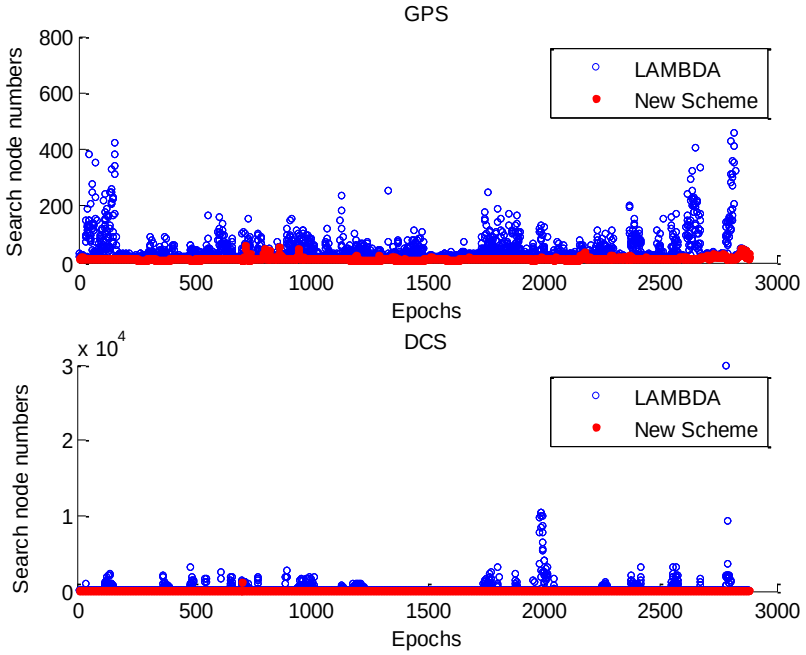

Figure 4-12 The search node numbers for LAMBDA and the new AR scheme of GPS and DCS

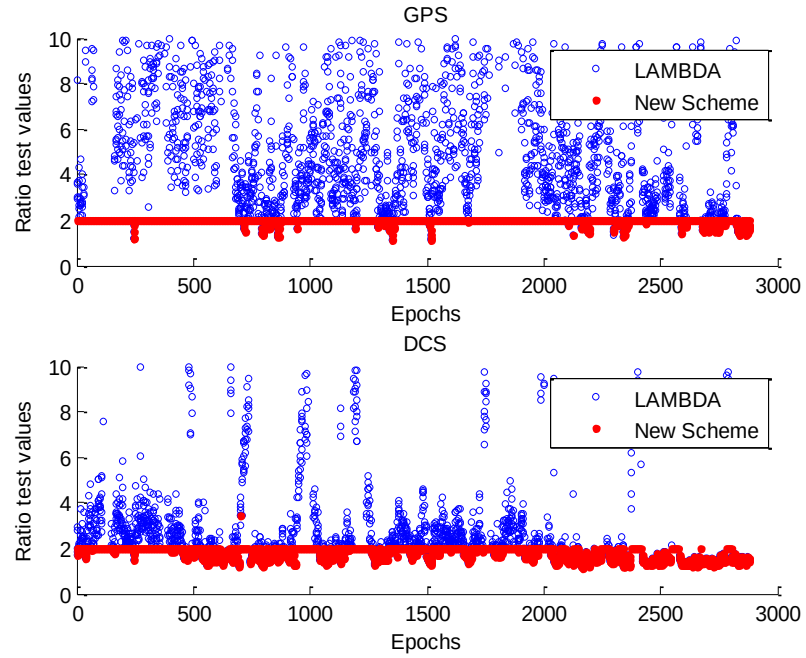

Figure 4-13 The ambiguity ratio-test values for LAMBDA and the new AR scheme of GPS and DCS

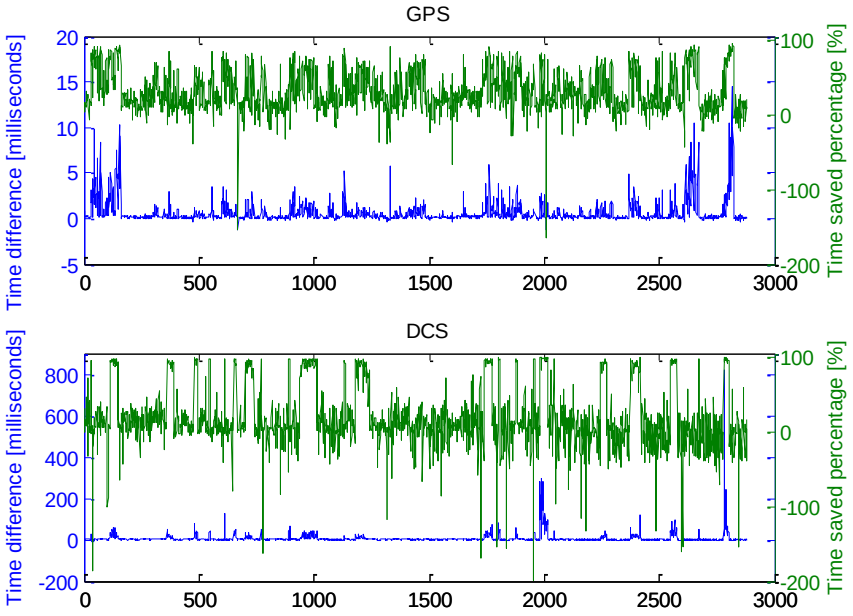

Figure 4-14 The ambiguity search CPU time difference between LAMBDA and the new AR scheme

Table 4-5 Statistical information of search CPU time for GPS and DCS case, respectively

	The mean of CPU time [milliseconds]		CPU time saved percentages
	LAMBDA	New Scheme	
GPS	1.30	0.69	47.1%
DCS	7.30	1.47	79.9%

4.6 Conclusions

The paper has investigated the properties of orthogonality defect and search-space size in GNSS integer least-squares processing and proposed a new ambiguity resolution scheme that combines the search and validation procedures. The decorrelation technique improves the search efficiency from two aspects: reducing the elongation of the search ellipsoid and precisely approximating the search-space size. The proposed new ambiguity resolution scheme combines the computation of search-space size with the ambiguity validation procedures into one procedure. The key procedure of the new scheme is to set the search-space size as $\chi^2 = \min\left(k \cdot \left\|\hat{\mathbf{z}} - \breve{\mathbf{N}}_b^1\right\|_{\mathbf{Q}_{\hat{\mathbf{z}}}}^2, \left\|\hat{\mathbf{z}} - \breve{\mathbf{N}}_b^k\right\|_{\mathbf{Q}_{\hat{\mathbf{z}}}}^2\right)$. This choice is based on the facts that (1) the success rates of the bootstrapping estimator solution $\breve{\mathbf{N}}_b$ of decorrelated ambiguities is the very sharp approximation of the success rate of the ILS solutions, thus two sets of integer solutions are mostly consistent; (2) a fixed empirically tolerance value k for the purpose of ambiguity validation is practically acceptable. The search space defined this way can meet the validation requirement without performing the ratio-test if there is just one candidate in the search space. In other words, the new scheme can deal with the case there are only one candidate, while the existing search methods require at least two candidates. It results in a smaller search-space size and higher computation efficiency, but retains the same AR validation outcomes. As a result, the same AR solutions as the usual ILS methods are obtained. In addition, the proposed AR scheme can be easily implemented following the given flowchart.

Experimental analysis for both simulated and real data sets has demonstrated that the orthogonality defect can also be utilized as a criterion of evaluating the performance

of a decorrelation method along with the decorrelation number and the condition number. However, the orthogonality defect shows better performance as a measure of the correlation between decorrelation impact and computational efficiency than the condition number as a measure in the numerical analysis. The numerical results have also shown that the search-space size is highly correlated with the efficiency of the search process.

The numerical results from the experiment with a 24 hour GPS data set have been obtained to verify the new AR scheme that combines the search and validation procedures. Particularly the setting of the search-space size can be used to improve the computational efficiency while retaining the same passing proportion of ratio-test. The new AR scheme will be more beneficial in dealing with high-dimension ambiguity resolutions where the search efficiency has become critical, referring to the result that the CPU time percentages saved in the DCS case is as high as 80% versus 47% in the GPS case. If the CPU time required for a computation is not considered critical in terms of absolute value with today's computers, the new AR scheme provides an elegant way to choose the size of the ambiguity search space.

Finally, it is necessary to note that in our work the efficiency of the proposed AR scheme is compared only with the released LAMBDA method which is available for our analysis. Many researchers have made research efforts to improve the search algorithms and implement some shrink procedures in their versions of the LAMBDA codes. The proposed scheme is one of these methods applicable to ILS, which may be easily implemented and tested against different approaches.

Acknowledgements

This work was partially supported by the CRC for Spatial Information project 1.03 " Regionally enhanced orbits and clocks to support multi-GNSS real-time positioning" 2011-2015. The first author also acknowledges the financial support received from the China Scholarship Council (Grant No: 2008466001). Special thanks go to anonymous reviewers whose comments have contributed to the improvement of the paper. Discussions with A/Prof. Sandra Verhagen have been very beneficial as well.

4.7 References

Cai J, Grafarend E, Hu C (2009) The total optimal search criterion in solving the mixed integer linear model with GNSS carrier phase observations. GPS Solutions 13 (3):221-230

Chang X-W, Zhou T (2007) MILES: MATLAB package for solving Mixed Integer LEast Squares problems. GPS Solutions 11 (4):289-294

De Jonge P, Tiberius C (1996) The LAMBDA method for integer ambiguity estimation: implementation aspects. Publications of the Delft Geodetic Computing Centre 12

Eisenbrand F (2010) Integer Programming and Algorithmic Geometry of Numbers. In: Jünger M, Liebling TM, Naddef D et al. (eds) 50 Years of Integer Programming 1958-2008. Springer Berlin Heidelberg, pp 505-559. doi:10.1007/978-3-540-68279-0_14

Euler HJ, Schaffrin B (1990) On a Measure for the Discernibility between Different Ambiguity Solutions in the Static-Kinematic GPS-Mode. Paper presented at the IAG Symposia no. 107, Kinematic Systems in Geodesy, Surveying, and Remote Sensing, New York

Feng Y (2005) Future GNSS performance predictions using GPS with a virtual Galileo constellation. GPS World 16 (3):46-52

Feng Y, Wang J (2011) Computed success rates of various carrier phase integer estimation solutions and their comparison with statistical success rates. Journal of Geodesy 85 (2):93-103. doi:10.1007/s00190-010-0418-y

Han S (1997) Quality-control issues relating to instantaneous ambiguity resolution for real-time GPS kinematic positioning. Journal of Geodesy 71 (6):351-361

Hassibi A, Boyd S (1998) Integer parameter estimation in linear models with applications to GPS. IEEE Transactions on signal processing 46 (11):2938-2952

Joosten P (2001) The lambda-method: Matlab implementation. Mathematical Geodesy and Positioning, Delft Universtiy of Technology, Tech Report

Knuth DE (1997) Art of Computer Programming, Volume 1: Fundamental Algorithms. Addison-Wesley Professional

Leick A (2004) GPS satellite surveying. Wiley

Liu L, Hsu H, Zhu Y, Ou J (1999) A new approach to GPS ambiguity decorrelation. Journal of Geodesy 73 (9):478-490

Svendsen J (2006) Some properties of decorrelation techniques in the ambiguity space. GPS Solutions 10 (1):40-44

Teunissen P, De Jonge P, Tiberius C (1996) The Volume of the GPS Ambiguity Search Space and its Relevance for Integer Ambiguty Resolution. Paper presented at the ION GPS-96 Kansas City Convention Center, Kansas City, Missouri, September 17-20

Teunissen PJG (1993) Least-Squares Estimation of the Integer GPS Ambiguities. Invited Lecture, Section IV, Theory and Methodology, IAG General Meeting

Teunissen PJG (1994) A new method for fast carrier phase ambiguity estimation. In: Position Location and Navigation Symposium, IEEE, 11-15 Apr 1994. pp 562-573

Teunissen PJG (1995) The least-squares ambiguity decorrelation adjustment: a method for fast GPS integer ambiguity estimation. Journal of Geodesy 70(1):65-82

Teunissen PJG (1998) Success probability of integer GPS ambiguity rounding and bootstrapping. Journal of Geodesy 72 (10):606-612

Teunissen PJG (1999) An optimality property of the integer least-squares estimator. Journal of Geodesy 73 (11):587-593

Teunissen PJG, Verhagen S (2009) The GNSS Ambiguity Ratio-Test Revisited: a Better Way of Using It. Survey Review 41 (312):138-151. doi:10.1179/003962609x390058

Tiberius CCJM, Jonge PJd (1995) Fast positioning using the LAMBDA method. In: Proceedings of the 4th International Symposium on Differential Satellite Navigation Systems DSNS'95, Bergen, Norway, April 24-28 1995.

Wang J, Feng Y, Wang C (2010) A Modified Inverse Integer Cholesky Decorrelation Method and the Performance on Ambiguity Resolution. In: Proceedings of CPGPS 2010 Navigation and Location Services: Emerging Industry and International Exchanges, Shanghai, China, August 2010. pp 153-166

Wang J, Stewart MP, Tsakiri M (1998) A discrimination test procedure for ambiguity resolution on-the-fly. Journal of Geodesy 72 (11):644-653

Xu P (2001) Random simulation and GPS decorrelation. Journal of Geodesy 75 (7-8):408-423

Xu P (2002) Isotropic probabilistic models for directions, planes and referential systems. In: Proceedings - Royal Society. Mathematical, physical and engineering sciences. London. August 8 2002. pp 2017-2038

Zhou Y (2010) A new practical approach to GNSS high-dimensional ambiguity decorrelation. GPS Solutions:1-7. doi:10.1007/s10291-010-0192-6

Chapter 5: Computed Success Rates of Various Carrier Phase Integer Estimation Solutions and Their Comparison with Statistical Success Rates

Statement of Contribution of Co-Authors

The authors listed below have certified that:

1. they meet the criteria for authorship in that they have participated in the conception, execution, or interpretation, of at least that part of the publication in their field of expertise;
2. they take public responsibility for their part of the publication, except for the responsible author who accepts overall responsibility for the publication;
3. there are no other authors of the publication according to these criteria;
4. potential conflicts of interest have been disclosed to (a) granting bodies, (b) the editor or publisher of journals or other publications, and (c) the head of the responsible academic unit, and
5. they agree to the use of the publication in the student's thesis and its publication on the Australasian Digital Thesis database consistent with any limitations set by publisher requirements.

In the case of this chapter:

Contributor	**Statement of contribution**
Jun Wang	Designd and conducted the experiment, wrote some parts of the manuscript and revised it
Yanming Feng	Developed experimental design, and wrote the manuscript

Principal Supervisor Confirmation

I have sighted email or other correspondence from all co-authors confirming their certifying authorship.

Yanming Feng		20-October-2012
Name	Signature	Date

Computed success rates of various carrier phase integer estimation solutions and their comparison with statistical success rates

Yanming Feng and Jun Wang

Faculty of Science and Technology

Queensland University of Technology, Australia

Phone: +61 7 31389111, Fax: +61 7 31389390, Email: jun.wang@student.qut.edu.au

Abstract

The success rate of carrier phase ambiguity resolution (AR) is the probability that the ambiguities are successfully fixed to their correct integer values. In existing works, an exact success rate formula for integer bootstrapping estimator has been given and used as a sharp lower bound for the integer least squares (ILS) success rate. Rigorous computation of success rate for the more general ILS solutions has been considered difficult, because of complexity of the ambiguity pull-in region and computational load of the integration of the multivariate probability density function. Contributions of this work are threefold. First, the ILS solutions pertaining to variations of observational and stochastic models and data processing strategies are examined, leading to simplification of the ILS success probability computation. Second, the pull-in region mathematically expressed by the vertices of a polyhedron is now represented by a multi-dimensional grid, at which the cumulative probability can be integrated with the multivariate normal cumulative density function (mvncdf) available in Matlab. The paper presents a study for the bivariate case where the pull-region is usually defined as a hexagon and the probability is easily obtained using mvncdf at all the grid points within the convex polygon. Third, the paper compares the computed integer rounding and integer bootstrapping success rates, the lower and upper bounds of the ILS success rates to the actual ILS AR success rates obtained from a 24 h GPS data set for a 21 km baseline. The results demonstrate that the upper bound probability of the ILS AR probability given the existing literatures agrees with the actual ILS success rate well, although the success rate computed with integer bootstrapping method is a quite sharp approximation to the actual ILS success rate.

The results also show that variations or uncertainty of the unit-weight variance estimates from epoch to epoch will affect the computed success rates from different methods significantly, thus deserving more attentions in order to obtain useful success probability predictions.

Keywords: GNSS, ambiguity resolution (AR), success rate, Integer Least Squares, multivariate cumulative normal density function, multi-dimensional grid.

5.1 Introduction

In the context of real time kinematic (RTK) positioning using Global Satellite Navigation System (GNSS) carrier phase measurements, the success rate of ambiguity resolution (AR) is the probability that ambiguities are successfully resolved and fixed to their correct integer values, thus also being known as Probability of Correct Fixing (PCF) by some researchers, such as O'Keefe et al. (2006). Knowing the success rate of carrier phase ambiguity resolution is important from both theoretical and application perspectives. Theoretically, once an AR model, method or processing procedure is proposed, it is preferable the AR performance of the estimation system can be predicted and compared in terms of AR success rate or reliability. Otherwise one may have to obtain the actual AR success rate through statistics results from the real data examples. From a user perspective, undetected incorrect integers may cause user state solutions to fail without notice. Predicable AR success probability can be used to define the reliability of RTK solutions or the Integrity Risk (IR) required in analysis of safety-critical or liability-critical applications.

The AR success rate or probability is defined as the integral of probabilistic density function of float ambiguity solutions over an ambiguity "Voronoi cell" as firstly defined in Hassibi and Boyd (1996 and 1998). In Teunissen (1998), the success rates for rounding and bootstrapping were defined over an ambiguity "pull-in region". Teunissen (1999) defined the pull-in region for the ILS case with three properties, leading to a larger class of a pull-in region than that of Voronoi cell constructed by Xu (2006). Construction of the ILS pull-in region or Voronoi cell can be complex for a high-dimension positive-definitive matrix, the computation of AR success probability is considered thus difficult in both works.

However, AR success probability problems have been approached from different perspectives to come up with useful conclusions. Referring to Teunissen (1998), the exact success rates for rounding were considered difficult to compute, but it was shown that this probability is bounded as

$$\prod_{i=1}^{m}[2\Phi(\frac{1}{2\sigma_{\hat{N}_i}})-1] \le P[(rounding(\hat{\mathbf{N}})=\mathbf{N})] \le \prod_{i=1}^{m}[2\Phi(\frac{1}{2\sigma_{\hat{N}_i|I}})-1] \quad (1)$$

with

$$\Phi(z) = \int_{-\infty}^{z} \frac{1}{\sqrt{2\pi}} \exp(-\frac{1}{2}x)dx \tag{2}$$

where m is the number of ambiguities parameters to be estimated; $\sigma_{\hat{N}i}$ and $\sigma_{\hat{N}i|I}$ are the standard deviation of the float integer estimate of the ith integer $\hat{N}_i$ and $\hat{N}_i \mid I$ where the shorthand notation $\hat{N}_i \mid I$ stands for the ith least-squares ambiguity obtained through a conditioning on the previous I={1,2,.., i-1} sequentially rounded ambiguities. As far as the probability of bootstrapping estimator is concerned, since the covariance matrix of the sequential conditional least-squares solution is diagonal, it was in (ibid) shown that the probability of correct integer estimation of the bootstrapped solution can be computed exactly:

$$\begin{aligned} &\prod_{i=1}^{m}[2\Phi(\frac{1}{2\sigma_{\hat{N}_i|I}}) - 1] = P(bootstrapping(\hat{N}) = N] \\ &\leq [2\Phi(\frac{1}{(2\pi)^{\frac{1}{m}}\sqrt{\text{ADOP}}}) - 1]^m \end{aligned} \tag{3}$$

where ADOP represents Ambiguity Dilution of Precision (ADOP), which is the determinant of the covariance matrix Cov($\hat{\mathbf{N}}$) in squared cycle units. The conclusions include: (1) rounding success rate is always poorer than, or as at the most as good as, bootstrapping; (2) for the bootstrapping, the given success-rate formula is an exact formula and easy-to-evaluate; (3) lower bound for success rate of rounding is obtainable and easy-to-evaluate; and (4) an invariant upper-bound for the successful rate of bootstrapping can be given via a decorrelation transformation of Cov($\hat{\mathbf{N}}$). Furthermore, Teunissen (1999) proved that of all integer estimators, the ILS estimator has the largest possible success rate. As a result, the bootstrapping success rate (after the decorrelating transformation process) was proposed as an easy-to-evaluate lower bound for the ILS success rate. In the mean time we notice that Teunissen (2000) also gave the computations of lower and upper bounds of the success probabilities of the ILS solutions

$$[2\Phi(\frac{1}{2\sqrt{\lambda_{\max}}})-1]^m \le P(\hat{N}|_{ILS}=N) \le [2\Phi(\frac{1}{2\sqrt{\lambda_{\min}}})-1]^m \quad (4)$$

with $\lambda_{\min}$ and $\lambda_{\max}$ the extreme eigenvalues of Cov($\hat{\mathbf{N}}$).

It is trivial to understand that the above three integer estimators become identical if the ambiguity covariance matrix is a diagonal matrix. If the ambiguity variance matrix is sufficiently close to a diagonal matrix, the success rate of integer rounding would be used as a sufficiently sharp lower bound of the ILS success rate. We also notice that Xu (2003 and 2006) and O'Keefe et al. (2006) argued that the lower bound is of more interests than the upper bound since the lower bound can be used to guarantee a minimal level of confidence in the solution. Success rate of bootstrapping has been frequently used as the lower bound of the ILS success rate in several recent efforts, such as Verhagen (2005) and O'Keefe et al. (2007). The question is that if the rounding or bootstrapping success rate is used as a lower bound of the success rate of the general ILS solutions, how close the bound is to the exact success rate of the ILS solutions; and how close the computed success rate of integer rounding or bootstrapping solutions is to their actual ILS success rate. In other words, the conclusion that the lower and upper bounds of the probability given or frequently used as success probability predictions needs to be substantiated with numerical proof from real world examples. Actual AR success rates are referred to the equation (38) in Section 5.3.

Theoretically, the success probability of ILS estimators can be defined by the integration of the multivariate normal density function over the ILS ambiguity pull-in region. A mathematical description of the pull-in region is complex, but possible by finding the vertices of a polytope of the pull-in region. Xu (2006) gives linear inequality constraints defining the Voronoi cell, showing a few lower-dimension examples. The problem is the computation complexity is attributed to double exponential numbers (ibid) and only realistic for a lower dimensional ambiguity vector. Albeit, a pull-in region can be constructed; the computational load of the integration process may still be unbearable as shown in Sect. 3. Therefore, we may alternatively seek to reduce the complexity of the ILS success probability computation problem.

In the following section, we briefly outline the Integer Least Square (ILS) models and solutions, and the cost functions for different integer estimations, including a special case of ILS solutions, namely Sequential ILS (SILS) solutions. This allows the problem of ILS success probability computations to be simplified, noting that the integer rounding and integer bootstrapping give approximations to ILS solutions instead of solutions in special cases. In Section 5.3, the pull-in region or Voronoi cell defined by the vertices of a polyhedron is represented by a multi-dimensional grid, at which the cumulative probability can be evaluated with the multivariate normal cumulative density function (mvncdf) available in Matlab. Due to the complexity of the computation for a high dimensional ambiguity vector, the paper presents a study for the bivariate case where the pull-region is usually defined as a hexagon and the cumulative probability is obtained using the mvncdf at all the grid points within the convex polygon. Section 5.4 describes numerical experiment schemes and results of computed and actual success rates with different integer estimations for the same AR problem. The final section summarises the findings from the theoretical developments and experiment results.

5.2 Integer Least Square (ILS) Solutions and Variations

We start with the general geometry-based linear observational models including user both coordinate vector and integer parameters:

$$\mathbf{L}=\mathbf{A}\delta\mathbf{x}+\mathbf{BN}+\mathbf{e} \tag{5}$$

where **L** is n-dimensional vector of observations; **A** and **B** are (n-by-3) and (n-by-m) observational matrices of full column rank, respectively; **δx** is a real-valued 3-dimensional coordinate vector and **N** is a m-dimensional integer vector, where n>m; e is the error vector of the observations **L**. In this paper, we assume the statistic characteristics of the vector e as follows:

$$\mathrm{E}(\mathbf{e})=\mathbf{0};\quad \mathrm{Cov}(\mathbf{e})=\sigma_{\mathbf{0}}^{\mathbf{2}}Q=\sigma_{\mathbf{0}}^{\mathbf{2}}W^{-1} \tag{6}$$

where $\sigma_0^2\mathbf{Q}$ or $\sigma_0^2\mathbf{W^{-1}}$ is the n-by-n covariance matrix that considers the correlation and relative variances between all the elements of the vector L; W is the inverse matrix of **Q**, namely weight matrix; σ_0^2 is a prior variance for the unit-weight

measurements. For convenience, we often name $\mathbf{Q}$ or $\mathbf{W}^{-1}$ as a covariance matrix as well. Amore general stochastic model is given as follows:

$$\sigma_0^2\mathbf{Q} = \sigma_0^2 \sum_{i=1}^{q} \alpha_i \mathbf{Q}_i \tag{7}$$

where α_i represents the variance-covariance components for different code and phase measurements and q is the number of the variance-covariance components to be estimated, $\mathbf{Q}_i$ represents the co-efficient matrices given to reflect the relative weighting within each group of measurements and correlation between groups of the measurements, for instance between L1 and L2 and between P1 and P2.

Generally, $\mathbf{L}$ is a collection of double-difference code and phase observables between GNSS receivers and satellites. These observables are generally formed from various linear combinations, such as among codes and phases, and different frequencies and observed and computed range (Feng and Li, 2009). The observational matrices $\mathbf{A}$ and $\mathbf{B}$ are obtained with respect to the observational vector $\mathbf{L}$, generally referring to the combined observables.

From the linear equation (5) and the stochastic model (6), the covariance matrix of the real-value least squares solutions is given as:

$$Cov\left(\begin{bmatrix}\boldsymbol{\delta}\hat{\mathbf{x}}\\ \hat{\mathbf{N}}\end{bmatrix}\right) = \sigma_0^2 \begin{bmatrix}\mathbf{A}^{\mathbf{T}}\mathbf{W}\mathbf{A} & \mathbf{A}^{\mathbf{T}}\mathbf{W}\mathbf{B}\\ \mathbf{B}^{\mathbf{T}}\mathbf{W}\mathbf{A} & \mathbf{B}^{\mathbf{T}}\mathbf{W}\mathbf{B}\end{bmatrix}^{-1} = \sigma_0^2 \begin{bmatrix}\mathbf{Q}_{\boldsymbol{\delta}\hat{\mathbf{x}}} & \mathbf{Q}_{\boldsymbol{\delta}\hat{\mathbf{x}}\hat{\mathbf{N}}}\\ \mathbf{Q}_{\hat{\mathbf{N}}\boldsymbol{\delta}\hat{\mathbf{x}}} & \mathbf{Q}_{\hat{\mathbf{N}}}\end{bmatrix} \tag{8}$$

where and $\mathbf{Q}_{\delta\hat{x}}$ and $\mathbf{Q}_{\hat{N}}$ are full positive-definite and symmetric matrices for the real valued estimates $\delta\hat{\mathbf{x}}$ and $\hat{\mathbf{N}}$; $\mathbf{Q}_{\delta\hat{x}\hat{N}}$ gives the cross-correlation between these two. The float ambiguity least squares solutions and the covariance matrix are given as

$$\hat{\mathbf{N}} = \mathbf{Q}_{\hat{\mathbf{N}}\boldsymbol{\delta}\hat{\mathbf{x}}}\mathbf{A}^{\mathbf{T}}\mathbf{W}\mathbf{L} + \mathbf{Q}_{\hat{\mathbf{N}}}\mathbf{B}^{\mathbf{T}}\mathbf{W}\mathbf{L} \tag{9}$$

$$\mathbf{Q}_{\hat{\mathbf{N}}} = [\mathbf{B}^{\mathbf{T}}\mathbf{W}\mathbf{B} - \mathbf{B}^{\mathbf{T}}\mathbf{W}\mathbf{A}(\mathbf{A}^{\mathbf{T}}\mathbf{W}\mathbf{A})^{-1}\mathbf{A}^{\mathbf{T}}\mathbf{W}\mathbf{B}]^{-1} \tag{10}$$

The Eqs. (8)-(10) give the float ambiguities and their covariance matrices for the linear Eq. (5), stochastic model 6. The next step is to resolve ambiguity integers from

these float solutions. The procedure is so-called ambiguity resolution (AR). Many AR methods have been developed over the past two decades, including the least squares ambiguity searching technique (Hatch 1990), Least squares AMBiguity Decorrelation Adjustment (LAMBDA) (Teunissen 1993) as well as Ambiguity Resolution with Constraint Equations method (Park et al. 1996) etc. Of these methods, LAMBDA is more widely used and referred by researchers due to its efficient integer searching performance (Teunissen 1999). The core of LAMBDA procedure is to decorrelate the float ambiguity vector $\hat{\mathbf{N}}$ and covariance matrix $\mathbf{Q}_{\hat{N}}$ with a transformation matrix **G**, which along with its inverse matrix $\mathbf{G}^{-1}$ have integer entries and |det(G)|=1, thus obtaining $\hat{\mathbf{Z}} = \mathbf{G}\hat{\mathbf{N}}$ and $\mathbf{Q}_{\hat{\mathbf{Z}}} = \mathbf{G}\mathbf{Q}_{\hat{\mathbf{N}}}\mathbf{G}^{\mathbf{T}}$. The integer search is then based on the minimization of the following cost function

$$F = (\mathbf{N} - \hat{\mathbf{N}})^{\mathbf{T}} \mathbf{Q}_{\hat{\mathbf{N}}}^{-1} (\mathbf{N} - \hat{\mathbf{N}}) = (\mathbf{Z} - \hat{\mathbf{Z}})^{T} Q_{\hat{Z}}^{-1} (\mathbf{Z} - \hat{\mathbf{Z}}) \tag{11}$$

After the integer vector **Z** is found, the integer **N** can be transferred from **Z**, i.e., $\mathbf{N} = \mathbf{G}^{-1}\mathbf{Z}$.

Substituting the known integer vector **N**, into the linear equation (5) parameters, the least square estimation of position vector $\breve{\mathbf{x}}$ can be obtained as follows:

$$\delta\breve{\mathbf{x}} = (\mathbf{A}^{\mathbf{T}}\mathbf{W}\mathbf{A})^{-1}\mathbf{A}^{\mathbf{T}}\mathbf{W}(\mathbf{L} - \mathbf{B}\mathbf{N}) \tag{12}$$

We also obtain the estimate of σ_0^2 as the post-priori variance:

$$\breve{\sigma}_0^2 = \frac{(\mathbf{L} - \mathbf{B}\mathbf{N} - \mathbf{A}\breve{\mathbf{x}})^{T}\mathbf{W}(\mathbf{L} - \mathbf{B}\mathbf{N} - \mathbf{A}\breve{\mathbf{x}})}{(n-3)} \tag{13}$$

The above estimate from measurements of a signal epoch is often very uncertain due to the low freedom (n-3). A weighted average obtained over a sufficiently long data period is more adequate for assessment of the AR success probability and position performance. The properly estimated variance $\breve{\sigma}_0^2$ reflects the overall noise level of the particular data set and re-balances between the code and phase noise levels.

With observational residuals using position estimations from integer-fixed measurements, it is possible to reliably estimate the variance–covariance components

to benefit real time AR and position estimation. The variance covariance estimation of the problem (7) in the context of ambiguity resolution and RTK is referred to the recent work by Li et al. (2008).

The integer rounding (IR) and integer bootstrapping (IB) solutions as outlined in Sect. 1 are two approximations of the general ILS integer solutions. IR solutions are obtained by directly rounding the floating ambiguity $\hat{\mathbf{Z}}$ to their nearest integers, and are equivalent to the ILS solutions being resolved by minimizing the following cost function

$$F_{IR} = \sum_{i=1}^{m} \frac{(Z_i - \hat{Z}_i)^2}{Q_{Zi}} \tag{14}$$

where $\mathbf{Q}_{\mathrm{Zi}}$ for i=1,2,…m are diagonal elements of the matrix $\mathbf{Q}_{\hat{Z}}$. Therefore, the nearer the matrix $\mathbf{Q}_{\hat{Z}}$ is to the diagonal, the nearer the integer rounding solutions to the ILS solutions under the cost function (11).

Integer bootstrapping (IB) is a sequential conditional least squares estimation, which is closely related to the triangular decomposition of the ambiguity covariance matrix, as shown in Teunissen (1999). As being explicitly stated by many authors such as Teunissen (1998), integer bootstrapping often applies to the floating solution $\hat{Z}$ and the covariance matrix $\mathbf{Q}_{\hat{Z}}$ after decorrelation. Let the decomposition of the covariance matrix be given as $\mathbf{Q}_{\hat{Z}} = \mathbf{U}^{\mathbf{T}}\mathbf{D}\mathbf{U}$, with $\mathbf{U}$ being a unit upper triangular matrix and $\mathbf{D}$ a diagonal matrix, then we have $(\mathbf{Z} - \hat{\mathbf{Z}}) = \mathbf{U}^{\mathbf{T}}(\mathbf{Z} - \tilde{\mathbf{Z}})$, where $\tilde{\mathbf{Z}}$ denotes the conditional least-squares solution obtained sequentially conditioning on the entries of $\hat{\mathbf{Z}}$. The covariance matrix of $\tilde{\mathbf{Z}}$ is given by the diagonal matrix $\mathbf{D}$.

$$F_{IB} = (\mathbf{Z} - \hat{\mathbf{Z}})^{\mathbf{T}} \mathbf{Q}_{\hat{\mathbf{Z}}}^{-1} (\mathbf{Z} - \hat{\mathbf{Z}}) = (\mathbf{Z} - \hat{\mathbf{Z}})^{\mathbf{T}} \mathbf{Q}_{\hat{\mathbf{Z}}}^{-1} (\mathbf{Z} - \tilde{\mathbf{Z}}) = \sum_{i=1}^{m} \frac{(Z_i - \tilde{Z}_i)^2}{D_i} \tag{15}$$

The integer solutions $\mathbf{Z}$ are obtained by directly rounding off each element of $\tilde{\mathbf{Z}}$ sequentially as

$$Z_1 = [\tilde{Z}_1], Z_2 = [\tilde{Z}_2], \cdots, Z_m = [\tilde{Z}_m] \tag{16}$$

Again, the original integer vector N is obtained through the transformation $\mathbf{N = G^{-1}Z}$.

A more general case is when different groups of integers are determined sequentially or independently under the cost function (11). This may be known as Sequential Integer Least Squares (SILS) estimation. In particular, the cost function (11) is changed to

$$F_{SILS} = (\mathbf{Z_a} - \hat{\mathbf{Z}}_\mathbf{a})^\mathrm{T} \mathbf{Q}_{\hat{\mathbf{Z}}\mathbf{a}}^{-1} (\mathbf{Z_a} - \hat{\mathbf{Z}}_\mathbf{a}) + (\mathbf{Z_b} - \hat{\mathbf{Z}}_\mathbf{b})^\mathrm{T} \mathbf{Q}_{\hat{\mathbf{Z}}\mathbf{b}}^{-1} (\mathbf{Z_b} - \hat{\mathbf{Z}}_\mathbf{b}) \tag{17}$$

The cost function (17) looks like an extension of (14) and (15), but it represents a special case of (11), instead of an approximation to the ILS solutions under (11). In practice, the float solutions of different groups of integers are often obtained from different methods or different data sets. For instance, the float solutions of the higher dimension vector $\mathbf{Z}_\mathrm{a}$ are derived from a period of observations; the covariance matrix $\mathbf{Q}_{\hat{Z}a}$ would be much nearer to a diagonal matrix. The vector $\mathbf{Z}_\mathrm{b}$ represents a small group of ambiguities, such as L1 and L2 integers for a new satellite pair. In general, such a sequential or independent partition does not necessarily lead to more reliable ambiguity resolution, but it affects AR success probability computation. As far as success probability computation is concerned, we shall consider this case.

5.3 Success Probability Computations

Using the IR and IB solutions as approximations to ILS solution or the SILS solution as an alternative to ILS solution, the ambiguity resolutions will be reduced. As a result, the complexity and difficulty of computation of ILS success probability can be reduced. In this section, we discuss the computation of the success probabilities of different integer solutions based on the cost functions (14), (15) and (16).

5.3.1 Integer least squares success probability

The ambiguity success rate is defined as the probability of correct integer ambiguity estimation, i.e., $P(\hat{Z} = \mathbf{Z})$ which equals to the integral of the probability density function of the float ambiguities $P_Z(x)$ over the pull-in region R:

$$P\left(\breve{\mathbf{Z}} = \mathbf{Z}\right) = \int_R P_z(x)dx \tag{18}$$

In general, for the float ambiguity vector, with a covariance matrix $\sigma_0^2 Q_{\hat{Z}}$ or the estimate $\breve{\sigma}_0^2 Q_Z$; the error vector $\boldsymbol{\varepsilon} = \hat{\mathbf{Z}} - \mathbf{Z}$,where Z is the unknown true integer vector. We assume $\hat{Z} \sim N(\mathbf{Z}, \sigma_0^2 \mathbf{Q}_{\hat{\mathbf{Z}}})$, or $\varepsilon \sim N(0, \sigma_0^2 \mathbf{Q}_{\hat{\mathbf{Z}}})$. With the cost function (11) and the full covariance matrix, the probability of the correct integer fix in the ILS solutions can be given as

$$P(\breve{\mathbf{Z}}{=}\mathbf{Z}) = \int_R N(Z, \sigma_0^2 \mathbf{Q}_{\hat{Z}})dX = \int_R \frac{1}{(2\pi)^{\frac{1}{m}} \left|\sigma_0^2 \mathbf{Q}_{\hat{\mathbf{Z}}}\right|^{1/2}} \exp[-\frac{1}{2\sigma_0^2}(\mathbf{X}-\mathbf{Z})^{\mathbf{T}} \mathbf{Q}_{\hat{\mathbf{Z}}}^{-\mathbf{1}} (\mathbf{X}-\mathbf{Z})]dX \tag{19}$$

where X represent the vector for the float ambiguity vector $\hat{\mathbf{Z}}$; R is the pull-in region defined by the positive covariance matrix $\sigma_0^2 \mathbf{Q}_{\hat{\mathbf{Z}}}$.

For SILS solutions, the integer vectors N_a and N_b are determined sequentially under the cost function (17). Substituting (17) into (19), the success probability of the varied ILS solutions is given as

$$\begin{aligned} P(\breve{\mathbf{N}} = \mathbf{N}) &= P(\breve{\mathbf{Z}}_{\mathbf{a}} = \mathbf{Z}_a) P(\breve{\mathbf{Z}}_{\mathbf{b}} = \mathbf{Z}_b) = P(\hat{\mathbf{Z}}_{\mathbf{a}} = \mathbf{Z}_a) \int_{Rb} N(\mathbf{Z}_b, \sigma_0^2 \mathbf{Q}_{\hat{\mathbf{Z}}\mathbf{b}})dX \\ &= \int_{Ra} \frac{1}{(2\pi)^{\frac{1}{m_a}} \left|\sigma_0^2 \mathbf{Q}_{\hat{\mathbf{Z}}\mathbf{a}}\right|^{\frac{1}{2}}} \exp[-\frac{1}{2\sigma_0^2}(\mathbf{X}_{\mathbf{a}}-\mathbf{Z}_{\mathbf{a}})^{\mathbf{T}} \mathbf{Q}_{\hat{\mathbf{Z}}\mathbf{a}}^{-\mathbf{1}} (\mathbf{X}_{\mathbf{a}}-\mathbf{Z}_{\mathbf{a}})]dX \\ &\times \int_{Rb} \frac{1}{(2\pi)^{\frac{1}{m_b}} \left|\sigma_0^2 \mathbf{Q}_{\hat{\mathbf{Z}}\mathbf{b}}\right|^{\frac{1}{2}}} \exp[-\frac{1}{2\sigma_0^2}(\mathbf{X}_{\mathbf{b}}-\mathbf{Z}_{\mathbf{b}})^{\mathbf{T}} \mathbf{Q}_{\hat{\mathbf{Z}}\mathbf{b}}^{-\mathbf{1}} (\mathbf{X}_{\mathbf{b}}-\mathbf{Z}_{\mathbf{b}})]dX \end{aligned} \tag{20}$$

where Ra and Rb are the pull-in regions for the ma-by-1 integer vector Na and the mb-by-1 integer vector Nb, respectively. Whilst the second integration is often a bivariate case of two ambiguities for a new satellite pair, the first integration has been well approximated by integer rounding or integer bootstrapping, due to the much nearer diagonal nature of $\mathbf{Q}_{\hat{Z}a}$. This shows a possibility to reduce the complexity of ILS success probability computations in theory through the

combination of integer rounding success rates and the ILS success rate for the bivariate case.

5.3.2 Construction and representation of ambiguity pull-in region

The cumulative probability of the multivariate normal distribution over the pull-in region R or Ra and Rb, gives the success probability of ILS solutions based on (19) or (20). Despite the fact that the pull-in region R is difficult to define and the integration (19) or (20) involves heavy computation, we intend to make further efforts toward construction of the pull-in region and completion of the ILS success probability computation procedures, referring to the existing methods such as pull-in region construction by Verhagen (2003) and Voronoi cell as suggested by Xu (2006). Our computations show that both methods generate the same pull-in region which is unique for a given positive-definite matrix after removal of redundant vertices. For a given covariance matrix $\mathbf{Q}_{\hat{z}}$, constructing a pull-in region is mathematically equivalent to finding all the vertices of the polytope or polyhedron defined by the following linear inequality constraints

$$\mathbf{z}^T\mathbf{Q}_{\hat{\mathbf{z}}}^{-1}\mathbf{x} \le \mathbf{z}^T\mathbf{Q}_{\hat{\mathbf{z}}}^{-1}\mathbf{z}/2 \quad \forall \mathbf{x} \in R^m \quad \mathbf{z} \ne 0 \tag{21}$$

where z takes different integer vectors to form a unique close polytope, depending on the correlation coefficient between diagonal elements of the matrix $\mathbf{Q}_{\hat{z}}$. Each of (21) gives a solution of a fundamental subsystem of (21). One can directly construct the Voronoi cell by finding all its vertices, and as a by-product of this procedure with Xu (2006), to identify and eliminate all the redundant constraints that do not form a face of dimension (m-1) for Voronoi cell from (21). Most methods of this kind have been based on the simple method of linear programming.

The next step is numerical integration of the multivariate normal distribution over the Voronoi cell. Discussion of the integration of this kind was also found in Teunissen (2000) and Xu (2006). In this work, thanks to the contributions by statisticians, especially, Genz and Bretz (1999 and 2002), the computation problem like (19) is more conveniently addressed by using the multivariate normal cumulative density function (mvncdf) implemented in the recent Matlab version. For two or more dimensions, mvncdf uses a quasi-Monte Carlo integration algorithm based on

methods developed by Genz and Bretz (1999 and 2002). Generally, given a mean vector, a positive-definite covariance matrix, the function mvncdf can return the cumulative probability at an array S that defines a multi-dimensional grid. Rows of the g-by-m matrix S correspond to grid points, and columns correspond to coordinates, where g is the number of grid points and can very large and m is the dimension of the multivariate vector. The multivariate normal cumulative probability at S is defined as the probability that a random vector X(i), for i=1,2,..., m, distributed as multivariate normal, will fall within the semi-infinite rectangle with upper limits defined by S, for example, $P\{X(1)\leq S(1), X(2) \leq S(2), ..., X(m) \leq S(m)\}$.

Computation of integration in (19) and (20) with a high-dimensional covariance matrix is very time consuming. We examine a bivariate case where two covariance matrices from a real data set. The covariance matrix is

$$Q_{(Amb1,Amb2)} = \begin{bmatrix} 0.1795 & 0.0781 \\ 0.0781 & 0.1707 \end{bmatrix} \tag{22}$$

The subscript Amb1 and Amb2 refer to the ambiguity variables for L1 and L2 phases respectively. Substituting (22) into the linear inequality (21), the coordinates of the six vertices for each pull-in region defined by (22) can be obtained, which are further represented by a two-dimensional grid as shown in Figure 5-1. Figure 5-2 shows the probability density function as defined in (19) or (20), while Figure 5-3 show their cumulative probability over the two-dimensional grid as given in Figure 5-1.

Following the above procedure for the two ambiguity variable cases, theoretically it is possible to obtain a Voronoi cell for a higher dimensional ambiguity covariance matrix, the mvncdf function can return the cumulative probability at the matrix, which defines the multi-dimensional grid with a very large number of rows, depending on the grid density. For instance, in the above two bivariate example, the number of the rows or grid points reached 1554, which is approximately 402. In a trivariate case, the member of rows can reach about 403. Practically, the computation load for a higher dimensional covariance matrix is unbearable. On the other hand, one may argue whether the construction of a complex pull-in region for a high dimensional ambiguity vector is really necessary. Although in general, the ellipsoid of the covariance matrix is conceptually not an approximation to the ILS ambiguity

pull-in region, the cumulative probability integration using mvncdf over an ellipsoid (or hyper-ellipsoid in higher dimensions) could be a very sharp approximation of the integration over the pull-in region. This is because the probability density takes very low or zero values for the grid points outside the overlap area of the pull-in region and ellipsoid. Figure 5-4 draws the contours of the probability density over the pull-in region. The low probability density values at the grid points outside the overlap area of the pull-region support the above argument. However, construction of a covariance ellipsoid is much easier. Using the same mvncdf function, the multivariate normal cumulative probability function may be evaluated over the ellipsoid, although the computational load is still too heavy for a high dimensional integer vector.

We note that Xu (2006) studied how to fit figures of simple shape to a Voronoi cell, both from inside and outside. An ellipsoid figure is an obvious choice. In the case when two ambiguities are highly correlated, the pull-in region may no longer be closely followed by an ellipse figure as implied by Xu (2006) and Teunissen (2000). The probability computation with the mvncdf function over an error ellipse may no longer be applicable.

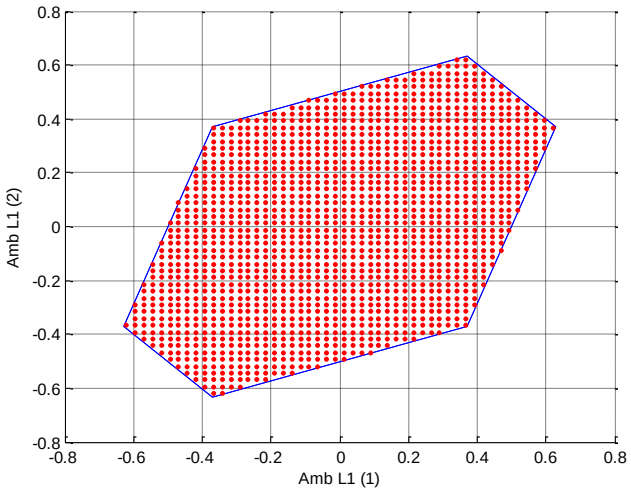

Figure 5-1 Illustration of the Voronoi cell defined by the covariance matrix (22) for the L1 and L2 ambiguity variables where the correct integers are (0, 0). The Voronoi cell is represented using a two-dimensional matrix grid, which consists of 1,554 rows or grid points

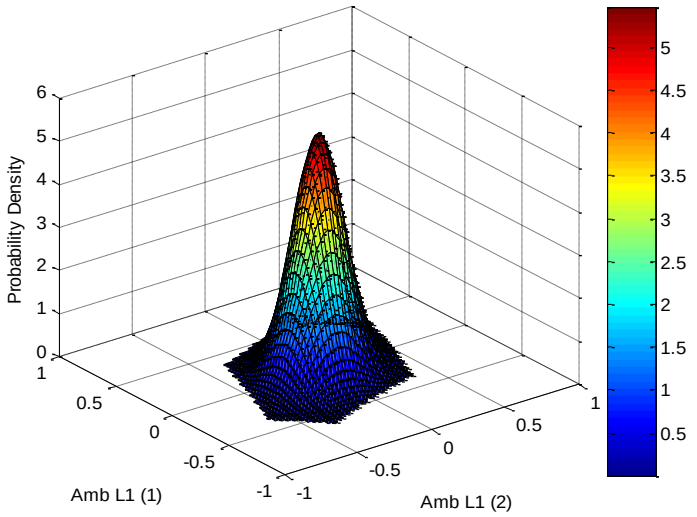

Figure 5-2 Illustration of probability density over the Voronoi represented by the 2-dimensional grid as shown in Figure 5-1

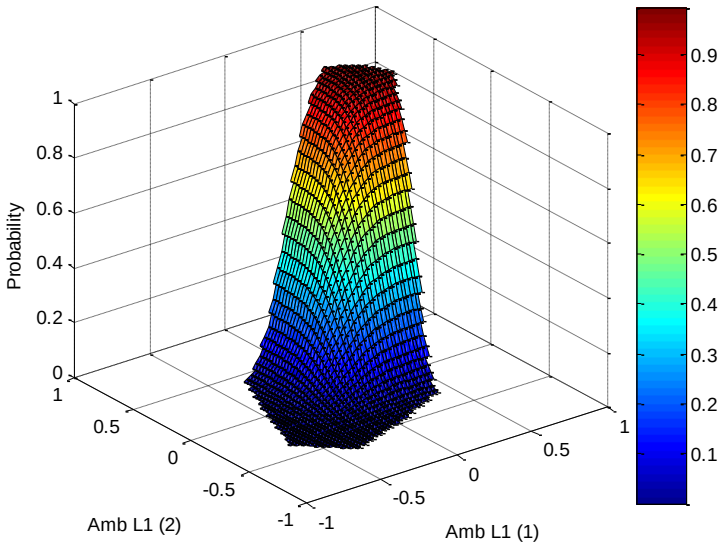

Figure 5-3 Illustration of the cumulative probability integrated over the Voronoi cell as shown in Figure 5-1

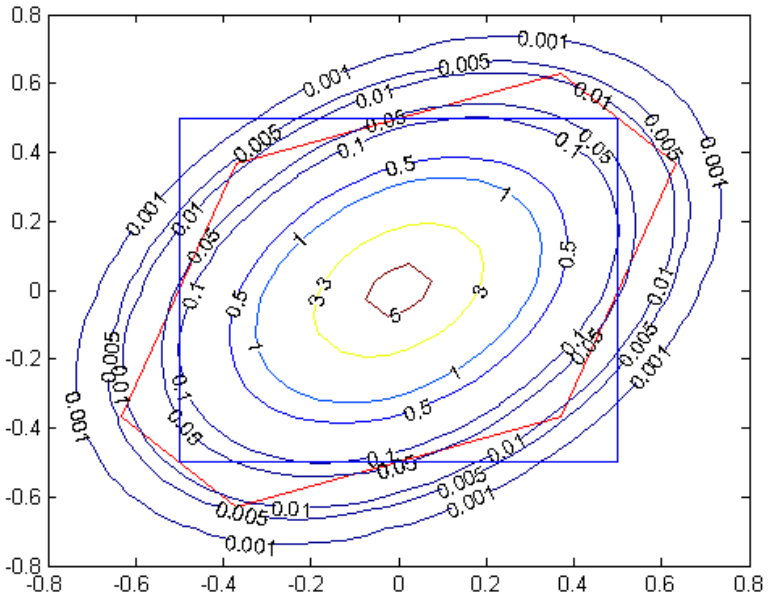

Figure 5-4 Probability density contours for the covariance matrix (22) plotted over the pull-in region and bound box (-0.5, 0.5), showing very low probability density values outside the pull-in region.

5.3.3 Integer rounding and integer bootstrapping success probability

Integer rounding is the simplest method, but very popularly used in GNSS data processing systems, such as network based ambiguity resolution for RTK services and advanced GPS analysis software systems like GAMIT and Bernese. Therefore, evaluation of integer rounding success probability is important in real world applications. In this context, integer rounding or integer bootstrapping success probabilities are used as approximations of the ILS success probability.

According to (14), the success probability of integer rounding for the decorrelated float ambiguities is approximated by the following:

$$P(\hat{Z}\,|_{rounding} = Z) \approx \prod_{i=1}^{m} \int_{R_0} \frac{1}{(2\pi)^{1/2}\sigma_0\sqrt{Q_{Zi}}} \exp[-\frac{(\mathbf{x}-Z_i)^2}{2\sigma_0^2 Q_{Zi}}]d\mathbf{x} \qquad (23)$$

Substituting (16) into (19), we can obtain the formula for computation of integer bootstrapping success rate:

$$P(\hat{\mathbf{Z}}\,|_{\text{bootstrapping}} = \mathbf{Z}) = \prod_{i=1}^{m} \int_{R_0} \frac{1}{(2\pi)^{1/2}\sigma_0\sqrt{D_i}} \exp[-\frac{(\mathbf{x}-Z_i)^2}{2\sigma_0^2 D_i}]d\mathbf{x} \qquad (24)$$

In both (23) and (24), **x** represents the float ambiguity $\hat{z}_i$ and the R0 is now the bounding box (Z-0.5, Z+0.5).

5.3.4 Actual success rate statistic

The AR success probabilities computed by (19), (23) and (24) are given with respect to each epoch or each data point when all the DD ambiguity parameters are determined. A data point is defined as one or multiple epochs during which one set of DD ambiguity parameters are estimated. The overall AR success rate over an observational period, for instance, 24 hours, is given as an average of the probabilities over all the epochs or data points, that is,

$$P = \frac{\sum_{j}^{M} P_j(\hat{\mathbf{Z}} = \mathbf{Z})}{M} \tag{25}$$

where M is the total number of epochs or data points for averaging. $P_j(\hat{\mathbf{Z}} = \mathbf{Z})$ denotes the success probability derived from (19), (23) and (24) for each data point.

It is important to note that the above probability estimations depend on not only the covariance matrix, but also the variance σ_0^2 that explicitly sets in the computations (19), (20) and (23) and (24). In other words, these variance parameters must be given or determined as reliable as possible in order to give the reliable approximation of a theoretical success rate. As suggested previously, σ_0^2 may be determined as a weighted average of single epoch estimate $\breve{\sigma}_0^2$ over a long and recent data period or until convergence. Numerical results given in the next section will also show the sensitivity of probability computations to the variance values used.

In the above probability computations, we are assuming the ambiguity estimates to be unbiased, it is well known that if the ambiguities are biased, the probably of correct resolution will rapidly approach zero as the bias approaches cycle (Teunissen 2001).

5.4 Experimental analysis

The purpose of the experimental analysis is twofold: (i) demonstrate the AR success rates of integer rounding integer bootstrapping and integer least squares solutions in the real data processing using the formulas given in Sects. 1–3; compare the computed success rates of different integer solutions with their actual success rate statistics from the same data set. Table 1 summarises the settings of the data set used in the experimental studies and variance-covariance and unit-weight variance settings in the geometry-based ILS problem (5) and (6).

The ILS solutions are obtained with the LAMBDA procedure on the epoch-to-epoch basis, where the unit-weight variance is estimated every single epoch, namely single-epoch variance. The overall $\breve{\sigma}_0$ =0.0021m is the square root of the weighted average of the variances over all sample epochs, namely all-epoch variance. Figure 5-5 shows the computed success rates of integer rounding solutions according to the integration of m-normal distribution function (23), where the single epoch unit-weight variance estimated from the ambiguity-fixed phase measurements are used for probability computation. Figure 5-6 shows the probability similarly computed using the same cumulative function (23), but with the all-epoch unit-weight variance (0.0021m)2 instead of the single-epoch variances varying from epoch to epoch. Figure 5-7 shows AR success rates of integer bootstrapping solutions computed from the product of integration of m-normal distribution function (24), where the variances take the diagonal elements of the decorrelated matrix $Q_{\hat{z}}$ and $\sigma_0^2 = (0.0021m)^2$. It is clearly observed that Figure 5-7 is slightly different from Figure 5-6. Figures 5-8 a, b plot the upper and lower bounds of the AR success probability of the ILS solutions according to the inequality formulas (4). Figure 5-9 plots the upper bound of the ILS AR success probability from epoch to epoch according to the inequality (3) where the determinant of the decorrelated covariance matrix is used. Figure 5-10 illustrates the position errors showing the impact of poor geometry around the a few epochs and instead of wrong integers.

Table 5-1 Description of data sets and settings in use of the geometry-based AR models (5)

Data information	
Data source/Date	http://www.ngs.noaa.gov/ on 1 January 2007
Data sets/format	P474 and P478/RINEX
Data length/total of epochs	24 h, 5760 epochs
Sample rates	15 seconds
Baseline	21 km
Cut-off angle	15 degrees
A priori variance-covariance settings for P1 and P2 code measurements	σ_{P1}^2 =(0.36m)2 σ_{P2}^2 =(0.54m)2 $\text{cov}(P1, P2) = (0.3286\text{m})^2$
A priori variance-covariance settings for phase measurement φL2 and φL2	$\sigma_{\phi 1}^2 = (0.0036m)^2$ $\sigma_{\phi 2}^2 = (0.0054m)^2$ $\text{cov}(\phi_{L1}, \phi_{L2}) = (0.003m)^2$
A priori variance of unit-weight measurements:	$\sigma_0^2 = (0.0036m)^2$
All-epoch post priori variance of unit-weight measurements	$\breve{\sigma}_0^2$ =(0.0021m)2

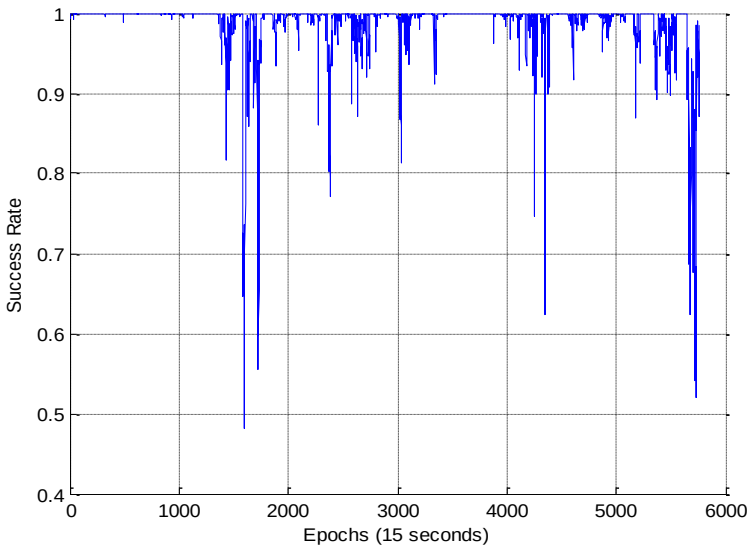

Figure 5-5 Illustration of computed integer rounding success probabilities according to the integration of m-normal distribution function (23) with single-epoch unit-weight variance estimates, referring to computation scheme I

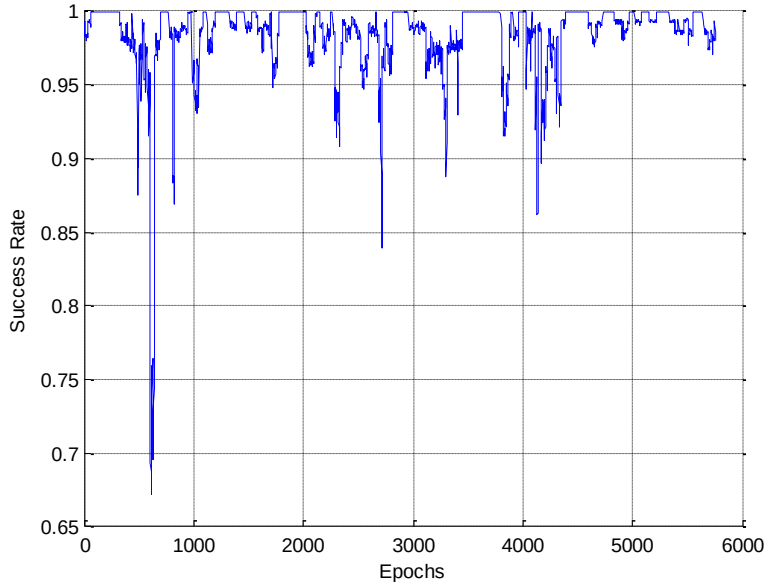

Figure 5-6 Illustration of computed integer rounding success probabilities according to the integration of m-normal distribution function (23) with the all-epoch variance estimate (see computation scheme II)

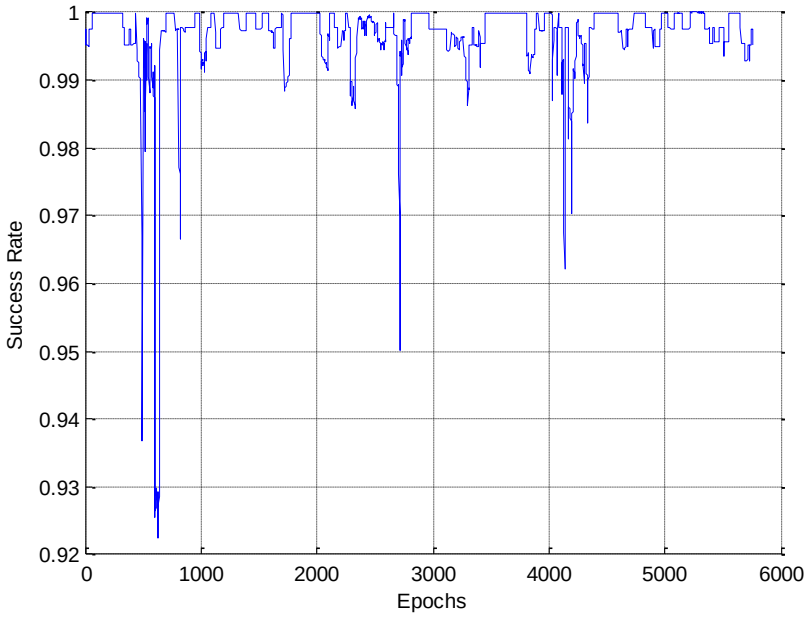

Figure 5-7 Illustration of computed integer bootstrapping success probabilities according to the integration of m-normal distribution function (24) (see computation scheme IV)

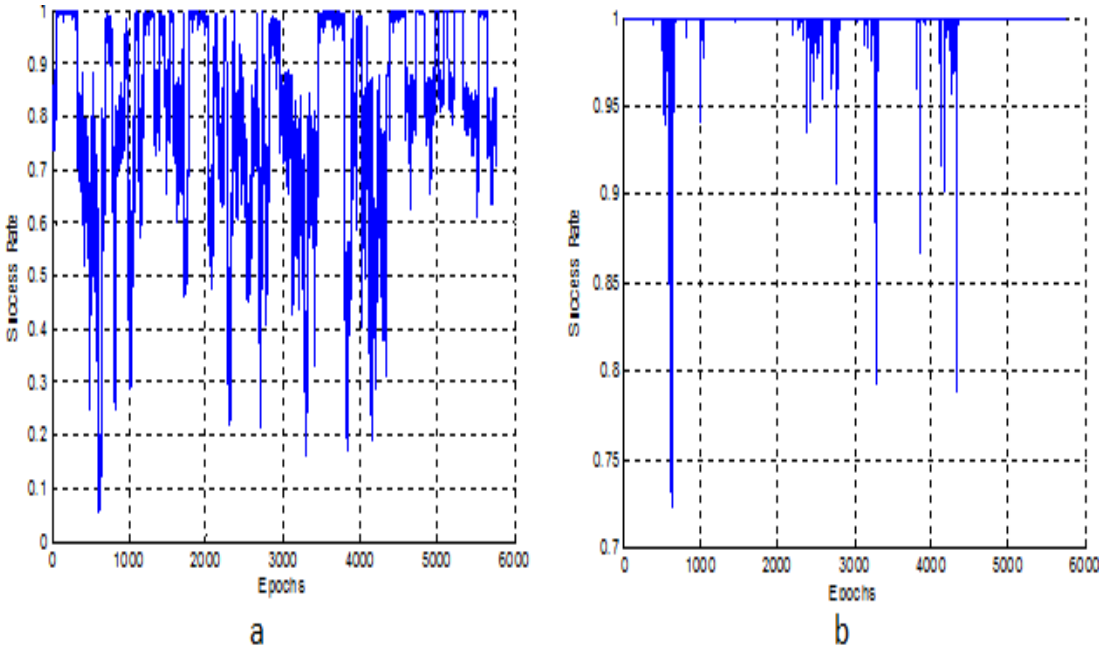

Figure 5-8 a Illustration of computed ILS lower-bound success probability according to the integration in the inequality (4) (see computation scheme V). b Illustration of computed ILS upper-bound success probability according to the integration in the inequality (4) (see computation scheme VI)

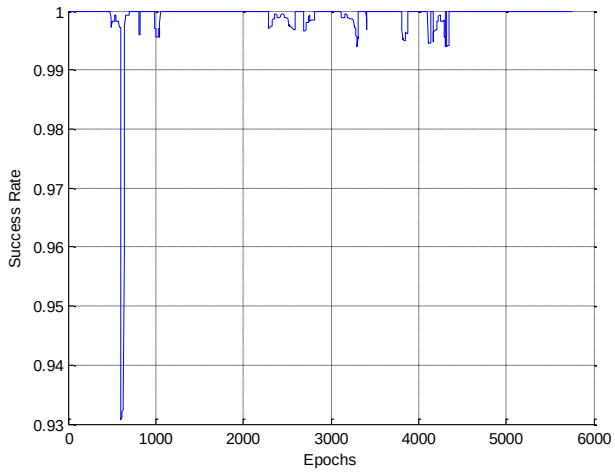

Figure 5-9 Illustration of computed ILS upper-bound success probability according to the right-hand integration in the inequality (3) (see computation scheme VII)

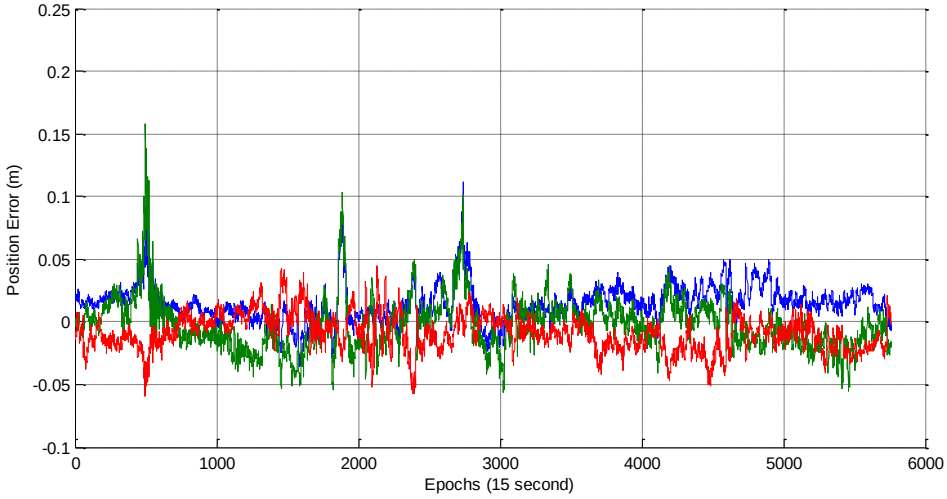

Figure 5-10 The positioning errors after integers are correctly fixed over all the epochs. The large errors show the impact of poor geometry instead of wrong integers.

Table 5-2 Summary of computational schemes and overall computed AR success probabilities and actual success rates

Formulas and settings	Computed success rate %	Actual success rate %
Integer rounding based on ambiguity decorrelation		
I (15),(23) and (25) single-epoch $\breve{\sigma}_0^2$	97.38	5666/5760 =98.37
II (15),(23) and (25) $(\sigma_0^2 = (0.0021m)^2$	98.44	
Integer bootstrapping based on ambiguity decorrelation		
III (16),(24) and (25) single-epoch $\breve{\sigma}_0^2$	98.87	5700/5760 =98.96
IV (16),(24) and (25) $(\sigma_0^2 = (0.0021m)^2$	99.67	
Integer Least Squares with ambiguity decorrelation		
V (11), (4) and (23) $(\sigma_0^2 = (0.0021m)^2$ Lower bound	81.91	
VI (11), (4) and (23) $(\sigma_0^2 = (0.0021m)^2$ Upper bound	99.91	5760/5760 =100
VII (11), (3) and (2) $(\sigma_0^2 = (0.0021m)^2$ Upper bound	99.92	

Table 5-2 summarises the computation schemes and computed success rate results of different integer estimators versus their actual success rates from the same data set. The actual success rate is defined by the ratio of the total number of data points at

which all integers are correct to the total number of data points. From the above figures and Table 5-2, we can obtain the following useful observations:

- Comparison between Figs. 5-5 and 5-6 shows strong effects of the unit–weight variance variations or uncertainties on the computed integer rounding probability. This implies that the unit–weight variance values taken in the probability formulas are equally important as the construction of pull-in regions, although estimation of unit-weight variances has attracted much less attentions in the context of success probability assessment.
- The overall computed success rate statistics from a 24 h data set confirm that the success rate of integer bootstrapping, 99.67%, is higher than that of integer rounding, 98.37%, but lower than the upper bound of the ILS estimation, 99.91%. The success rates of the first two methods indeed give lower bounds of the ILS success-rate as demonstrated from the real GPS data.
- Comparison between the computed success rates and actual success rate statistics demonstrates that the computed success rate of the integer bootstrapping 99.67% is a sharp approximation of the actual success rate, 100%, achieved in the ILS solutions, when the all-epoch unit-weight variance $\sigma_0^2 = (0.0021\text{m})^2$ is used. The computed success rate of integer bootstrapping solutions with the single epoch unit-weight variance is 98.87%, which agrees less to the actual ILS success rate of 100%.
- It is observed that the upper bound of ILS success rate 99.91% computed with (4) or 99.92% with (3) is an even sharper approximation to the actual ILS success rate of 100%, while the lower bound 81.91% is far too low as an approximation of the actual ILS success rates. However, it is noted that this agreement may depend on the setting in the stochastic model (6), especially the unit-weight variances, which are used in both actual AR processing and probability computations.

Although we cannot generalise the above findings from a single experimental study, the close agreement between the upper-bound of the ILS success probability and the actual success rate do imply that the multivariate normal cumulative probability integration (19) would be less dependent on the rigor of the ILS ambiguity pull-in region or Voronoi cell. Instead, the knowledge of the ambiguity bias vector Z0

caused by systematic errors and the unit-weight variance σ_0^2 the multivariate or univariate normal distribution function perhaps could be more dependent factors for the accurate probability computation, thus deserving more research attentions and experimental studies.

It is important to note that the consistence between the computed success rates and experimental results has only achieved in statistic results from the 24 h data set used. In fact, from the Figs. 5-5, 5-6, 5-7, 5-8, and 5-9, it is observed that low success rate spikes did not necessarily lead to wrong integer solutions at these epochs. Instead, poor satellite geometries may have been the direct causes for these probability spikes.

5.5 Concluding remarks

Rigorous computation of success rate of general integer least square solutions has been considered difficult due to the complexity of the pull-in region and heavy probability integration. The paper has introduced the cost function for sequential integer least-squares (SILS) estimation, allowing the complexity of ILS success probability computation to be reduced. The pull-in region that is mathematically expressed as the vertices of a polyhedron has been represented by a multidimensional grid, at which the cumulative probability can be computed with the multivariate normal cumulative density function (mvncdf) available in Matlab. A study has been presented for the bivariate case where the pull-in region is usually defined as a hexagon and the probability is easily obtained using the mvncdf function at all the grid points of the convex polygon. Based on the above studies, the paper has also argued that although the ellipsoid of a covariance matrix is not considered as an approximation to the ILS ambiguity pull-in region, the cumulative probability over the ellipsoid could still be a good approximation of the ILS success probability because of low or zero probability density values being taken at the grid points outside the pull-in region.

Using a 24 h GPS data set for a 21 km baseline, the paper has compared the computed success probabilities of integer rounding, integer bootstrapping solutions and lower and upper bounds of ILS success rates with the actual success rate obtained from the ILS solutions. The results have demonstrated that the upper bound probability of the ILS success rate, 99.91%, agrees with the actual ILS success rate

100% well, although the success rate computed with integer bootstrapping method 99.67% using decorrelated covariance matrices is a sharp approximation to the actual ILS success rate as well. Finally, results have also shown that the effects of the unit-weight variance variations or uncertainties on the computed integer rounding probability. In other words, the unit-weight variance values taken in the probability formulas are as important as the construction of pull-in regions, although estimation of unit-weight variances has attracted much less attentions in AR success probability assessment.

5.6 References

Blewitt G (1989) Carrier-phase ambiguity resolution for the Global Positioning System applied to geodetic baselines up to 2000 km. *J Geophys Res 94 (B8): 10.187-10.302.*

Dong D, Bock Y (1989) Global Positioning System network analysis with phase ambiguity resolution applied to crustal deformation studies in California. *J Geophys Res* 94: 3949-3966.

Feng Y (2008) GNSS three carrier ambiguity resolution using ionosphere-reduced virtual signals, J of Geodesy, 82 (12): 847 – 862.

Feng Y, Rizos C (2009) Network-Based Geometry-Free Three Carrier Ambiguity Resolution and Phase Bias Calibration, *GPS Solutions*, 13 (1):43-56.

Feng, Y, Li B (2008) Three Carrier Ambiguity Resolutions: Generalised Problems, Models and Solutions, *J. of Global Positioning Systems*, 8(2): 115-123.

Genz A, Bretz F (1999) Numerical Computation of Multivariate t Probabilities with Application to Power Calculation of Multiple Contrasts. *J. of Statistical Computation and Simulation.* 63: 361–378.

Genz A, Bretz F (2002) Comparison of Methods for the Computation of Multivariate Probabilities. *J. of Computational and Graphical Statistics*, 11(4): 950–971.

Hassibi A, Boyd S (1996) Integer parameter estimation in linear models with applications to GPS, in *Proc. IEEE Conf. Decision and Control*, Kobe, Japan: 3245–3251.

Hassibi A, Boyd A (1998) Integer parameter estimation in linear models with applications to GPS, *IEEE Trans. Signal Process.* 46(11):2938–2952.

O'Keefe K, Julien O, Cannon M E, Lachapelle G (2006) Availability, accuracy, reliability, and carrier-phase ambiguity resolution with Galileo and GPS, *Acta Astronautica*, 58(8): 422–434.

O'Keefe K, Petovello M, Lachapelle G, Cannon M E (2007) Assessing probability of correct ambiguity resolution in the presence of time-correlated errors, *Navigation*, 53 (4): 269–282.

Shannon C E (1959) Probability of error for optimal codes in a Gaussian channel, *Bell Syst. Techn. J.*, 38:611–656

Teunissen P (1997) A canonical theory for short GPS baselines, Part I: the baseline precision, *J. of Geodesy*, 71: 320-336.

Teunissen P. (1998) Success probability of integer GPS ambiguity rounding and bootstrapping, *J. of Geodesy*, 72:606–612.

Teunissen P (1999) A optimal property of the integer least-squares estimator, J. of Geodesy, 73:587–593

Teunissen P (2001) Integer estimation in the presence of biases', J of Geodesy, 75: 399-407.

Verhagen,S (2005) On the reliability of integer ambiguity resolution, *Navigation*, 52 (2):98–110.

Verhagen, S(2003) On the approximation of the integer least-squares success rate: which lower or upper bound to use. Journal of Global Positioning Systems, (2)**,** 117-124

Xu P (2001) Random simulation and decorrelation phase ambiguities, *J. of Geodesy, 75:408–423*

Xu P (2003) Voronoi cells, probabilistic bounds and hypothesis testing in mixed integer linear models, *Paper presented at IUGG 2003 in Sapporo, Hokkaido, Japan, June 30-11 July 2003.*

Xu P(2006) Voronoi cells, probabilistic bounds and hypothesis testing in mixed integer linear models, *IEEE Transaction on Information Theory*, 52(2):3122–3138

Chapter 6: Reliability of Partial Ambiguity Fixing with Multiple GNSS Constellations

Statement of Contribution of Co-Authors

The authors listed below have certified that:

1. they meet the criteria for authorship in that they have participated in the conception, execution, or interpretation, of at least that part of the publication in their field of expertise;
2. they take public responsibility for their part of the publication, except for the responsible author who accepts overall responsibility for the publication;
3. there are no other authors of the publication according to these criteria;
4. potential conflicts of interest have been disclosed to (a) granting bodies, (b) the editor or publisher of journals or other publications, and (c) the head of the responsible academic unit, and
5. they agree to the use of the publication in the student's thesis and its publication on the Australasian Digital Thesis database consistent with any limitations set by publisher requirements.

In the case of this chapter:

Contributor	**Statement of contribution**
Jun Wang	Conducted all the experiments and data analysis, wrote the manuscript
Yanming Feng	Reviewed and revised the manuscript

Principal Supervisor Confirmation

I have sighted email or other correspondence from all co-authors confirming their certifying authorship.

Yanming Feng		20-October-2012
Name	Signature	Date

Reliability of partial ambiguity fixing with multiple GNSS constellations

Jun Wang, Yanming Feng

Faculty of Science and Technology

Queensland University of Technology, Australia

Phone: +61 7 31389111, Fax: +61 7 31389390, Email: jun.wang@student.qut.edu.au

Abstract

Reliable ambiguity resolution (AR) is essential to Real-Time Kinematic (RTK) positioning and its applications, since incorrect ambiguity fixing can lead to largely biased positioning solutions. A partial ambiguity fixing technique is developed to improve the reliability of AR, involving partial ambiguity decorrelation (PAD) and partial ambiguity resolution (PAR). Decorrelation transformation could substantially amplify the biases in the phase measurements. The purpose of PAD is to find the optimum trade-off between decorrelation and worst-case bias amplification. The concept of PAR refers to the case where only a subset of the ambiguities can be fixed correctly to their integers in the integer least-squares (ILS) estimation system at high success rates. As a result, RTK solutions can be derived from these integer-fixed phase measurements. This is meaningful provided that the number of reliably resolved phase measurements is sufficiently large for least-square estimation of RTK solutions as well. Considering the GPS constellation alone, partially fixed measurements are often insufficient for positioning.

The AR reliability is usually characterised by the AR success rate. In this contribution an AR validation decision matrix is firstly introduced to understand the impact of success rate. Moreover the AR risk probability is included into a more complete evaluation of the AR reliability. We use 16 ambiguity variance-covariance matrices with different levels of success rate to analyse the relation between success rate and AR risk probability. Next, the paper examines during the PAD process, how a bias in one measurement is propagated and amplified onto many others, leading to more than one wrong integer and to affect the success probability. Furthermore, the paper proposes a partial ambiguity fixing procedure with a predefined success rate criterion and ratio-test in the ambiguity validation process. In this paper, the Galileo constellation data is tested with simulated observations. Numerical results from our experiment clearly demonstrate that only when the computed success rate is very high, the AR validation can provide decisions about the correctness of AR which are close to real world, with both low AR risk and false alarm probabilities. The results also indicate that the PAR procedure can automatically chose adequate number of ambiguities to fix at given high-success rate from the multiple constellations instead of fixing all the ambiguities. This is a benefit that multiple GNSS constellations can offer.

Keywords: Reliability, Partial ambiguity resolution, Partial ambiguity decorrelation, Multiple GNSS

6.1 Introduction

Global navigation satellite system (GNSS) linear observation equations are generally expressed as

$$\mathbf{L}=\mathbf{Ax}+\mathbf{BN}+\mathbf{e} \tag{1}$$

and the criterion of least-squares (LS) solutions of the equation (1) is given as

$$\min_{\mathrm{x,N}} \left\{ \left\| \mathbf{L}-\mathbf{Ax}-\mathbf{BN} \right\|_{\mathbf{Q}_L}^2 , \mathbf{x}\in R^n, \mathbf{N}\in Z^k \right\} \tag{2}$$

where **L** is the *m*-vector of 'observed minus computed' double-difference (DD) observations; **A** is the $m\times n$ design matrix for the vector of real-valued unknowns $\mathbf{x}$; **B** is the $m\times k$ design matrix for the vector of integer DD ambiguities **N**; $\mathbf{Q}_{\mathrm{L}}$ is the variance-covariance (vc-) matrix of observables; **e** is the vector of unmodelled effects and measurement noise and $\left\|\cdot\right\|_{\mathbf{Q}_L}^2 = (\cdot)^T \mathbf{Q}_L^{-1}(\cdot)$. The solution of the problem (2) is equivalent to the solution of the integer least-squares (ILS) problem

$$\breve{\mathbf{N}} = \arg\min_{N} \left\{ \left\| \hat{\mathbf{N}}-\mathbf{N} \right\|_{\mathbf{Q}_{\hat{\mathbf{N}}}}^2 , \mathbf{N}\in Z^k \right\} \tag{3}$$

where $\hat{\mathbf{N}}$ is a float ambiguity vector with the vc-matrix $\mathbf{Q}_{\hat{\mathbf{N}}}$ and $\breve{\mathbf{N}}$ is the estimated integer ambiguity vector. In general, $\mathbf{Q}_{\hat{\mathbf{N}}}$ has high correlation due to the DD geometry and correlation between measurement errors which makes the search progress inefficient. Decorrelation techniques have been developed and applied in order to reduce the elongation and size of the search space, referring to Teunissen (1993); Hassibi and Boyd (1998); Grafarend (2000), and Xu (2001). The essence of decorrelation is to apply an admissible integer unimodular matrix **Z** to eliminate or reduce the size of the off-diagonal elements of $\mathbf{Q}_{\hat{\mathbf{N}}}$. This can be expressed as

$$\hat{\mathbf{N}}_{\mathbf{dec}} = \mathbf{Z}^{\mathbf{T}}\hat{\mathbf{N}},\ \mathbf{Q}_{\hat{\mathbf{N}}_{\mathbf{dec}}} = \mathbf{Z}^{\mathbf{T}}\mathbf{Q}_{\hat{\mathbf{N}}}\mathbf{Z} \tag{4}$$

Therefore the ILS problem (3) is transformed as

$$\breve{\mathbf{N}}_{\mathrm{dec}} = \arg\min_{N}\left\{\left\|\hat{\mathbf{N}}_{\mathrm{dec}} - \mathbf{N}_{\mathrm{dec}}\right\|^2_{\mathbf{Q}_{\hat{\mathbf{N}}_{\mathrm{dec}}}}, \mathbf{N}_{\mathrm{dec}} \in Z^k\right\} \tag{5}$$

Due to the integer constraint $\mathbf{N}_{\mathrm{dec}} \in Z^k$, the solution $\breve{\mathbf{N}}_{\mathrm{dec}}$ of (5) must be obtained by virtue of a search process. Once we get $\breve{\mathbf{N}}_{\mathrm{dec}}$, $\breve{\mathbf{N}}$ can be easily obtained from $\breve{\mathbf{N}} = \left(\mathbf{Z}^{\mathbf{T}}\right)^{-1}\breve{\mathbf{N}}_{\mathbf{dec}}$. In the last step, the remaining real-valued parameter estimates $\hat{\mathbf{x}}$ can be updated due to the correlation with the ambiguities as

$$\breve{\mathbf{x}} = \hat{\mathbf{x}} - \mathbf{Q}_{\hat{\mathbf{x}}\hat{\mathbf{N}}}\mathbf{Q}_{\hat{\mathbf{N}}}^{-1}(\hat{\mathbf{N}} - \breve{\mathbf{N}}) \tag{6}$$

and

$$\mathbf{Q}_{\breve{\mathbf{x}}} = \underbrace{\mathbf{Q}_{\hat{\mathbf{x}}} - \mathbf{Q}_{\hat{\mathbf{x}}\hat{\mathbf{N}}}\mathbf{Q}_{\hat{\mathbf{N}}}^{-1}\mathbf{Q}_{\hat{\mathbf{N}}\hat{\mathbf{x}}}}_{1} + \underbrace{\mathbf{Q}_{\hat{\mathbf{x}}\hat{\mathbf{N}}}\mathbf{Q}_{\hat{\mathbf{N}}}^{-1}\mathbf{Q}_{\breve{\mathbf{N}}}\mathbf{Q}_{\hat{\mathbf{N}}}^{-1}\mathbf{Q}_{\hat{\mathbf{N}}\hat{\mathbf{x}}}}_{2} \tag{7}$$

Only if $\mathbf{Q}_{\breve{\mathbf{N}}}$ is very close to 0, the integer ambiguities can be considered deterministic which guarantees the precision of the fixed solution better than the float solution, because term 2 of (7) can be omitted in this case. Hence it is essential to have measures to decide whether the integer ambiguities can be assumed to be deterministic (Verhagen 2005). If only part of $\hat{\mathbf{N}}$ or $\hat{\mathbf{N}}_{\mathrm{dec}}$ can be fixed, we should group the remaining float ambiguities with the other real-valued parameters $\hat{\mathbf{x}}$ before updating them by (6), which implies the remaining float ambiguity set is also corrected and improved (Cao W 2009).

The success rate of ambiguity resolution (AR) is an important measure which gives a quantitative assessment of the probability of correct fixing and thus provides a reliability measure of AR (Teunissen et al. 1999a). The reliability decision depends on the functional and stochastic model, as well as the chosen method of integer ambiguity estimation. A more complete definition of the AR reliability should include the AR risk probability and other associate probabilities. The computed success rate of AR is defined as the integral of probabilistic density function of float ambiguity solutions over an ambiguity "Voronoi cell" (Hassibi and Boyd 1998) or "Pull-in region" (Teunissen 1998). Unfortunately, construction of the ILS pull-in region or Voronoi cell can be complex, the real-time computation of the AR success

rate is considered difficult and impractical. However various lower and upper bounds of the ILS success rate have been proposed and some of them have been proved good approximations of the actual success rate (Teunissen 1998, 2000, 2001, 2003; Verhagen 2003). Numerical experiment schemes and results have demonstrated that the success rate computed with the integer bootstrapping method is quite a sharp approximation to the actual ILS success rate (Verhagen 2003; Feng and Wang 2011). The performance of different bounds on the ILS success rate will be investigated and analysed in different cases.

Theoretically, once an AR model, method or processing procedure is proposed, the success rate can be predicated to evaluate the strength of the model or the reliability of AR. However, the success rate computation does not involve actual measurements, but a prior knowledge of the overall measurement noise level. Any biases in the actual measurements may affect the actual success rate although the computed success rate could be high. Therefore one cannot simply make the decision to accept the integer solution depending on the success rate only, because the float ambiguity can be located very near the boundary for the ILS pull-in region in practice. In that case, the integer solution cannot be distinguished from others with sufficient confidence. An ambiguity validation procedure is used to determine the integer solution uniquely. A popularly used validation technique is called ratio-test (Euler and Schaffrin 1990). The ratio-test tests the closeness of the float ambiguity to its nearest integer compared to the second-nearest integer. The integer solution is considered with high discernibility only when the ratio-test value exceeds a threshold value, for instance, 1.5 (Han and Rizos 1996), 2 (Wei and Schwarz 1995) or 3 (Leick 2004).

The success rate and the ratio-test are known as “model-driven” and “data-driven” approaches respectively by Teunissen and Verhagen (2008). The problem is that the dependence of the AR validation decisions on the AR success rate is not clear. In fact, the AR validation decisions are made without consideration of success rates. The AR reliability is currently defined by its success probability. A more complete evaluation of the AR reliability should at least include the AR risk probability. Similar to the probability of false alarm and missed detection usually used in the field of integrity monitoring (Kovach et al. 1995), the concepts of false alarm and missed detection are thus introduced in this paper to describe different AR integrity conditions as well.

Worldwide users expect significant performance benefits from the deployment of multiple GNSS constellations, which may be measured in terms of the availability, accuracy, reliability and continuity. O'Keefe (2001) presented the combined GPS/Galileo system had better performance than a single system in terms of horizontal dilution of precision (HDOP) and maximum horizontal position error (HPE), showing the availability and reliability advantages of integration systems. However since both HDOP and HPE are predicted parameters measures, the effects of actual measurement errors are not considered. Cao et al. (2008b) also claimed that the GPS/Galileo combined system offered a great improvement in terms of reliability and using dual-frequency GPS/Galileo together outperformed triple-frequency GPS or Galileo alone in terms of time required to achieve a given success rate. In addition to the benefits of the GPS/Galileo combined system, Ong et al. (2009) presented a GPS/GLONASS RTK methodology to estimate the position in several environments where residual analysis is applied to evaluate the accuracy and reliability of the RTK solutions. It indicated that the addition of GLONASS did improve the performance of RTK solutions in the given examples. However, fixing the full set of ambiguities of multiple constellations does not come without cost. One is the possible decrease of the success rate despite extra geometric information being considered. The idea of the partial ambiguity resolution (PAR) technique, which means resolving a subset of the ambiguities, was suggested to maintain a sufficiently high success rate and applied to the geometry-free model (Teunissen et al. 1999b). Choice of an ambiguity subset could be based on ambiguity variance, pre-defined subset sizes, elevation-ordering and linear combinations (Mowlam and Collier 2004). As far as the efficiency of the PAR technique for multiple constellations, Cao et al. (2007) numerically demonstrated that a combination of constellations can achieve higher success rates and positioning accuracies in shorter observation periods as compared to a single constellation used independently. In a later effort by Cao et al. (2008a), it was observed that different subsets of available ambiguities provided different advantages. But it was not clear how the PAR performance benefit from adding another observations either from additional frequencies or systems. Another PAR technique was developed to deal with the presence of biased observations (Parkins 2011). But, the technique is very time-consuming as it will run the LAMBDA algorithm for each subset until fixed. In the mean time, Henkel and Günther (2009) proposed partial ambiguity fixing with partial integer decorrelation in the presence of

biases in the case of single satellite differences. In this research effort, a PAR procedure with means of a predefined success rate is proposed and tested in both single constellation and multiple-constellation. The parameters, such as success rates, ADOPs, ratio-test values as well as positioning errors, are examined together as part of the analysis of the AR reliability, through the comparison between the PAR method and the traditional full AR method, that is, the LAMBDA method used in the context of this work.

The remainder of this paper is organised as follows. Section 6.2 briefly reviews the AR reliability related concepts, including the pull-in region, success rate and ADOP. Ambiguity validation and the related decision matrix are the subjects of Section 6.3. In Section 6.4, the impact of bias amplification in ambiguity decorrelation transformation is described. Section 6.5 describes a PAR procedure with a predefined success rate. In Section 6.6, numerical experiment schemes and results for different cases are provided to demonstrate the advantages of this proposed PAR method with multiple GNSS constellations. Finally, the main research findings achieved in this work are summarised.

6.2 Reliability Characteristics of Ambiguity Resolution

Incorrect integer solutions of AR, when passed the validation tests without an alert, will often lead to unacceptable positioning errors. Therefore, an index to denote the quality of AR is needed to provide the reliability information to users. The ambiguity dilution of precision (ADOP) is introduced as an AR performance measure (Teunissen and Odijk 1997). The success rate of ambiguity resolution (AR) is another important measure which gives a quantitative assessment of the probability of correct fixing (Teunissen 1998, 2000; O'Keefe et al. 2006; Verhagen 2005). The computation of these indices of the AR reliability is described in this section.

6.2.1 ADOP

Like the dilution of precision measure commonly used to describe the impact of receiver-satellite geometry on the positioning precision, the concept of ADOP is introduced to measure the intrinsic precision characteristics of the ambiguities. It is defined as

$$ADOP = \sqrt{\left|\mathbf{Q}_{\hat{\mathbf{N}}}\right|^{\frac{1}{k}}} \quad \text{(cycle)} \tag{9}$$

It is suggested that an ADOP of 0.15 cycles or less would be required if the success rate is required to be above 0.99 (Verhagen et al. 2010).

6.2.2 Pull-in region and success rate of integer least-squares

The success rate is defined as the integral of the probabilistic density function of float ambiguity solutions over an ambiguity "Voronoi cell" (Hassibi and Boyd 1998) or "Pull-in region" (Teunissen 1998). The probability P_S of correct integer estimation in the case of ILS is defined as follows

$$P_S = P(\breve{\mathbf{N}} = \mathbf{N}) = \int_R f_{\hat{N}}(x)dX \tag{10}$$

where R and $f_{\hat{N}}(x)$ denote the pull-in region and the probability density function of the float ambiguities $\hat{\mathbf{N}}$ respectively. In general, we assume the float ambiguity is normally distributed, e.g. $N(\mathbf{N}, \sigma_0^2\mathbf{Q}_{\hat{\mathbf{N}}})$. Therefore, the success rate can be expressed as

$$\begin{aligned} P_S &= \int_R N(\mathbf{N}, \sigma_0^2\mathbf{Q}_{\hat{\mathbf{N}}})dX \\ &= \int_R \frac{1}{(2\pi)^{\frac{1}{m}}\left|\sigma_0^2\mathbf{Q}_{\hat{\mathbf{N}}}\right|^{1/2}} \exp[-\frac{1}{2\sigma_0^2}(\mathbf{X}-\mathbf{N})^{\mathrm{T}}\mathbf{Q}_{\hat{\mathbf{Z}}}^{-1}(\mathbf{X}-\mathbf{N})]dX \end{aligned} \tag{11}$$

where σ_0^2 is the variance of the unit-weight measurements. Figure 6-1 shows an example of a two-dimensional ILS pull-in region and its corresponding probability density function (PDF) over the ILS pull-in regions respectively.

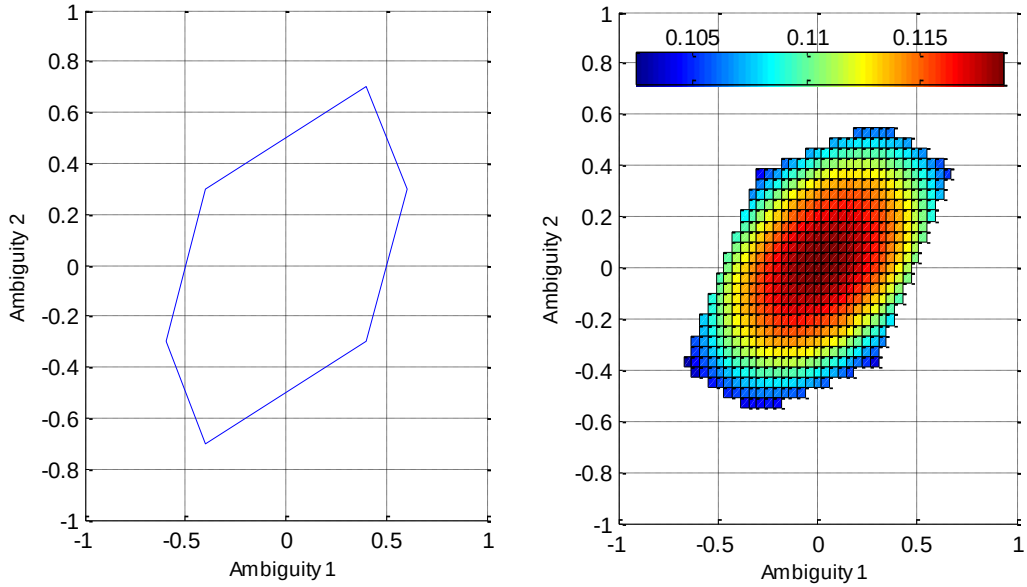

Figure 6-1 Illustration of the pull-in region (*left*) and the probability density (*right*) of 2-dimensional matrix

Nevertheless, construction of the ILS pull-in region or Voronoi cell can be complex, and the real-time computation of the AR success rate is considered difficult and impractical. Fortunately, various lower and upper bounds of the ILS success rate have been proposed and some of them have been proved to be good approximations of the actual success rate.

6.2.3 Computation of success rates

The success rate of the integer bootstrapping formula is an exact formula and easy to evaluate. Teunissen (1999) proved that of all the integer estimators, the ILS estimator has the highest possible success rate. As a result, the bootstrapped success rate was widely used as a lower bound for the ILS success rate (O'Keefe et al. 2006; Cao et al. 2007). Numerical experiment schemes and results have demonstrated that the success rate computed with the integer bootstrapping method is quite a sharp approximation to the actual ILS success rate (Verhagen 2003; Feng and Wang, 2011). The results also showed that variations or uncertainty in the unit–weight variance estimates from epoch to epoch will affect the computed success rates obtained via different methods significantly, thus deserving more attention in order to obtain useful success probability predictions. Teunissen (2000) also gave the computations of the lower and upper bounds of the ILS success rate based on the extreme eigenvalue of $\mathbf{Q}_{\hat{\mathbf{N}}_{\mathbf{dec}}}$. But having biases unaccounted for will affect the success rate. Hence a bias-affected

bootstrapped success rate is studied to evaluate the bias robustness of AR (Teunissen 2001). In addition, another upper bound and approximation of the ILS success rate were given based on the ADOP using different formulas (Teunissen 2003; Verhagen 2003). An overview of the bounds and approximations is given in Table 6-1.

Table 6-1 A summary of AR success rates computing algorithms as approximations to the actual AR success rate

Methods	Approximations	References
P_{low}, P_{up1}, lower and upper bounds based on maximum and minimum eigenvalue	$P_{low} = [2\Phi(\frac{1}{2\sqrt{\lambda_{\max}}}) - 1]^k \le P(\breve{\mathbf{N}} = \mathbf{N})$ $\le P_{up1} = [2\Phi(\frac{1}{2\sqrt{\lambda_{\min}}}) - 1]^k$	(Teunissen 2000)
P_{boot}, lower bound based on bootstrapping	$P_{boot} = \prod_{i=1}^{k} \left[2\Phi\left(\frac{1}{2\sigma_{\hat{N}_i \mid I}} \right) - 1 \right] \le P(\breve{\mathbf{N}} = \mathbf{N})$	(Teunissen 1998)
P_{bias}, bias-affected on bootstrapped success rate	$P_{bias} = \prod_{i=1}^{m} \left[\Phi\left(\frac{1-2\beta_i}{2\sigma_{\hat{N}_i \mid I}} \right) + \Phi\left(\frac{1-2\beta_i}{2\sigma_{\hat{N}_i \mid I}} \right) - 1 \right] \le P_{boot}$	(Teunissen 2001)
P_{up2}, upper bound based on ADOP	$P_{up2} = P\left(\chi^2(k,0) \le \frac{c_k}{ADOP^2} \right) \ge P(\breve{\mathbf{N}} = \mathbf{N})$	(Teunissen 2003; Verhagen 2003)
P_{adop}, approximation of Ps and upper bound of P_{boot} based on ADOP	$P(\breve{\mathbf{N}} = \mathbf{N}) \approx P_{adop} = \left[2\Phi\left(\frac{1}{2\mathrm{ADOP}} \right) - 1 \right]^k \ge P_{boot}$	(Teunissen 2003)

Note: $\Phi(t) = \int_{-\infty}^{t} \frac{1}{\sqrt{2\pi}} \exp(-\frac{1}{2}x^2)dx$, $c_k = \frac{\left(\frac{k}{2}\Gamma\left(\frac{k}{2}\right)\right)^{\frac{2}{k}}}{\pi}$, and β_i is the ith entry of the bias vector $L^{-1}b$.

6.3 Ambiguity Validation Decision Matrix

Unlike the success rate which indicates the strength of the underlying model and assumption of the variance of measurement noises and is not directly dependent on the actual measurements, the ratio-test value is the data-driven index of the reliability of AR (Teunissen and Verhagen 2008). In this research effort, we introduce an ambiguity validation decision matrix for four ratio-test results that can occur under conditions of high or low success rates. The probability consequences in different situations reflect the reliability of AR and other associated parameters.

6.3.1 Ratio test

For the ambiguity validation purpose, most validation techniques need at least two integer candidates with the minimum quadratic form of integer ambiguities residuals, and the second minimum one. The ratio-test is a popular acceptance test and given by

$$\text{Accept } \breve{\mathbf{N}} \text{ if: } \frac{\left\|\hat{\mathbf{N}}-\breve{\mathbf{N}}_2\right\|^2_{\mathbf{Q}_{\hat{\mathbf{N}}}}}{\left\|\hat{\mathbf{N}}-\breve{\mathbf{N}}\right\|^2_{\mathbf{Q}_{\hat{\mathbf{N}}}}} \geq t \tag{12}$$

where $\breve{\mathbf{N}}_2$ is the second best integer ambiguity candidate and t is an empirically critical value. The ratio-test actually tests the closeness of the float ambiguity to its nearest integer compared to the second-nearest integer. The critical value of t actually determines how close between two candidates the user will choose. In general t can be chosen 1.5 (Han and Rizos 1996), 2 (Wei and Schwarz 1995) or 3 (Leick 2004). Referring to the integrity concepts as shown in Kovach (1995), there are four ratio-test results that can occur under conditions of high or low success rates, as shown in Table 6-2:

N_R − Normal operation, while the integer ambiguity is fixed correctly and the ratio test is passed, whether the success rate is high or low;

F_R − False alarm, while the integer ambiguity is fixed correctly, but the ratio test is rejected, whether the success rate is high or low;

M_R − Missed detection, while the integer ambiguity is fixed incorrectly, but the ratio test is passed when the success rate is either high or low;

D_R − Detection, while the integer ambiguity is fixed incorrectly, the ratio test is indeed rejected when the success rate is either high or low.

According to the definition of these four probabilities, the result of each probability is easy to compute. For instance, the normal operation probability P_{N_R} equals the number of those correct samples passing the ratio-test divided by the number of total samples. The relationship between all of the probabilities is

$$P_{N_R} + P_{M_R} + P_{D_R} + P_{F_R} = 1 \tag{13}$$

The ideal situation is that P_{N_R} is close to 1, and all the others are close to zero. The next best situation is the sum of $P_{N_R} + P_{D_R}$ is close to 1 and the P_{M_R} and P_{F_R} are close to zero. Neither a high P_{F_R}, nor a low P_{N_R} is preferred since the result does not lead to optimal position solutions. The worst case is the high missed detection rate, since wrong integer ambiguities often lead to the fixed solution being further away from the true solution than the float solution itself. In that situation, the event is referred to AR risk probability. Therefore, it is desirable to keep the probability P_{M_R} of missed detection as low as possible. The analysis in Section 6.6 numerically examines these probability parameters obtained under different success probabilities and numbers of satellites. All these probabilities in Table 6-2 can be obtained statistically from the actual results.

Table 6-2 AR probability outcomes from the ratio test decision under high and low AR success rates

Ratio Test	Correct Ambiguity	Wrong Ambiguity
Pass	Normal Operation (P_{N_R})	Missed Detection (P_{M_R})
Reject	False Alarm (P_{F_R})	Detection (P_{D_R})

Note: The subscript $_R$ denotes the decision based on ratio test

6.4 Partial Ambiguity Decorrelation

Although it is already possible to decorrelate $\mathbf{Q}_{\hat{\mathbf{N}}}$ within one iteration, the iterative decorrelation procedure is generally necessary in terms of the integer Gaussian elimination method (Teunissen 1993). The purpose of Teunissen's **Z** transformation is two-fold: (1) to decorrelate, (2) to flatten ambiguity spectrum (i.e. to reduce diagonal terms of D-matrix in $L^T DL$ decomposition). The reason for an iterative solution is that the decorrelation is to eliminate or reduce the size of the off-diagonal elements of $\mathbf{Q}_{\hat{\mathbf{N}}}$, while the permutation focuses on the diagonal elements, but also affects the off-diagonal elements. Hence, a subsequent decorrelation is required. Teunissen developed the ambiguity transformation for a zero-mean Gaussian measurement noise, i.e. it solely depends on $\mathbf{Q}_{\hat{\mathbf{N}}}$, without considering the measurement biases, which are linearly combined by the **Z** transformation. The linear combination could suppress but also substantially amplify the biases,

depending on the signs of the elements in **Z** and signs of the biases. According to (4), the $\mathbf{Z}^{\mathbf{T}}$ matrix transforms the float ambiguity bias vector $bias_{\hat{\mathbf{N}}}$ into

$$bias_{\hat{\mathbf{N}}_{\mathbf{dec}}} = \mathbf{Z}^{\mathbf{T}} bias_{\hat{\mathbf{N}}} \tag{14}$$

whose absolute value can be upper bounded by

$$abs\left(bias_{\hat{\mathbf{N}}_{\mathbf{dec}}}\right) = abs\left(\mathbf{Z}^{\mathbf{T}}\right) \cdot abs\left(bias_{\hat{\mathbf{N}}}\right) \tag{15}$$

where *abs*() is an absolute value operator. Therefore, Henkel and Günther (2009) suggested a partial integer decorrelation, which uses a reduced number of decorrelation steps to lower the magnitude of the elements in **Z** and, thereby, find the optimum trade-off between decorrelation and worst-case bias amplification.

To exemplify the amplification of biases in decorrelation, we consider two cases: single bias and multiple biases. We assume that the magnitude of the biases in the float solution is 0.1 cycles which corresponds to approximately 2 cm – a typical value for phase multipath and uncorrected satellite phase biases in a Precise Point Positioning (PPP) solution (Henkel and Günther 2009, 2012). Table 6-3 shows the impact of the bias vector on decorrelated solutions with a different transformation matrix **Z**. The decorrelation function implemented in the LAMBDA method is modified to record the number of iterative decorrelation procedures and the corresponding information, for example, the transformation matrix **Z**. $\mathbf{Z_1}$ and $\mathbf{Z_2}$ are obtained after 2 and 4 iterations respectively. Obviously the performance of decorrelation by $\mathbf{Z_2}$ is better than $\mathbf{Z_1}$, but the impact of bias on the decorrelated solution of $bias_2$ is worse than that of $bias_1$ in both cases. The $bias_2$ with the decorrelation process by $\mathbf{Z_2}$ is not only amplified but propagated, whilst the decorrelation process by $\mathbf{Z_1}$ still keeps $bias_1$ of 0.1 cycles in Case 1. We also notice that the second float ambiguity element decorrelated by $\mathbf{Z_2}$ is biased 0.5 cycles in Case 2, which possibly leads to an erroneous fixing. On the contrary, the biases by $\mathbf{Z_1}$ were less than 0.2 cycles, which still allows a correct fixing.

Table 6-3 The impact of biases on decorrelated solutions of different decorrelation levels

Q	Z_1	Z_2	cond (Q)	cond (Q_1)	cond (Q_2)
$\begin{bmatrix} 6.29 & 5.97 & 1.54 \\ 5.97 & 7.29 & 4.34 \\ 1.54 & 4.34 & 9.28 \end{bmatrix}$	$\begin{bmatrix} 1 & 0 & 0 \\ -1 & -1 & 1 \\ 0 & 1 & 0 \end{bmatrix}$	$\begin{bmatrix} 1 & 2 & 1 \\ 0 & -2 & -1 \\ 0 & 1 & 0 \end{bmatrix}$	43.18	16.10	5.01
Case 1:*bias*	$\lvert bias_1 \rvert$	$\lvert bias_2 \rvert$	Case 2:*bias*	$\lvert bias_1 \rvert$	$\lvert bias_2 \rvert$
$\begin{bmatrix} 0.1 \\ 0 \\ 0 \end{bmatrix}$	$\begin{bmatrix} 0.1 \\ 0 \\ 0 \end{bmatrix}$	$\begin{bmatrix} 0.1 \\ 0.2 \\ 0.1 \end{bmatrix}$	$\begin{bmatrix} 0.1 \\ 0.1 \\ 0.1 \end{bmatrix}$	$\begin{bmatrix} 0.2 \\ 0.2 \\ 0.1 \end{bmatrix}$	$\begin{bmatrix} 0.1 \\ 0.5 \\ 0.2 \end{bmatrix}$

Generally, the higher the dimension of **Q**, the larger the number of iterative decorrelation steps. Figure 6-2 shows the bootstrapped success rate P_{boot} in the case with no bias, with a bias of 0.01 cycles, and with a bias of 0.1 cycles on a ten-dimensional matrix for different iteration numbers of decorrelation steps. The ten-dimensional matrix is derived from a GPS dual-frequency phase with 6 visible satellites. It is clear that the success rate of the case with the bias of 0.01 cycles is almost the same as the one without bias. This means the bias of 0.01 cycles actually can be considered as part of a random error rather than a bias. On the contrary, the success rate with the bias of 0.1 cycles is significantly different from the original one. In some extreme cases, the biased success rate with 0.1 cycles is lower than 10% while the unbiased success rate is actually high than 90%, see iteration numbers from 250 to 300. Figure 6-3 gives the corresponding bootstrapping solution for these three cases. It is easy to find out the success rate of the bootstrapping solution, with the bias of 0.1 cycles starting to be different from the other two solutions after 100 iterations but being closer to that of the other solutions after 310 iterations. But from Figure 6-3, it is seen that while the solutions with biases of 0 or 0.01 cycles are all correctly approaching zero after 250 iterations, the same integer solutions affected by the bias of 0.1 cycles remain incorrect through to the end of the iterations.

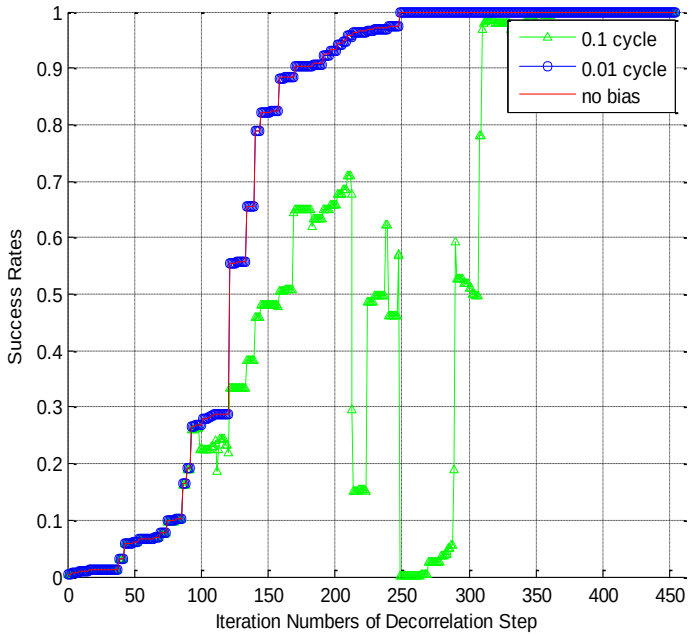

Figure 6-2 The success rate P_{boot} in the case with no bias, with a bias of 0.01 cycles, and a bias of 0.1 cycles on a ten-dimensional matrix for different numbers of decorrelation steps

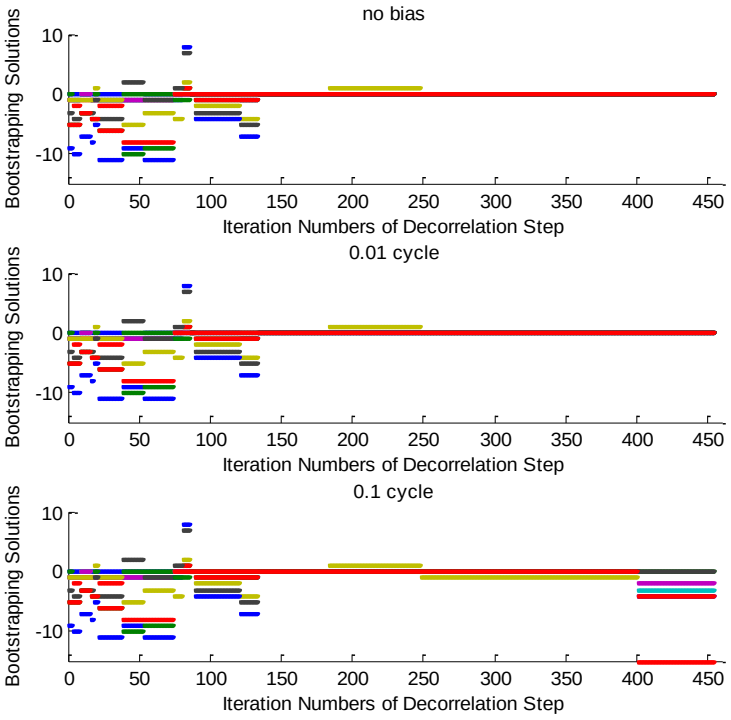

Figure 6-3 Illustration of effects of measurement biases on bootstrapping ambiguity solutions with consideration of the cases with no bias, a bias of 0.01 cycles, and a bias of 0.1 cycles. The dimension of the Q matrix is 10 and the decorrelation iteration run from 1 to 450 steps.

6.5 Partial Ambiguity Fixing With Indices of Success Rate and Ratio Test

In this study, a modified partial ambiguity resolution procedure is used in order to find a subset of integers which can be fixed with a certain confidence under conditions when a correct resolution of the whole set of integers in the linear equation system is not possible. Unlike the usual method, the modified PAR procedure combines indices of both the success rate and the ratio test. Figure 6-4 presents the flowchart of this PAR procedure. As shown, the PAR process starts with the decorrelation of the ambiguities. Next, the bootstrapped success rate Ps is computed and compared to the Ps (*predefined*). If $\mathrm{Ps} \geq \mathrm{Ps}(\textit{predefined})$, the usual AR process is followed. If $\mathrm{Ps} < \mathrm{Ps}(\textit{predefined})$, the diagonal elements of the decorrelated matrix are sorted in the ascending order, and a minimum required success rate is chosen. If the number of selected ambiguities is less than three, only the float solutions are made available. The integer solutions which can satisfy both the requirement of the success rate and the ratio test will be used to derive the fixed solutions, although in practice the measurements with the float ambiguities may also be used to derive the position solutions if proper weights can be given. The results of this proposed procedure will be shown to work much better with the multiple GNSS constellations than the single-GNSS constellation.

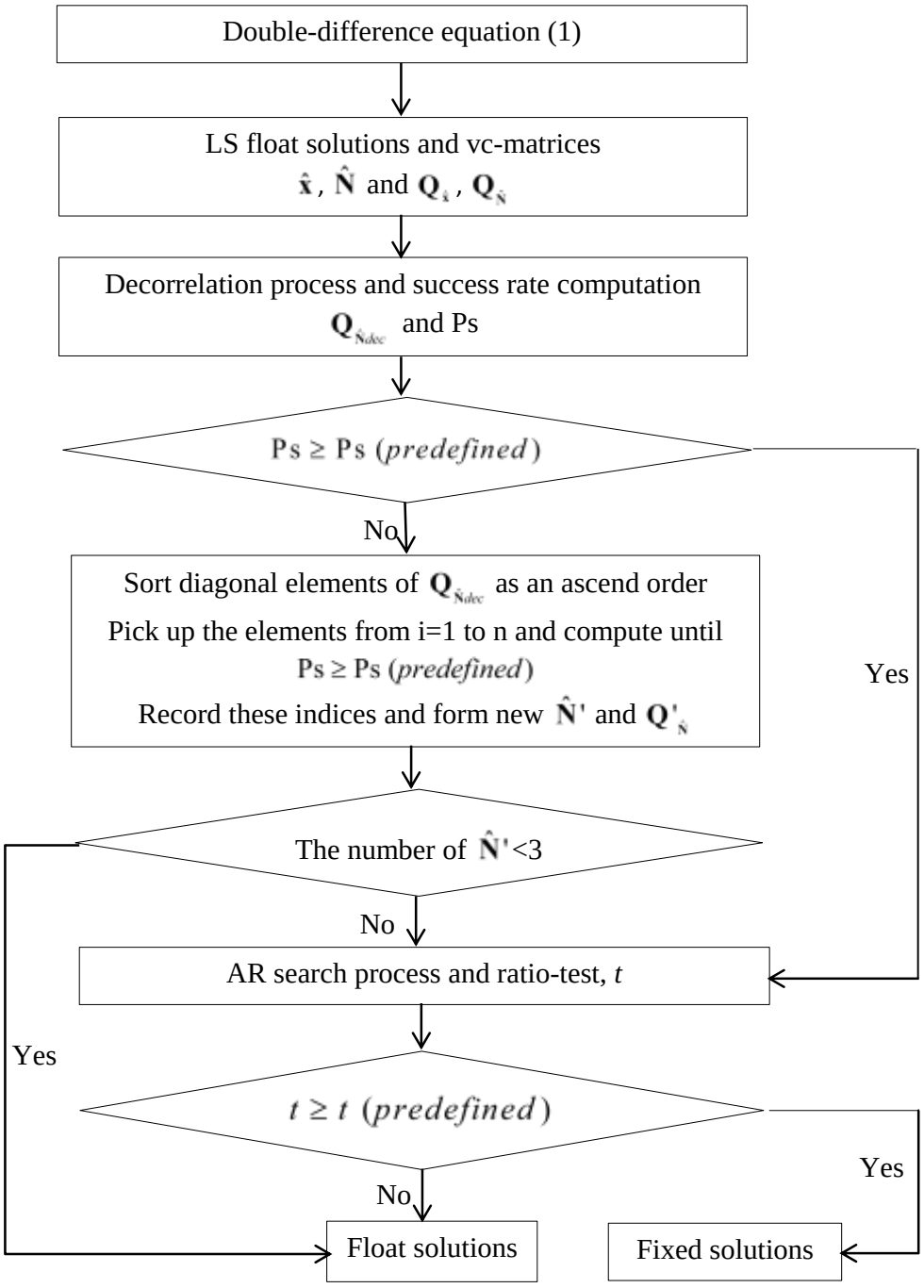

Figure 6-4 The flowchart of partial ambiguity resolution with predefined success rate

6.6 Experimental Analysis

The AR reliability is the key to real-time precise positioning with carrier phase measurements. It has been widely expected in the GNSS community that with the multiple GNSS signals, the AR reliability can be improved or promised. Will this be exactly the case? With various probability parameters and the ambiguity validation decision matrix given in the previous sections, we numerically examine how these parameters are related to each other. In particular, we examine how the ambiguity validation decision will depend on the computed AR success probabilities, ratio-test values and their variations under condition of different number of satellites. The reliability performance of PAR in the multiple GNSS constellation is specifically discussed in the following subsection. The virtual Galileo constellation (VGC) method is applied to simulate the virtually real data of another GNSS constellation (Feng 2005). The concept is to combine the GPS measurements data sets recorded at two epochs separated by a few hours, and compute the user state parameters for the two different epochs. It is emphasised that two reference satellites are selected for GPS and VGC respectively. For convenience, the linear DD equation for combination of GPS and VGC is given by

$$\begin{bmatrix} \mathbf{L}_{gps} \\ \mathbf{L}_{vgc} \end{bmatrix} = \begin{bmatrix} \mathbf{A}_{gps} & \mathbf{B}_{gps} & 0 \\ \mathbf{A}_{vgc} & 0 & \mathbf{B}_{vgc} \end{bmatrix} \begin{bmatrix} \mathbf{x} \\ \mathbf{N}_{gps} \\ \mathbf{N}_{vgc} \end{bmatrix} + \begin{bmatrix} \mathbf{e}_{gps} \\ \mathbf{e}_{vgc} \end{bmatrix} \tag{16}$$

where $\mathbf{L}_{gps}$ and $\mathbf{L}_{vgc}$ are the DD observations for GPS and VGC respectively; $\mathbf{A}_{gps}$ and $\mathbf{A}_{vgc}$ are their design matrices with respect to the user position states $\mathbf{x}$; $\mathbf{B}_{gps}$ and $\mathbf{B}_{vgc}$ are their design matrices with respect to the DD ambiguities; $\mathbf{e}_{gps}$ and $\mathbf{e}_{vgc}$ are the corresponding measurement noises. Both code and carrier phase measurements are involved in (16).

6.6.1 AR success rates, ratio-test values and AR validation outcomes

AR success rates computing algorithms as approximations to the actual AR success rate are referred to Table 6-1 and the ambiguity validation decision parameters are referred to Table 6-2. The covariance matrices for the single constellation (12 and 16 ambiguities) and dual constellations (DCS) (20 and 24 ambiguities) are obtained

from a real GPS baseline where the DCS are simulated using the concept of GPS + VGC (Feng 2005). A total of 16 ambiguity vc-matrices are adopted in the experimental analysis. The vc-matrices are chose to take four success rate P_{boot} values: low, medium, high and very high in each integer dimension case. For each ambiguity vc-matrix, 10,000 simulation samples from $N(\mathbf{0}, \sigma_0^2 \mathbf{Q}_{\hat{\mathbf{N}}})$ and the corresponding vc-matrix $\sigma_0^2 \mathbf{Q}_{\hat{\mathbf{N}}}$ are used as input for the ILS estimation. The output of this estimator should be a zero vector if it is correct. Next, we can count correct samples and obtain the actual success rate. The actual success rate over an observational period is given as an average of the probabilities over all the epochs or data points, that is, the number of correct samples divided by the total number of samples 10,000.

Table 6-4 summarises the computed and actual success rates against different AR probability results under different ratio test thresholds. Table 6-4 confirms that overall the computed ILS success rate P_{boot}, is a sharp approximation to the actual success rate from the statistics, although P_{adop} has a better evaluation performance for case with the dimension of 12. It is clear that the actual success rate P_{actual} maintain good agreement with the predicted success rate P_{boot}. The mean of the critical value *t* increases along with P_{boot} within the same dimension of ambiguity vc-matrix. Table 6-4 also indicates that the risk probability P_{M_R} of AR decreases in accordance with increase of the success rate P_{boot} or the critical value *t*. For example, in the cases when the success rate P_{boot} achieves either 0.99 (with the dimension of 12) or 1.00 (with the dimension of 16), both the AR risk probability P_{M_R} and the detection probability P_{D_R} become zero when the critical value *t* equals 1.5, or 2, or 3.

Table 6-4 Statistical information of AR success rates, AR risk parameters, and ratio-test thresholds in the single-constellation case

Dimension	12	12	12	12	16	16	16	16
P_{boot}	**0.67**	**0.80**	**0.96**	**0.99**	**0.46**	**0.65**	**0.81**	**1.00**
P_{low}	0.06	0.11	0.37	0.65	0.00	0.03	0.05	0.64
P_{up1}	1.00	1.00	1.00	1.00	1.00	1.00	1.00	1.00
P_{up2}	0.89	0.94	1.00	1.00	0.81	1.00	1.00	1.00
P_{adop}	**0.74**	**0.81**	**0.98**	**1.00**	**0.57**	**0.94**	**1.00**	**1.00**

Correct integer numbers	7166	8772	9866	9984	4970	6652	8084	10000
Incorrect integer numbers	2834	1228	134	16	5030	3348	1916	0
Actual success rate P_{actual}	**0.72**	**0.88**	**0.99**	**1.00**	**0.50**	**0.67**	**0.81**	**1.00**
Mean of t for all samples	1.58	2.19	3.66	4.85	1.22	1.29	1.41	6.05
Mean of t for correct samples	1.70	2.32	3.69	4.86	1.28	1.35	1.46	6.05
Mean of t for incorrect samples	1.25	1.25	1.24	1.17	1.15	1.17	1.21	Nan
t =1.5, P_{N_R}	0.37	0.64	0.93	0.98	0.08	0.15	0.29	1.00
t =1.5, P_{M_R}	0.04	0.02	0.00	0.00	0.02	0.02	0.01	0.00
t =1.5, P_{F_R}	0.34	0.23	0.06	0.02	0.42	0.51	0.52	0.00
t =1.5, P_{D_R}	0.25	0.11	0.01	0.00	0.48	0.32	0.18	0.00
t =1.5, pass samples	4108	6598	9296	9838	998	1696	3108	9996
t =2, P_{N_R}	0.16	0.43	0.79	0.94	0.01	0.03	0.06	1.00
t =2, P_{M_R}	0.01	0.03	0.00	0.00	0.00	0.00	0.00	0.00
t =2, P_{F_R}	0.55	0.45	0.20	0.06	0.49	0.64	0.75	0.00
t =2, P_{D_R}	0.28	0.12	0.01	0.00	0.50	0.33	0.19	0.00
t =2, pass samples	1710	4302	7964	9372	152	278	588	9966
t =3, P_{N_R}	0.03	0.18	0.50	0.75	0.00	0.00	0.00	0.95
t =3, P_{M_R}	0.00	0.00	0.00	0.00	0.00	0.00	0.00	0.00
t =3, P_{F_R}	0.69	0.70	0.49	0.25	0.50	0.66	0.81	0.05
t =3, P_{D_R}	0.28	0.12	0.01	0.00	0.50	0.34	0.19	0.00
t =3, pass samples	312	1802	5028	7510	8	18	32	9480

Table 6-5 shows the AR success rates and AR risk conditions with different ratio test thresholds obtained for the ambiguity dimensions of 20 and 24 respectively. In general, the observations regarding the agreements between P_{boot} and P_{actual} remain the same in the dual-constellation case. Most of computed AR probability bounds listed in Table 6-1 show more spacious approximations to the actual success rate in the dual-constellation case, but the bootstrapped success rate can still be a good lower bound and a sharp approximation of the ILS success rate. From Table 6-4 and Table 6-5, additional comments are given as follows:

- Comparing the ambiguity validation decision parameters among the cases of the critical values of t being 1.5, 2 and 3, it is clearly seen that the probability of "Normal Operation" in each case is distinctively far from the actual success rate, except for the case when the actual success rate is very close to 1. The false alarm and detection rates, P_{F_R} and P_{D_R} remain very high until the success rate is close to 1, such as 0.99. This situation is worsened in the dual constellation case. A positive behaviour of the

validation process is that the missed detection rate P_{M_R} is always relatively small, especially in the dual-constellation case or, understandably, when t is larger. In general, when the computed success rate is very high (close to 1), the AR validation with a lower ratio-test threshold will provide the decisions about the correctness of AR close to the real world with both low AR risk and false alarm probabilities.

- The implication of achieving high computed success rates, e.g. close to 1 for all tests, becomes clear from the results in both Table 6-4 and 6-5. The high success rate not only guarantees the correctness of AR, but also restricts the AR risk probability, and keeps false alarm and detection rates very low. For instance, we can see that the probabilities of P_{M_R}, P_{F_R} and P_{D_R} are all zeros when the success rate is very close to 1.

Table 6-5 Statistical information of AR success rates, AR risk parameters, and ratio-test thresholds in the dual-constellations case

Dimension	20	20	20	20	24	24	24	24
P_{boot}	**0.66**	**0.81**	**0.96**	**0.99**	**0.66**	**0.81**	**0.96**	**1.00**
P_{low}	0.01	0.02	0.17	0.59	0.01	0.01	0.18	0.64
P_{up1}	1.00	1.00	1.00	1.00	1.00	1.00	1.00	1.00
P_{up2}	1.00	1.00	1.00	1.00	1.00	1.00	1.00	1.00
P_{adop}	**0.99**	**1.00**	**1.00**	**1.00**	**1.00**	**1.00**	**1.00**	**1.00**
Correct integer numbers	6766	8080	9608	10000	6770	8136	9580	10000
Incorrect integer numbers	3234	1920	392	0	3230	1864	420	0
Actual success rate P_{actual}	**0.68**	**0.81**	**0.96**	**1.00**	**0.68**	**0.81**	**0.96**	**1.00**
Mean of t for all samples	1.19	1.27	1.65	10.61	1.15	1.22	1.52	12.05
Mean of t for correct samples	1.22	1.30	1.66	10.61	1.18	1.24	1.54	12.05
Mean of t for incorrect samples	1.11	1.14	1.16	Nan	1.09	1.11	1.12	Nan
t =1.5, P_{N_R}	0.05	0.12	0.60	1.00	0.02	0.05	0.49	1.00
t =1.5, P_{M_R}	0.00	0.01	0.00	0.00	0.00	0.00	0.00	0.00
t =1.5, P_{F_R}	0.63	0.69	0.36	0.00	0.66	0.76	0.47	0.00
t =1.5, P_{D_R}	0.32	0.18	0.04	0.00	0.32	0.19	0.04	0.00
t =1.5, pass samples	540	1254	6040	10000	202	566	4906	10000
t =2, P_{N_R}	0.01	0.01	0.16	1.00	0.00	0.00	0.07	1.00
t =2, P_{M_R}	0.00	0.00	0.00	0.00	0.00	.00	0	0.00
t =2, P_{F_R}	0.67	0.80	0.80	0.00	0.68	0.81	0.89	0.00
t =2, P_{D_R}	0.32	0.19	0.04	0.00	0.32	0.19	0.04	0.00
t =2, pass samples	26	66	1638	10000	6	14	720	10000

t =3, P_{N_R}	0.00	0.00	0.00	1.00	0.00	0.00	0.00	1.00
t =3, P_{M_R}	0.00	0.00	0.00	0.00	0.00	0.00	0.00	0.00
t =3, P_{F_R}	0.68	0.81	0.96	0.00	0.68	0.81	0.96	0.00
t =3, P_{D_R}	0.32	0.19	0.04	0.00	0.32	0.19	0.04	0.00
t =3, pass samples	0	2	52	10000	0	0	12	10000

6.6.2 Reliability Performance of PAR in the case of a dual-constellation

The remaining numerical analysis aims to further evaluate the reliability of AR in different situations with real data, including comparison of the computed success rates, the ADOPs and the critical values *t*. The analysis also demonstrates the benefits of the proposed PAR technique and multiple GNSS constellations. A total of 2500 epochs of dual-frequency (L1 and L2) data set collected at the interval of 30 seconds on 1 January 2007 about a 21 km baseline was processed for analysis. A typical elevation cut-off angle of 15° is used. Prior variance settings for code and phase measurements are given as 30 cm^2 and 0.5 cm^2 respectively. The geometry-based model is used in this experiment and the solutions are resolved epoch-by-epoch in kinematic mode. In this case, the chosen predefined thresholds of the success rate and critical value are 99% and 2 respectively. Four situations to be examined include: full AR process with GPS and DCS data respectively and PAR process with GPS and DCS. The computing schemes are named as GPS, DCS for full AR process and GPS (PAR) and DCS (PAR) for PAR process. The LAMBDA method is applied for AR in this experiment.

The number of fixed ambiguities at each situation during this experimental period is shown in Figure 6-5. It is noted that the GPS (PAR) process results in much fewer number of fixed ambiguities in order to achieve the predefined success rate of 99%. This process may lead to zero fixed ambiguities, as shown in Figure 6-5. This situation can be significantly improved in the dual-constellation case. The DCS (PAR) process with the same predefined success rate of 99% can always result in a good number of fixed ambiguities, for instance, 16 in the given data. Figure 6-6 shows the results of ADOP in the four situations. The ADOP values in the GPS full AR process are the highest among the results of other three situations where ADOP values are mostly less than 0.15 cycles. Hence, from the perspective of ADOP, the results of AR are expected to be more reliable in the cases of GPS (PAR), DCS and

DCS (PAR), which are agreeable with the work of Verhagen et al. (2010). Particularly, all the ADOP values of DCS (PAR) are less than 0.1 cycles.

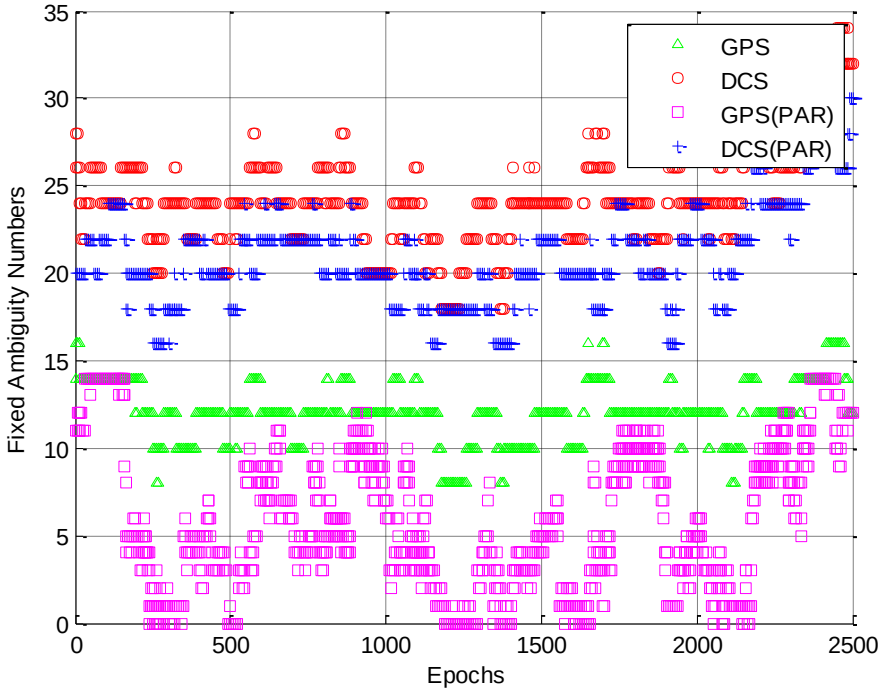

Figure 6-5 Fixed ambiguity numbers of GPS, DCS, GPS (PAR) and DCS (PAR)

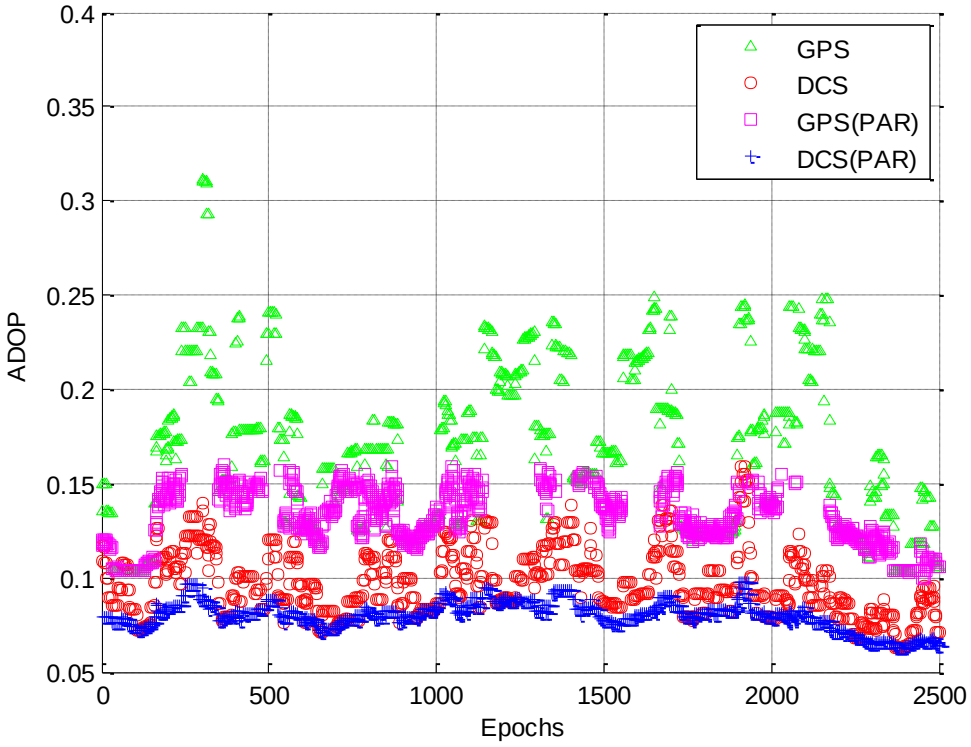

Figure 6-6 ADOPs of GPS, DCS, GPS (PAR) and DCS (PAR)

In terms of the computed success rates, the results of bootstrapped success rates are shown in Figure 6-7. There are some epochs when the success rate information is not available in the GPS (PAR) process, because of no fixed ambiguity solutions. In addition, the success rate obtained with the PAR technique is more stable than that of the traditional AR method. This is because of the application of a predefined success rate. Figure 6-8 shows the results of the success rate approximated from ADOP. The ADOP-approximated success rate is similar to the bootstrapped success rate in the GPS situation as shown in Figure 6-7. However, the result of the ADOP-approximated success rate seems to be over-optimistic in the DCS situation. Figure 6-9 shows the results of ratio tests. In general, the critical values in the PAR process are larger than those obtained from the full AR process. This fact also implies that the ratio-test function works more effectively with the high success rate shown in Figure 6-7.

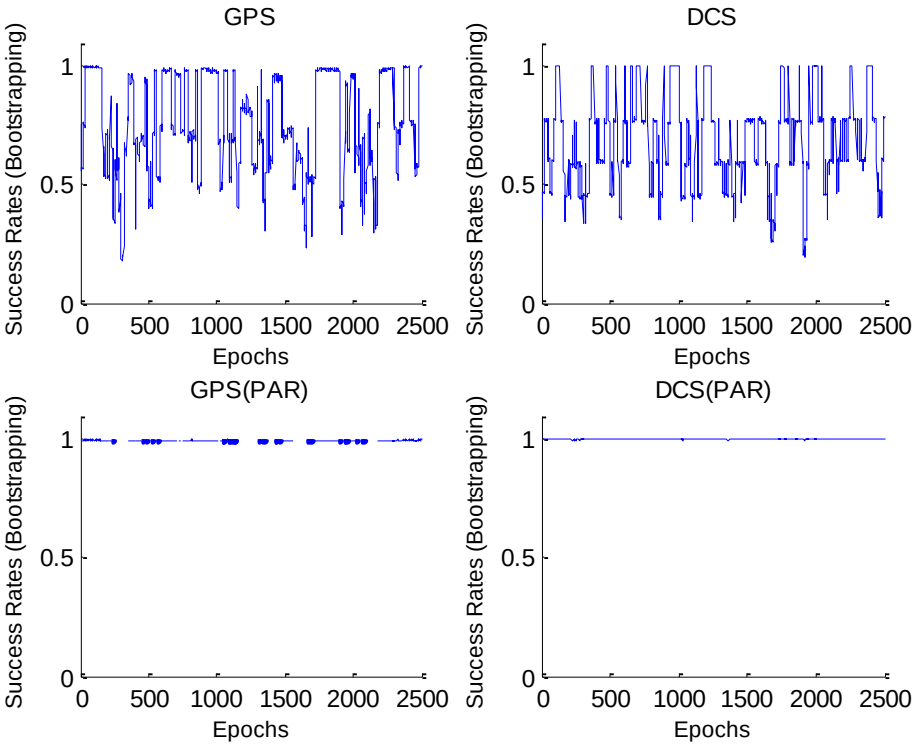

Figure 6-7 Bootstrapped success rates of GPS, DCS, GPS (PAR) and DCS (PAR)

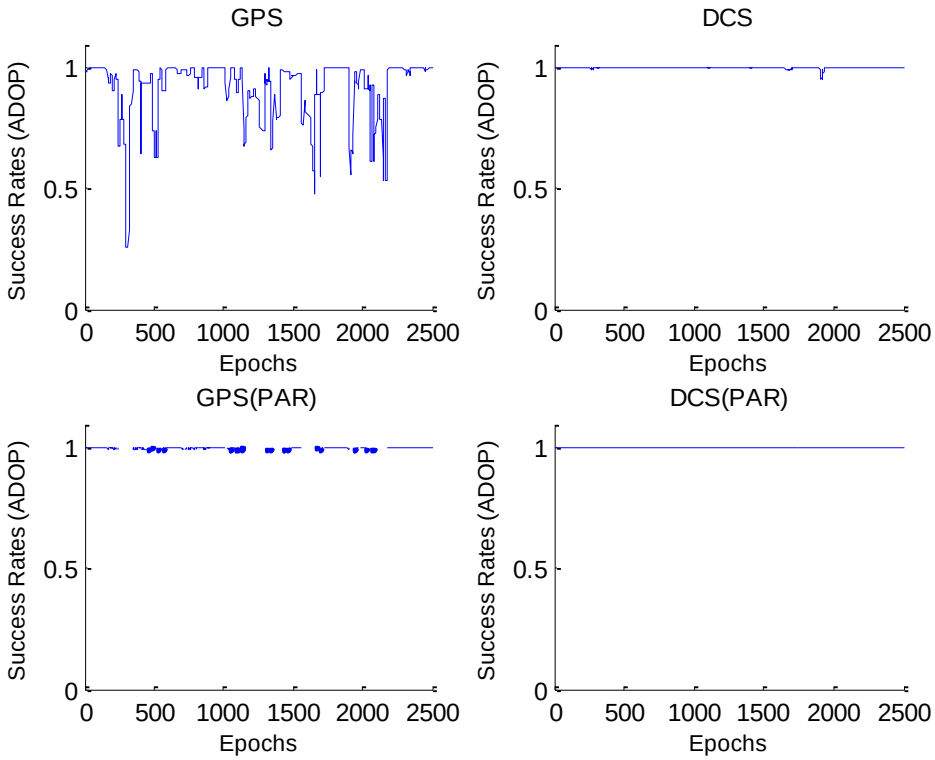

Figure 6-8 ADOP-approximated success rates of GPS, DCS, GPS (PAR) and DCS (PAR)

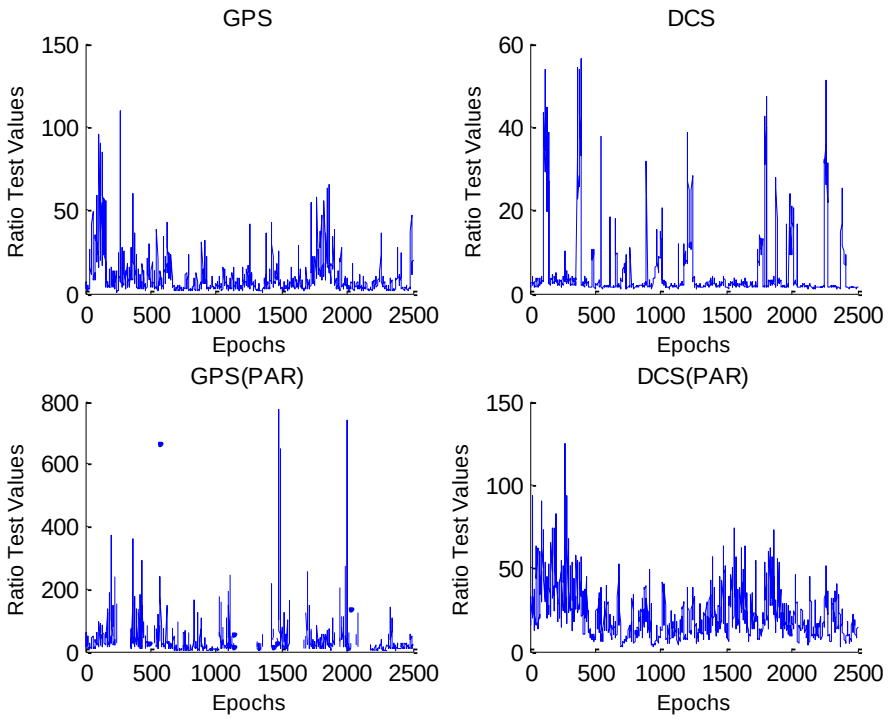

Figure 6-9 Ratio Test Values of GPS, DCS, GPS (PAR) and DCS (PAR)

The mean values of the different success rates, ADOPs and the critical values of ratio-test are given in Table 6-6. Apparently, the situation of DCS (PAR) has outperformed the other three situations. The means of the critical values of the ratio test of PAR are larger than for the full AR process. Since there is only one epoch with incorrect fixed ambiguities in the case of GPS, we did not analyse the AR risk probability in this experiment. Instead, the percentages of passed ratio test samples with different given thresholds are listed in Table 6-7. Once again, it is proved that the performance of DCS (PAR) is better than that for other situations. Figure 6-10 illustrates the position errors showing the impact of the AR solution for different situations. Obviously, both DCS and DCS (PAR) have good positioning results while GPS (PAR) has worse positioning results regardless of its highly reliable ambiguity solutions. The reasons why can be explained as follows: first, the number of fixed ambiguities is fewer; second, the geometry of fixed ambiguities for (6) is too poor.

Table 6-6 The mean of the success rate, ADOP and the critical value of ratio-test

Constellations	P_{boot}	P_{adop}	P_{low}	P_{up1}	P_{up2}	ADOP	t
GPS	0.76	0.92	0.25	1.00	0.97	0.17	8.87
DCS	0.69	0.99	0.12	1.00	1.00	0.10	4.52
GPS (PAR)	0.99	1.00	0.83	1.00	1.00	0.13	30.12
DCS (PAR)	1.00	1.00	0.63	1.00	1.00	0.08	20.86

Table 6-7 The percentage of past ratio-test values with given thresholds

Constellations	R≥1.5	R≥2	R≥3
GPS	98%	94%	78%
DCS	83%	51%	25%
GPS (PAR)	99%	98%	64%
DCS (PAR)	100%	100%	99%

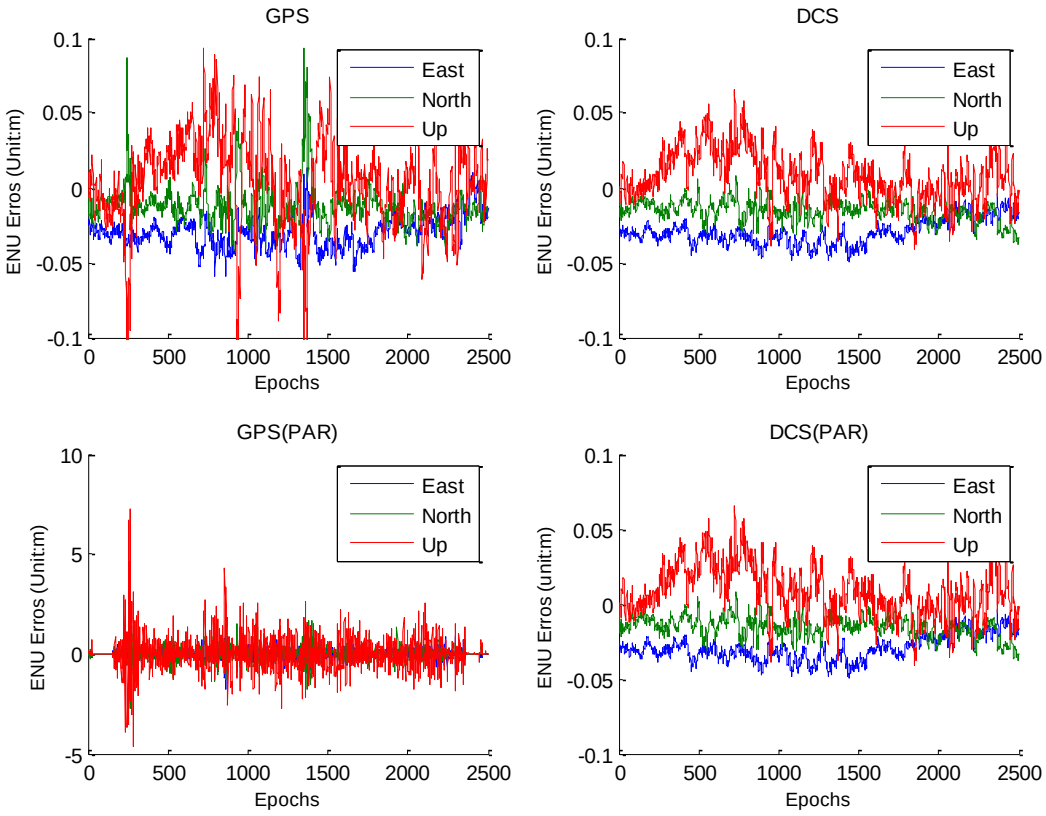

Figure 6-10 XYZ Positioning errors of GPS, DCS, GPS (PAR) and DCS (PAR)

6.7 Conclusions

This paper has examined the reliability characteristics of partial ambiguity resolution solutions with the aim of being able to promise the reliable ambiguity solutions in multiple GNSS situations. The existing AR reliability defined by its success probability is considered incomplete, due to lack of links to ambiguity validation decisions. A more complete concept of the AR reliability should also refer to the AR risk probability and false alarm probability etc. On the other hand, AR validation results depend on the success rates. This paper has proposed an ambiguity validation decision matrix to consider AR risk probability and false alarm probability as well. As a part of the contributions, the paper has presented a modified partial ambiguity fixing procedure with a predefined success rate and ratio-test in the ambiguity validation process.

Numerical results from simulations and real data have clearly demonstrated that only when the computed success rate is very high, the ambiguity validation with a lower ratio-test threshold can provide decisions about the correctness of AR close to real world situations with both low AR risk and false alarm probabilities. The proposed modified PAR procedure with predefined success rate in the validation process can effectively assure the reliability of PAR solutions. This procedure may result in a much fewer number of fixed ambiguities in single-constellation cases in order to achieve a predefined success rate of as high as 99%. However, in the dual-constellation cases, the PAR process with the same predefined success rate of 0.99 can automatically result in a good number of reliably fixed ambiguities. This finding indicates that the benefit of PAR with multiple GNSS signals is that a subset of satellites or signals may be selected to achieve a very high success rate, instead of using all satellites. As a result, higher AR reliability can be achieved with multiple GNSS signals. A more general conclusion is that the signals or measurements in the multiple GNSS constellations can be selected to assure the success rates, while the proposed PAR procedure achieves this purpose via a predefined success rate criterion.

Acknowledgements

This work was partially supported by the CRC for Spatial Information project 1.04 "Delivering Precise Positioning Services in Regional Areas" 2007-2010. The first author also acknowledges the financial support received from the China Scholarship Council (Grant No: 2008466001). Special thanks go to anonymous reviewers whose comments have contributed to the improvement of the paper. Discussions with Dr Patrick Henkel have been very beneficial as well.

6.8 References

Cao W, O'Keefe K, Cannon M (2007) Partial ambiguity fixing within multiple frequencies and systems. In: Proceedings of ION GNSS07, The Satellite Division of the Institute of Navigation 20th International Technical Meeting, Fort Worth, TX, September 25-28 2007, pp 312-323.

Cao Wei, O'Keefe K, Cannon M (2008a) Performance Evaluation of GPS/Galileo Multiple-frequency RTK Positioning Using a Single-difference Processor. In: Proceedings of the 21st International Technical Meeting of the Satellite Division of The Institute of Navigation, Savannah, GA, September 2008, pp. 2841-2849.

Cao W, O'Keefe K, Petovello M, Cannon M (2008b) Simulated Performance of Multiple-signal and Multiple-system Positioning for Land Vehicle Navigation. In: Proceedings of the 2008 National Technical Meeting of The Institute of Navigation, San Diego, CA, January 2008, pp. 603-613.

Cao W (2009) Multi-frequency GPS and Galileo kinematic positioning with partial ambiguity fixing. Master thesis, University of Calgary.

Euler HJ, Schaffrin B (1990) On a measure for the discernibility between different ambiguity solutions in the static-kinematic GPS-mode. Paper presented at the IAG Symposia no. 107, Kinematic Systems in Geodesy, Surveying, and Remote Sensing, Springer-Verlag, New York, pp 285-295.

Feng Y (2005) Future GNSS performance predictions using GPS with a virtual Galileo constellation. GPS World 16 (3):46-52.

Feng Y, Wang J (2011) Computed success rates of various carrier phase integer estimation solutions and their comparison with statistical success rates. J Geod 85 (2):93-103. doi:10.1007/s00190-010-0418-y.

Grafarend EW (2000) Mixed integer-real valued adjustment (IRA) problems: GPS initial cycle ambiguity resolution by means of the LLL algorithm. GPS Solut 4 (2):31-44.

Han S, Rizos C (1996). Integrated methods for instantaneous ambiguity resolution using new-generation GPS receivers. In: Proceedings of IEEE PLANS'96, Atlanta GA: 245-261.

Hassibi A, Boyd S (1998) Integer parameter estimation in linear models with applications to GPS. IEEE Transactions on signal processing 46 (11):2938-2952.

Henkel P, Günther C (2009) Partial integer decorrelation: optimum trade-off between variance reduction and bias amplification. J Geod 84 (1):51-63.

Henkel P, Günther C (2012) Reliable integer ambiguity resolution: multi-frequency code carrier linear combinations and statistical a priori knowledge of attitude. Navigation 59 (1): 61-75.

Kovach K, Maquet H, Davis D (1995) PPS RAIM algorithms and their performance. Navigation (Washington, DC) 42 (3):515-529.

Leick A (2004) GPS satellite surveying. 3rd edition. John Wiley and Sons, New York.

Mowlam AP, Collier PA (2004) Fast ambiguity resolution performance using partially-fixed multi-GNSS phase observations. Paper presented at the the 2004 International Symposium on GNSS/GPS, Sydney, Australia, 6-8 December.

O'Keefe K (2001) Availability and reliability advantages of GPS/Galileo integration. In: Proceedings of the 14th International Technical Meeting of the Satellite Division of The Institute of Navigation (ION GPS 2001), Salt Lake City, UT, September 2001, pp. 2096-2104.

O'Keefe K, Petovello M, Lachapelle G, Cannon ME (2006) Assessing probability of correct ambiguity resolution in the presence of time-correlated errors. Navigation (Washington, DC) 53 (4):269-282.

Ong RB, Petovello MG, Lachapelle G (2009) Assessment of GPS/GLONASS RTK under a variety of operational conditions. Proceedings of the 22nd International Technical Meeting of The Satellite Division of the Institute of Navigation, Savannah, GA, September 2009, pp. 3297-3308.

Parkins A (2011) Increasing GNSS RTK availability with a new single-epoch batch partial ambiguity resolution algorithm. GPS Solut 15(4): 391-402.

Teunissen PJG (1993) Least-squares estimation of the integer GPS ambiguities. Invited lecture, Section IV Theory and Methodology, IAG General Meeting, Beijing, China, August, also in Delft Geodetic Computing Centre LGR series, No. 6, 16 pp.

Teunissen PJG (1998) Success probability of integer GPS ambiguity rounding and bootstrapping. J Geod 72 (10):606-612.

Teunissen PJG (1999) An optimality property of the integer least-squares estimator. J Geod 73 (11):587-593.

Teunissen PJG (2000) The success rate and precision of GPS ambiguities. J Geod 74 (3):321-326.

Teunissen PJG (2001) Integer estimation in the presence of biases. J Geod 75 (7):399-407.

Teunissen PJG (2003) An invariant upperbound for the GNSS bootstrapped ambiguity success rate. JGPS 2 (1):13-17.

Teunissen PJG, Odijk D (1997) Ambiguity dilution of precision: definition, properties and application. In: Proceedings of the 10th International Technical Meeting of the Satellite Division of The Institute of Navigation, Kansas City, MO, September 16 - 19 1997, pp 891 - 899.

Teunissen PJG, Verhagen S (2008) GNSS ambiguity resolution: when and how to fix or not to fix? In: VI Hotine-Marussi Symposium on Theoretical and Computational Geodesy: Challenge and Role of Modern Geodesy, Wuhan, China, 29 May-2 June 2006, Series: International Association of Geodesy Symposia, 132, pp 143-148.

Teunissen PJG, Joosten P, Odijk D (1999a) The reliability of GPS ambiguity resolution. GPS Solut 2 (3):63-69.

Teunissen PJG, Joosten P, Tiberius C (1999b) Geometry-free ambiguity success rates in case of partial fixing. In: Proceedings of the 1999 National Technical Meeting of The Institute of Navigation, San Diego, CA, January 25 - 27 1999, pp 201-207.

Verhagen S (2003) On the approximation of the integer least-squares success rate: which lower or upper bound to use. JGPS 2 (2):117-124.

Verhagen S (2005) On the reliability of integer ambiguity resolution. Navigation (Washington, DC) 52 (2):99-110.

Verhagen S, Odijk D, Teunissen PJG, Huisman L (2010) Performance improvement with low-cost multi-GNSS receivers. In: Satellite Navigation Technologies and European Workshop on GNSS Signals and Signal Processing (NAVITEC), 2010 5th ESA Workshop on, 8-10 December 2010, pp 1-8.

Wei M, Schwarz KP (1995) Fast ambiguity resolution using an integer nonlinear programming method. In: Proceedings of the 8th International Technical Meeting of the Satellite Division of The Institute of Navigation (ION GPS 1995), Palm Springs, CA, September 1995, pp. 1101-1110.

Xu P (2001) Random simulation and GPS decorrelation. J Geod 75(7): 408-423.

Chapter 7: Satellite Selection Strategy for Achieving High Reliability Ambiguity Resolution with Multi-GNSS Constellations

Statement of Contribution of Co-Authors

The authors listed below have certified that:

1. they meet the criteria for authorship in that they have participated in the conception, execution, or interpretation, of at least that part of the publication in their field of expertise;
2. they take public responsibility for their part of the publication, except for the responsible author who accepts overall responsibility for the publication;
3. there are no other authors of the publication according to these criteria;
4. potential conflicts of interest have been disclosed to (a) granting bodies, (b) the editor or publisher of journals or other publications, and (c) the head of the responsible academic unit, and
5. they agree to the use of the publication in the student's thesis and its publication on the Australasian Digital Thesis database consistent with any limitations set by publisher requirements.

In the case of this chapter:

Contributor	**Statement of contribution**
Jun Wang	Conducted all the experiments and data analysis, wrote the manuscript
Yanming Feng	Reviewed and revised the manuscript

Principal Supervisor Confirmation

I have sighted email or other correspondence from all co-authors confirming their certifying authorship.

Yanming Feng | | 20-October-2012

Name | Signature | Date

Satellite Selection Strategy for Achieving High Reliability of Ambiguity Resolution with Multi-GNSS Constellations

Jun Wang, Yanming Feng

Faculty of Science and Technology

Queensland University of Technology, Australia

Phone: +61 7 31389111, Fax: +61 7 31389390, Email: jun.wang@student.qut.edu.au

Abstract

Reliability of carrier phase ambiguity resolution (AR) of an integer least-squares (ILS) problem depends on ambiguity success rate (ASR), which in practice can be well approximated by the success probability of integer bootstrapping solutions. With the current GPS constellation, sufficiently high ASR of geometry-based model can only be achievable at certain percentage of time. As a result, high reliability of AR cannot be assured by the single constellation. In the event of multi-GNSS constellations including GPS, GLONASS, Galileo and Beidou which provide tens of satellites in view, one is expected significant performance benefits such as high reliability of AR and precise positioning solutions. Simply using all the satellites in view for AR and positioning is a straightforward solution, but does not necessarily lead to high reliability as it is hoped. In addition, multi-GNSS receivers do mean high hardware and software complexity and operational cost, such as higher power consumption and computational burden to deal with a large number of satellites and signals which may be a problem for many low-cost applications.

The paper presents an alternative approach that selects a subset of the visible satellites to achieve a higher reliability performance of the AR solutions in a multi-GNSS environment, instead of using all the satellites. Traditionally, satellite selection algorithms are mostly based on the position dilution of precision (PDOP) in order to meet accuracy requirements. In this contribution, some reliability criteria are introduced for GNSS satellite selection, and a novel satellite selection algorithm for reliable ambiguity resolution (SARA) is developed. The SARA algorithm allows receivers to select a subset of satellites for achieving high ASR such as above 0.99.

Numerical results from both single and dual constellation cases show that with the SARA procedure, the percentages of ASR values in excess of 0.99 and the percentages of ratio-test values passing the threshold 3 are both higher than those directly using all satellites in view, particularly in the case of dual-constellation, the percentages of ASRs (>0.99) and ratio-test values (>3) could be as high as 98.0% and 98.5% respectively, compared to 18.1% and 25.0%. In addition, the PDOP values resulted from SARA process. It is worth noting that the implementation of SARA is simple and the computation time is low, which can be applied in most real-time data processing applications.

Keywords: *Satellite Selection Algorithm; Ambiguity success rate; Reliability; Multi-GNSS signals; Ambiguity resolution*

7.1 Introduction

Global Navigation Satellite Systems (GNSSs) is the generic term for all jurisdictional satellite navigation systems including the United States Global Position System (GPS), Russia's GLONASS, European Space Agency's Galileo, China's Beidou, Japan's Quasi Zenith Satellite System (QZSS) and India's Indian Regional Navigation Satellite Systems (IRNSS) (Hofmann-Wellenhof et al. 2008). In the very future, there will be 25-45 satellites in view depending on users' locations. Australia is one of many countries eventually receiving maximum numbers of satellite signals from all six systems simultaneously. In addition, most of satellite systems operate with three and more frequencies. Intrinsically, use of more satellite systems and signals can improve the performance of the positioning, navigation and timing (PNT) solutions, especially accuracy, integrity, continuity, availability and reliability. O'Keefe et al. (2002) have investigated and demonstrated that a combined GNSS system provides significantly improved availability for navigation in obstructed areas, where navigation with GPS alone is currently difficult. In the context of three carrier ambiguity resolutions (TCAR), Feng and Li (2008) show that one benefit of multi-frequency signals for a regional scale network-based real time kinematic positioning is that the inter-station distances of the network could be doubled. Li et al. (2009) have demonstrated that using three frequency signals can efficiently determine the ambiguities over several minutes without distance constraints. Verhagen et al. (2010) have investigated the high-precision relative positioning performance of low-cost single-frequency RTK receiver in the dual-constellation and presented that instantaneous ASR above 99% can be obtained with 15km baseline in clear sky conditions. However, these performance benefits do not come without cost. Generally speaking, multi-GNSS hardware will consume more power to deal with more satellites and signals which may be a problem for many low-cost applications. High computational burden is another issue for high timeliness applications. Transmission of GNSS corrections for a large number of satellites and signals will cause bandwidth congestion problems, for instance, potential disadvantages due to the co-existence of multiple GNSS systems in the same frequency bands. Benefits that multi-GNSS and multi-frequency signals can bring to users may be maximized by selective use of satellite systems, or signals, or subset of visible satellites from different systems in order to achieve required positioning performance at affordable

costs. This is certainly the case for real-time kinematic positioning or other precise positioning based on successful resolutions of carrier phase ambiguities of satellite signals. This research work will prove that it is possible to select a subset of satellites from two constellations in order to achieve higher reliability of carrier phase ambiguity resolutions, thus assuring the reliability and accuracy of the RTK solutions (Grejner-Brzezinska et al. 2005; Feng and Wang 2008). In the contrast, use of too many redundant satellites may likely cause low success probability of ambiguities, thus affecting the reliability of the RTK solutions.

For integer least–squares (ILS) solutions of a linear system with integer parameters, the ambiguity dilution of precision (ADOP) and the ambiguity success rate (ASR) have been introduced to capture and analyze the precision and reliability characteristics of the ambiguities (Teunissen and Odijk 1997; Teunissen 1998; Teunissen et al. 1999). Theoretically only when the ASR is very close to 1, the integer ambiguities can be considered deterministic, thus guaranteeing the precision of fixed solution better that the float solution (Verhagen 2005b). Since incorrect ambiguity fixing can lead to largely biased positioning solutions, so it is always worthwhile to have an AR solution with the high ASR. An approach to achieve the high ASR is to apply the concept of partial ambiguity resolution (PAR), which is a technique for fixing a subset of the ambiguities with a higher ASR of resolving them correctly (Teunissen et al. 1999). This study is focused on the geometry-free model; however the success rate of the geometry-based model cannot guaranteed to be increased with less satellites imposed because of the poor geometry. Cao et al. (2007) has also numerically demonstrated that the ASR decreases as the number of ambiguities increases and a combination of constellations can achieve a higher ASR in shorter observation periods compared to a single constellation used independently. In addtion, his work is also presented that the ambiguities with more satellites observed at a low latitude can be fixed much faster than that of middle and high latitudes with fewer observed satellites on the geometry-based model, which implies that the ambiguities number has great impact on ambiguity fixing. The recent work by the authors clearly have demonstrated that only when the computed success rate is very high, the AR validation can provide the decisions about the correctness of AR close to real world with both low AR risk and false alarm probabilities. The results from that work also indicate that an advantage of using multi-GNSS signals for PAR

is that actually only part of satellites or signals are needed to archive a very high-success rate instead of using all satellites. This is how high reliability of PAR can be achieved with multi-GNSS signals.

On the other hand, once the number of selected satellite reaches certain numbers, such as more than ten, the rate of position dilution of precision (PDOP) values is no longer evident, perhaps because the geometry has reached a good balance. The improvement of ASR is still remarkable, thus deserving more investigation. Figure 7-1 shows the PDOP, ADOP and ASR of four different ten-satellite subsets from overall fifteen satellites. It is clear that the PDOP values are fluctuating between 0.9 and 1.5, while the ADOP values and the ASR values are portioned into four separate layers. The hierarchical structure of the ASR is more obvious than that of the ADOP. Moreover, it is interesting to see that in some samples, ASR values are very close to 1, which indicates their integer ambiguities will be reliable. This implies that it is possible to find a subset of satellites which maintains both the low PDOP and the high ASR when the total visible satellite number is large enough. This research effort develops and tests a satellite selection strategy that allows high reliability of AR to be achieved with multi-constellations. For sake of convenience, the method is known as Satellite selection Algorithm for Reliable Ambiguity resolution (SARA), which can be applied in both single constellation and multi-constellations. Results from numerical analysis will confirm that SARA can result in better ASR outcomes without loss of positioning accuracy.

The remainder of this paper is organized as follows. Section 7.2 briefly reviews the existing satellite selection algorithms. In Section 7.3, the measures of least squares solution reliability are described, which are related to the ADOP and the ASR. Section 7.4 describes the satellite-selection algorithm for reliable ambiguity resolution (SARA). In Section 7.5, numerical experiment results for different constellations are provided to demonstrate the advantage of this proposed algorithm over other satellite selection algorithms and contribution to high reliability of ambiguity resolutions comparing no satellite selection. Finally, the main research findings from this work are summarized.

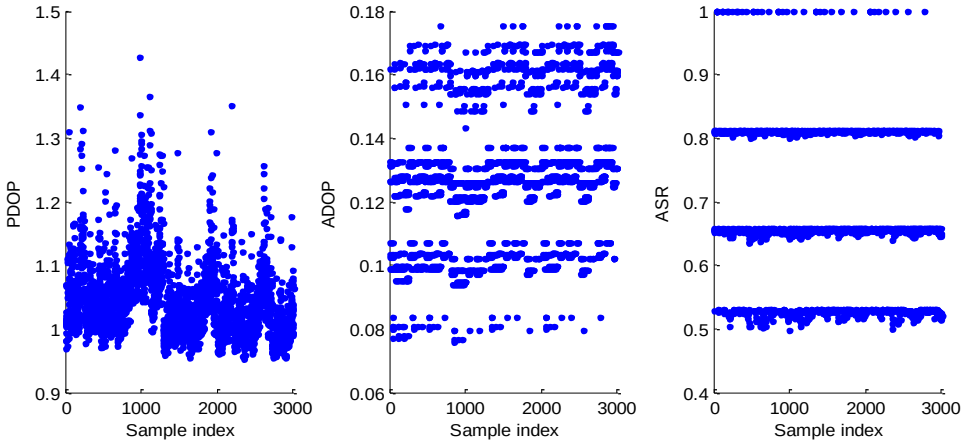

Figure 7-1 PDOP, ADOP and ASR of different ten satellites from fifteen satellites

7.2 Existing Satellite Selection Algorithms

In the context of GNSS-based positioning, the idea of selection of satellites started with the first commercial GPS receiver, the Texas Instruments TI 4100 NAVSTAR Navigator (Henson et al. 1985) which has to select the best four satellites with a minimum position dilution of precision (PDOP) in order to complete the position estimation. The definition of PDOP is given as (Hofmann-Wellenhof et al. 2008)

$$PDOP = \sqrt{Trace\left[\left(\mathbf{A}^T\mathbf{A}\right)^{-1}\right]} \tag{1}$$

$$\mathbf{A} = \begin{bmatrix} a_{x1} & a_{y1} & a_{z1} \\ a_{x2} & a_{y2} & a_{z2} \\ \vdots & \vdots & \vdots \\ a_{xn} & a_{yn} & a_{zn} \end{bmatrix} \tag{2}$$

where A is the design matrix, the $\mathbf{a_i} = (a_{xi}, a_{yi}, a_{zi})$ are the unit vectors from the station to the location of the *i*th satellite and *n* is the satellite number. Several algorithms of selecting a subset of the satellites have been developed to find the minimal PDOP with given satellite number. One early contribution was the maximum volume algorithm(MVA) (Kihara and Okada 1984). The four-step satellites selection algorithm by Li et al. (1999) are developed to select four satellites to form near optimal geometry. Park (2001) proposed the quasi-optimal satellite selection algorithm (QOSSA) for GPS receivers used in low earth orbit (LEO) application, which can select any required number of satellites. A heuristic method

combining the maximum volume algorithm and the redundancy technique is developed to mitigate computational burdens while maintaining benefits of the combined navigation satellite systems and called multi-constellations satellite selection algorithm (MCSSA) (Roongpiboonsopit and Karimi 2009). Although low PDOP usually indicates good estimation accuracy, it does not yet hold true in terms of the system reliability. The reliability requirement is also of great importance within safety-critical and liability-critical applications. Until recently, no work has been reported on selecting a subset of the satellites towards achieving a high reliability of a positioning system.

However, one cannot exclude the possibility that selection algorithms based on accuracy criterion can also provide good reliability. A brief overview of five different satellite selection algorithms is given in the following. Their advantages and disadvantages are described and discussed. Numerical results from some of selection algorithms will be also analysed against reliability of ambiguity resolution.

7.2.1 Highest Elevation Satellite Selection Algorithm

The highest elevation satellite selection algorithm (HESSA), which selects the highest elevation angles with reference to the user's position as its literal sense, is simple to utilize. The computation burden for this selection process is very low. However, the decision of the threshold of satellite elevation is often made experientially. Sometimes, if the threshold is too large, either the satellite number will be seldom or the geometry will be very poor.

7.2.2 Maximum Volume Algorithm

Kihara and Okada (1984) proposed the maximum volume algorithm (MVA) for selecting four satellites. The idea is based on the fact that PDOP tends to be inversely proportional to the volume of the tetrahedron form by unit vectors $\mathbf{a}_i$. The algorithm consists of the following three steps.

Step 1: Select the satellite (S1) with the highest elevation.

Step 2: Select the satellite (S2) which has the angle to S1 close to 109.5°.

Step 3: Select the other two satellites (S3 and S4).

It is shown that this algorithm provides a near-optimal geometry with a small

computation time. However, for the purpose of reliability, specific, in the relative positioning application, more than four satellites are desirable to select to increase estimation robustness.

7.2.3 Quasi-Optimal Satellite Selection Algorithm

Park (2001) introduced the quasi-optimal satellite selection algorithm (QOSSA) for selecting any number of satellites. The logic of this algorithm is to eliminate redundant satellites which are close to each other or form a collinear. The algorithm includes the following steps.

Step 1: Calculate the redundancy value of each visible satellite with respect to all the other visible satellites.
Step 2: Eliminate the satellite with maximum redundancy value.
Step 3: Return to step 1 until the predefined number of satellites is selected.

The implementation and computation of this algorithm is simple, nevertheless, the aim of QOSSA was designed for GPS receivers used in LEO applications that the elevation angles are lower compared with terrestrial users. Besides, the predefined number of selected satellites is based on one's experience.

7.2.4 Multi-Constellations Satellite Selection Algorithm

Roongpiboonsopit and Karimi (2009) developed the multi-constellations satellite selection algorithm (MCSSA) to mitigate computational burdens and maintain benefits of the combined GNSS constellations. MCSSA combines the strength of MVA and QOSSA together. MCSSA is not limited to any specific number of satellites and can provide sub-optimal satellite geometry. The procedure of MCSSA can be summarized as follows.

Step 1: Define the number of selected satellites (n).
Step 2: Select the first four satellites based on MVA from all the candidate satellites.
Step 3: Remove the four satellites to selected satellites from the candidate satellites.
Step 4: Calculate the redundancy value of the remaining candidate satellite.

Step 5: Select the satellite with minimum redundancy value and remove the satellite to selected satellites from the candidate satellites

Step 6: Return to step 4 until the predefined number of satellites is selected.

Though MCSSA is fairly simple and provides the set of satellites with good geometry resulting near-optimal PDOP, the criterion of the predefined number of selected satellites is not yet given.

7.3 Reliability Criteria for Ambiguity Resolution

Traditionally, reliability is the measure of the capability of a system to detect blunders or biases in the measurements and to estimate the effects that undetected blunders may have on a solution. Redundancy number is an important factor in reliability theory which refers to the contribution of the *i*th observation of the linear observation system to the degree of freedom (DOF). There are two measures of reliability: internal reliability represented by the minimum detectable bias (MDB) and external reliability quantified by the effect of undetectable bias in the observation (Baarda 1968; Cross et al. 1994). Internal reliability and external reliability are used to characterize the least squares solutions of unknown parameters. The reliability criteria are referred to the parameters to be used in selection of satellites for achieving reliable ambiguity solution in processing GNSS carrier phase measurements. The criteria include concepts of internal and external reliability from the traditional real-value least-squares estimation and the concepts of the ADOP and the ASR that is directly related to the ILS solutions' reliability. This section will introduce the internal and external reliability concept first, followed by the ADOP and success rate computations and numerical analysis regarding the reliability criteria.

7.3.1 Internal reliability and external reliability

A linear observational model is defined by

$$\mathbf{y} = \mathbf{A}\mathbf{x} + \mathbf{e}, \quad \mathbf{e} \sim \left(0, \sigma_0^2 \mathbf{Q}\right) \tag{3}$$

where **y** is the observation vector, **x** is the unknown parameter vector, **e** is the random error vector, σ_0^2 is the variance of the unit-weight measurements and **Q** is the cofactor matrix. We have the weight matrix $\mathbf{P} = \mathbf{Q}^{-1}$.

The redundancy number r_i is given as

$$r_i = (\mathbf{Q}_{vv}\mathbf{P})_{ii} \tag{4}$$

with a normal equation matrix

$$\mathbf{N} = \mathbf{A}^T\mathbf{P}\mathbf{A} \tag{5}$$

and a cofactor matrix for residuals

$$\mathbf{Q}_{vv} = \mathbf{Q} - \mathbf{A}\mathbf{N}^{-1}\mathbf{A}^T \tag{6}$$

The internal reliability measure is represented by the minimal detectable bias (MDB) as (Baarda 1968; Cross et al. 1994)

$$|\nabla_{0i}| = \frac{\delta}{\sqrt{r_i}}\sigma_i \tag{7}$$

where σ_i is the standard deviation of the *i*th observation, which is a function of the diagonal element of Q_{vv} and σ_0^2; δ is the non-centrality parameter depending on the level of significance α and the power of the test β.

The external reliability is the influence of each of the MDBs on the estimated parameters. The effect of the blunder or the bias ∇_i in *i*th observation is

$$\nabla_{\mathbf{x}} = \mathbf{N}^{-1}\mathbf{A}^T\mathbf{P}\mathbf{c}_i\nabla_i \tag{8}$$

where the **c**-vector takes the form $(0,...,1,...,0)^T$, with the 1 as the *i*th entry of **c**. Consequently, the impact of the MDB ∇_{0i} is given as

$$\nabla_{\mathbf{x}_{0i}} = \mathbf{N}^{-1}\mathbf{A}^T\mathbf{P}\mathbf{c}_i\nabla_{0i} \tag{9}$$

Baarda (1968) suggested the follow alternative expression:

$$\lambda_{0i}^2 = \frac{\nabla_{\mathbf{x}_{0i}}^T \mathbf{N} \nabla_{\mathbf{x}_{0i}}}{\sigma_0^2} \tag{10}$$

The value λ_{0i}^2 is considered to be a measure of global external reliability. When the external reliability becomes large, the global falsification caused by a blunder or bias can be significant (Verhagen 2005a).

7.3.2 ADOP

Like the PDOP measure commonly used to describe the impact of receiver-satellite geometry on the positioning precision, the concept of the ADOP is introduced to measure the intrinsic precision characteristics of the ambiguities (Teunissen and Odijk 1997). It is defined as

$$\text{ADOP} = \sqrt{\left|\mathbf{Q}_{\hat{\text{N}}}\right|}^{\frac{1}{m}} \quad \text{(cycle)} \tag{11}$$

where $\mathbf{Q}_{\hat{\text{N}}}$ is the variance-covariance (vc-) matrix of the *m*-dimensional float ambiguities.

Smaller ADOP values imply more precise estimation of the float ambiguities and higher possibility of successful ambiguity validation. It is suggested that for successful AR the ADOP should be smaller than 0.15 cycles (Verhagen et al. 2010). For a short observation time span, the approximation of the ADOP can be expressed as (Takac 2006)

$$\text{ADOP} \approx m^{\frac{1}{2(m\text{-}1)}} \cdot \left(\frac{\sigma_\phi^2}{\sigma_p^2}\right)^{\frac{m\text{-}4}{4(m\text{-}1)}} \cdot \left(\frac{\sigma_\phi \sigma_p}{k\lambda_1\lambda_2}\right)^{\frac{1}{2}} \quad \text{(cycle)} \tag{12}$$

where σ_p^2 denotes the variance of code, σ_ϕ^2 denotes the variance of phase, λ_1 and λ_2 denote the wavelengths of L1 and L2, and *k* denotes the number of epochs.

Figure 7-2 shows the precision and the precision change rate of the ADOP computed by (12) with increasing satellites in the case of $\sigma_p = 0.3m$, $\sigma_\phi = 0.003m$ and *k*=1. It is shown that the ADOP only falls below 0.15 cycles when there are 5 or more satellites. In fact, the ADOP decreases when the number of redundant satellites

increases. However, the change rate will reduce to less than 10% when m>10 which we can assume that the contribution of more satellites on ADOP is not significant anymore.

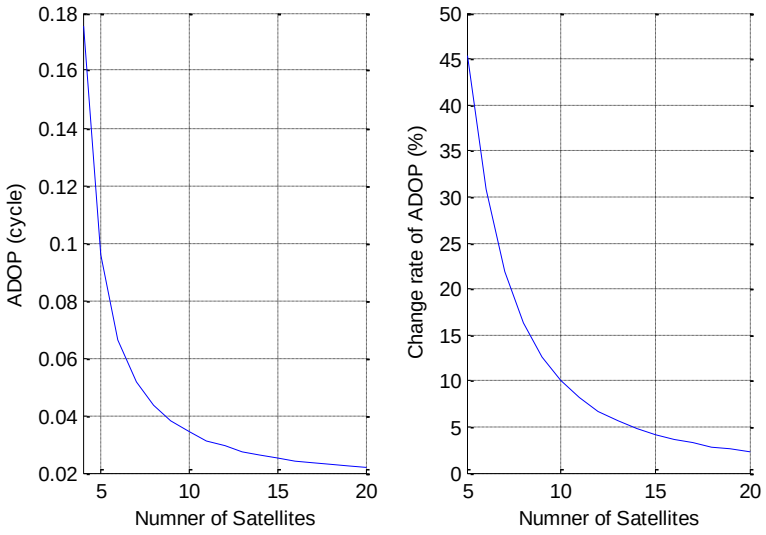

Figure 7-2 The precision and change rate of the ADOP with increasing number of satellites

7.3.3 Success Rate

The success rate is defined as the integral of probabilistic density function of float ambiguity solutions over an ambiguity "Voronoi cell" (Hassibi and Boyd 1998) or "Pull-in region"(Teunissen 1998). The probability P_S of correct integer estimation in the case of ILS is defined as follows

$$P_S = P(\breve{\mathbf{N}} = \mathbf{N}) = \int_R f_{\hat{N}}(x)dX \tag{13}$$

where R and $f_{\hat{N}}(x)$ denote the ILS pull-in region and the probability density function of the float ambiguities $\hat{\mathbf{N}}$ respectively. In general, we assume the float ambiguity is normally distributed, e.g., $N(\mathbf{N}, \sigma_0^2\mathbf{Q}_{\hat{\mathbf{N}}})$. Therefore, the success rate can be expressed as

$$\begin{aligned} P_S &= \int_R N(\mathbf{N}, \sigma_0^2\mathbf{Q}_{\hat{\mathbf{N}}})dX \\ &= \int_R \frac{1}{(2\pi)^{\frac{1}{m}}\left|\sigma_0^2\mathbf{Q}_{\hat{\mathbf{N}}}\right|^{1/2}} \exp[-\frac{1}{2\sigma_0^2}(\mathbf{X}-\mathbf{N})^{\mathrm{T}}\mathbf{Q}_{\hat{\mathbf{Z}}}^{-1}(\mathbf{X}-\mathbf{N})]dX \end{aligned} \tag{14}$$

Nevertheless, construction of the ILS pull-in region or Voronoi cell can be complex, the real-time computation of AR success rate is considered difficult and impractical. Fortunately the success rate of bootstrapping estimator has been proved to be a sharp lower bound and good approximations of the actual success rate, expressed as (Teunissen 1998; Feng and Wang 2011)

$$P(\breve{\mathbf{N}} = \mathbf{N}) \geq P_{boot} = \prod_{i=1}^{m} \left[2\Phi\left(\frac{1}{2\sigma_{\hat{N}_i|I}} \right) - 1 \right] \tag{15}$$

with

$$\Phi(t) = \int_{-\infty}^{t} \frac{1}{\sqrt{2\pi}} \exp(-\frac{1}{2}x^2) dx \tag{16}$$

The invariant ADOP can be used to obtain an upperbound for the bootstrapped ASR as (Teunissen 2003)

$$P_{boot} = \prod_{i=1}^{m} \left[2\Phi\left(\frac{1}{2\sigma_{\hat{N}_i|I}} \right) - 1 \right] \leq \left[2\Phi\left(\frac{1}{2\mathrm{ADOP}} \right) - 1 \right]^m \tag{17}$$

From (17), we can conclude that the smaller ADOP will get a higher upperbound of ASR. It is suggested that an ADOP of 0.15 cycles or less would be required if the success rate is required to be above 0.99 (Verhagen et al. 2010).

7.3.4 Reliability criteria for satellite selection

Figure 7-3 shows the redundancy numbers (RNUM), the MDBs and the external global reliabilities of a dual-constellation design matrix for 1000 samples that can be generated from the experiment data in Section 7.5 *Experiments and Analysis*. It is interesting to note that those relevant reliability values are grouped into two separate Clusters. To be specific, the values of redundancy numbers (RNUM) are either close **1** or below 0.9 while the MDB values are either close or **0.21** or below 0.4 and the external global reliabilities (EXTR) are either around **0.3** or around 2.5. Besides, Figure 7-3 also shows the selected satellites with extreme values in terms of RNUM (>0.9), MDB (>0.15) and EXTR (<0.4) are the same. Taking a sample with 11 satellites as an example, the redundancy numbers, the MDBs and the external global

reliabilities are listed in Table 7-1. It is shown that the maximum redundancy number and MDB and the minimum external global reliability can be easily identified. The question naturally is whether the removal of the measurements with extreme values from the observation system can sufficiently assure the higher success rate of AR in the ILS solutions. Alternatively, the question is if the high AR success rates necessarily require the removal of the extreme measurements. These questions are not easily answered theoretically. However, Section 7.5 will seek the answers to the questions numerically.

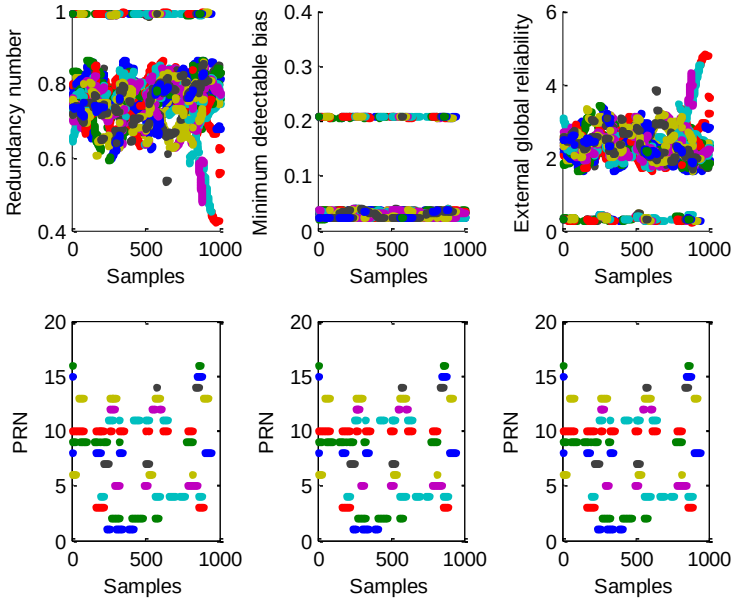

Figure 7-3 The redundancy number, minimum detectable bias and external global reliability of a dual-constellation design matrix for 1000 samples with the correspondent satellites of extreme values

Table 7-1 The extreme values of redundancy number (RNUM), MDB and external global reliability (EXTR)

PRN	1	2	3	4	5	**6**	7	8	9	10	11
RNUM	0.77	0.83	0.79	0.67	0.69	**0.99**	0.77	0.77	0.73	0.73	0.77
MDB	0.02	0.02	0.03	0.02	0.02	**0.20**	0.03	0.03	0.03	0.03	0.02
EXTR	2.21	1.83	2.10	2.85	2.71	**0.32**	2.21	2.21	2.46	2.46	2.21

7.4 Satellite-selection Algorithm for Reliable Ambiguity-resolution (SARA)

Based on the given reliability criteria in the previous section, this section presents a satellite- selection algorithm for reliable ambiguity-resolution (SARA), which searches for a subset of satellites with a high ASR and low computational burden. In addition, this algorithm assumes that there are adequate satellites, for instance, in the case of multiple constellations where the PDOP requirement is easy to satisfy. The purpose or the advantage of SARA is to improve the ASR compared to other satellite selection algorithms, whereas, the computation load of SARA is maintained at a low level.

In fact, it is simple to implement the SARA algorithm which only consists of the following four steps.

Step 1: Create a list of visible satellites and form the design matrix A of un-differenced model with all the satellites.
Step 2: Calculate the reliability parameters mentioned in Section 7.3.1.
Step 3: Remove the satellite with extreme values.
Step 4: Select the remaining satellites.

Unlike the existing algorithms in Section 7.2, there is no need for a predefined number of selected satellites for SARA, because SARA can make the decision with its own reliability characteristics. As shown in Figure 7-4 and Table 7-1, the criteria for the extreme redundancy number, the MDB and the external global reliability give the equivalent results. The criterion of selecting the subset of satellites can be based on any of the three parameters. In Step 3, usually there are two options: Option 1 is to remove all the satellites with the extreme RNUM, or MDBs or EXTR values; Option 2 is to remove the satellite with the most extreme value and return to Step 2. Figure 7-4 gives the flowchart of Option 1 and Option 2. Obviously, the second scheme is more complicated. Figure 7-5 shows the ASR difference between these two options based on SARA. It is shown that the ASR performances of these two options are just the same in most samples in spite of having some ignorable difference, smaller than 0.1% in other samples. Therefore, the SARA algorithm adopts the first option that removes the high redundant satellites at once. The

fourteen satellites selected by SARA from eighteen satellites are plotted in Figure 7-6. Considering inter constellation biases, the different reference satellites are used in their corresponding system respectively.

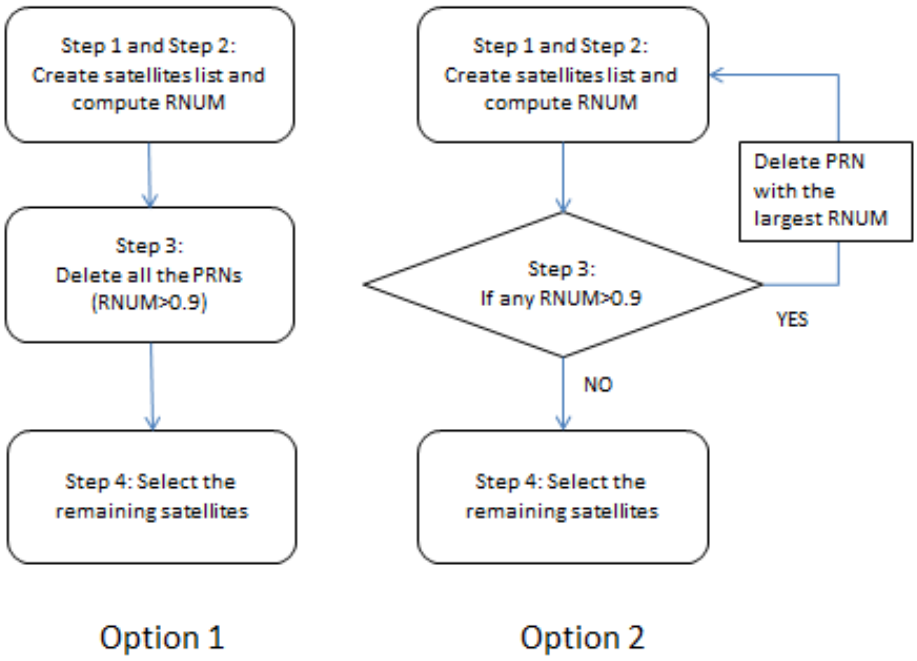

Figure 7-4 The two options of SARA algorithm

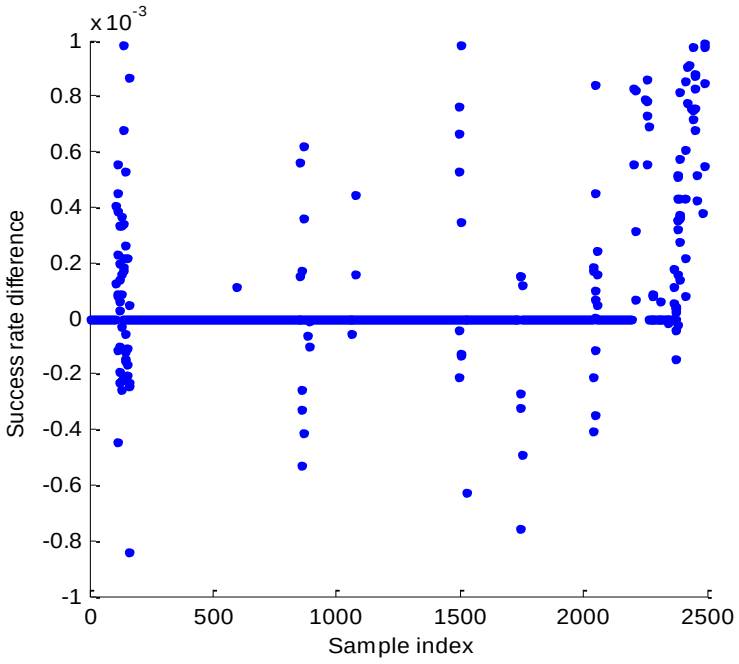

Figure 7-5 The ASR difference between option 1 and option 2 in SARA algorithm

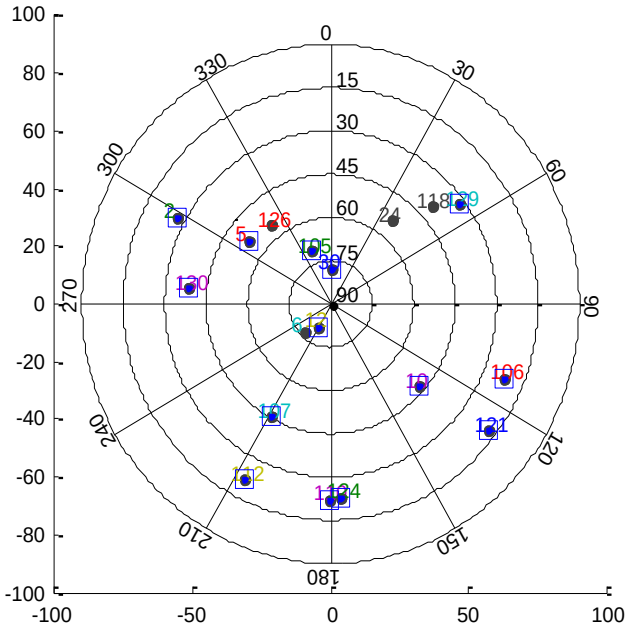

Figure 7-6 The sky plot of selected 14 visible satellites as an example from 18 visible satellites by SARA, ☐ denotes the selected satellite

7.5 Experiments and Analysis

To demonstrate the efficiency of SARA, results from both the single GPS constellation system and the dual-constellation system (DCS) are analyzed. A total of 2500 epochs of dual-frequency (L1 and L2) data set collected at the interval of 30 seconds on 1 January 2007 about a 21 km baseline was processed for analysis. A typical elevation cut-off angle of 15° is used. Prior variance settings for code and phase measurements are given as 30 cm2 and 0.5 cm2 respectively. The geometry-based model and the LAMBDA method are used in this experiment and the solutions are resolved epoch-by-epoch in kinematic mode.

The virtual Galileo constellation (VGC) method is applied to simulate the data of another GNSS constellation and the time-latency for deriving VGS data is 300 epochs (Feng 2005). It is noticed that the maximum volume algorithm and the four-step satellite selection algorithm are only capable to selecting four satellites, while the quasi-optimal satellite selection algorithm is originally design for the receiver in LEO application. We therefore choose to compare the SARA with the highest elevation satellite selection algorithm (HESSA) and the multi-constellations satellite selection algorithm (MCSSA) in terms of positioning accuracy and AR reliability

performance. In this work, the SARA uses the extreme redundancy number (RNUM>0.9) as the criterion to remove all the corresponding satellites as the concept of redundancy number is more familiar and simple too.

For ambiguity validation purposes, the ratio-test is a popular acceptance test and given as

$$\text{Accept } \breve{\mathbf{N}} \text{ if: } \frac{\left\|\hat{\mathbf{N}}-\breve{\mathbf{N}}_2\right\|^2_{\mathbf{Q}_{\hat{\mathbf{N}}}}}{\left\|\hat{\mathbf{N}}-\breve{\mathbf{N}}\right\|^2_{\mathbf{Q}_{\hat{\mathbf{N}}}}} \geq t \tag{18}$$

where $\breve{\mathbf{N}}_2$ is the second best integer ambiguity candidates and t is an empirically critical value. The ratio-test actually tests the closeness of the float ambiguity to its nearest integer candidate. The critical value of t actually determines how closeness the user will choose. In general t can be chosen 1.5 (Han and Rizos 1996), 2 (Wei and Schwarz 1995) or 3 (Leick 2004). The ratio test values are also compared among these algorithms.

Case 1: Single GPS constellation system

As already discussed in Section 7.2, both HESSA and MCSSA need a predefined number of selected satellites. Hence, to make the comparison among these algorithms reasonable, the number determined by SARA is applicable for HESSA and MCSSA too. Additionally, the algorithm of using all the satellites is also considered. There are in total four schemes for comparison. Figure 7-7 shows the ADOPs results with each algorithm. The title GPS indicates that all the GPS satellites are adopted. Overall all the ADOP values have the similar pattern, but it is clear seen that the ADOPs of MCSSA are larger than others. Figure 7-8 shows the ASR comparison among the four cases. The ASR values are computed by (15). The ASR from MCSSA has much more ASRs smaller than 50% compared to others possibly because of its larger ADOPs. The ASR performances of HESSA and SARA through selecting satellites have some slight improvements as compared to using all the satellites. The reliability parameters including the redundancy number, the minimal detectable bias and the external global reliability are also compared among the algorithms, and are shown in Figure 7-9, 7-10 and 7-11 respectively. It can be observed that the results of HESSA and SARA are very similar. In the meantime, the

results of GPS show the hierarchical structure patterns. Figure 7-12 compares the PDOP values from different algorithms. It is understandable the case of all the satellites has the best performance and MCSSA has the second-best performance. The PDOP results of HESSA and SARA have more epochs with values above 2 than other two algorithms. Figure 7-13 illustrate the position errors. It is clearly seen that MCSSA has a few epochs of abnormal position errors about several meters due to the impact of wrong integers. This result also demonstrates the significance of the reliability of AR. Figure 7-14 gives the histograms of AR ratio-test values to each algorithm. It is shown that HESSA and SARA have more number of larger ratio-test values than other two algorithms. The corresponding statistical information will be summarized in Table 7-2. Provided that the larger ratio-test values, the more reliable AR solutions, we can deduce that HESSA and SARA have more reliable AR solutions.

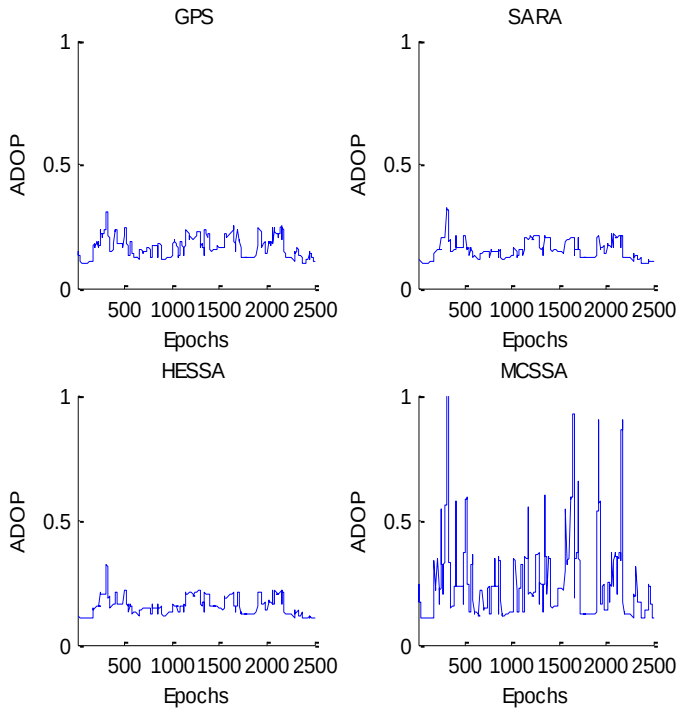

Figure 7-7 ADOPs computed with four schemes: GPS, SARA, HESSA and MCSSA

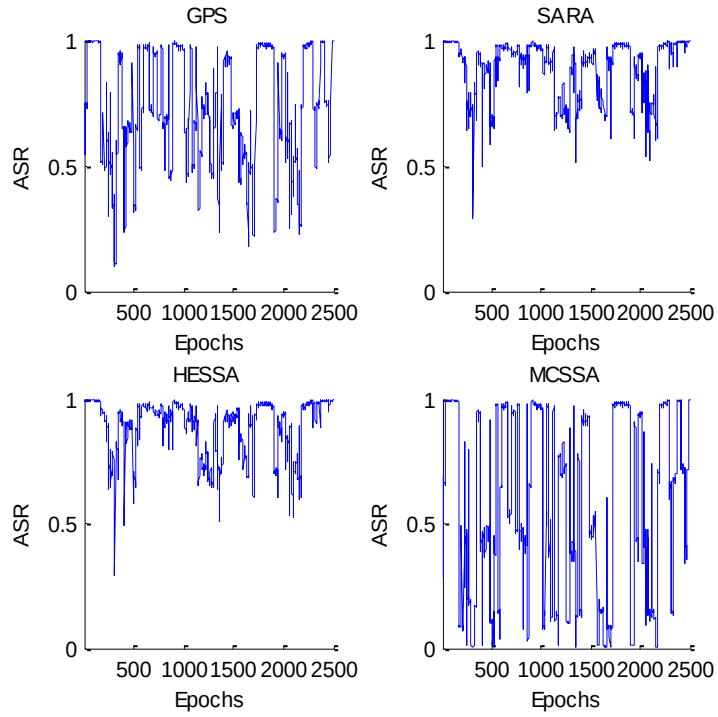

Figure 7-8 ASRs computed with four schemes: GPS, SARA, HESSA and MCSSA

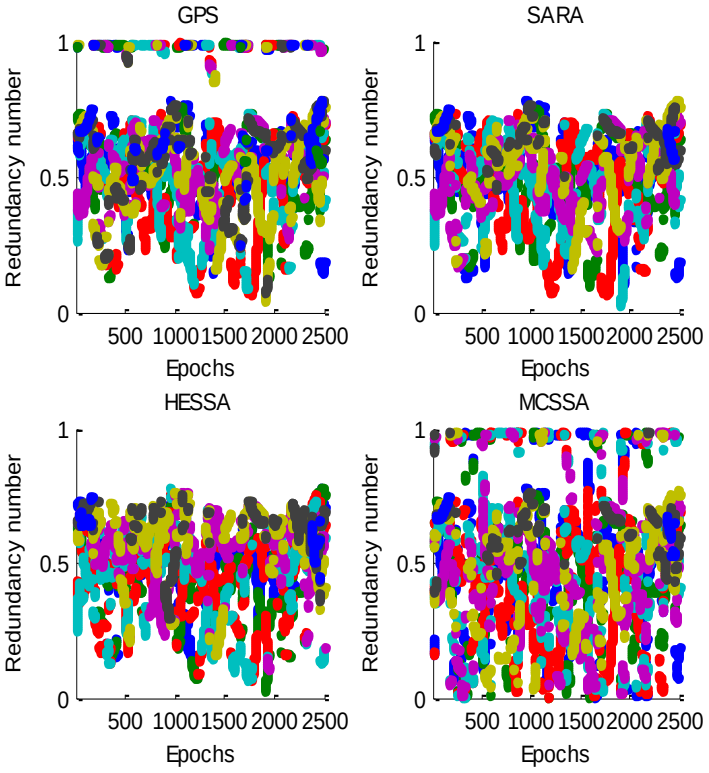

Figure 7-9 Redundancy number computed with four schemes: GPS, SARA, HESSA and MCSSA

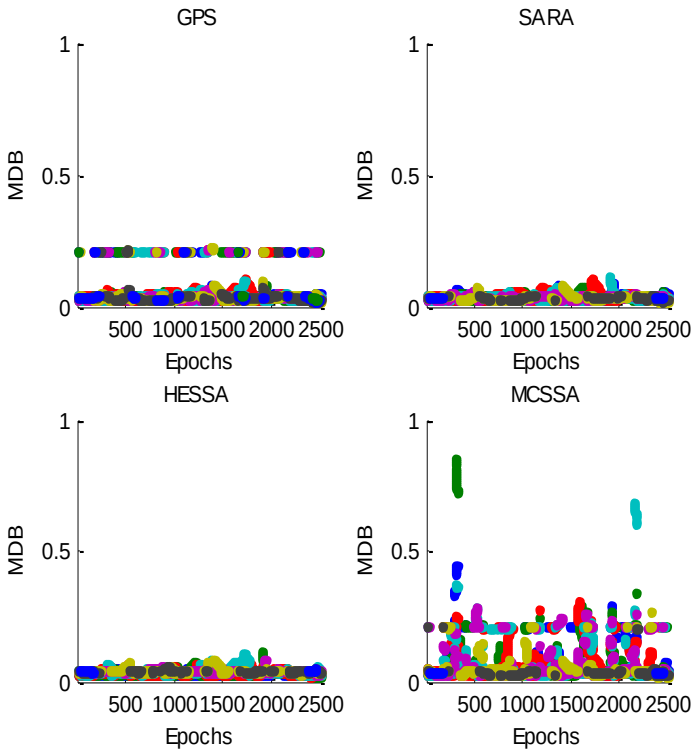

Figure 7-10 MDB computed with four schemes: GPS, SARA, HESSA and MCSSA

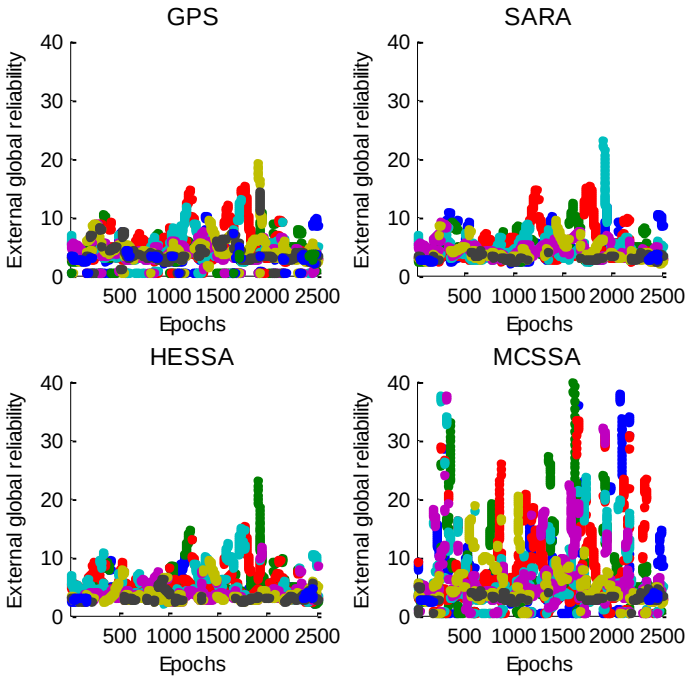

Figure 7-11 External reliability computed with four schemes: GPS, SARA, HESSA and MCSSA

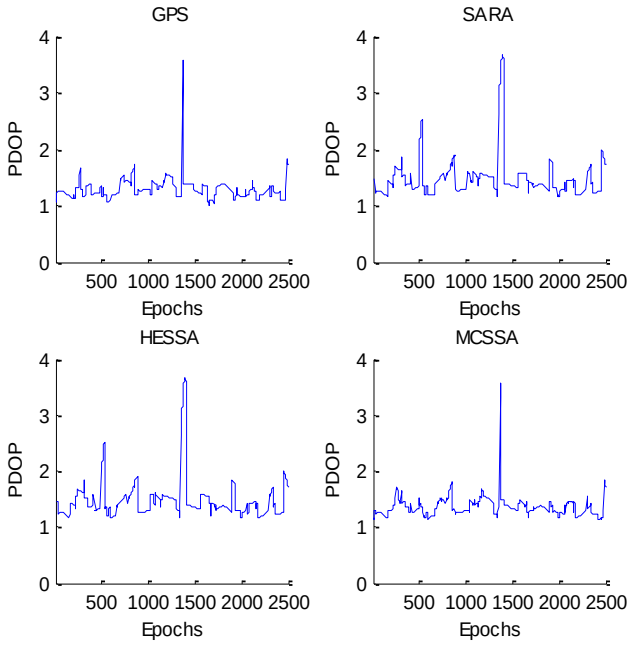

Figure 7-12 PDOP computed with four schemes: GPS, SARA, HESSA and MCSSA

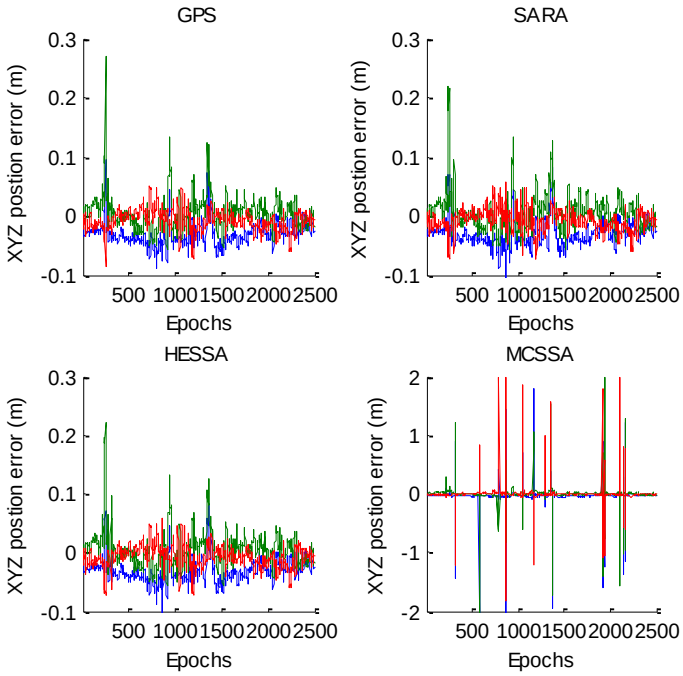

Figure 7-13 XYZ position error computed with four schemes: GPS, SARA, HESSA and MCSSA.

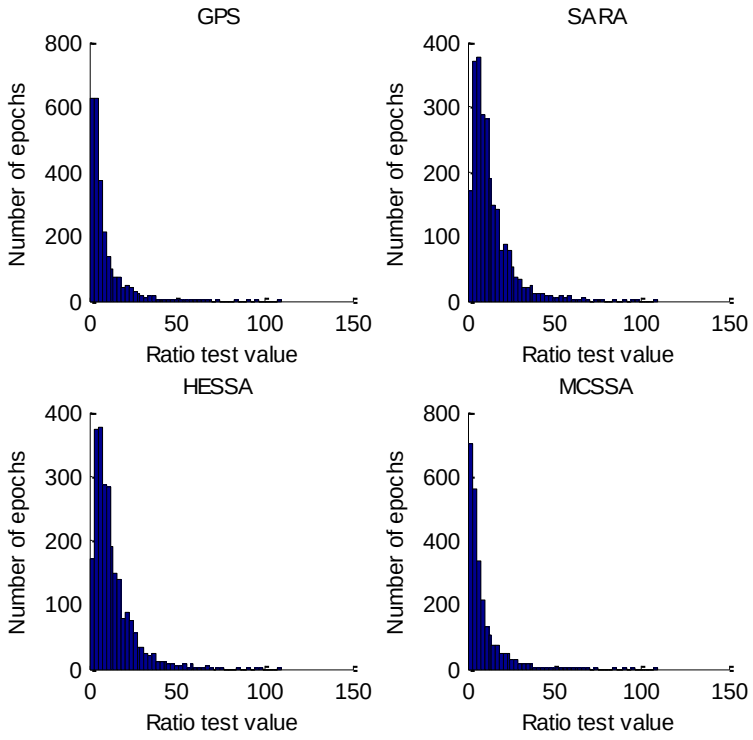

Figure 7-14 Ratio Test values computed with four schemes: GPS, SARA, HESSA and MCSSA

Case 2: the Dual-Constellation System

To further demonstrate the performance of SARA, we repeat the process and analysis with the same schemes as for Case 1 in the case of a dual-constellation system. The term DCS is referred to the scheme that computes the relevant parameters using all the GPS and VGC satellites. Figure 7-15 shows the ADOPs results with each algorithm. ADOP values obtained from these algorithms are all below 0.15 cycles except for MCSSA. Figure 7-16 illustrates the ASR results. A remarkable phenomenon is that the ASR values from the SARA and HESSA scheme exceed 90%. More specifically, most ASR values over the 2500 samples are over than 90% and very close to 100%, whereas the ASR values from the DCS and MCSSA schemes are fluctuated between 0 and 1. For the sake of conciseness, only the results of redundancy numbers are given as Figure 7-17. Obviously, SARA removes all the observations with the redundancy number of 0.9 or higher, while HESSA still retains a few observations with extreme RNUM values. In contrast, the results from the DCS and MCSSA schemes illustrate two distinct structural patterns involving extremely

large redundancy numbers. Figure 7-18 illustrates the PDOP values from all the schemes. As we can see, DCS and MCSSA schemes result in smaller PDOPs than HESSA and SARA, however, the PDOPs of SARA are still good enough with the values from 0.8 to 1.2. In fact Figure 7-19 illustrates the positional errors from all the four algorithms, which are very close. In general, the PDOP values and positioning errors resulted from SARA process are limited to be smaller than 1.2 and 5 centimeters. Figure 7-20 gives the histograms of AR ratio-test values obtained from each algorithm. Compared to Figure 14, HESSA and SARA have more numbers of larger ratio-test values than in single constellation, while DCS and MCSSA have more numbers of small ratio-test values. Figure 7-21 shows the satellite numbers of original methods and those with satellite selection algorithms. SARA can detect and delete more satellites with the increasing of satellites number. It is shown that the maximum deleted satellites number in dual-constellation is 6 and the minimum satellites number of dual-constellation with SARA is not smaller than 10 in this experiment.

Table 7-2 summarizes the percentages of samples whose ratio-test values exceed the given ratio-test critical values (1.5, 2, and 3) and the percentages of samples whose ASR values exceed the given thresholds (0.90, 0.95 and 0.99) in the both GPS and DCS cases. These percentages given under different *t* thresholds (columns 3, 4 and 5) and ASR thresholds (columns 6, 7 and 8) actually indicate, to large extend, the acceptance rates of correct integer solutions and the reliability of AR. From the above figures and Table 7-2, it can be concluded that SARA process gives much higher ASR percentages than these obtained from all the visible satellites in both single and dual constellation cases. The HESSA process gives the results similar to SARA, but the predefined number of satellites in HESSA process is given by SARA search results. As a specific example, we compare the rows 3 with 2, rows 7 with 6 in Table 7-2. It is noticed that only 82.9%, 50.5% and 25.0% of samples passed the ratio tests when the critical value is 1.5, 2 and 3, respectively, in the DCS case using all the satellites in view. These percentage turn out to be 100%, 99.7% and 98.6% if the SARA procedure is applied. In terms of ASR values, it is clearly demonstrated that the SARA process increases those samples with ASR values larger than 0.99 from 18.1% to 98.0%. This result may vary when different data sets or periods are used, but the distinctive difference indeed shows the significant advantages of the

SARA method with respect to the scheme of without adopting satellite selection strategy.

As mentioned, HESSA requires a predefined satellite number to select. In this numerical analysis, this is given by SARA instead of an arbitrary option. This number varies from epoch to epoch. This may be because the strength of the underlying GNSS model is varying. Figure 7-22 displays the ASR values from HESSA with different fixed satellites numbers, showing how a predefined number may affect the ASR performance of HESSA. The ASRs with fixed 9 satellites and 11 satellites are clearly smaller than another two situations in a few of epochs. Particularly, those events that the ASRs of 9 satellites are smaller than those of 10 satellites imply that with fewer satellites does not necessarily have higher ASR. The problem is that the HESSA algorithm itself cannot automatically determine the number of satellites needed. SARA however can automatically find the required satellite number in the selection process

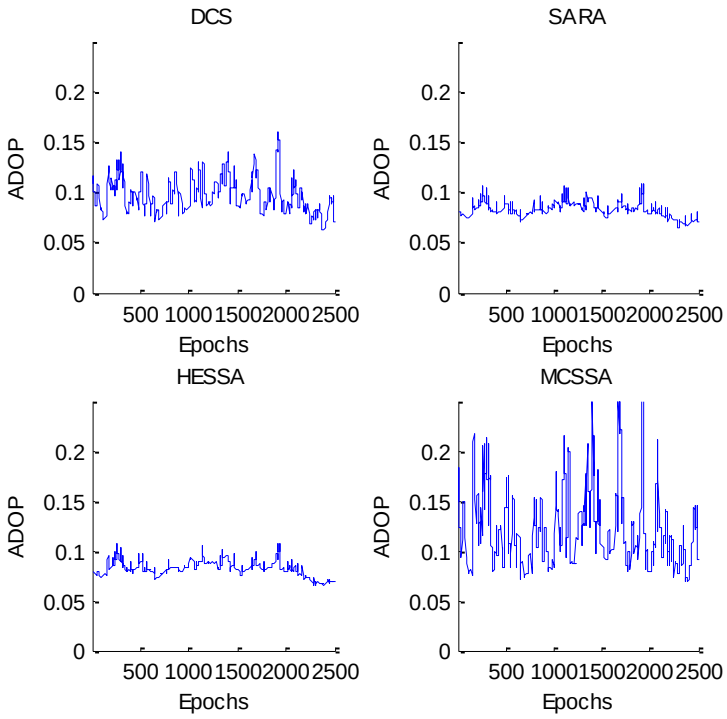

Figure 7-15 ADOPs computed with four schemes: DCS, SARA, HESSA and MCSSA

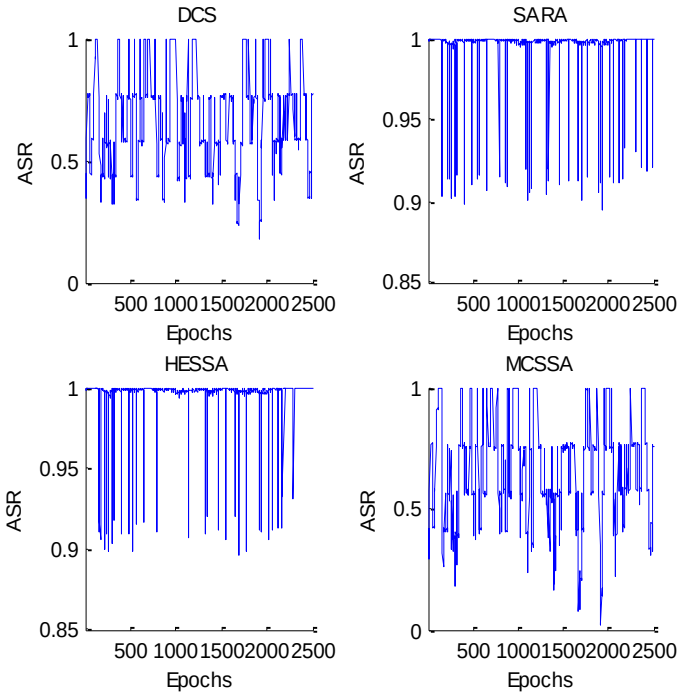

Figure 7-16 ASRs computed with four schemes: DCS, SARA, HESSA and MCSSA

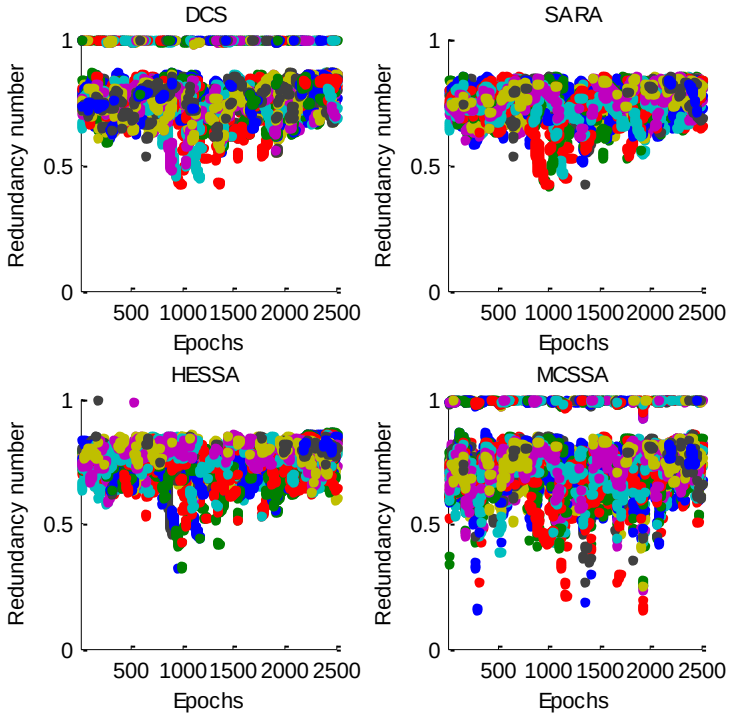

Figure 7-17 Redundancy number computed with four schemes: DCS, SARA, HESSA and MCSSA

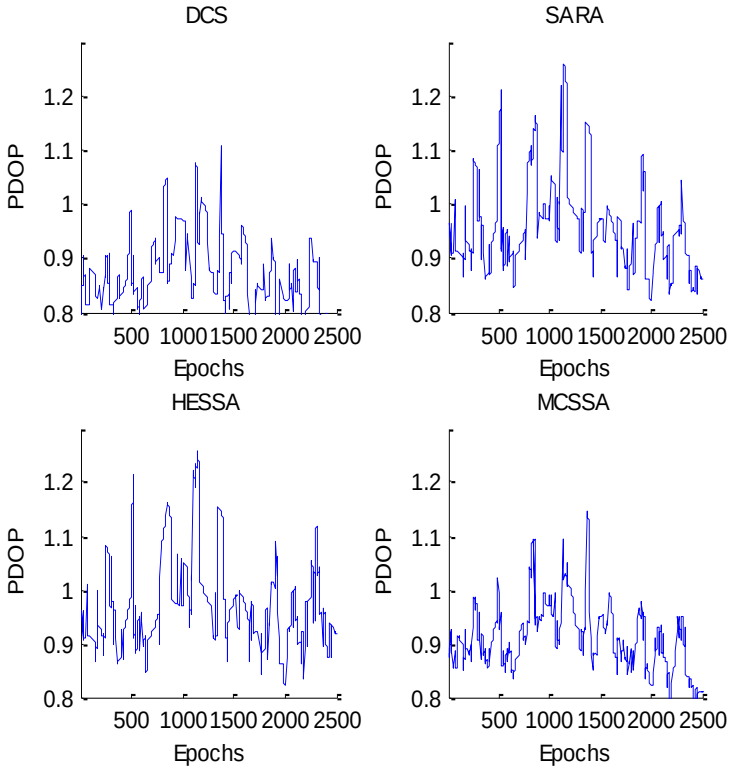

Figure 7-18 PDOP computed with four schemes: DCS, SARA, HESSA and MCSSA

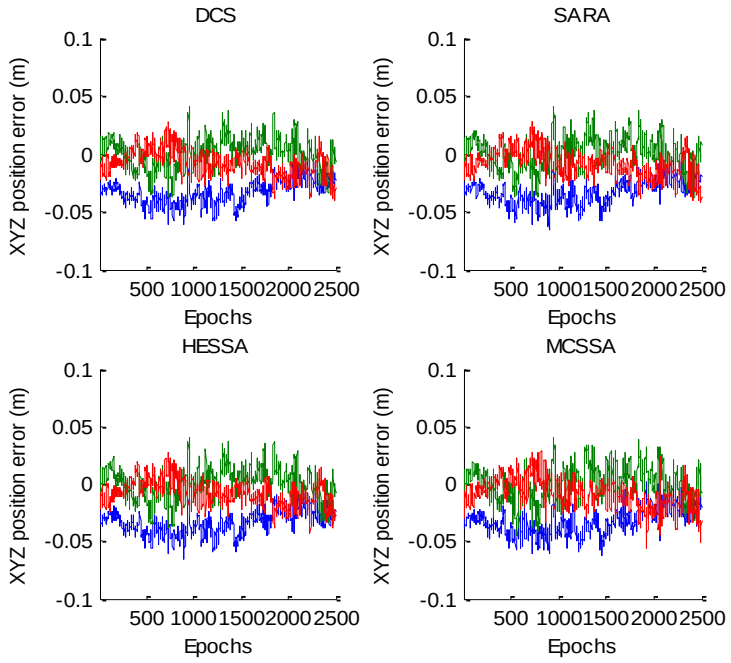

Figure 7-19 XYZ position error computed with four schemes: DCS, SARA, HESSA and MCSSA

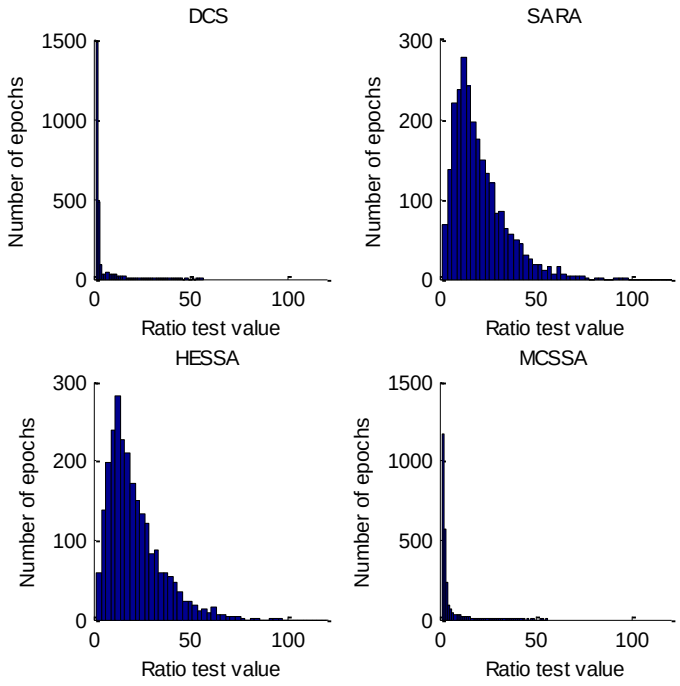

Figure 7-20 Ratio Test values with four schemes: DCS, SARA, HESSA and MCSSA

Table 7-2 The percentage of samples number for ratio test and ASR with given critical values

1		*t>1.5*	*t>2*	*t>3*	*ASR>0.9*	*ASR>0.95*	*ASR>0.99*
2	*GPS*	*98.4%*	*94.2%*	*78.3%*	*36.5*	*29.9%*	*8.0%*
3	*GPS (SARA)*	*99.6%*	*98.7%*	*94.2%*	*65.2%*	*41.1%*	*10.3%*
4	*GPS (HESSA)*	*99.6%*	*98.7%*	*94.2%*	*65.2%*	*41.2%*	*10.2%*
5	*GPS (MCSSA)*	*94.0%*	*88.9%*	*74.6%*	*36.5%*	*29.9%*	*8.0%*
6	*DCS*	*82.9%*	*50.5 %*	*25.0%*	*18.9%*	*18.1%*	*18.1%*
7	*DCS (SARA)*	*99.9%*	*99.6%*	*98.5%*	*99.9%*	*98.0%*	*98.0%*
8	*DCS (HESSA)*	*100%*	*99.7%*	*98.6%*	*99.8%*	*98.4%*	*98.4%*
9	*DCS (MCSSA)*	*89.2%*	*64.4%*	*35.9%*	*18.8%*	*18.1%*	*18.1%*

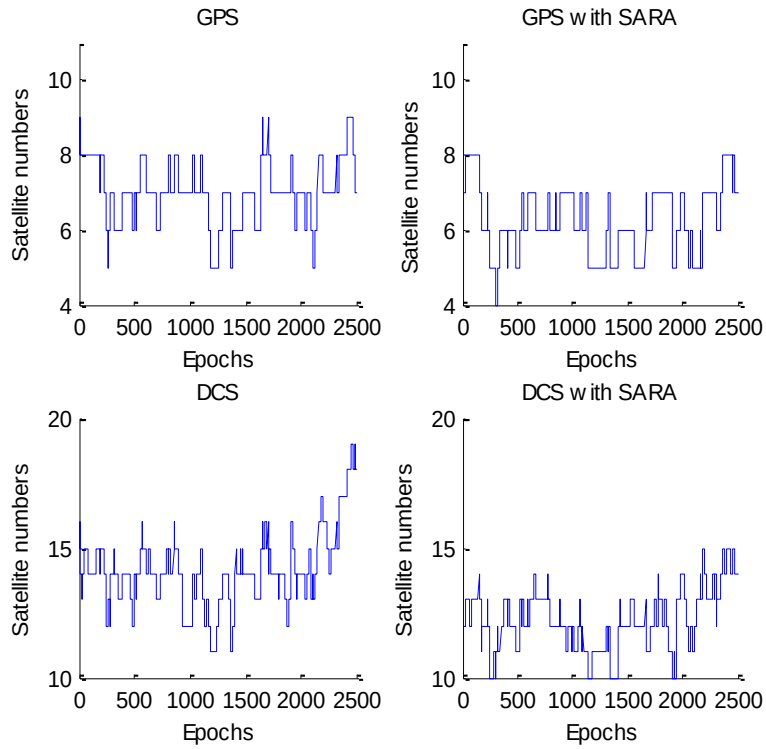

Figure 7-21 Satellites number with four schemes: GPS, GPS (SARA), DCS and DCS (SARA)

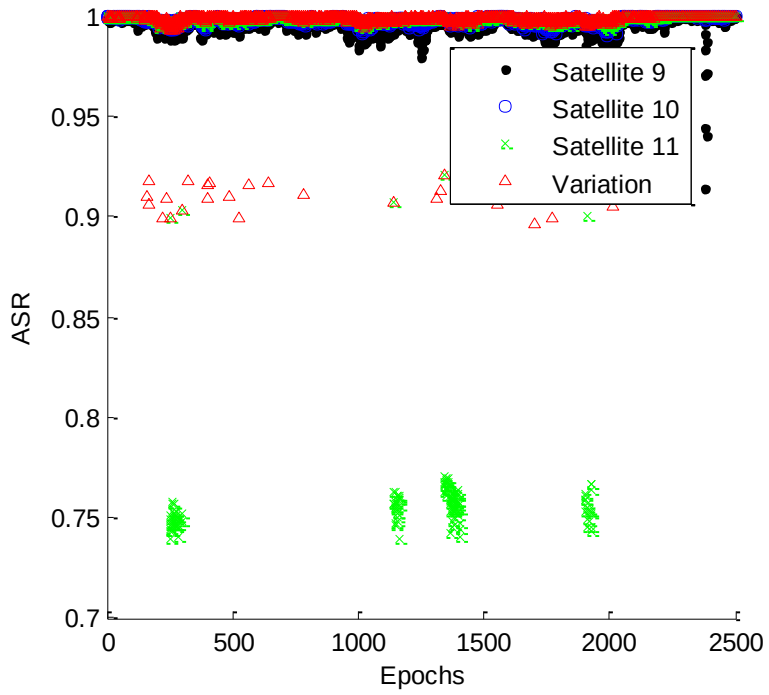

Figure 7-22 ASR computed by HESSA with different satellites

In addition to the performance of reliability and accuracy, computation time is also an important factor in real-time applications. Obviously, HESSA requires little computational load since the elevation of satellite is generally a common parameter in GNSS data processing. MCSSA has bad performance in terms of the ASR; therefore, here we only analyze the time performance of SARA compared to using all the satellites. Figure 7-23 shows the time performance of SARA in single- and dual-constellation respectively. The above part of this figure shows the time cost including ambiguity resolution and position estimation, while the below part only shows the time cost of the implementation of SARA satellites selection steps. It is clearly that though SARA requires higher computation time when the number of visible satellites increases, SARA still does not cost too much time (less than 0.02 seconds) to select the corresponding satellites in both the single constellation and the dual-constellation. There are a few events cost several seconds of computation in the dual-constellation regardless of SARA implementation. The computational speed is still a challenging problem for AR with high dimensions (Chang et al. 2005), but this disadvantage is not caused by SARA itself.

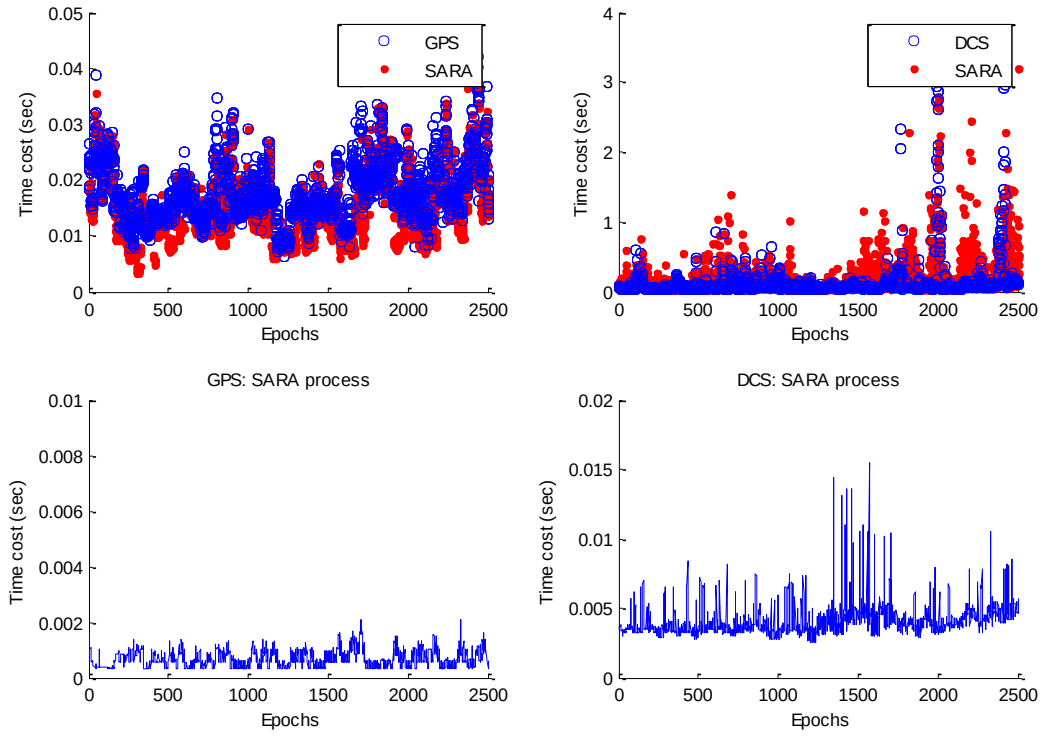

Figure 7-23 Time cost of SARA method in single- and dual-constellation

7.6 Conclusions and Future work

Benefits from multi-GNSS and multi-frequency signals could be significant, but do not come without cost. The receiver could have fewer channels or less computational power to process all the visible satellites. For real time kinematic positioning users, the major benefits of multi-GNSS and multi-frequency signals may be the option for the selective use of satellite systems, or signals, or subsets of visible satellites from different systems to assure the required reliability and accuracy of the RTK solutions.

The paper has developed a new satellite selection algorithm for reliable ambiguity resolution, namely SARA, which can select a subset of visible satellites from a single or multiple constellations based on reliability criteria while giving low PDOP values as well. The purpose is to achieve high ambiguity resolution success rate and reliable position solutions. The logic behind SARA strategy is to remove those satellites with extreme large redundancy number or MDB, or with extremely small external global reliability parameters. Experimental analysis has demonstrated that SARA process gives much higher acceptance rate of correct integer solutions and much higher ASR percentages than these obtained from all the visible satellites in both single and dual constellation cases. The HESSA process gives the results similar to SARA, but the predefined number of satellites in HESSA process is given by SARA search results. This result may vary from different data sets or periods being used, but the difference shows the significant advantages of the SARA method with respect to the case where no selection strategy is adopted.

Though the SARA algorithm can select satellite to achieve much higher ASR in a dual-constellation system, there are still some epochs where ASR values are not high enough to assure AR reliability. A possible future research effort may combine the SARA with the partial ambiguity resolution (PAR) algorithm to further improve AR reliability. Ultimately, the proposed algorithms and theory have to pass verification using a large number of real time multi-GNSS data sets, which however are not available yet.

Acknowledgements

This work was partially supported by the CRC for Spatial Information project 1.04 "Delivering Precise Positioning Services in Regional Areas" 2007-2010. The first

author also acknowledges the financial support received from the China Scholarship Council (Grant No: 2008466001). Special thanks go to anonymous reviewers whose comments have contributed to the improvement of the paper.

7.7 Reference

Baarda W (1968) A testing procedure for use in geodetic networks. Delft, Kanaalweg 4, Rijkscommissie voor Geodesie, 1968.

Cao W, O'Keefe K, Cannon M (2007) Partial ambiguity fixing within multiple frequencies and systems. In: Proceedings of ION GNSS07, The Satellite Division of the Institute of Navigation 20th International Technical Meeting, Fort Worth, TX, September 25-28 2007, pp 312-323.

Chang, X. W., Yang, X., Zhou, T. (2005). MLAMBDA: A modified LAMBDA method for integer least-squares estimation. J Geod 79(9): 552-565.

Cross P, Hawksbee D, Nicolai R (1994) Quality measures for differential GPS positioning. The Hydrographic Journal 72:17-22.

Feng Y (2005) Future GNSS Performance Predictions Using GPS with a Virtual Galileo Constellation. GPS World 16 (3):46-52.

Feng Y, Li B (2008) A benefit of multiple carrier GNSS Signals: regional scale network-based RTK with doubled inter-station distances. J SPAT SCI 53 (2):135-147.

Feng, Y, Wang, J. (2008). GPS RTK Performance Characteristics and Analysis. J GPS, 7 (1): 1-8.

Feng Y, Wang J (2011) Computed success rates of various carrier phase integer estimation solutions and their comparison with statistical success rates. J Geod 85 (2):93-103. doi:10.1007/s00190-010-0418-y

Grejner-Brzezinska, D. A., Kashani, I., Wielgosz, P. (2005). On accuracy and reliability of instantaneous network RTK as a function of network geometry, station separation, and data processing strategy. GPS Solut, 9(3): 212-225.

Han S, Rizos C Integrated method for instantaneous ambiguity resolution using new generation GPS receivers. In: Position Location and Navigation Symposium, 1996., IEEE 1996, 22-26 Apr 1996 1996. pp 254-261.

Hassibi A, Boyd S (1998) Integer parameter estimation in linear models with applications to GPS. IEEE Transactions on signal processing 46 (11):2938-2952.

Henson DJ, Collier EA, Schneider KR Geodetic Applications of the Texas Instruments TI4100 GPS Navigator. In, 1985. pp 15-19.

Hofmann-Wellenhof B, Lichtenegger H, Wasle E (2008) GNSS - global navigation satellite systems : GPS, GLONASS, Galileo, and more. Springer, Wien ; New York

Kihara M, Okada T (1984) A satellite selection method and accuracy for the global positioning system. Navigation 31 (1):8-20.

Leick A (2004) GPS satellite surveying. 3rd edition. John Wiley and Sons, New York

Li B, Feng Y, Shen Y (2009) Three carrier ambiguity resolution: distance-independent performance demonstrated using semi-generated triple frequency GPS signals. GPS Solut 14 (2):177-184.

Li J, Ndili A, Ward L, Buchman S GPS Receiver Satellite/Antenna Selection Algorithm for the Stanford Gravity Probe B Relativity Mission. In: Institute of Navigation, National Technical Meeting 'Vision 2010: Present and Future', San Diego, CA, January 25-27 1999. pp 541-550.

O'Keefe, K., Ryan, S., Lachapelle, G. (2002). Global availability and reliability assessment of the GPS and Galileo global navigation satellite systems. Canadian Aeronautics and Space Journal, 48,123–132.

Park C-W (2001) Precise relative navigation using augmented CDGPS. Ph.D. Dissertation, Stanford University, United States

Roongpiboonsopit D, Karimi HA (2009) A Multi-Constellations Satellite Selection Algorithm for Integrated Global Navigation Satellite Systems. Journal of Intelligent Transportation Systems: Technology, Planning, and Operations 13 (3):127 - 141.

Takac FaW, J. (2006) Leica System 1200 - High Performance GNSS Technology for RTK Applications. In: Proceedings of ION GNSS 2006, Fort Worth, Texas, Septemeber 26-29 2006. pp. 217-225.

Teunissen PJG (1998) Success probability of integer GPS ambiguity rounding and bootstrapping. J Geod 72 (10):606-612.

Teunissen PJG (2003) An invariant upperbound for the GNSS bootstrapped ambiguity success rate. J GPS 2 (1):13-17.

Teunissen PJG, Joosten P, Odijk D (1999) The Reliability of GPS Ambiguity Resolution. GPS Solut 2 (3):63-69.

Teunissen PJG, Joosten P, Tiberius C (1999) Geometry-free ambiguity success rates in case of partial fixing. In: Proceedings of the 1999 National Technical Meeting of The Institute of Navigation, San Diego, CA, January 25 - 27 1999, pp 201-207.

Teunissen PJG, Odijk D (1997) Ambiguity Dilution of Precision: Definition, Properties and Application. In: Proceedings of the 10th International Technical Meeting of the Satellite Division of The Institute of Navigation, Kansas City, MO, September 16 - 19 1997. pp 891 - 899.

Verhagen S (2005a) The GNSS integer ambiguities: estimation and validation. Technische Universiteit Delft (The Netherlands)

Verhagen S (2005b) On the reliability of integer ambiguity resolution. Navigation (Washington, DC) 52 (2):99-110.

Verhagen S, Odijk D, Teunissen PJG, Huisman L (2010) Performance improvement with low-cost multi-GNSS receivers. In: Satellite Navigation Technologies

and European Workshop on GNSS Signals and Signal Processing (NAVITEC), 2010 5th ESA Workshop on, 8-10 Dec. 2010. pp 1-8.

Wei M, Schwarz KP (1995) Fast ambiguity resolution using an integer nonlinear programming method. In: Proceedings of the 8th International Technical Meeting of the Satellite Division of The Institute of Navigation (ION GPS 1995), Palm Springs, CA, September 1995, pp. 1101-1110.

Chapter 8: Conclusions and Recommendations

The research problem under investigation in this thesis mainly concerns one of the most challenging and significant issues for high precision positioning and navigation with GNSS: how to achieve the high reliability of AR with respect to the ILS method in the context of multi-GNSS constellations. The high reliability requirement is especially important for those safety-critical and liability-critical operations such as aviation applications. In the context of a single-GNSS constellation, it is impossible to maintaining a high ASR of 99% or higher during a long operational period, e.g. 24 hours. An alternative way to achieve high ASR is to take advantage of the PAR technique; nevertheless, the accuracy requirement of centimetre cannot be satisfied even with the high ASR due to the insufficient number of fixed ambiguities. However, these problems can be solved with multiple-GNSS constellations; thus, the potential to have positioning solutions with both high reliability and accuracy is applicable.

In this thesis, we have studied the integer ambiguity decorrelation technique first, which is described as a modified inverse integer Cholesky decorrelation (MIICD) method. Both simulations and real data have demonstrated the MIICD could significantly reduce the condition numbers and improve the decorrelation performance. Next we have investigated the properties of orthogonality defect and search-space size in GNSS integer least-squares processing and proposed a new ambiguity resolution scheme that combines the LAMBDA search and validation procedures, resulting in a smaller search-space size and higher computation efficiency, but retaining the same AR validation outcomes. Experimental analysis has shown that the orthogonality defect presents better performance in measuring the correlation between decorrelation impact and computational efficiency than the condition number. It has been observed that the search-space size is of great importance in controlling the efficiency of the search process. The decorrelation technique improves the search efficiency from two aspects: reducing the elongation of the search ellipsoid and precisely approximating the search-space size.

Furthermore, this research work has explored the variations of ILS solutions according to the observational and stochastic models used and data processing strategies, leading to simplification of the ILS success probability computations. Results have shown that the computed ambiguity success rates (ASR) from different cases are very sensitive to the uncertainty of the unit-weight variance, which implies the fact of the dependence of the success probability prediction on correct variance and variance settings. In addition, numerical experiment schemes have also demonstrated that the ASR computed with the integer bootstrapping method is quite a sharp approximation to the actual ILS ASR. Herein, the ASR of the bootstrapped estimator is applied to be the measure of the reliability characteristics of AR with the ILS method. In fact, the low ASR is not the worse situation, since if we know the AR solution is doubtful in advance we can undertake some complementary operation to the user, e.g. an alert of the positioning result. The worst case is the missed detection cases, that is, the ASR is very high but the integer ambiguity is incorrect. In that situation, the event is said to generate Hazardous Misleading Information. Therefore, an ambiguity validation decision matrix is suggested to consider the success rate and ratio-test.

In the following two parts of the work, we demonstrate the benefits of multiple GNSS constellations to the ASR. We have examined the reliability characteristics of partial ambiguity resolution (PAR) solutions in order to obtain reliable ambiguity solutions in multiple-GNSS situations. The PAR process with the same predefined ASR of 99% can always result in a good number of reliably fixed ambiguities in the dual-constellation cases. It is proved that only when the ASR is very high, can the AR validation provide the decisions about the correctness of AR close to the real world, with both low AR risk and false alarm probabilities. Additionally, we have also examined that during the partial decorrelation process, how a bias in one measurement can be propagated and amplified onto many others, leading to more than one wrong integers and affecting the success probability.

Instead of achieving high ASR by the PAR technique, a new Satellite-selection Algorithm for Reliable Ambiguity-resolution, namely SARA, has been presented, which can select a subset of visible satellites from a single or multiple constellations based on reliability criteria while giving low PDOP values as well. Numerical results from both single and dual constellation cases have shown that with the SARA

procedure, the percentages of ASR values in excess of 90% and 95% and the percentages of ratio-test values passing the thresholds are both significantly higher than those of algorithms that use all of the satellites in view. Moreover, the implementation of SARA is simple and easy, thus, the SARA is suitable for real-time data processing to reduce high hardware and software complexity and operational cost, which is applicable for many low-cost applications.

8.1 Summary of Key Contributions

During this research project study, we have made the following findings and contributions:

- *Development of a new ambiguity decorrelation technique.* A modified inverse integer Cholesky decorrelation method is proposed and has been proved to be more effective than other methods in terms of decorrelation performance.
- *Introduction of a new measure of decorrelation performance.* The orthogonality defect is introduced as a criterion for measuring decorrelation performance. Experimental results present that it has a better performance in measuring the correlation between decorrelation impact and computational efficiency than the condition number and the decorrelation number.
- *Development of a new AR scheme*. In fact, the new AR scheme gives an alternative to set the search space size considering the ambiguity validation requirement. The new scheme can not only improve the search efficiency but also guarantee the same AR reliability as the LAMDA method. This characteristic of the scheme is attractive especially, in the high dimensional AR case.
- *Assessment of the ASR performance with actual PCF*. Various bounds and approximations of ILS ASR have been investigated, which lead to the fact that the ASR of the bootstrapping method can be a very good approximation and a close low bound of the ASR of the ILS method.
- *Evaluation of AR risk probability instead of ASR*. The ASR provides the information of AR reliability; however, the worst case is that the integer ambiguities are fixed incorrectly while the users still treat them as correct. This case refers to the probability of missed detection, or AR risk probability.

Simulation study has demonstrated that when the ASR is very high, the AR risk probability is close to zero with proper ratio-test critical values.

- *Assessment of PAR performance in the case of multi-constellations*. The experiment has shown that maintenance of the 0.99 ASR with high accurate positioning results is possible in the case of dual-constellations, while this objective is difficult to achieve in a single constellation.
- *Development of an original satellite selection algorithm*. The algorithm called SARA is proposed and it is proven that it can make the AR reliable by selecting a specific subset of the all of the visible satellites. The performance of AR reliability is significantly improved by SARA in contrast to using all of the visible satellites. SARA also provides a criterion of selected number of satellites. Moreover, SARA is simple and easy to implement in the future GNSS data processing.

8.2 Recommendations for Future Work

Based on the theoretical and practical results obtained in this work, the following recommendations are made for future work:

(1) In the very near future, the increase in satellite availability will also increase the number of ambiguity parameters. Nonetheless, the search efficiency of existing ILS methods is still slow when dealing with high-dimensional ambiguity parameters. The proposed MIICD method can have a better decorrelation performance, but the time cost of MIICD will also increase. Therefore, a better and faster decorrelation method is desirable. In addition, the proposed AR scheme (Chapter 4) could be adopted in the procedure of setting search space size χ^2 in a high-dimensional ambiguity matrix.

(2) Since we have already discussed that the computed ASR is very sensitive to the value of the prior unit-weight variance factor σ_0^2, how to determine an accurate value of σ_0^2 becomes more critical in the application of evaluation and prediction of the quality of AR. Either conservative or optimistic conclusions could be generated from an improper value of σ_0^2. In addition, the stochastic model refinement is also desirable for more precise evaluation.

(3) When we use the PAR technique, sometimes, the positioning results are still not satisfied regardless of its highly reliable ambiguity solutions. This is possible because the number of fixed ambiguities is too a few. Besides this reason, the relationship between the selected ambiguities and positioning result precision still needs more investigation.

(4) Vast amounts of real multi-GNSS data are supposed to verify our proposed algorithms. Particularly, more studies and investigation of AR method for GLONASS are needed to demonstrate the availability of SARA method.

BIBLIOGRAPHY

Baarda W (1968) A testing procedure for use in geodetic networks. Delft, Kanaalweg 4, Rijkscommissie voor Geodesie, 1968

Blewitt G (1989) Carrier phase ambiguity resolution for the Global Positioning System applied to geodetic baselines up to 2000 km. Journal of Geophysical Research 94 (B8):10.187-110.203

Bona P (2000) Precision, Cross Correlation, and Time Correlation of GPS Phase and Code Observations. GPS Solutions 4 (2):3-13. doi:10.1007/pl00012839

Cai J, Grafarend E, Hu C (2009) The total optimal search criterion in solving the mixed integer linear model with GNSS carrier phase observations. GPS Solutions 13 (3):221-230

Cao W, O'Keefe K, Cannon M (2007) Partial ambiguity fixing within multiple frequencies and systems. In: Proceedings of ION GNSS07, The Satellite Division of the Institute of Navigation 20th International Technical Meeting, Fort Worth, TX, September 25-28 2007, pp 312-323.

Cao Wei, O'Keefe K, Cannon M (2008a) Performance Evaluation of GPS/Galileo Multiple-frequency RTK Positioning Using a Single-difference Processor. In: Proceedings of the 21st International Technical Meeting of the Satellite Division of The Institute of Navigation, Savannah, GA, September 2008, pp. 2841-2849.

Cao W, O'Keefe K, Petovello M, Cannon M (2008b) Simulated Performance of Multiple-signal and Multiple-system Positioning for Land Vehicle Navigation. In: Proceedings of the 2008 National Technical Meeting of The Institute of Navigation, San Diego, CA, January 2008, pp. 603-613.

Chadha K (1998) The global positioning system: Challenges in bringing GPS to mainstream consumers. In, 1998. IEEE, pp 26-28

Chang X-W, Zhou T (2007) MILES: MATLAB package for solving Mixed Integer LEast Squares problems. GPS Solutions 11 (4):289-294

Chang XW, Yang X, Zhou T (2005) MLAMBDA: A modified LAMBDA method for integer least-squares estimation. Journal of Geodesy 79 (9):552-565

Chen D, Lachapelle G (1995) A comparison of the FASF and least-squares search algorithms for on-the-fly ambiguity resolution. Navigation-Washington 42 (2):371-390

Compass navigation system web (2011) Retrieved from www.beidou.gove.cn. Accessed November 9 2001

Cross P, Hawksbee D, Nicolai R (1994) Quality measures for differential GPS positioning. The Hydrographic Journal 72:17-22

Dao THD (2005) Performance evaluation of multiple reference station GPS RTK for a medium scale network. M.Sc., University of Calgary, Canada

de Jonge P, Tiberius C (1996) The LAMBDA method for integer ambiguity estimation: implementation aspects. Publications of the Delft Geodetic Computing Centre 12

Eisenbrand F (2010) Integer Programming and Algorithmic Geometry of Numbers. In: Jünger M, Liebling TM, Naddef D et al. (eds) 50 Years of Integer Programming 1958-2008. Springer Berlin Heidelberg, pp 505-559. doi:10.1007/978-3-540-68279-0_14

Euler HJ, Schaffrin B (1990) On a Measure for the Discernibility between Different Ambiguity Solutions in the Static-Kinematic GPS-Mode. Paper presented at the IAG Symposia no. 107, Kinematic Systems in Geodesy, Surveying, and Remote Sensing, New York,

European Commission Enterprise and Industry (2011) Launch of first 2 operational Galileo IOV Satellites. Ec.europa.eu (2011-10-21). Retrieved from http://ec.europa.eu/enterprise/policies/satnav/galileo/satellite-launches/index_en.htm. Accessed 9 November 2011

European Space Agency Web (2011) http://www.esa.int/esaNA/galileo.html. Accessed October 17 2011

Feng S, Ochieng W, Moore T, Hill C, Hide C (2009) Carrier Phase Based Integrity Monitoring for High Accuracy Positioning. GPS Solutions 13 (1):13-22

Feng S, Ochieng WY (2006) User Level Autonomous Integrity Monitoring for Seamless Positioning in All Conditions and Environments. In: European Navigation Conference GNSS Manchester International Convention Centre, Manchester, UK, 8th-10th May 2006.

Feng Y (2005) Future GNSS Performance Predictions Using GPS with a Virtual Galileo Constellation. GPS World 16 (3):46-52

Feng Y (2008) GNSS three carrier ambiguity resolution using ionosphere-reduced virtual signals. Journal of Geodesy 82 (12):847-862

Feng Y, Li B (2008) A benefit of multiple carrier GNSS Signals: regional scale network-based RTK with doubled inter-station distances. Journal of Spatial Science 53 (2):135-147

Feng Y, Wang J (2011) Computed success rates of various carrier phase integer estimation solutions and their comparison with statistical success rates. Journal of Geodesy 85 (2):93-103. doi:10.1007/s00190-010-0418-y

Frei E, Beutler G (1990) Rapid static positioning based on the fast ambiguity resolution approach FARA: theory and first results. Manuscripta Geodaetica 15 (6):325-356

Godet J, De Mateo JC, Erhard P, Nouvel O (2002) Assessing the Radio Frequency Compatibility between GPS and Galileo. In Proceedings of the 15th International Technical Meeting of the Satellite Division of The Institute of Navigation, Portland, OR, USA, September 2002, pp. 1260-1269

Grafarend EW (2000) Mixed Integer-Real Valued Adjustment (IRA) Problems: GPS Initial Cycle Ambiguity Resolution by Means of the LLL Algorithm. GPS Solutions 4 (2):31-44

Griffiths J, Ray J (2009) On the precision and accuracy of IGS orbits. Journal of Geodesy 83 (3):277-287. doi:10.1007/s00190-008-0237-6

Groves PD (2008) Principles of GNSS, inertial, and multisensor integrated navigation systems. Artech House, Boston, Mass. ; London :

Han S (1997a) Carrier phase-based long-range GPS kinematic positioning. Ph.D. Thesis, University of New South Wales, Australia

Han S (1997b) Quality-control issues relating to instantaneous ambiguity resolution for real-time GPS kinematic positioning. Journal of Geodesy 71 (6):351-361

Han S, Rizos C (1996) Integrated method for instantaneous ambiguity resolution using new generation GPS receivers. In: Position Location and Navigation Symposium, 1996., IEEE 1996, 22-26 Apr 1996 1996. pp 254-261

Hassibi A, Boyd S (1998) Integer parameter estimation in linear models with applications to GPS. IEEE Transactions on signal processing 46 (11):2938-2952

Hatch R (1990) Instantaneous Ambiguity Resolution. In: Proceedings of KIS'90, Banff, Canada, 10-13 September 1990. pp 299-308

Hatch R, Jung J, Enge P, Pervan B (2000) Civilian GPS: The Benefits of Three Frequencies. GPS Solutions 3 (4):1-9. doi:10.1007/pl00012810

Hein G (2006) GNSS Interoperability: Achieving a Global System of Systems or "Does Everything Have to Be the Same?". Inside GNSS Premiere issue 1 (1)

Henkel P, Günther C (2009) Partial integer decorrelation: optimum trade-off between variance reduction and bias amplification. Journal of Geodesy 84 (1):51-63. doi:10.1007/s00190-009-0343-0

Henkel P (2010) Reliable carrier phase positioning. Ph.D. Thesis, Technische Universität München, Germany

Henson DJ, Collier EA, Schneider KR (1985) Geodetic Applications of the Texas Instruments TI4100 GPS Navigator. In: Proc of the First International Symposium on Precise Positioning with the Global Positioning System 1, Apr. 15-19 1985, Rockville, Maryland. pp 15-19

Hofmann-Wellenhof B, Lichtenegger H, Wasle E (2008) GNSS - global navigation satellite systems : GPS, GLONASS, Galileo, and more. Springer, Wien ; New York

Hopfield, H.S. (1969) Two–quadratic tropospheric refractivity profile for correction satellite data. Journal of Geophysical Research 74(18): 4487 – 4499

Japan Aerospace Exploration Agency (2011) CALL FOR APPLICATIONS: Hosting sites for Multi-GNSS Monitoring Network. Retrieved from http://www.satnavi.jaxa.jp/e/news/qz-1106012_e.html. Accessed November 9 2011

Ji S (2008) Positioning performance improvements with European multiple-frequency satellite navigation - Galileo. Ph.D., Hong Kong Polytechnic University, Hong Kong

Ji S, Chen W, Ding X, Chen Y, Zhao C, Hu C (2010) Ambiguity validation with combined ratio test and ellipsoidal integer aperture estimator. Journal of Geodesy 84 (10):597-604. doi:10.1007/s00190-010-0400-8

Johannes Mach ID, Robert Wolf, Theo Zink (2005) Real-time station clockl synchronization for GNSS integrity monitoring. Paper presented at the ION GNSS 18th International Technical Meeting of the Satellite Division, Long Beach, USA, 13-16 September

Jonkman, N.F. (1998) The Geometry-Free Approach to Integer GPS Ambiguity Estimationc. In Proceedings of the 11th International Technical Meeting of the Satellite Division of The Institute of Navigation (ION GPS 1998), Nashville, TN, September 1998, pp. 369-379.

Jung J, Enge P, Pervan B (2000) Optimization of cascade integer resolution with three civil GPS frequencies. In: Proceedings of the 13th International Technical Meeting, 2000. p 2191-2201

Kaplan ED, Hegarty C (2006) Understanding GPS : principles and applications. 2nd edn. Artech House, Boston

Kihara M, Okada T (1984) A satellite selection method and accuracy for the global positioning system. Navigation 31 (1):8-20

Kim D, Langley RB (1999) An optimized least-squares technique for improving ambiguity resolution performance and computational efficiency. In: Proceedings of ION GPS'99, Nashville, Tennessee, 14-17 September 1999. pp 1579-1588

Kleusberg A, Teunissen PJG (1998) GPS for geodesy. 2nd, completely rev. and extended edn. Springer, Berlin ; New York

Klobuchar J (1996) Ionospheric effects on GPS. Global Positioning System: Theory and applications 1:485-515

Kovach K, Maquet H, Davis D (1995) PPS RAIM algorithms and their performance. Navigation(Washington, DC) 42 (3):515-529

Kuusniemi HC (2005) User-level reliability and quality monitoring in satellite-based personal navigation. C821132, Tampereen Teknillinen Korkeakoulu, Finland

Leick A (2004) GPS satellite surveying. John Wiley & Sons, Inc

Lenstra AK, Lenstra HW, Lovász L (1982) Factoring polynomials with rational coefficients. Mathematische Annalen 261 (4):515-534

Li B, Feng Y, Shen Y (2009) Three carrier ambiguity resolution: distance-independent performance demonstrated using semi-generated triple frequency GPS signals. GPS Solutions 14 (2):177-184

Li B, Shen Y (2010) Global Navigation Satellite System Ambiguity Resolution with Constraints from Normal Equations. Journal of Surveying Engineering 136 (2):63-71

Li J, Ndili A, Ward L, Buchman S (1999) GPS Receiver Satellite/Antenna Selection Algorithm for the Stanford Gravity Probe B Relativity Mission. In: Institute of Navigation, National Technical Meeting 'Vision 2010: Present and Future', San Diego, CA, January 25-27 1999. pp 541-550

Liu L, Hsu H, Zhu Y, Ou J (1999) A new approach to GPS ambiguity decorrelation. Journal of Geodesy 73 (9):478-490

Luk, FT, Qiao, S. (2007). Numerical properties of the LLL algorithm. Paper presented at the Advanced Signal Processing Algorithms, Architectures, and Implementations XVII, 2007

Luk FT, Tracy DM (2008) An improved LLL algorithm. Linear Algebra and its Applications 428 (2-3):441-452

Misra P, Enge P (2006) Global positioning system : signals, measurements, and performance. 2nd edn. Ganga-Jamuna Press, Lincoln, Mass.

Mok E, Cross PA (1994) A Fast Satellite Selection Algorithm for Combined GPS and GLONASS Receivers. The Journal of Navigation 47 (03):383-389. doi:10.1017/S0373463300012327

Mowlam AP, Collier PA (2004) Fast Ambiguity Resolution Performance using Partially-Fixed Multi-GNSS Phase Observations. Paper presented at the the 2004 International Symposium on GNSS/GPS, Sydney, Australia, 6-8 December

NAVSTAR (1996) NAVSTAR Gloabl Positioning System (GPS) On DoD User Equipment (trans: group saicsad).

O'Keefe K (2001) Availability and reliability advantages of GPS/Galileo integration. In: Proceedings of the 14th International Technical Meeting of the Satellite Division of The Institute of Navigation (ION GPS 2001), Salt Lake City, UT, September 2001, pp. 2096-2104.

O'Keefe K, Petovello M, Lachapelle G, Cannon ME (2006) Assessing probability of correct ambiguity resolution in the presence of time-correlated errors. Navigation (Washington, DC) 53 (4):269-282.

Ober PB (1999) Towards High Integrity Positioning. In: The proceedings of ION GPS-99, 12th International Technical Meeting of the Satellite Division of the Institute of Navigation, Nashville Convention Center, Nashville, Tennessee 1999.

Ong RB, Petovello MG, Lachapelle G (2009) Assessment of GPS/GLONASS RTK under a variety of operational conditions. Proceedings of the 22nd International Technical Meeting of The Satellite Division of the Institute of Navigation, Savannah, GA, September 2009, pp. 3297-3308.

Park C, Kim I, Lee JG, Jee GI (1996) Efficient ambiguity resolution using constraint equation. In Position Location and Navigation Symposium, 1996. IEEE, pp 277-284

Park CW (2001) Precise relative navigation using augmented CDGPS. Ph.D. Thesis, Stanford University, USA

Parkins A (2009) Performance of precise marine positioning using future modernised global satellite positioning systems and a novel partial

ambiguity resolution technique. Ph.D. Thesis, University College London, United Kingdom

Parkins A (2010) Increasing GNSS RTK availability with a new single-epoch batch partial ambiguity resolution algorithm. GPS Solutions:1-12. doi:10.1007/s10291-010-0198-0

Parkinson BW, Spilker JJ, Axelrad P, Enge P (1996) Global Positioning System: Theory and Applications Volume II. Progress in astronautics and aeronautics 163

Perepetchai V (2000) Global positioning system receiver autonomous integrity monitoring. M.Sc., McGill University, Canada

Pervan BS (1996) Navigation integrity for aircraft precision landing using the global positioning system. Stanford University, USA

Peter J. Buist PJGT, Gabriele Giorgi, and Sandra Verhagen (2009) Multiplatform Instantaneous GNSS Ambiguity Resolution for Triple- and Quadruple-Antenna Configurations with Constraints. International Journal of Navigation and Observation 2009. doi: 10.1155/2009/565426

Roongpiboonsopit D, Karimi HA (2009) A Multi-Constellations Satellite Selection Algorithm for Integrated Global Navigation Satellite Systems. Journal of Intelligent Transportation Systems: Technology, Planning, and Operations 13 (3):127 - 141

Russian Space Agency Information page. (2011) http://www.glonass-ianc.rsa.ru/en/. Accessed October 17 2011

Sagar Kulkarni in Hyderabad (2007) India to develop its own version of GPS. Retrieved from http://www.rediff.com/news/2007/sep/27gps.htm. Accessed November 9 2011

Saastamoinen, J (1973) Contribution to the theory of atmospheric refraction. Bulletin Geodesique 107: 13-34

Satellite navigation. (2011) Comparison of systems. Retrieved from http://en.wikipedia.org/wiki/Satellite_navigation#cite_note-0. Accessed October 31 2011

Segall P, Davis JL (1997) GPS applications for geodynamics and earthquake studies. Annual Review of Earth and Planetary Sciences 25 (1):301-336

Svendsen J (2006) Some properties of decorrelation techniques in the ambiguity space. GPS Solutions 10 (1):40-44

Takac FaW, J. (2006) Leica System 1200 - High Performance GNSS Technology for RTK Applications. In: Proceedings of ION GNSS 2006, Fort Worth, Texas, Septemeber 26-29 2006.

Tang C (1996) Accuracy and reliability of various DGPS approaches. M.Sc., University of Calgary, Canada

Teunissen P, De Jonge P, Tiberius C (1996) The Volume of the GPS Ambiguity Search Space and its Relevance for Integer Ambiguty Resolution. Paper presented at the ION GPS-96 Kansas City Convention Center, Kansas City, Missouri, September 17-20 1996

Teunissen PJG (1993) Least-Squares Estimation of the Integer GPS Ambiguities. Invited Lecture, Section IV, Theory and Methodology, IAG General Meeting

Teunissen PJG (1994) A new method for fast carrier phase ambiguity estimation. In: Position Location and Navigation Symposium, 1994., IEEE, 11-15 Apr 1994. pp 562-573

Teunissen PJG (1995) The least-squares ambiguity decorrelation adjustment: a method for fast GPS integer ambiguity estimation. Journal of Geodesy 70 (1):65-82

Teunissen PJG (1997) A canonical theory for short GPS baselines. Part IV: precision versus reliability. Journal of Geodesy 71 (9):513-525. doi:10.1007/s001900050119

Teunissen PJG (1998a) Minimal detectable biases of GPS data. Journal of Geodesy 72 (4):236-244

Teunissen PJG (1998b) On the integer normal distribution of the GPS ambiguities. Artificial Satellites 33 (2):49-64

Teunissen PJG (1998c) Success probability of integer GPS ambiguity rounding and bootstrapping. Journal of Geodesy 72 (10):606-612

Teunissen PJG (1999a) The Mean and the Variance Matrix of the 'Fixed'GPS Baseline. Acta Geodaetica et Geophysica Hungarica 34 (1-2):33-40

Teunissen PJG (1999b) An optimality property of the integer least-squares estimator. Journal of Geodesy 73 (11):587-593

Teunissen PJG (2000) The success rate and precision of GPS ambiguities. Journal of Geodesy 74 (3):321-326

Teunissen PJG (2001) Integer estimation in the presence of biases. Journal of Geodesy 75 (7):399-407

Teunissen PJG (2003a) Towards a unified theory of GNSS ambiguity resolution. Journal of Global Positioning Systems 2 (1):1-12

Teunissen PJG (2003b) A carrier phase ambiguity estimator with easy-to-evaluate fail-rate. Artificial Satellites - Journal of Planetary Geodesy 38 (3):89-96

Teunissen PJG (2003c) An invariant upperbound for the GNSS bootstrapped ambiguity success rate. Journal of Global Positioning Systems 2 (1):13-17

Teunissen PJG (2004) Penalized GNSS Ambiguity Resolution. Journal of Geodesy 78 (4):235-244

Teunissen PJG (2005) Integer aperture bootstrapping: a new GNSS ambiguity estimator with controllable fail-rate. Journal of Geodesy 79 (6):389-397

Teunissen PJG, de Jonge PJ, Tiberius CCJM (1997) The least-squares ambiguity decorrelation adjustment: its performance on short GPS baselines and short observation spans. Journal of Geodesy 71 (10):589-602

Teunissen PJG, Joosten P, Odijk D (1999) The Reliability of GPS Ambiguity Resolution. GPS Solutions 2 (3):63-69

Teunissen PJG, Joosten P, Tiberius C (1999b) Geometry-free ambiguity success rates in case of partial fixing. In: Proceedings of the 1999 National Technical Meeting of The Institute of Navigation, San Diego, CA, January 25 - 27 1999, pp 201-207.

Teunissen PJG, Odijk D (1997) Ambiguity Dilution of Precision: Definition, Properties and Application. In: Proceedings of the 10th International Technical Meeting of the Satellite Division of The Institute of Navigation, Kansas City, MO, September 16 - 19 1997. pp 891 - 899

Teunissen PJG, Verhagen S (2004) On the foundation of the popular ratio test for GNSS ambiguity resolution. Paper presented at the ION GNSS, Long Beach, California, USA

Teunissen PJG, Verhagen S (2008) GNSS Ambiguity Resolution: When and How to Fix or not to Fix? In: VI Hotine-Marussi Symposium on Theoretical and Computational Geodesy. pp 143-148

Teunissen PJG, Verhagen S (2009) The GNSS Ambiguity Ratio-Test Revisited: a Better Way of Using It. Survey Review 41 (312):138-151. doi:10.1179/003962609x390058

Teunissen PJG, Verhagen S (2011) Integer Aperture Estimation-A Framework for GNSS Ambiguity Acceptance Testing. Inside GNSS (March/April):66-73

Tiberius CCJM, de Jonge PJ (1995) Fast positioning using the LAMBDA method. In: Proceedings of the 4th International Symposium on Differential Satellite Navigation Systems DSNS'95, Bergen, Norway, April 24-28 1995.

US Government's GPS page. (2011). http://gps.gov/systems/gps/space/. Accessed October 17 2011

Verhagen S (2003) On the approximation of the integer least-squares success rate: which lower or upper bound to use. Journal of Global Positioning Systems 2 (2):117-124

Verhagen S (2004) Integer ambiguity validation: an open problem? GPS Solutions 8 (1):36-43

Verhagen S (2005a) The GNSS integer ambiguities: estimation and validation. Technische Universiteit Delft, The Netherlands

Verhagen S (2005b) On the reliability of integer ambiguity resolution. Navigation(Washington, DC) 52 (2):99-110

Verhagen S (2006) Improved performance of multi-carrier ambiguity resolution based on the LAMBDA method. In: Proc. 3rd ESA Workshop on Satellite Navigation User Equipment Technologies, NAVITEC 2006.

Verhagen S, Odijk D, Teunissen PJG, Huisman L (2010) Performance improvement with low-cost multi-GNSS receivers. In: Satellite Navigation Technologies and European Workshop on GNSS Signals and Signal Processing (NAVITEC), 2010 5th ESA Workshop on, 8-10 Dec. 2010. pp 1-8

Vollath U, Birnbach S, Landau H, Fraile-Ordonez JM, Martin-Neira M (1999) Analysis of three-carrier ambiguity resolution technique for precise relative positioning in GNSS-2. Navigation(Washington, DC) 46 (1):13-23

Wang J (2000) An approach to GLONASS ambiguity resolution. Journal of Geodesy 74 (5):421-430

Wang J, Feng Y (2011) Reliability of partial ambiguity fixing with multi-GNSS constellations. Submitted to Journal of Geodesy

Wang J, Feng Y, Wang C (2010) A Modified inverse integer Cholesky decorrelation method and the performance on ambiguity resolution. Journal of Global Positioning Systems 9 (2):156-165

Wang J, Stewart MP, Tsakiri M (1998) A discrimination test procedure for ambiguity resolution on-the-fly. Journal of Geodesy 72 (11):644-653

Xu P (2001) Random simulation and GPS decorrelation. Journal of Geodesy 75 (7-8):408-423

Xu P (2002) Isotropic probabilistic models for directions, planes and referential systems. In: Proc. Royal Soc. London A, Vol. 548, No. 2024. August 2002, pp. 2017-2038

Xu P (2006) Voronoi cells, probabilistic bounds, and hypothesis testing in mixed integer linear models. IEEE Transactions on information theory 52 (7):3122-3138

Xu P (2011) Parallel Cholesky-based reduction for the weighted integer least squares problem. Journal of Geodesy:1-18. doi:10.1007/s00190-011-0490-y

Zhang X (2012) Beidou launched the 13th and 14th satellites. Retrieved from http://www.beidou.gov.cn/2012/09/25/2012092511b5b9aea020447aa2d8b4b041cf776c.html. Accessed May 9 2012

Zhou Y (2010) A new practical approach to GNSS high-dimensional ambiguity decorrelation. GPS Solutions:1-7. doi:10.1007/s10291-010-0192-6